INFORMATION TO USERS

This manuscript has been reproduced from the microfilm master. UMI films the text directly from the original or copy submitted. Thus, some thesis and dissertation copies are in typewriter face, while others may be from any type of computer printer.

The quality of this reproduction is dependent upon the quality of the copy submitted. Broken or indistinct print, colored or poor quality illustrations and photographs, print bleedthrough, substandard margins, and improper alignment can adversely affect reproduction.

In the unlikely event that the author did not send UMI a complete manuscript and there are missing pages, these will be noted. Also, if unauthorized copyright material had to be removed, a note will indicate the deletion.

Oversize materials (e.g., maps, drawings, charts) are reproduced by sectioning the original, beginning at the upper left-hand corner and continuing from left to right in equal sections with small overlaps.

Photographs included in the original manuscript have been reproduced xerographically in this copy. Higher quality 6" x 9" black and white photographic prints are available for any photographs or illustrations appearing in this copy for an additional charge. Contact UMI directly to order.

Bell & Howell Information and Learning
300 North Zeeb Road, Ann Arbor, MI 48106-1346 USA
800-521-0600

Université d'Ottawa • University of Ottawa

Concrete Columns Confined with Scrap Tires

by

Adel Abdulmoula Bugaldian

A thesis submitted to
the Faculty of Graduate Studies and Research
in partial fulfillment of
the requirement for the degree of

Master of Applied Science
in Civil Engineering*

Department of Civil Engineering
University of Ottawa
Ottawa, Ontario, Canada
April 1999

* The M.A.Sc. Program in Civil Engineering
is a joint program with the Carleton University,
administrated by the Ottawa-Carleton Institute for Civil Engineering

To my mother and my wife

for their love

and continuous support

Abstract

The majority of column failures observed during recent earthquakes were attributed to poor column behavior, due to lack of inelastic deformability. Column deformability can be improved by confining potential plastic hinge regions by properly designed transverse reinforcement, consisting of closely spaced perimeter hoops, overlapping hoops, crossties or spirals. This ensures dissipation of seismic induced energy without a significant loss of strength. However, the requirements of confinement reinforcement can be labor intensive, uneconomical and potentially leading to construction difficulties due to the congestion of column cages with reinforcing steel. It is therefore essential to find new and improved techniques to confine concrete columns.

One possible alternative to conventional transverse reinforcement is to use scrap tires for column confinement. However, there is currently no experimental data available on the effectiveness of scrap tires as confinement reinforcement. It is the objective of the current research program to conduct experimental and analytical investigation to explore the possibilities of using scrap steel-belted tires as transverse column reinforcement for bridge columns.

The experimental investigation included testing six large-scale circular columns, confined with scrap tires, under simulated seismic loading. Three different arrangements of tires were used as confinement reinforcement which allowed the investigation of different parameters of confinement on column behavior. The columns were tested under two different levels of axial load, consisting of 11% or 21% of their concentric capacities. The results indicated that the columns behaved in a ductile manner when confined with steel-belted scrap tires, developing lateral drifts comparable to those expected in columns confined with conventional transverse steel reinforcement.

Analyses of columns were also conducted using the computer program COLA, which had been developed for inelastic static analysis of conventionally reinforced concrete columns. The analytical moment-displacement relationships were compared favourably with hysteretic moment-displacement relationships obtained experimentally. The comparisons indicate that the analytical models and techniques commonly used for conventional reinforced concrete columns can also be used for tire-reinforced concrete columns. Flexural capacities recorded experimentally agreed well with those computed on the basis of the current design practice.

It was shown both experimentally and analytically that steel-belted tires can be used effectively to confine concrete in reinforced concrete columns. This new approach eliminates many of the construction difficulties involved in building seismic resistant concrete columns, while protecting steel against corrosion.

Acknowledgments

First of all, thanks to Almighty God for giving me the opportunity, courage, strength and support to undertake this research. The author wishes to express his sincere appreciation and gratitude to his thesis supervisors, Dr. Murat Saatcioglu and Dr. Vinod K. Garga for their continued guidance, advice, encouragement, and stimulating discussions during the period in which this study was carried out. Their inspiring ideas and positive feedback have been invaluable for the progress of research.

Technical supports, suggestions and help received from Mr. Richard Moore during the constructions of column specimens, which went far beyond his duties as the laboratory technician, are highly appreciated. Many thanks to Dr. Mongi Grira for his assistance in constructing and testing the specimens. Thanks are also extended to the technical staff of the Civil Engineering Department and the technical staff at the Machine Shop for their services and help in constructing the specimens.

My sincere appreciation and thanks are extended to my mother and my family for their patience, advice, support, encouragement and continuous prayer. Not least of all, my wife Awatef and my children Yousif, Mabrouka, and Salsabeal deserve my deepest gratitude for their patience, sacrifice, encouragement, support and continuous prayer throughout the many years of my studies.

Many special thanks are extended to my brothers Abdulla and Hafez for their advice, encouragement and support throughout this research. The encouragement and advice of my father-in-law and mother-in-law are sincerely appreciated and not forgotten.

I also wish to thanks my fellow graduate students friends for their valuable help during this research project, especially Dr. Cem Yalcin, Mr. Derek Mes, Mr. Jule-Anges Infante, and Dr. Vince O'Shaughnessy.

Finally, I am grateful to Derna University, Derna, Libya for awarding me the scholarship to study for the M.A.Sc. degree.

Table of Contents

List of Tables

List of Figures

Notations

d	=	Diameter of circular column section.
F	=	Lateral force acting on the column.
$f'c$	=	Concrete compressive strength obtained from standard cylinder test.
h	=	The cross-section diameter of column.
L	=	Height of column.
M	=	Base moment in column caused by lateral force.
M_c	=	Confined moment.
M_u	=	Unconfined moment.
P	=	Axial force acting on the column.
P_o	=	Concentric axial load capacity of reinforced concrete column.
Δ	=	Lateral displacement.
θ_t	=	Total rotations.
θ_{as}	=	Rotation due to anchorage slip.
θ_f	=	Rotation due to flexure.

CHAPTER 1

INTRODUCTION

1.1 General

In seismic applications, lack of column ductility is a source of concern among Structural Engineers. Many structural failures during earthquakes were attributed to poor column behavior in the inelastic range. It is therefore recommended to design columns of structures to withstand large inelastic deformations without a significant strength decay. These deformations take place at the ends of columns, creating critical areas which are sensitive to rapid degradation of strength. Ductility and energy absorption capacities of these critical regions are of paramount importance for seismic resistance of structures.

Ductility of a member is defined as the ability to deform beyond its elastic limit without a significant strength decay. In moment-resisting frame buildings, columns may be the critical lateral load resisting elements. Often, attempts are made to ensure that the columns remain elastic during seismic response, since they are responsible for the overall strength and stability of the entire structure. However, it is usually not possible to prevent yielding and plastic hinging of columns, especially at the first storey level. Concrete columns are particularly susceptible to damage caused by inelasticity, since concrete is a brittle material. Ductility (deformability) of concrete columns can be achieved by suitably confining the plastic hinge regions by transverse reinforcement. This involves confinement of the core concrete. In addition, tension dominant flexural response is promoted to absorb and dissipate seismic induced energy.

Earthquake resistant reinforced concrete columns are typically confined by conventional

hoops, overlapping hoops, crossties and spirals. However, the required reinforcement often creates congestion of column cage, resulting in concrete placement problems. New and innovative approaches to confine concrete columns are always sought, for improved structural performance and ease of construction. Use of steel belted scrap tires may offer the required qualities to confine concrete, though at first instance it appears to be unlikely, in view of the volumetric ratio of transverse steel typically used in conventional columns. The current research project is dedicated to this topic, with the objective and scope discussed in the following sections.

1.2 Research Objectives

The objective of this research program is to explore the possibility of using scrap steel belted tires as transverse confinement reinforcement in circular columns. The objective also includes investigation of the behavior of steel belted tires as transverse reinforcement in circular concrete columns, with the view that similar materials may also be used for structural applications.

1.3 Scope of Research

The scope of this research consists of experimental and analytical investigations, and includes the following steps:

- Review of previous research on experimental investigation of column confinement under simulated seismic loading.
- Design of six full-scale circular columns with conventional longitudinal reinforcement and tires as transverse reinforcement.
- Design and construction of an experimental set-up suitable for testing large-scale columns under constant axial load and incrementally increasing lateral load reversals.

- Design, construction and instrumentation of steel reinforced concrete footings for column specimens.
- Construction and instrumentation of six full-size reinforced concrete columns for testing under simulated seismic loading.
- Testing all six columns under combined axial compression and incrementally increasing lateral deformation reversals, while recording the relevant test data by means of two data acquisition systems.
- Evaluation of test data, and investigation of the effects of test parameters.
- Analytical predictions of column behavior and computation of inelastic force-displacement relationships for comparison with experimental results.
- Generation of design recommendation for circular columns confined with scrap tires.
- Preparation of thesis and presentation of results.

1.4 Previous Research on Column Confinement

Confinement of reinforced concrete columns with scrap tires is a new concept, with no reported previous research in the literature. The research reported in the literature on use of scrap tires as a reinforcement material is limited to geotechnical engineering applications. There is no data available on structural engineering applications with the exception of using tire chips in concrete (Eldin and Senouci 1993). Therefore, only a review of column confinement by conventional steel reinforcement has been reported in this chapter.

Many structural failures during earthquakes were attributed by previous researchers to poor column behavior in the inelastic range. The mechanism of concrete confinement was discussed by Razvi (1995), and explained that lateral reinforcement reduces the internal cracking associated with lateral expansion of concrete under axial compression. The main variables affecting concrete confinement have been established by previous researchers. These include spacing of confinement reinforcement, concrete strength and type, percentage and distribution of longitudinal reinforcement, tie arrangement, rate of loading, level of axial compression, size

and section geometry, and the volumetric ratio or ratio of lateral steel volume to the volume of concrete core. The following literature survey on column confinement highlights the current state-of-the-art on column confinement.

Chan (1955), Roy and Sozen (1964), and Kent and Park (1971), conducted experimental investigations to study the behavior of confined concrete. They proposed analytical models to describe stress-strain relationships for confined concrete. The main variables considered in these investigation were the spacing and amount of lateral reinforcement, strength, cross-sectional size and shape, and the rate of loading. Before 1975, researchers did not consider the distribution of longitudinal reinforcement and the tie arrangement as confinement parameter (Bresler and Gilbert 1961, Pfister 1964, Hudson 1966, Somes 1970, Burdette and Hilsdorf 1971).

Sheikh and Uzumeri at the University of Toronto(1980), tested twenty-four tied columns under monotonic axial compression. The specimens had a square cross-section, with 305 mm sectional dimension and 1960 mm high. Column reinforcement included four different tie configurations and eight to sixteen longitudinal bars. The main variables considered in this investigation were tie arrangement, volumetric ratio, spacing and characteristics of lateral steel, and distribution and amount of longitudinal steel around the core perimeter. From this investigation, it was concluded:

- Strength and ductility were improved by increasing the amount of lateral steel.
- The amount of longitudinal steel, within the range of 1.7% to 3.7%, had small effect on concrete confinement.
- The strength of concrete increased up to 70%, and significant improvement in ductility was observed when confined with rectangular ties and well distributed longitudinal steel.
- Enhancement of strength and ductility was observed when tie spacing was reduced, even if the same volumetric ratio was used.

Scott, Park and Priestley (1982), at the University of Canterbury in New Zealand tested twenty-five square columns under high and low strain rates. The cross-sectional dimension was 450 mm and the column heigh was 1200 mm. Each column contained either eight or twelve longitudinal steel bars and different arrangements of square or octagonal steel hoops. The variables considered were the effect of longitudinal steel distribution on enhancement of concrete strength and ductility. The following conclusions were reported from this investigation:

- By increasing the amount of lateral reinforcement, the peak stress for concrete core increased and the slope of falling branch of the stress-strain relationship for concrete core decreased.
- By increasing the spacing of lateral reinforcement, the confinement efficiency for the same amount of lateral reinforcement decreased.
- Concrete showed significant improvement in compressive strength by proper confinement.
- Increasing the number of longitudinal reinforcing bars, while maintaining a constant longitudinal reinforcement area, showed a good improvement in confinement. This was shown by reducing the longitudinal bar spacing.

Fafitis and Shah (1985), developed simple equations to predict the stress-strain relationship of confined concrete. By using these equations they compared the predicted behavior of confined columns with the available experimental data. Distribution of longitudinal steel, tie spacing and tie configuration were not included in their equation.

Ozcebe and Saatcioglu (1987, 1989), tested sixteen full size columns with different confinement configurations under constant axial compression and incrementally increasing lateral load reversals. All columns were tested under 600 kN of constant compressive axial load. The specimens had 350 mm square cross sections, and 900 mm high. The main variables considered in this investigation were the effectiveness of arrangement, spacing and volumetric ratio on concrete confinement. It was concluded that inelastic response of columns

improved very significantly by proper confinement of core concrete. Crossties supporting the longitudinal bars had high efficiency in providing proper confinement only if they were properly supported by lateral reinforcement.

Mander, Priestley and Park (1988 a), tested thirty-one circular, rectangular and square columns with different arrangement of reinforcement under low and high strain rates, with different volumetric ratios and spacings of confinement reinforcement. The strength increased due to the increase in the volumetric ratio of confinement reinforcement.

Razvi and Saatcioglu (1989 a and b), tested thirty-four small scale columns confined with different combinations of welded-wire fabric as confinement reinforcement under monotonic axial compression. The results of this investigation showed a significant improvement in strength and ductility of columns. This indicated that welded-wire fabric could be effective in confining the core concrete.

Saatcioglu and Razvi (1992), developed an analytical model for confined concrete. The model was compared with different shapes of cross sections and different confinement configurations (spirals, cross ties, welded wire fabric, and rectilinear hoops). This model was used to produce good predictions of concrete behavior under concentric and eccentric loadings, as well as slow and fast strain rates.

Sheikh and Khoury (1993), tested six square columns under cyclic lateral loading accompanied by simultaneously applied axial compression. The cross-sectional dimension was 305 mm, and the column height was 1473 mm. The columns were cast integrally with a stub. The main variables in this investigation were level of axial load, amount of lateral steel, configurations of lateral steel, and the stub effect. The researchers concluded that the increase in the amount of lateral steel, the effectiveness of confinement reinforcement, and reduction in axial load, increases the ductility and energy-absorbing capacity of the columns.

It was also observed that the stub effect was to enhance the strength of the adjacent section by 20%.

Sheikh and Khoury (1997), reviewed the confinement of the ACI Code provisions which based on the available experimental data. They proposed a new design approach in which the amount of lateral steel required is a function of the column ductility performance. They concluded that the proposed equation produced good agreement with the test data when applied to realistically-sized specimens.

Also a number of experimental programs were conducted on confined concrete columns by other researchers (Kent and Park, 1971, Park, Priestley and Gill 1982, Sheikh and Uzumeri, 1982, Sheikh and Yeh 1986, Lipien 1995, Saatcioglu et al. 1995, Baingo 1996, and Grira 1998). The results obtained from these research programs led to similar conclusions as before.

In summary, concrete columns can be confined to behave in a ductile manner. The most significant parameters of confinement are the amount, spacing and arrangement of transverse reinforcement. Axial compression decreases column deformabilty. Furthermore, column deformability decreases with increasing concrete strength. In light of these conclusions, it was felt that steel belted tires would be a good candidate as a new and innovative waste material to be used for concrete confinement.

CHAPTER 2

Properties of Tires as Civil Engineering Material

2.1 Introduction

There has been a growing concern over the past twenty years regarding the volume of waste products requiring disposal. Disposal of the scrap tires is a growing issue, since the accumulation of discarded automobile tires causes environmental, fire, and health hazards worldwide. They contribute to the problem of pollution when burned to dispose, as shown in Fig. 2.1. Waste tires require large space for storage, due to their shape, quantity, compaction resistance, and they are non-biodegradable. The mechanical properties of the tires remain available even after their ordinary life as a car wheel element has expired (O'Shaughnessy 1997).

In the United States, it is estimated that more than 200 million automobile tires and 40 million truck tires are discarded every year (Williams 1987). In the same country, more than 250 million tires are scrapped each year (South Carolina Department of Health and Environmental Control Office of Solid Waste Reduction and Recycling 1999). That's the equivalent of almost one tire for every man, woman and child in the country. Only in the State of Iowa alone 3 million waste tires are generated each year. Also, in South Carolina, the law now prohibits the storage of scrap tires without a permit, and it is illegal to dispose off whole tires in county or public landfills. In France, more than 450,000 tones of old tires are thrown away every year. Only 150,000 - 200,000 tones are recycled in one form or another (Long 1990). In the UK, 25-30 million tires are disposed every year. All these numbers indicate that scrap tires are a major problem on an international scale.

There are several methods used for tire disposal. For instance, putting the scrap tires in stockpiles as shown in Fig. 2.2, burying them or dumping in landfills, retreading, reclamation, burning, shredding, and reusing them for other purposes such as boat fenders, children swing etc., and many of these methods require large disposal areas. Only 25 % or fewer are used as fuel or as raw materials for manufacturing rubber goods. The province of Ontario generates more than 10 million passenger tires per year. Forty percent are disposed in tire stockpiles or landfills (O'Shaughnessy 1997).

Dumping scrap tires in landfills create problems in land use. Retreading is not a solution because the tire still has to be disposed. Furthermore, only a few tires with good sidewalls can be retreaded. Reclamation is a very limited use because only a low grade rubber can be obtained. New tires can only contain up to 5% reclaimed rubber. Tire shredding costs about $1 per tire, and can be expensive because it requires special equipment. The stockpile method is not desirable since it adds a significant pressure to the environment by providing a good breeding habitat for disease-carrying insects and vermin (O'Shaughnessy 1997). Inappropriate storage can cause a potential fire hazard which results in serious environmental damage and high cleanup cost. Tire combustion as a source of energy was discouraged in the past due to the emission of sulfur, a major precursor to "acid rain", and heavy metals and/or their oxides. Now, however, processes are being developed to remove the metals and sulfur to yield a clean-burning, environment-friendly hydrocarbon (Iowa's Waste Tire Collection Program; Iowa City / Coralville Area, 1998). Therefore, tire combustion is not a good idea either. Burying scrap tires in landfills is waste to the land and costly.

To offset added disposal costs and to deter customers from bringing in tires, many landfills are currently charging $2 per tire for accepting whole tires ("Scrap" 1988). Some stores in Ontario are charging customer $5 per tire for accepting hole tires which is costly. All these methods are wasteful and costly, and require large disposal areas, and combined with various problems. However, scrap tires are abundant, and may be utilized economically as a civil engineering material, if the mechanical properties of the material are found to be of adequate

quality for the application involved. One such application, considered in this research program, is the use of tires as a construction material, specifically in building and bridge construction as column transverse reinforcement and formwork. Hence, the properties of tires examined and discussed in this chapter, should be viewed with this application in mind.

2.2 Tire Types and Constituents

There are four major categories of tires used in the world. Passenger, truck, farm, and off-road tires. The passenger tires form the most common type, representing 80% of the market (Deese et al 1981). Passenger tires come in rim sizes of 12 to 15 inches (305 mm to 381 mm) and truck tires come in rim sizes of 15 to 16 inches (381 mm to 406 mm) for lightweight vehicles, and 15 to 24 inches (381 mm to 610 mm) for heavyweight vehicles. They weigh approximately 10 kg, 13.5 to 27 kg, and 41 to 91 kg, respectively. The average weight of steel used for a passenger tire is 0.7 kg per tire.

There are three types of passenger tire; radial, bias-ply, and bias-belted. The most common one is the radial tire. The physical tire constituents consist of fabric, bed wire, and rubber compound. Radial tires are fabricated with vulcanized rubber that contains reinforcing textile cords, high-strength steel wire reinforcing bead, and high-strength steel. The major tire components by weight are given in Table 2.1.

The main chemical components for tire rubber are given in Table 2.2. The most commonly used tire rubber is styrene-butadiene-copolymer (SBR), containing about 25% styrene. Other tire rubbers used are cis-polybutadiene, natural rubbers (cis-polyisoprene), and synthetic cis-polyisoprene (O'Shaughnessy 1997). Carbon black is added to strengthen rubber and increase abrasion resistance. Other constituent materials are also used for specific functions. Extender oil, which is a mixture of aromatic hydrocarbons, is used to increase the workability of the rubber while also softening it. Sulphur is used to harden the rubber by cross-linking the polymer chains within the rubber to prevent deformations at high temperature

(O'Shaughnessy 1997). Zinc oxide, stearic acid and organo-sulphure accelerator are used to aid in the vulcanization process and also to enhance the physical properties of rubber (Williams et al. 1990).

Tires consist of three major parts; tread, two sidewalls, and two rims. These components are presented in Fig. 2.3. The tread is the important part which contains a number of strong cords coated with rubber. The steel belt or cord under the tread of radial tires and rims contains high-tensile steel, which contains a high percentage of carbon. The steel in the tread and rim are well protected by a rubber coating. Figure 2.4 shows a typical cross-sectional view of a tire. These cords have a very high tensile strength of up to approximately 2000 MPa to 2500 MPa at ultimate. The different components of a radial tire are shown in Fig. 2.5.

According to the information obtained from a steel manufacture, typical cord diameters used consist of 0.25,0.22, 0.28,0.30, and 0.32 mm. Each cord contains four wires. The diameter for each wire is 0.25 mm, resulting 0.048 mm^2 area. This means that the area of each cord is; 4 x 0.048 = 0.192 mm^2/ cord. Some manufactures put three to four wires per cord, while others may put up to 10 wires per cord. However, the majority places four wires in each cord. The number of cords per tire in the tread varies among different companies. Some common figures are 14, 15, 17, 20, and 22 cords per inch (25.4 mm). The average weight of steel used in passenger tires is 0.7 kg/tire (1.54lb/tire). The tire reinforcement used in this research program consists of scrap tires, either as whole tire (sidewalls and a tread) or with the sidewalls removed (tread), stacked together on top of each other or tied together continuously to resist lateral pressure due to concrete expansion.

2.3 Tires as a Civil Engineering Material

Old tires have excellent mechanical properties as a waste material, and are readily available in large quantities. Dealers and garages can supply them free of charge to construction sites, except for the cost of transportation. Scrap tires can be an excellent substitute for expensive

civil engineering materials. Scrap tires have been used successfully as reinforcement for several years in many countries (O'Shaughnessy 1997). There are many applications of scrap tires in civil engineering, such as lightweight fill for retaining walls, highway crash barriers, insulated layers in roadways, drainage material, road subgrade, reinforcement for slopes, river protection, sound barriers, energy dissipators, artificial reefs, breakwaters, source of energy, and rubberized asphalt. Tires are used in civil engineering projects according to their material characteristics (WYMCC 1977), which are highlighted below.

Durability: Tires are non-biodegradable. There are some tires in museums that are as much as eighty years old. The deterioration of an old tire is usually caused by the effects of sunlight and water. However, recent tires contain antioxidants and other additives to prevent deterioration. When tires are not used for transport purposes, chemists advised that the life of most tires would be of at least 100 years (O'Shaughnessy 1997). AB-Malek and Stevenson (1986) studied the physical condition of vulcanized rubber submerged in 24 m of sea water for a period of 42 years. Their investigation showed that no serious deterioration of the rubber had occurred.

High Radial Strength: Tires can resist very large tensile forces due to their circular geometry which enables them to develop hoop tension. Hence, they may be used as transverse reinforcement in concrete building and bridge columns. When used to confine concrete against lateral expansion, caused by transverse strains, they may have the required ability to resist lateral pressure. This characteristics forms the objective of the current study.

Handling and Transportation: Handling tires is easy and can be done by traditional construction equipment and labor. Tires can be easily transported to the site in loads from 600 to 1000 tires per truck. Off loading of the tires can be readily accomplished by one worker.

Economy and Availability: Scrap tires, as waste material, are readily available and may be supplied to construction site free of charge, except for transportation costs.

Flexibility and Extensibility: Tires are able to extend and deform without cracking. They are very flexible and able to deform more than most other materials.

There are several applications in which tires could be used as a structural media, while utilizing the properties highlighted above. These are listed below:

- Sea defense
- Crash barriers
- Noise barriers
- Land terracing
- Bridge abutments
- Gravity retaining walls
- Facing for reinforced earth walls
- Screening mounds for solid waste disposal units
- Enabling embankments to be built with steeper side slopes
- Enabling embankments to take tension within base layers which is very important for embankments on poor ground

2.4 Previous Research on Using Scrap Tires in Civil Engineering Applications

Engineers and researchers are interested in civil engineering materials that are more economical but otherwise comparable to existing materials. Scrap tires have received wide acceptance for a variety of applications as soil reinforcement in geotechnical engineering. The American experience showed that construction of reinforced earth structures using scrap tires can provide an alternative solution to many geotechnical problems. Tire structures have been achieved in many countries like Brazil, France, Germany, Switzerland, and United States, at lower costs than those that involved conventional techniques for reinforcement.

In France, research on the use of scrap tires in geotechnical engineering to reinforce soils or earth structures for improved mechanical properties of soils, started in 1976 . In 1990 Long reported a number of applications involving the use of scrap tires. A retaining wall, 54 m

length and 5 m height, was constructed at Fertrupt (1984) in France, utilizing scrap tires. Energy absorption structure was constructed at La Grave (1984) with a length of 120 m, and a thickness of 1 m, to prevent avalanches or rock slides. More than 250 tire-reinforced soil structures were constructed in France in 1993. Twelve structures have been constructed in Algeria by using scrap tires to reinforce soils.

One of the first practical applications in the United States, using discarded tires, was the repair of a hill side fill slip along Calif-236, north of Santa-Cruz, built in mid 1970s (Forsyth and Egan 1976). In South Carolina, they add up to almost 3.5 million tires each year. Research in the States also concentrated on the use of shredded tires as a form of a lightweight fill in roads and retaining wall construction (Giesler et al. 1989, Eldin and Senouci 1992, and Drescher and Newcomb 1994). The results published by Giesler et al. 1989, Eldin and Senouci 1992, Drescher and Newcomb 1994, Humphrey and Eaton 1995 indicate that the shredded tires increase the shear strength of soils. Shredded tires produce a lightweight fill that reduces settlements up to 50% and increase the stability of the road embankment. Shredded tires do not present any major handling and placement problems in road construction, and also have good thermal properties. According to Drescher and Newcomb 1994, many other tire projects have been undertaken in California. They used scrap truck tires to control shoulder erosion of an embankment on Rout 32, in Tehama County.

The Minnesota Department of Natural Resources studied the use of automobile tires as reinforcement to determine if roads constructed over highly compressible soils in Saint-Louis County could improve the subgrade performance (Drescher and Newcomb 1994). The settlements were reported to be less than those expected from a conventional soil embankment without the reinforcement. Also, on State Route 111, near Palm Springs, they used automobile tire piles and tied tire walls to supply temporary barriers against wind blown sand.

In United Kingdom, the first project using scarp tires was the construction of an experimental

gravity wall at the mechanical engineering services at Lofthouse in West Yorkshire Metropolitan County Council (WYMCC 1977). The heigh of the tire wall was 3.7 m and the length of the structure, with 4500 tires, was 45 m with an average tire layer thickness of 0.15m. Whole passenger tires were used, ranging from R-13 to R-15 (radius of the tire rim in inches) with corresponding tire widths varying from 125 to 200 mm. It was observed that the effective interlock at the face of the tire wall was difficult for slopes steeper than 1 to 1. The cost of this project was estimated to be approximately one quarter the cost of a similar traditional retaining wall. In 1982 Dalton and Hoban reported another tire wall that was constructed in England.

Eldin and Senouci (1993), performed an experimental study to examine the potential of using tire chips and crumb rubber as aggregate in Portland-cement concrete. They used different amounts of rubber-tire particles of several sizes as aggregate to examine strength and toughness properties of concrete. More than 200 (150 mm in diameter x 300 mm high) concrete cylinders were tested. Their results showed that the concrete mixtures presented lower compressive and splitting-tensile strengths than did normal concrete. These mixtures also demonstrated a ductile plastic failure, and had the ability to absorb a large amount of plastic energy under both compression and tension. The researchers suggested the use of rubber aggregates for the following applications:

- Architectural applications such as nailing concrete, stone backing, false facades, and interior construction because of its light unit weight.
- Low-strength concrete applications such as sidewalks, and driveways.
- Crash barriers around bridges because of their high ability to absorb plastic energy.

Garga and O'Shaughnessy (1997) constructed a test embankment, reinforced with scrap tires. The tires were used either as whole tires, or with one sidewall removed. In the reinforced fill section, tires were tied together as a mat, followed by a compacted backfill layer of soil, 0.3m thick, followed by the next layer of the tire mat. Tires were stacked on top of each other in a staggered manner. To assess the load deformation behavior of the composite materials,

three large plate loading tests were performed on the surface of the completed test fill. They concluded that this embankment proved the practical feasibility of using scrap tires as soil reinforcement technique for tire reinforced slopes and tire reinforced gravity retaining walls.

Table 2.1 : Tire Constituents by Weight (Humpstone et al. 1972)

Tire Constituents	Weight (kg)	Weight (%)
Fabric	1.41	10
Bead Wire	0.46	4
Rubber Compound	9.80	86
Total	11.67	100

Table 2.2 : Typical Composition of Tire Rubber (Williams et al. 1990)

Component	Weight (kg)	Weight (%)
Rubber Polymer (SBR)	6.088	62.1
Carbon Black	3.039	31.0
Extender Oil	0.186	1.9
Zinc Oxide	0.186	1.9
Stearic Acid	0.118	1.2
Sulphur	0.107	1.1
Accelerator	0.069	0.7
Total	≅ 9.80	99.9

Figure 2.1: Burning the Tire in Open Air

Figure 2.2 : Scrap Tires in Stockpiles

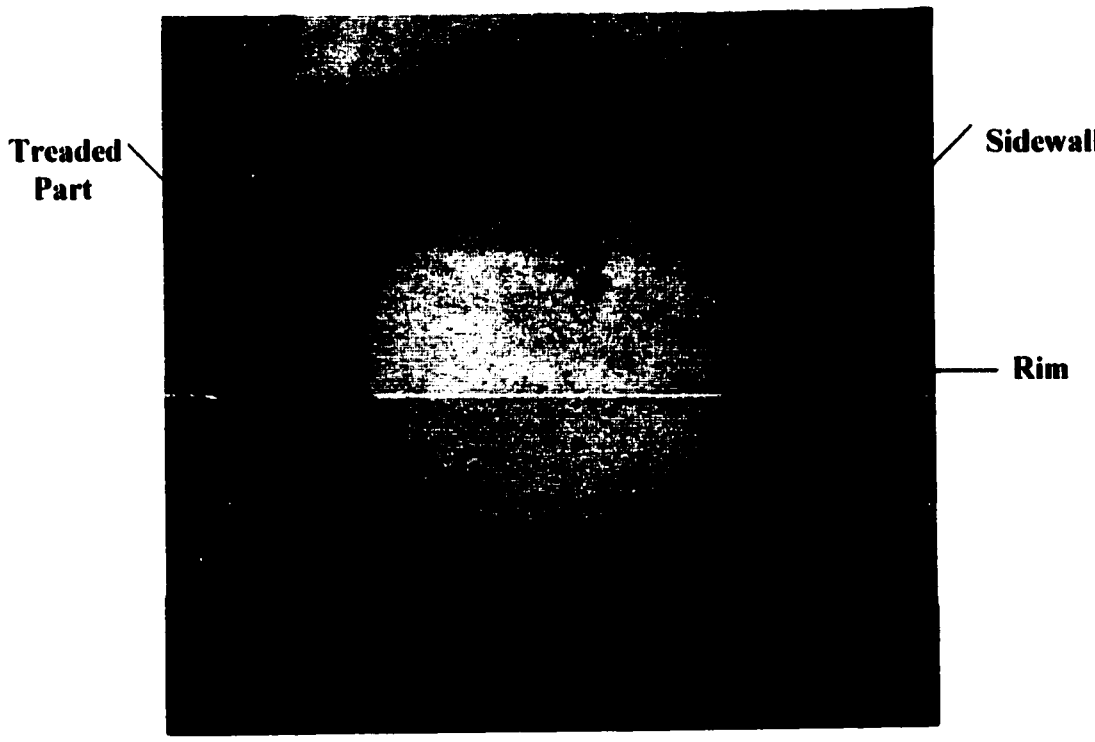

Figure 2.3 : The Components of the Tire

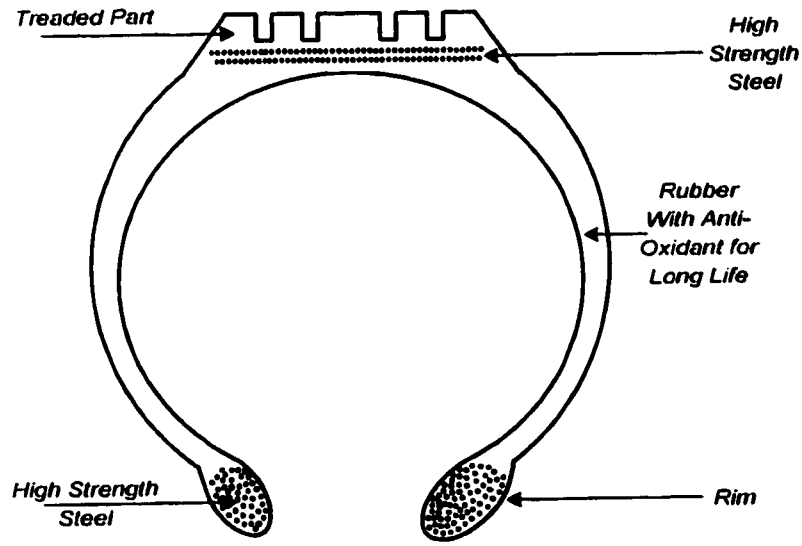

Figure 2.4 : Tire Construction

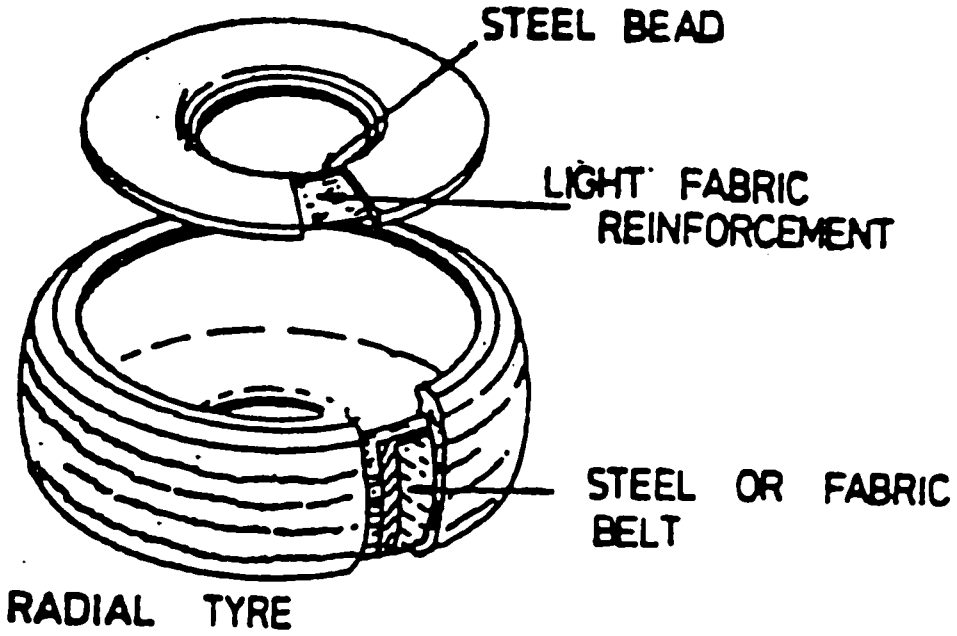

Figure 2.5 : The Different Components of A radial Tire

CHAPTER 3

Experimental Program

3.1 General

The experimental program was designed to investigate the effectiveness of scrap steel belted tires as transverse confinement reinforcement in circular columns. The test program involved construction and testing of six circular columns under axial compression and lateral load reversals. Tires were used in whole or in part (treaded part) to provide confinement to the column. Passenger tires with 13-inch (330 mm) rim diameter (Size 13) were used in all columns. The main test parameter was the arrangement of reinforcement, consisting of conventional longitudinal bars and steel belted tires as transverse reinforcement. The construction of test specimens, material properties and instrumentation are described in this chapter, as well as the test set up, and test procedure. The test results, observed behavior and evaluation of data are discussed in Chapter 4.

3.2 Description of Test Specimens

Six circular full-scale column specimens were designed, built and tested. An important consideration in column design was the use of a realistic column size that would also permit the use of one of the standard sizes of scrap tires, while being representative of the columns used in practice. This would eliminate potential size effects. The column specimens represented part of a first story column or a bridge column between the footing and inflection point. Each specimen consisted of a column and a footing. The specimens were labelled as TC-1 through TC-6. The cross-section of each column was 545 mm in diameter except TC-3 and TC-4 which had 600 mm diameter. The column height was 2000 mm measured from the

column-footing interface to the point of inflection. The lateral load was applied at the point of inflection located 2000 mm from the column-footing interface (shear span = 2000mm). This height included 1725 mm of concrete column and 275 mm of steel loading block. It represented a prototype column with an inter-story height of 4.0 m, which is typical of columns used in practice. Figure 3.1 shows geometric details of column specimens.

Design strength of the concrete used was 30 MPa for all columns. The columns were poured from the same batch of concrete. Each column had a heavily reinforced concrete footing. Control cylinders were cast from the same batch of concrete to monitor strength gain. The 28 day cylinder strength of the concrete used in columns was 36 MPa. It was 38 MPa during the period of column testing. The dimensions of the footing were 1730 mm x 1400 mm x 520 mm. Plywood formwork was prepared for two footings to facilitate casting of two footings at a time. The concrete strength of the footing was 30 MPa after 28 days.

Four plastic (PVC) tubes with an outside diameter of 80.5 mm were placed near the corner of the footing to secure the footing to the laboratory strong floor by four bolts with a diameter of 70 mm and a length of 1800 mm. Eight plastic (PVC) tubes with an inside diameter of 38 mm were placed on the right and left sides of the footing to fix vertical actuators to the top of the footing with eight bolts having a diameter of 38 mm.

All longitudinal reinforcement of the column specimens consisted of twelve 19.5 mm diameter (No. 20) deformed bars, with an average yield strength of 453 MPa. The longitudinal reinforcement ratio for TC-1, TC-2, TC-5, and TC-6 was 1.54%, for TC-3 and TC-4 it was 1.27%. The longitudinal bars extended 405 mm into the footing and were bent to form 90 degree hooks. The hook extension was 500 mm, which conformed to the development length requirement of CSA standard A23.3-1994. Each column had eight Grade 8, 19 mm diameter bolts embedded in the concrete at the top of the column, vertically protruding to facilitate the attachment of the loading beam to the top of the column. The columns did not have any concrete cover for protection purposes, since they were enclosed by steel belted tires, which

were exposed and functioned as transverse confinement reinforcement, although the longitudinal reinforcement had some concrete cover inside the tires. This is illustrated in Figs. 3.2, 3.4 and 3.6.

Three different arrangements of tires were used as confinement reinforcement. These arrangements of tires allowed the investigation of different parameters of confinement on column behavior. Passenger tires with size 13 (13 inch rim diameter) were used in this investigation. In the first pair of columns, steel was placed inside the sidewalls of the tire by punching through the sidewalls; these were labelled TC-1 and TC-2. In the second pair, the column was confined with the treaded part only, having removed both sidewalls; these were labelled TC-3 and TC-4. The third pair of columns had the longitudinal reinforcement placed inside the rim; these were labelled TC-5 and TC-6.

All columns were confined with tires only, except for the second pair (TC-3 and TC-4), which also had individual circular hoops at a spacing of 275 mm, (which was the radius of the cross section). The circular hoops used were 11.3 mm diameter (No.10) deformed bars, with a yield strength of 407 MPa. The properties of tire reinforcement are discussed in details in subsequent sections. The design variables considered in the test program included the arrangement of longitudinal reinforcement inside the tire and the level of axial load. Figures 3.2 through 3.5 show the photographs and general details of reinforcement cages for column specimens, including the tire confinement, for TC-1 thorough TC-4. Figures 3.6 and 3.7 show the general details of reinforcement cages and tire confinement used in TC-5 and TC-6.

3.3 *Material Properties*

3.3.1 *Properties of Concrete*

The same batch of concrete was used to cast all columns. The concrete was of normal weight, with 100-mm slump, ordinary Portland cement (ASTM Type I), natural sand, and 20-mm maximum size aggregate. The mix was designed to obtain a target strength of 30 MPa.

A total of 30 standard cylinders (152 x 305-mm) were cast along with the columns, to establish concrete strength. All cylinders were capped with sulphur compound to ensure uniform application of load. Strength-age relationship for concrete was developed by performing standard cylinder tests at frequent intervals. Cylinders were tested after 7, 14, 28 days, and the time of column tests. Table 3.1 illustrates the strength development of test specimens with respect to time. The average of at least three cylinders was used at each interval to define these relationships. These relationships were used to determine compressive strength f'c for all the specimens. The strain data was obtained from displacement measurements provided by extensometer. The instrumentation and testing of standard cylinders are presented in Fig 3.8. The strength gain over time and the stress-strain relationship of concrete are shown in Figures 3.9 and 3.10. The cylinders were tested by a Forney testing machine.

3.3.2 *Properties of Longitudinal and Transverse Deformed Steel Reinforcement*

All longitudinal and transverse reinforcements were ordered from a local supplier. The longitudinal reinforcement for all column specimens consisted of twelve 19.5 mm diameter (No. 20) deformed bars. Transverse hoops were used only in TC-3 and TC-4, and consisted of 11.3 mm diameter (No. 10) deformed bars. Three randomly selected coupons were tested

to establish the stress-strain relationships of #20 and #10 bars. The average yield strengths for longitudinal and transverse reinforcements were 453 MPa and 407 MPa, respectively. Figures 3.11 and 3.12 show the stress-strain relationships for deformed bars used in columns.

3.3.3 Properties of Steel-Belted Tires

Scrap steel belted tires were used as transverse confinement reinforcement in all columns. Although three different brand names of tires were used in the investigation, it was made sure that the tires in critical regions, consisting of the bottom six tires in each pair, were of identical brand and type to ensure consistency. For the first and second pair (TC-1, TC-2, TC-3, and TC-4) Motomaster tires were used, while for the last pair (TC-5 and TC-6) Michelin tires were used. From the seventh tire until the top end of the column, different brand names of same size tires were used. In the absence of a standard test for tires, three coupons were prepared and tested in tension for each brand name. Tests of these coupons provided stress-strain relationships for each type of tire. As well, three randomly chosen coupons from other brand names were also tested. Figure 3.13 shows the general geometry and dimensions of tire coupons tested.

The tire coupons were taken from the treaded part of the tire, which consisted of a number of strong steel cords coated with rubber of different brand names. The diameter of the cord per tire varied in size and was 0.22, 0.25, 0.28, 0.30, and 0.32 mm. Every cord contains four wires. The diameter for each wire was 0.25 mm, giving an area of 0.049 mm^2, which resulted in an area of $4 \times 0.049 = 0.196$ mm^2 for each cord. Some manufactures put three or four wires per cord, and others put up to 10 wires per cord. The majority, however, used four wires per cord. The brand names of tires which were tested or used in this investigation had four wires per cord. The numbers of cords per tire in the treaded part varied among the brand names. The numbers were 14, 15, 17, 20, and 22 cords per inch (25.4 mm). Motomaster tires, used in this investigation, had 17 cords per inch. Michelin tires, also used in the current investigation, had 17 cords per inch (25.4 mm). The average of at least three coupons per

brand name were tested in direct tension to define the stress-strain relationships. The average strength at which the steel cord in the tire ruptured was 1905 MPa for Motomaster tire (used in TC-1 through TC-4), 2000 MPa for Michelin (used in TC-5 and TC-6) and 2140 MPa for other random coupons (consisting of Goodyear, Bridgestone and Yokohama).

The stress-strain relationships for type I (Motomaster), type II (Michelin), and other brand names (random, consisting of Goodyear, Bridgestone and Yokohama), obtained by standard coupons tests, are shown in Figs. 3.14 through 3.16. Table 3.2 illustrates the average strength of different coupons. Strain data was established from displacement measurements obtained by extensometers with a 51 mm gage length. The coupon tests were conducted using a Tinius Olsen Universal Testing machine. Figures 3.17 and 3.18 show general views of test setup and typical failure of a tire coupon.

3.4 Preparation of Test Specimens

3.4.1 Construction of Columns

The construction of all test specimens was done at the Structures Laboratory of the University of Ottawa in five phases; i) the assembly of steel reinforcement cages for footings and columns, ii) installation of strain gauges for longitudinal reinforcement and circular hoops if any, iii) installation of strain gauges on the tread and rim of tires, iv) Drilling holes through sidewalls of tires used for the first pair, and cutting of the sidewalls for the second pair, v) construction of formwork for footings and columns, and vi) casting of footings, two at a time, and subsequently casting of all columns at once.

Three different arrangements of tire configurations were used as confinement reinforcement, as discussed previously. The details of tire arrangements, including the longitudinal reinforcement are described in the following section. The columns were prepared in identical pairs, for testing under two different levels of axial compression.

Strain gauges for longitudinal reinforcement and hoops were installed at predetermined locations and the necessary wiring was soldered to gauge terminals prior to cage assembly. Strain gauges for tires were installed after the footing was cast. The details of strain gauge locations are described in Section 3.5. The assembly of steel cages was executed in stages. First the footing cages were built without some of the top bars, then the longitudinal column bars were secured in the center of the footing, then the remaining footing reinforcement was built around and through the column cage.

A plywood formwork was prepared for two footings, and reused for the second and third pairs. The formwork was held together by a combination of screws at the joints and triangular pieces of plywood were placed all around the formwork to give lateral support. To prevent warping and bulging of the formwork due to lateral concrete pressure, threaded rods and nuts were used to tie the sides of the formwork. The steel cages for footing were placed in formwork with the aid of a laboratory crane, after that the PVC tubes were fixed in the formwork. The construction process of a typical specimen cage, strain gauges, formwork and placement of reinforcement cages are seen in Figs. 3.19 through 3.22. A total of three batches of concrete were prepared and delivered to the laboratory for casting of footings, by a local ready mix company, with a specified concrete strength of 30 MPa. Concrete was cast in layers and vibrated throughly. Figure 3.23 illustrates the casting of footings.

3.4.2 Assembly of Tires and Reinforcement Cages

Tires in columns were stacked on top of each other in a circular manner. Ten tires per column were used for all specimens. Tires are used in whole or in part (treaded part) to provide confinement to concrete. Passenger tires with a size of 13 inches (P175 / 75 R 13 and P180 / 75 R 13) have been used in this investigation, where P stands for passenger car tires, 175 indicates width of the tire in millimeters, 75 indicates height to width ratio, R stands for radial, and 13 is the diameter of the well, in inches. Tires were supplied to the lab free of charge, except for transportation cost. All tire preparation (cleaning, cutting, drilling holes

and inserting reinforcement) was performed at the Structures Laboratory of the University of Ottawa.

The tires used to build TC-1 and TC-2 were punched in the sidewalls to allow for insertion of longitudinal reinforcement. The holes in the sidewalls were made using a cutter steel tube, fixed into a drill. A special plywood template was manufactured to align the holes, with dowels made of plywood. Both the plywood template and the cutter steel tube were designed and prepared in the laboratory. Figure 3.24 illustrates the general view of the tire template and cutter tube. A series of photographs are included in Fig. 3.25 to show the fabrication of holes in sidewalls using the template and cutter tube. The tires for TC-1 and TC-2 were inserted through longitudinal bars, on top of each other, with longitudinal bars passing through the sidewalls. Figure 3.26 illustrates this procedure. These columns were confined by the steel in treads, covering the entire exterior surface of column, as well as the steel in the tire rim, proving hoops further into the concrete.

Columns TC-3 and TC-4 were confined by the treads only, since the sidewalls had been cut off, including the steel in the rims. These columns also had conventional hoop steel tied to the longitudinal reinforcement. These hoops were made of 11.3 mm diameter (No. 10) deformed reinforcement with overlapping ends, and were placed at 275 mm spacing, with the first hoop located at 135 mm from the column-footing interface. The sidewalls were removed in the lab, using a jigsaw, as shown in Fig. 3.27. In this pair of columns, 35 mm plastic spacers were used to keep the spacing between the tire treads and the steel cage. This was necessary to maintain the alignment of tires on top of each other, as this application resulted in a flexible rubber shell, once the sidewalls were removed. Stacking tires on top of each other was very difficult to maintain. The tires were tied along their top edges to the longitudinal reinforcement, to keep them stacked in a circular manner. Figure 3.28 illustrates the steps involved in putting together the steel-tire assembly used in TC-3 and TC-4.

Columns TC-5 and TC-6 had whole tires used, placed on top of each other, with longitudinal

reinforcement placed inside the rim. Figure 3.29 depicts the procedure of positioning the tires and the longitudinal reinforcement. This arrangement allowed both the rims and the treads provide confinement to concrete, while the rims would also provide support to the longitudinal bars against buckling. The main disadvantage of this arrangement was the reduction in the interior lever arm and associated reduction in moment capacity. Small holes were drilled in the sidewalls, to release air and to avoid concrete placement problems during casting.

Formwork for all columns consisted of 24-inch (610 mm) diameter sona tubes. Sona tubes were tied with ropes to the footing from four sides, to stabilize the cage. A batch of concrete was prepared and delivered to the laboratory by a local ready mix company, with a specified strength of 30 MPa, for casting of all the columns at once. The slump of concrete was approximately 100 mm. A team of students was available to aid in casting. Concrete was cast in layers and vibrated thoroughly to ensure proper placement. The photographs included in Fig. 3.30 show column specimens before and after casting. Figure 3.31 shows cleaned specimens ready for testing.

3.5 Instrumentation

Two types of strain gauges were used in this investigation. KYOWA strain gauges, model KFG-10-120-C1-11 with a gauge length of 10 mm were used on longitudinal reinforcement, and SR-4 strain gauges, model FAE-25-35-PET with gauge length of 6.35 mm were used for tires. The first type of strain gauge was placed on longitudinal reinforcement of all columns, as well as the ties of TC-3 and TC-4. The specimens were also instrumented with transducers to measure lateral displacements and rotations of the hinging region. The loads were measured by means of the load cells contained in MTS actuators.

Strain gauges were placed on tires to measure lateral pressure on treads as rims. The locations of these strain gauges varied depending on the specimen. The data were recorded

using a Vishey data acquisition system, which was connected to a Pentium personnel computer 166 MHz, and an MTS controller connected to a second personnel computer, Dell model 486/MXV. The Vishey data acquisition system consisted of two scanners of model 5520. Figure 3.32 illustrates the schematic network diagram, data acquisition system, and MTS controller device.

All columns had six strain gauges attached to two extreme longitudinal bars, three gauges on each side (east and west), except for TC-3 and TC-4, which had extra six strain gauges attached to the first three ties from the column-footing interface. Two gauges were placed on longitudinal bars at column-footing interface (one in east and one in west). Additional two gauges were placed at 135 above the column-footing interface, while two others were placed at 135 mm below the column-footing interface. The data obtained from these six strain gauges were used to obtain strain profiles in longitudinal reinforcement, which indicated yield penetration into the footing. Figure 3.33 illustrates the gauge locations. The tie steel in TC-3 and TC-4 had strain gauges, beginning at 135 mm above the column-footing interface, continuing on to the next two hoops with a 275 mm interval. Figure 3.34 shows strain gauge locations for TC-3 and TC-4.

The first column in each pair had fifteen strain gauges attached to treads and rims of the first three tires, except for the second pair (TC-3 and TC-4), which had twelve strain gauges on the treaded part only, since this pair did not have any side walls (no rim). The gauge locations are shown in Figs. 3.35 and 3.36.

A total of seven LVDTs were used to measure elongations and/or displacements. Six of these transducers were placed vertically to measure total rotations within the assumed hinging region, as well as the anchorage slip rotation that occurs at the end of the column. The LVDTs labeled as 1, 2, 3, and 4, had 51 mm (2 in) stroke. LVDTs 5 and 6 had a stroke of 25.4 mm (1 in). The seventh LVDT was manufactured by Temposonic, and had high precision. This LVDT was used to measure the horizontal displacement of the point of

application of horizontal actuator, 2000 mm above the footing (the shear span of column). The displacement reading was used during the test to impose the pre-determined deformation history. All LVDTs were secured with brackets on six threaded rods that had been cast in column concrete on either side. These three pairs of threaded rods were spaced at 25 mm, 275 mm (h/2), and 550mm (h) above the footing for rotation measurements within respective lengths. LVDTs 1 and 3 were placed to measure the total rotation within the assumed plastic hinge length (550 mm, equal to depth of the cross section). LVDTs 2 and 4 were placed at a distance of 275 mm above the surface, to measure the total rotation within this segment, while LVDTs 5 and 6 were placed only 25 mm above the footing to record the member end rotation due to anchorage slip. LVDTs 1, 3, 5 and 6 were positioned at approximately 50 mm away from the face of the column, and 2 and 4 at 100 mm from the face of the column. The difference between vertical readings of two opposite LVDTs, divided by the horizontal distance between the two, gave the rotation of that segment.

The Temposonic LVDTs were mounted with brackets to a light steel mecano frame, which was constructed using slotted steel angles. This frame was fixed onto the column footing by means of four screws, so that all readings of displacements were relative to the column footing. The Temposonic LVDTs had a stroke of ± 250 mm. Figure 3.37 shows locations of LVDTs on a typical specimen. Figure 3.38 shows a photographic view of instrumentation for a typical column specimen.

3.6 Description of Test Setup

The columns were tested under constant axial compression and lateral displacement reversals. This type of loading necessitated a loading system in which vertical and horizontal actuators could be controlled separately. Three servo-controlled MTS hydraulic actuators and a steel loading beam assembly were used to apply the loading. Each MTS actuator had a load capacity of 1000 kN in compression and tension. The hydraulic pressure for the MTS actuators was provided by a 33 GPM gear driven pump, and was controlled by an MTS

servo-valve to apply the required load. The maximum stroke of the actuator was 500 mm, which allowed ± 250 mm relative to the neutral position. The actuator were equipped with multi directional swivels at the ends. These swivels eliminated the risk of damage to the actuators due to any accidental eccentricity and /or force component that may be developed perpendicular to their axis. Figure 3.39 illustrates the overall geometry of a typical MTS actuator.

A single MTS actuator was used to apply the horizontal force reversals. The actuator was first positioned horizontally, and attached to the steel loading beam that had been bolted on the column. A pair of steel A-frames were used to support the horizontal actuator at the other end. The A-frames were bolted on three pairs of C-channels. These channels were placed back-to-back and secured to the laboratory strong floor by means of 1800mm long, and 64 mm diameter Grade 400 MPa bolts. The actuator ends were connected using grade 8 high-strength bolts, which were 400 mm long and 38 mm in diameter. The maximum force applied by the horizontal actuator during testing was 365 kN, which was applied to Column TC-3. Figures 3.40 and 3.41 illustrate the details of the horizontal load setup.

The vertical load setup consisted of two MTS actuators and a steel loading beam assembly, which also contained concrete spacer blocks. The actuators were placed vertically on either side of the column . The top ends were connected to the loading beam assembly, and the bottom ends were attached to the column footing, using high strength bolts. The front view of the vertical load setup is shown in Fig. 3.42.

The loading beam assembly consisted of two parts. The upper part was a built-up box section beam, which was attached to the vertical actuators by means of 400 mm long, 38 mm diameter Grade 8 bolts. The bottom part was a built-up I section spacer block, which was used to connect the horizontal actuator to the column specimen. Because the vertical actuators rested on top of the column footing, an additional reinforced concrete spacer was necessary to allow for full height of actuators. The spacer block was connected to the built-up

box section beam from the top, and the built-up I section spacer block from the bottom, by means of eight 25 mm diameter, 100 mm long grade 8 bolts. The details of the loading beam assembly and the concrete spacer block are illustrated in Fig. 3.43.

3.6.1 Lateral Restraints

A pair of steel frames, made out of hollow steel sections, were positioned on either side of a test column to provide lateral bracing and additional safety against unexpected out-of-plane failure at high inelastic deformations. The frames were secured to the laboratory strong floor and connected to each other at the top by two hollow section steel box beams. The photographs, included in Fig. 3.44, show the lateral bracing system.

3.7 Test Procedure and Loading Program

The first step in the test procedure was to fix the specimen in the test setup. The 10-ton overhead crane of the Structures Laboratory was used for this purpose. The column footing was then fixed to the laboratory strong floor by means of four bolts. The vertical actuators were attached to column footing on either side of the column. The loading beam assembly, including the reinforced concrete spacer block, was subsequently attached to the column. The actuator ends were bolted to the bottom flange of the loading beam. The horizontal actuator was then positioned and connected to the web of the spacer block. Finally the strain gauges and LVDTs were connected to the data acquisition system, and calibrated and initialized for data collection.

Testing started by applying the required level of axial compression. Two levels of axial load were applied to each pair, consisting of 11% and 21% of column concentric capacity (P_o). The axial load was kept at the same level for the entire duration of test. Columns TC-2, TC-3, and TC-5 were tested under 1900 kN of axial compression (21% of P_o). This force level corresponded to the maximum capacity of actuators. TC-1, TC-4, and TC-6 were tested

under 1000 kN (11% of P.). The horizontal load was then applied in displacement control mode, following a loading program that consisted of incrementally increasing inelastic displacement reversals. Displacement levels were expressed in terms of lateral drift ratio. The drift ratio was defined as the ratio of column top deflection to column heigh. Figure 3.45 illustrates the loading program followed for lateral displacements. Every column was subjected to three full elastic cycles at approximately 0.5% drift. The drift level was increased incrementally to 1.0%, 2.0%, 3.0%, etc. until failure. Three deformation cycles were applied at each level of drift. Testing continued until the lateral load resistance of the column dropped by at least 20% of the peak load. Total duration of a typical test was about two to three hours, depending on the ductility of the column.

Table 3.1 : Development of Concrete Strength with Time

Time (days)	Average Strength (MPa)
7	28
14	32
28	36
Test period	38

Table 3.2 : Strength of Tire Coupons

Tire Type	Average Ultimate Strength (MPa)
Motomaster (I)	1905
Michelin (II)	2000
Random (III)	2140

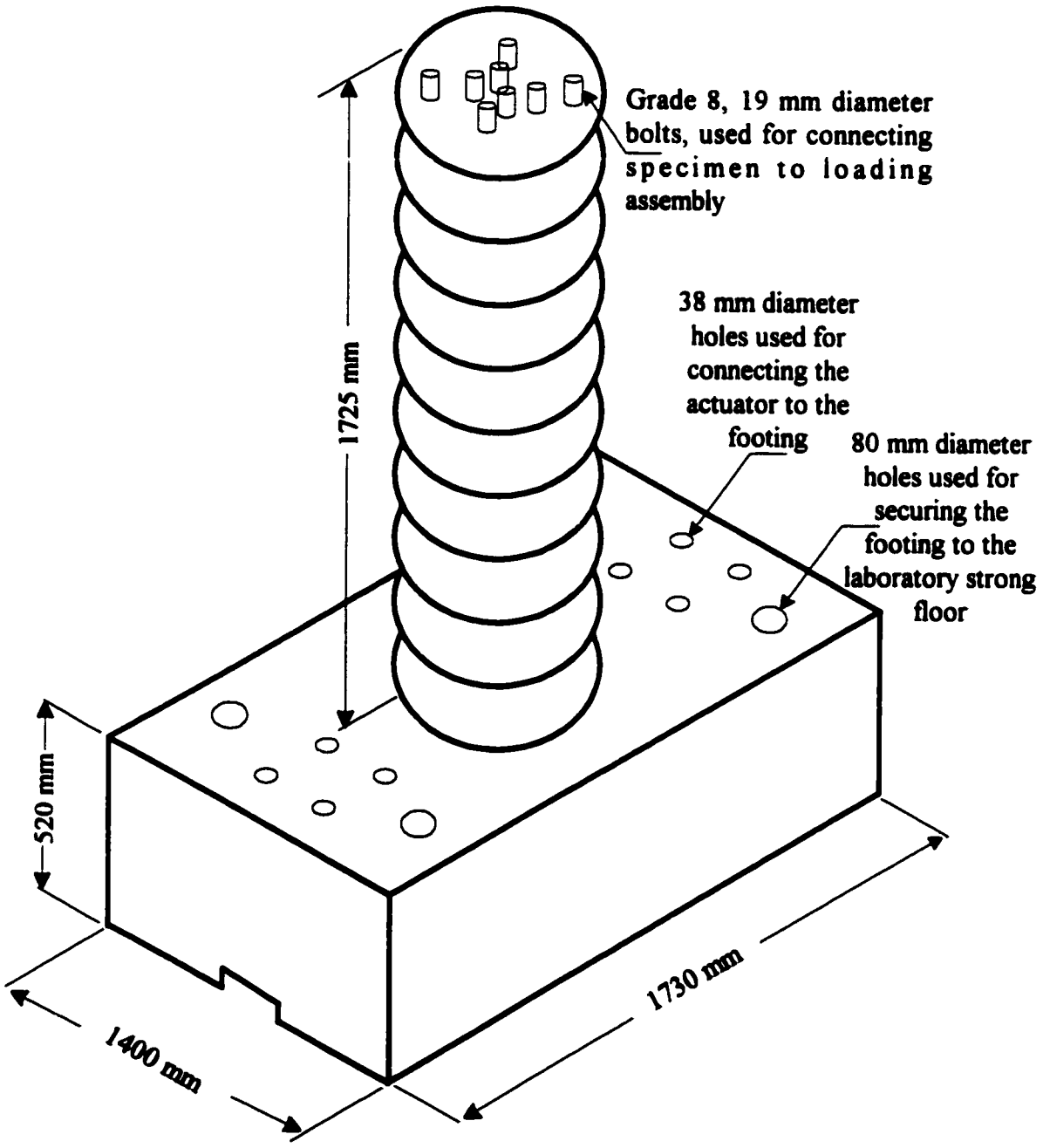

Figure 3.1 : Geometry of a Typical Specimen

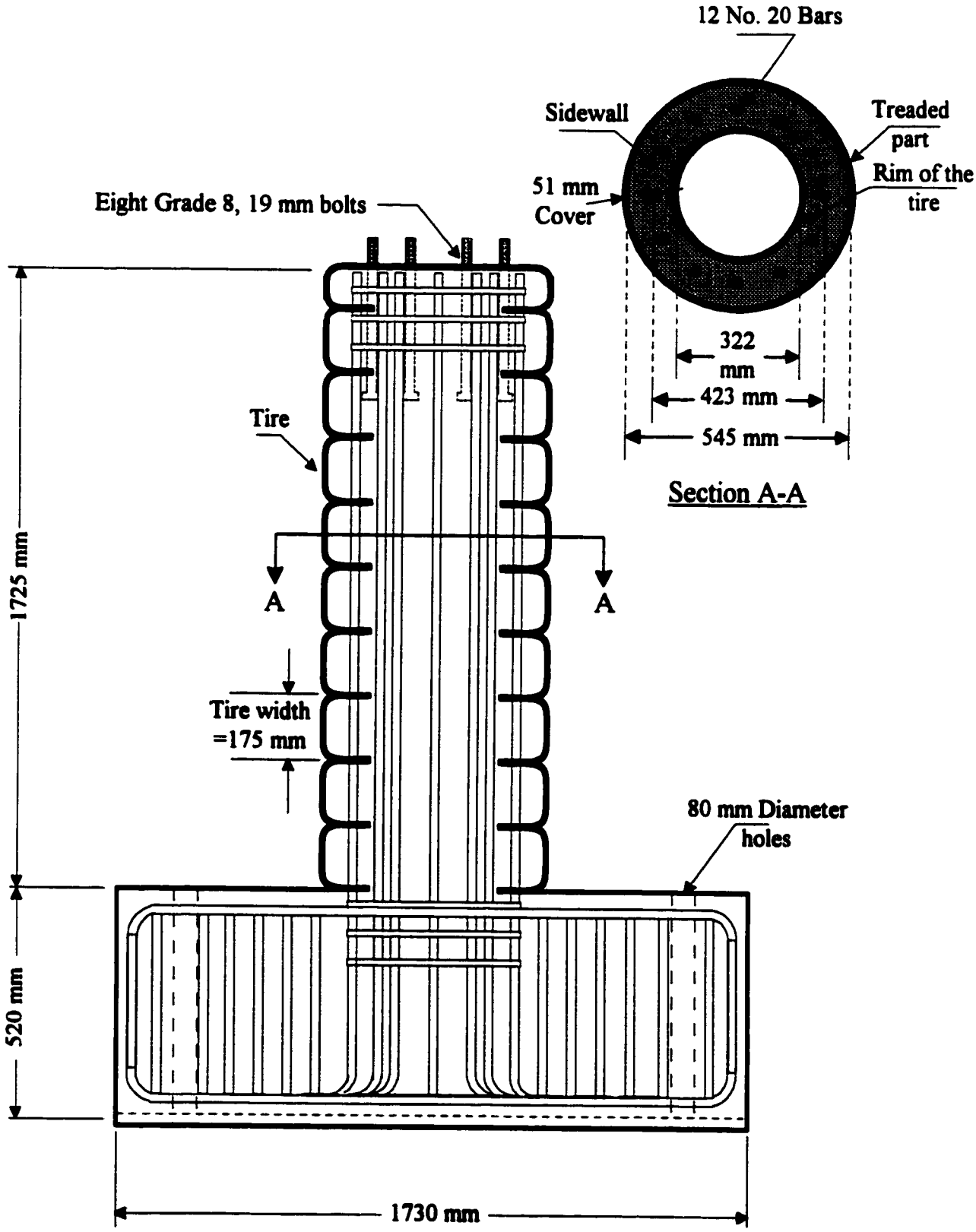

Figure 3.2 : Reinforcement Details for Columns TC-1 and TC-2

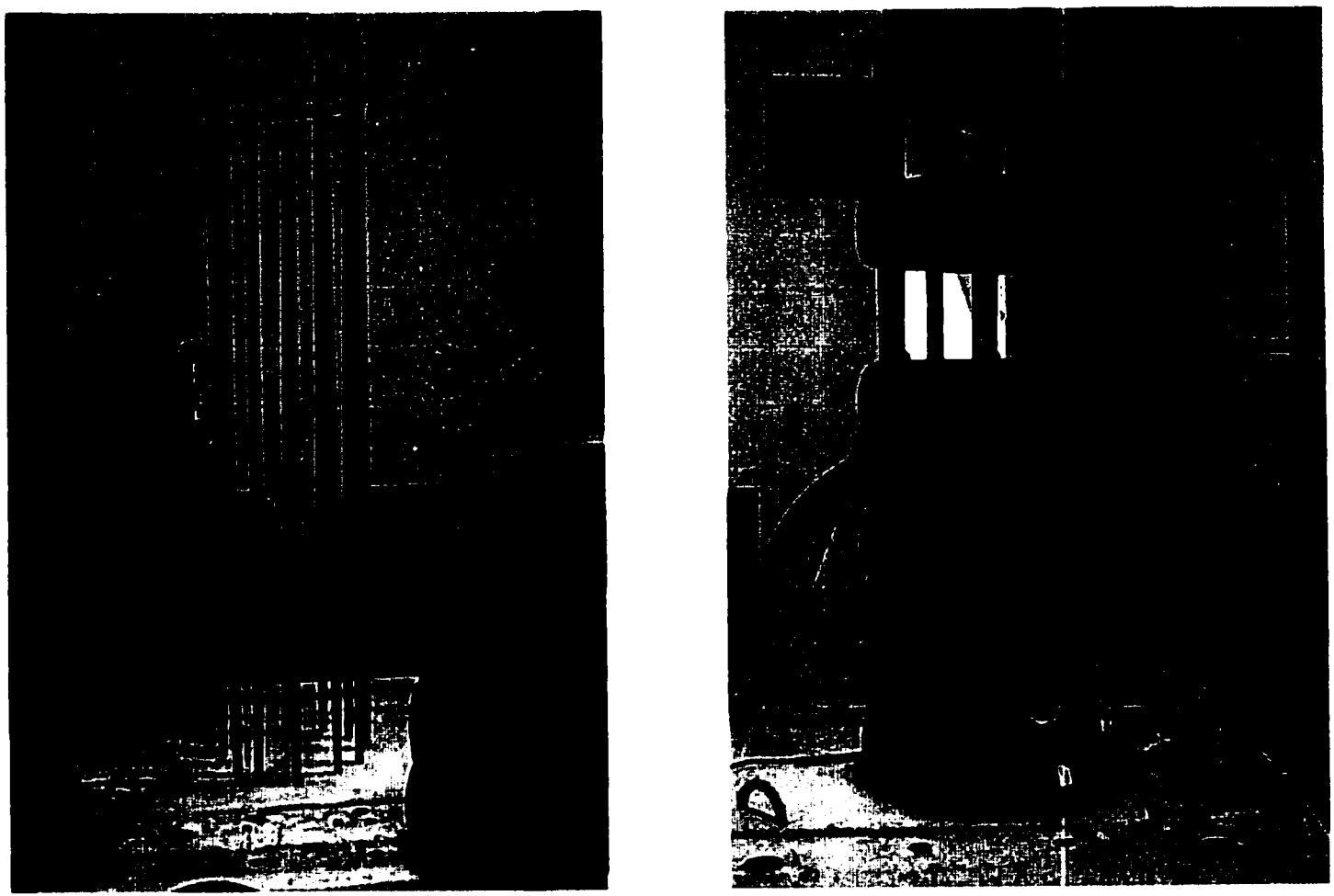

Figure 3.3 : Construction of Column Reinforcement Cages for TC-1 and TC-2

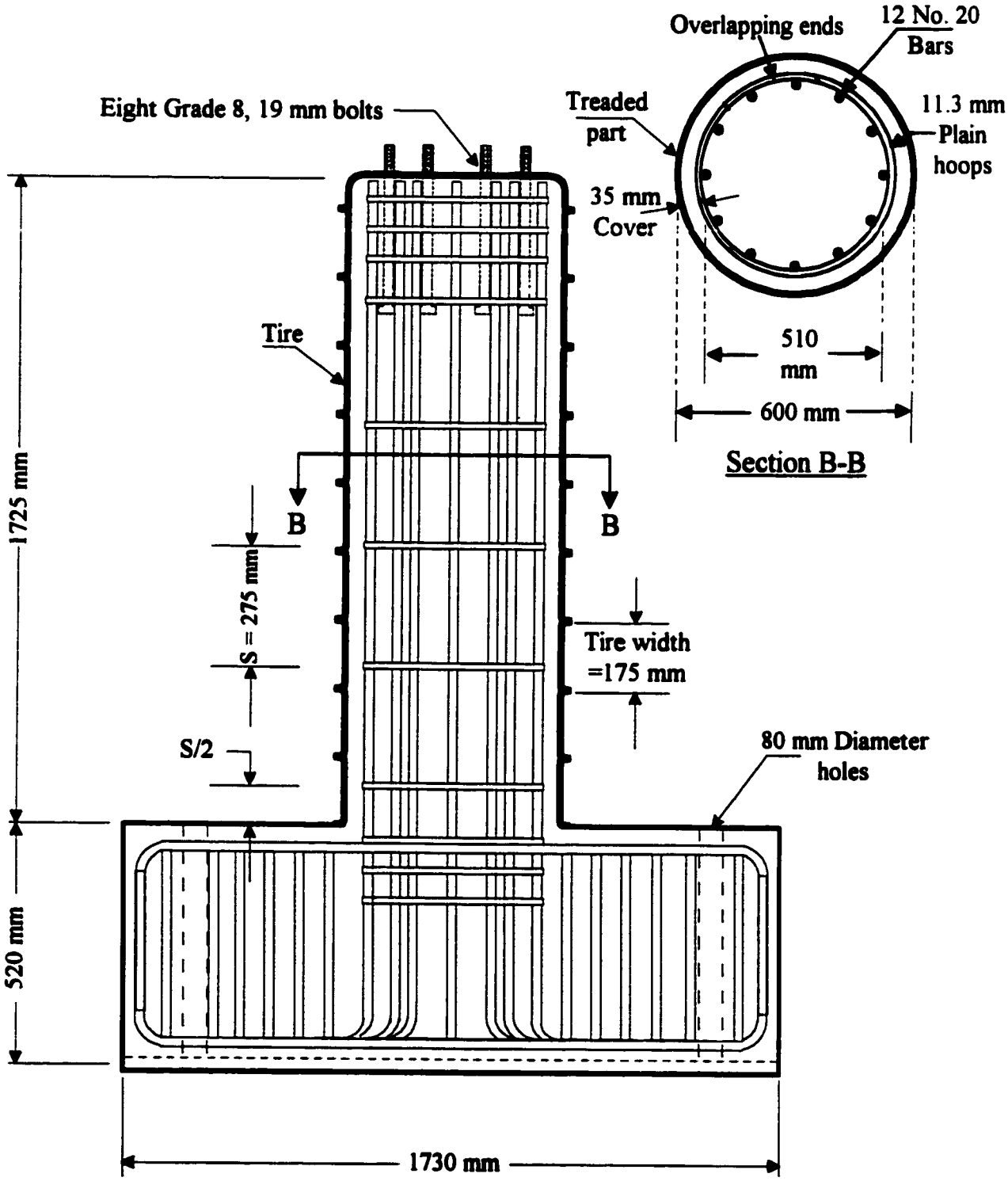

Figure 3.4 : Reinforcement Details for Columns TC-3 and TC-4

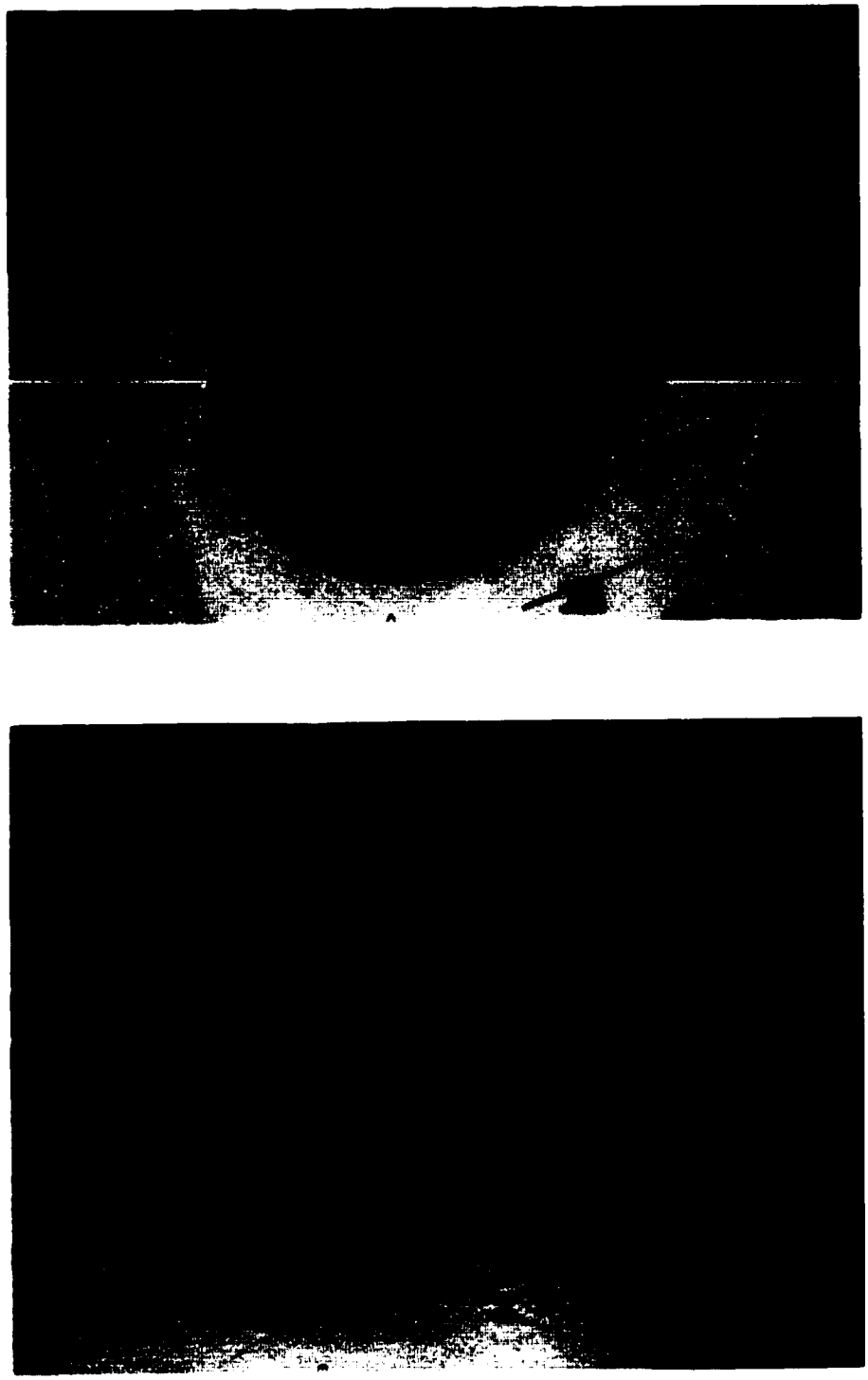

Figure 3.5 : Construction of Column Reinforcement Cages for TC-3 and TC-4

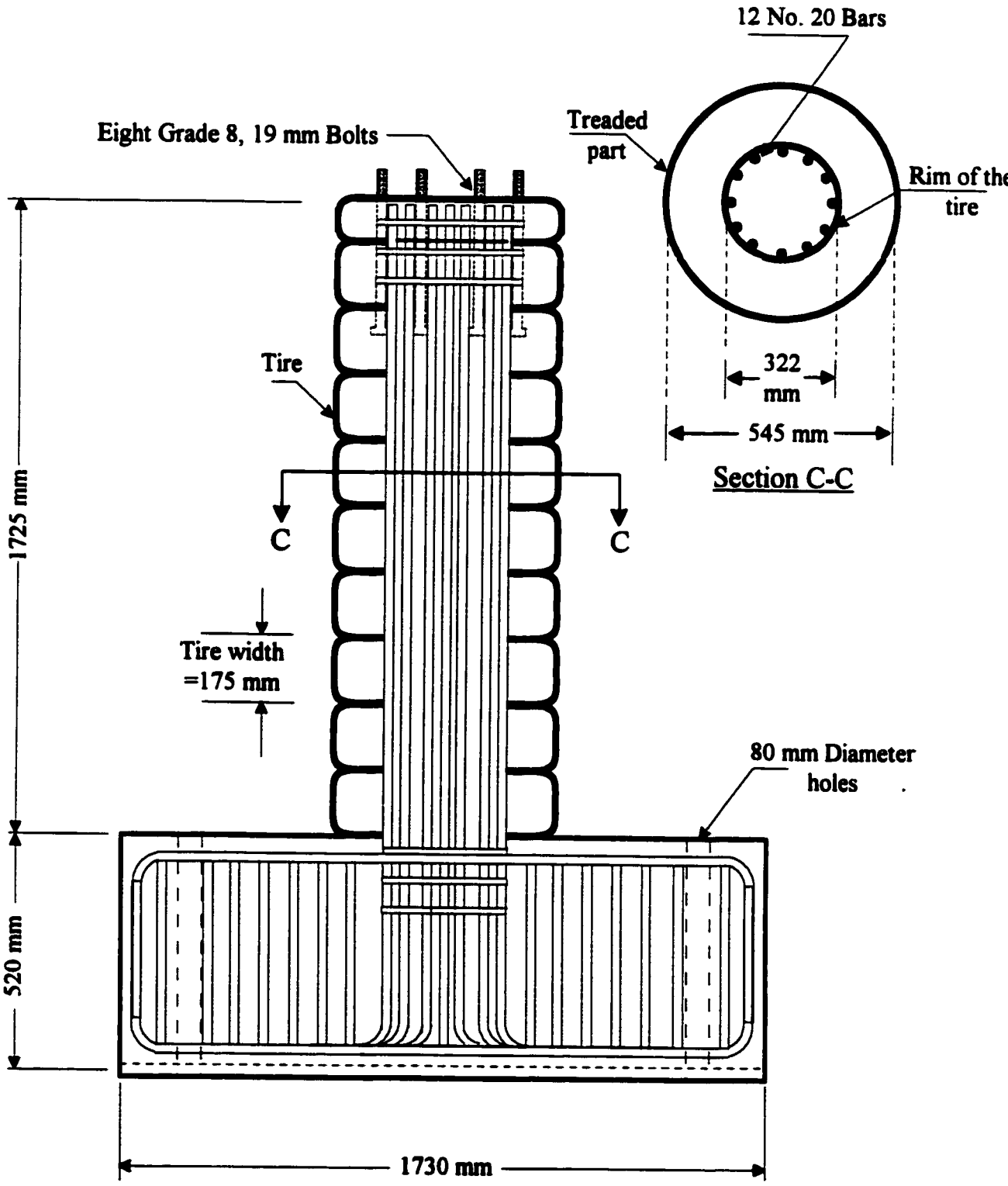

Figure 3.6 : Reinforcement Details for Columns TC-5 and TC-6

Figure 3.7 : Construction of Column Reinforcement Cages for TC-5 and TC-6

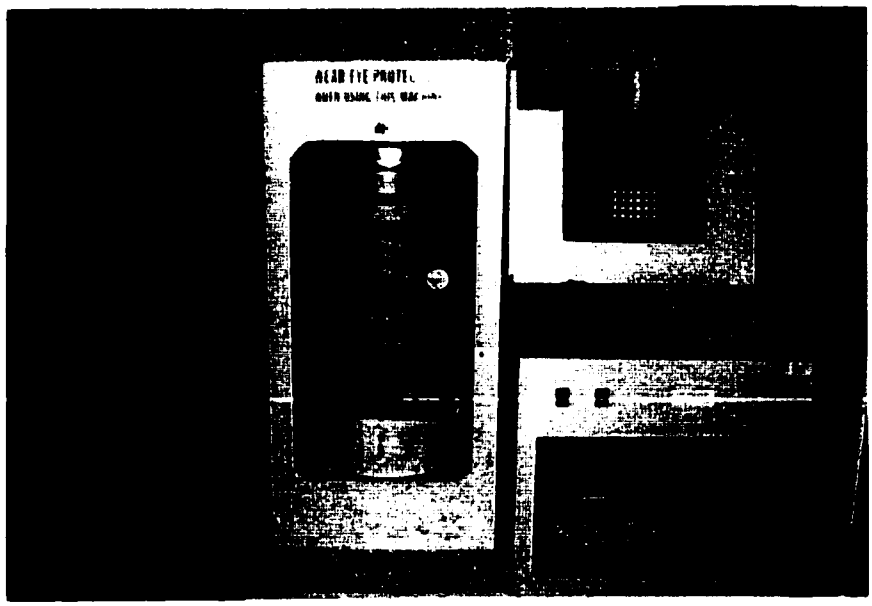

(a) Testing of Cylinder on a Forney Testing Machine

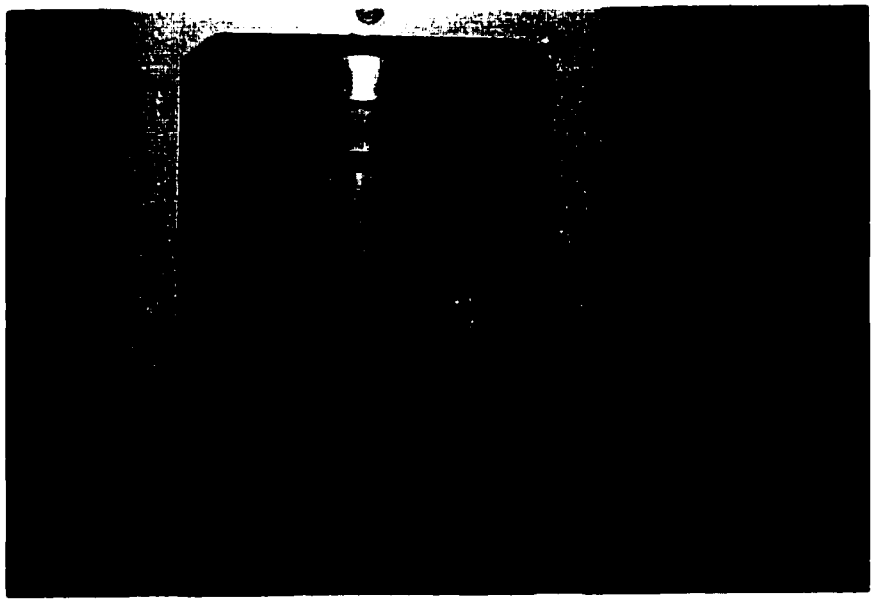

(b) Cylinder After Testing

Figure 3.8 : Instrumentation and Testing of Standard Cylinders

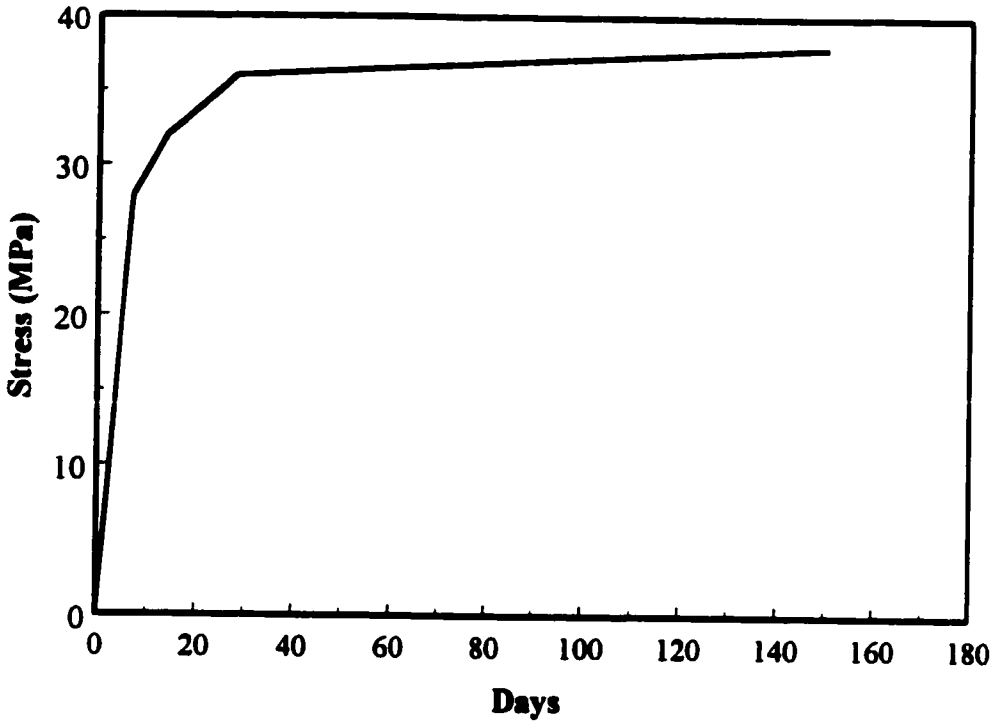

Figure 3.9 : Stress Development over Time of Concrete Cylinders

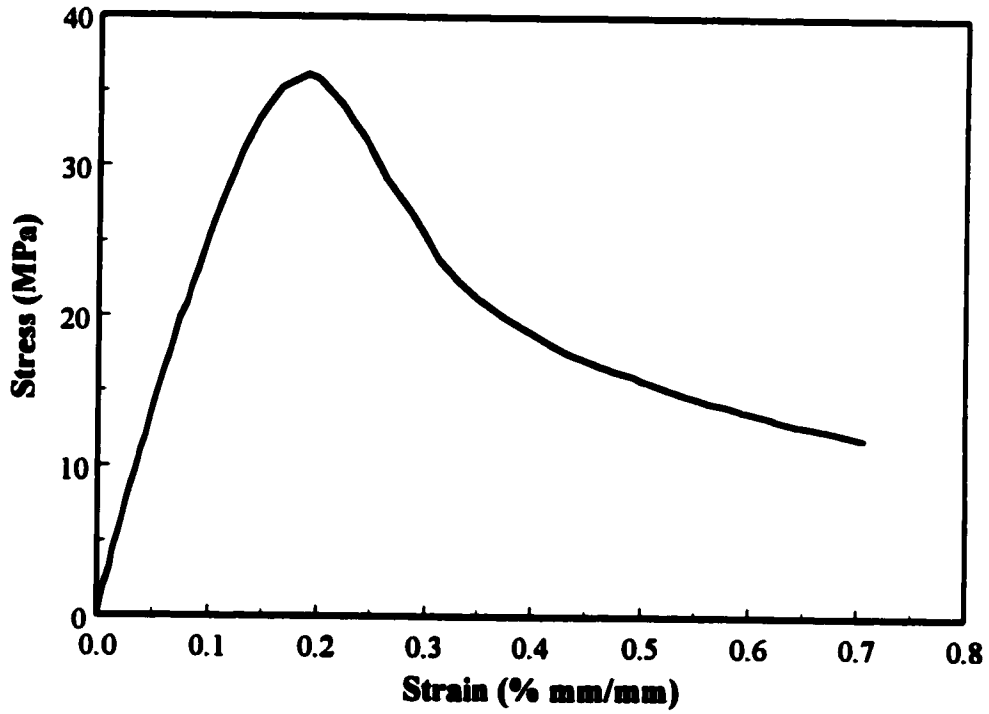

Figure 3.10 : Stress-Strain Relationships for Concrete Columns

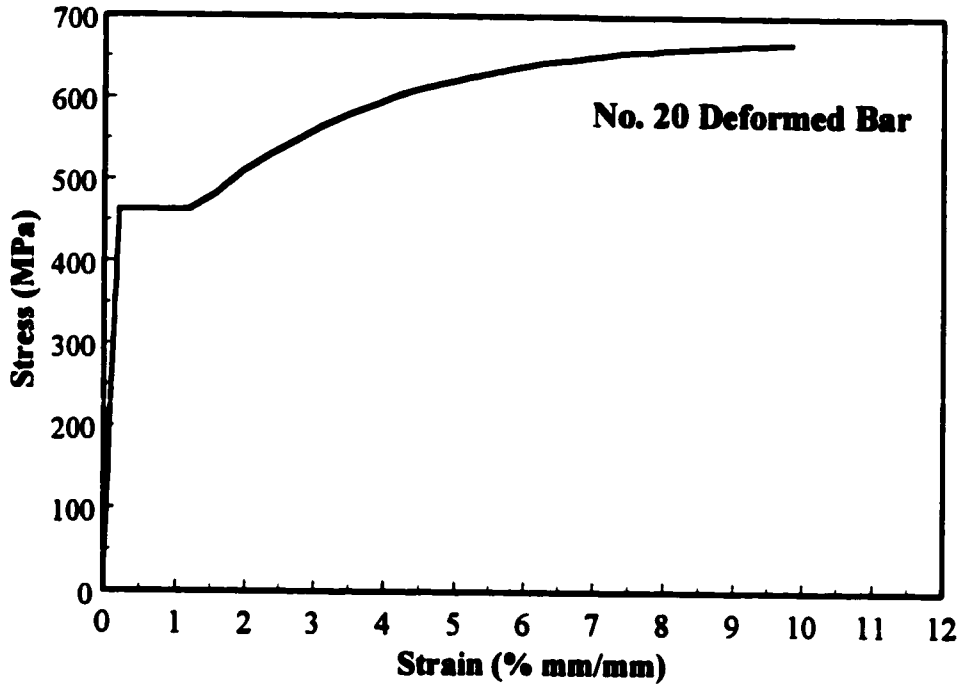

Figure 3.11 : Stress-Strain Relationship of Longitudinal Reinforcement for all Columns

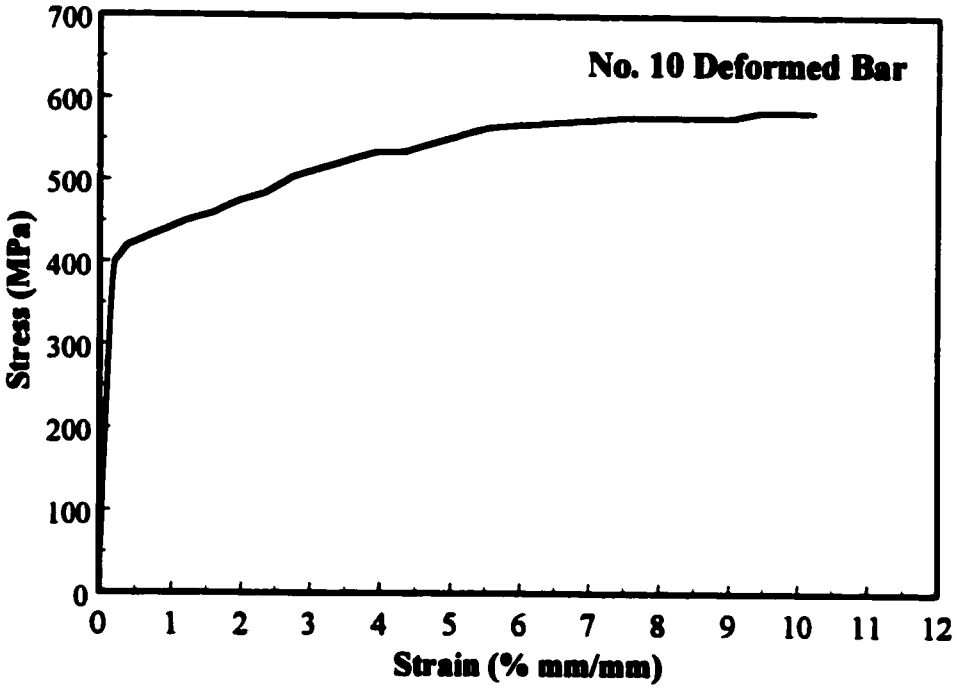

Figure 3.12 : Stress-Strain Relationship of Transverse Reinforcement for Columns TC-3 and TC-4

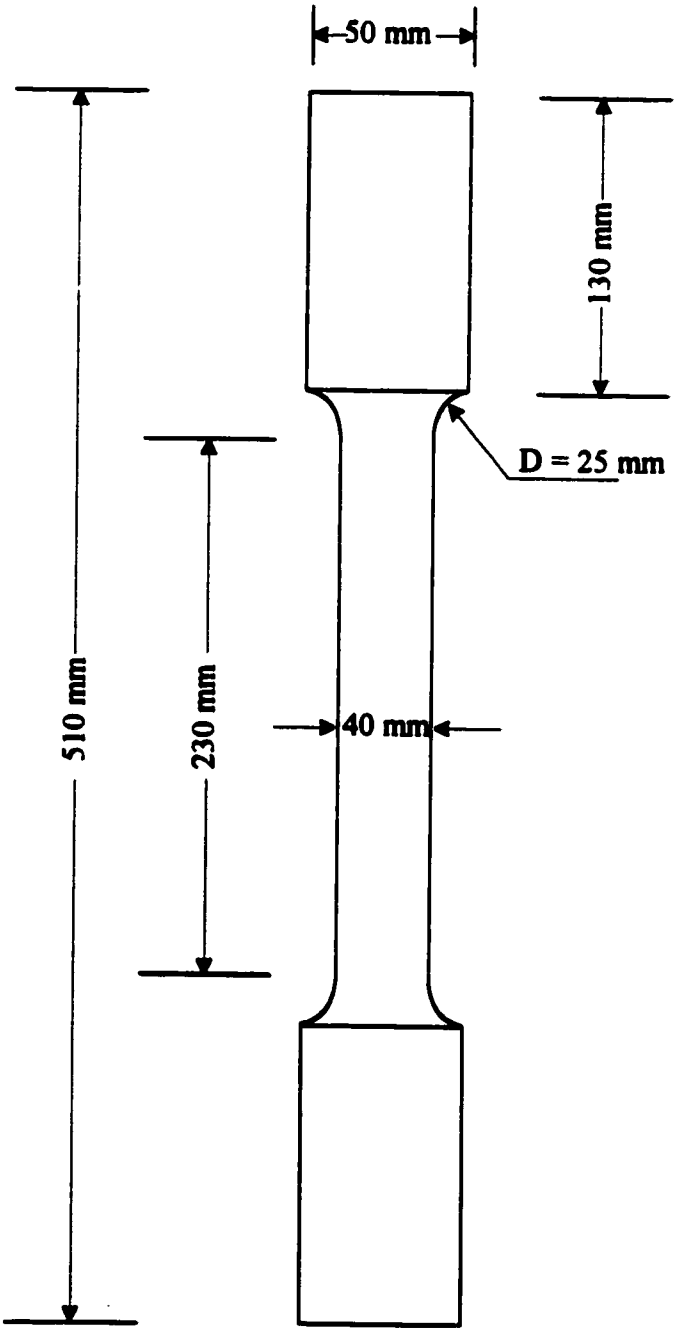

Figure 3.13 : Geometry of a Typical Tire Coupon

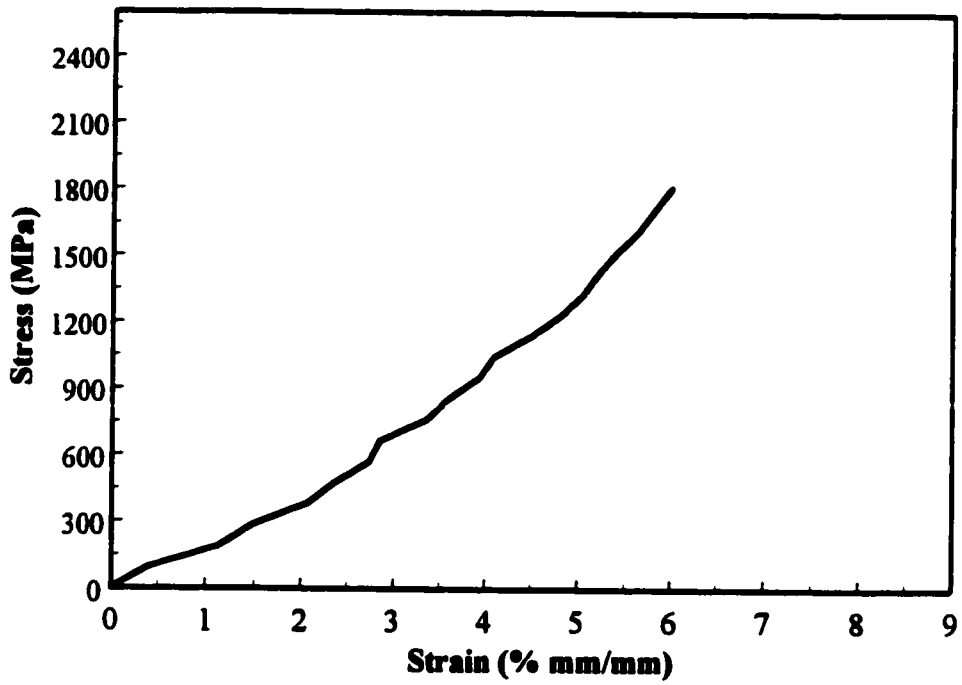

Figure 3.14 : Stress-Strain Relationship for Type I Tire (Motomaster) for Columns TC-1 through TC-4

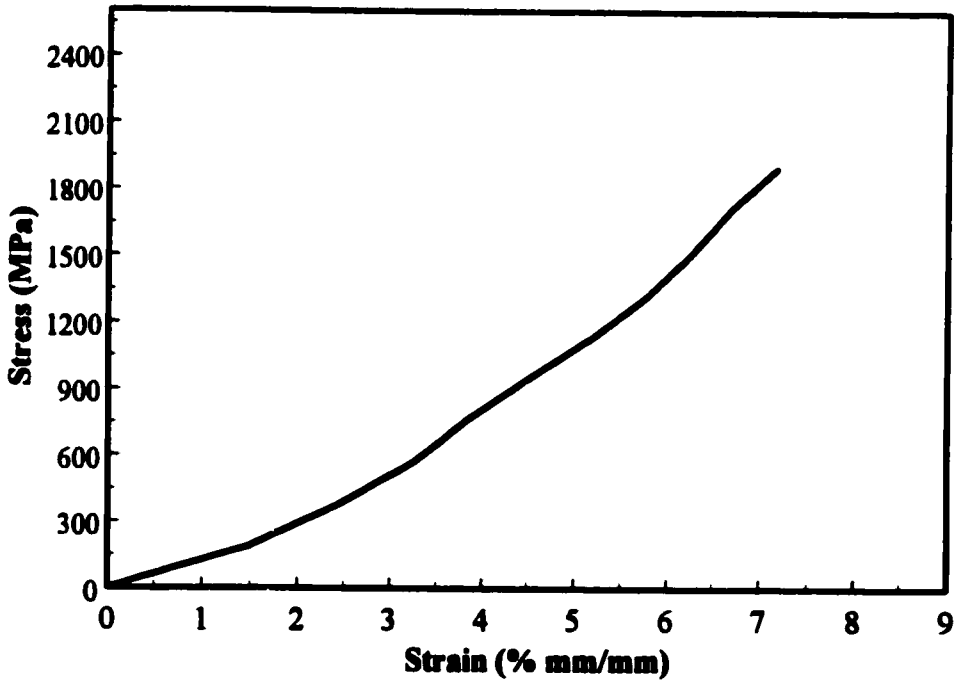

Figure 3.15 : Stress-Strain Relationship for Type II Tire (Michelin) for Columns TC-5 and TC-6

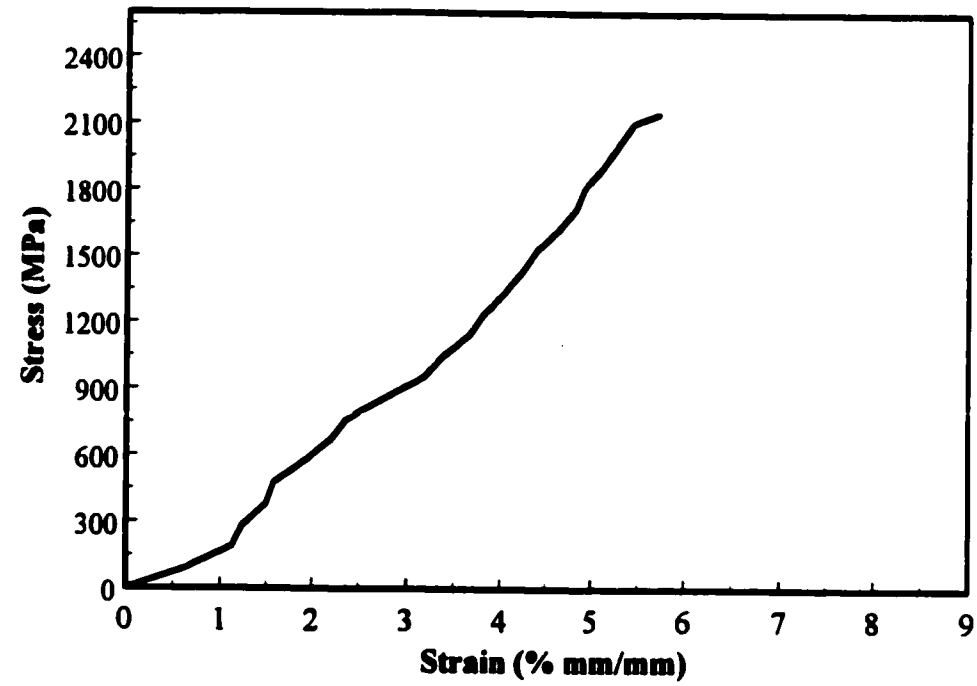

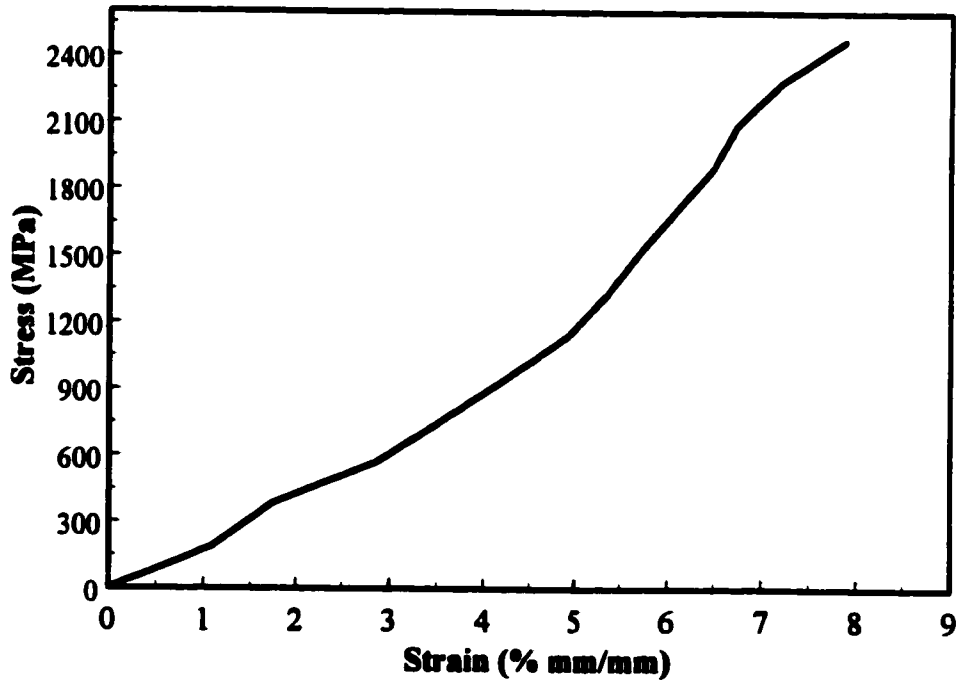

Figure 3.16 : Stress-Strain Relationships for other Brand Tires Used in Columns TC-1 through TC-6

(a)Overall View of a Tire Coupon

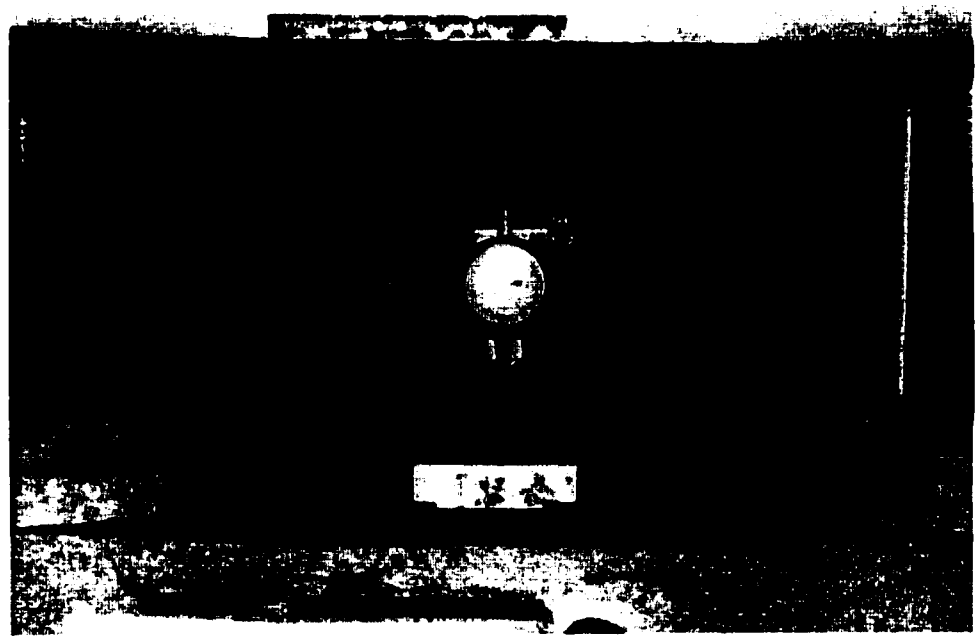

(b) Test Setup of Tire Coupon on Tinius Olsen Universal Testing Machine

Figure 3.17 : General View and Test Setup of Standard Tire Coupon

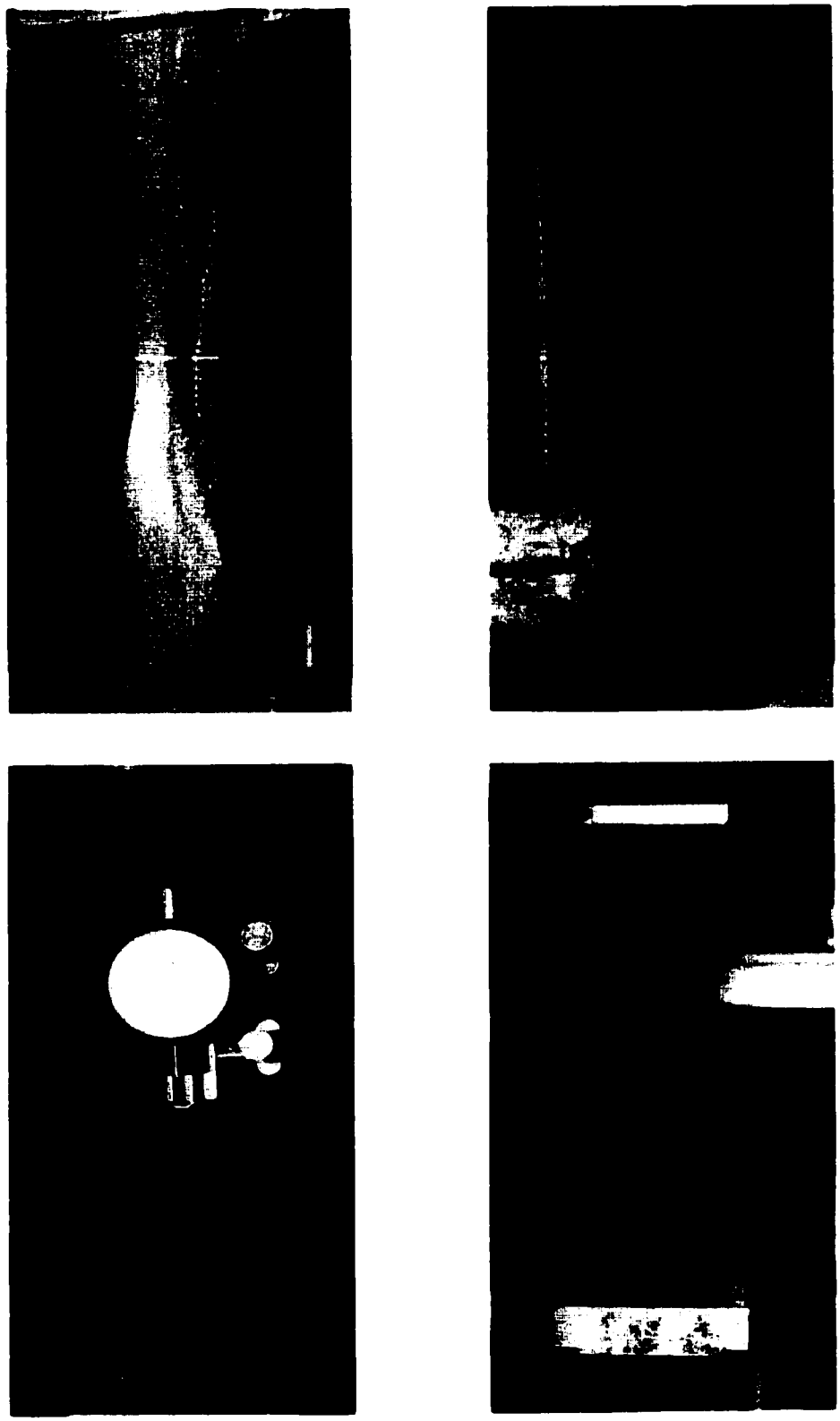

Figure 3.18 : Typical Tire Coupons During Tension Tests

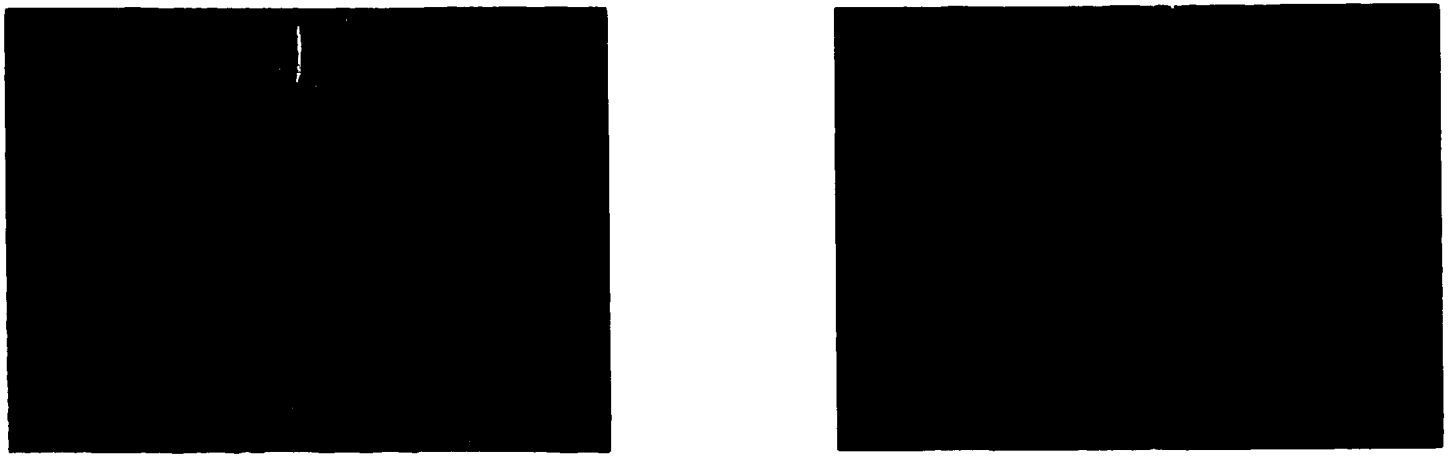

Figure 3.19 : Assembly of a Typical Footing Reinforcement Cage

Figure 3.20 : Strain Gauges and Wiring on Completed Reinforcement Cages

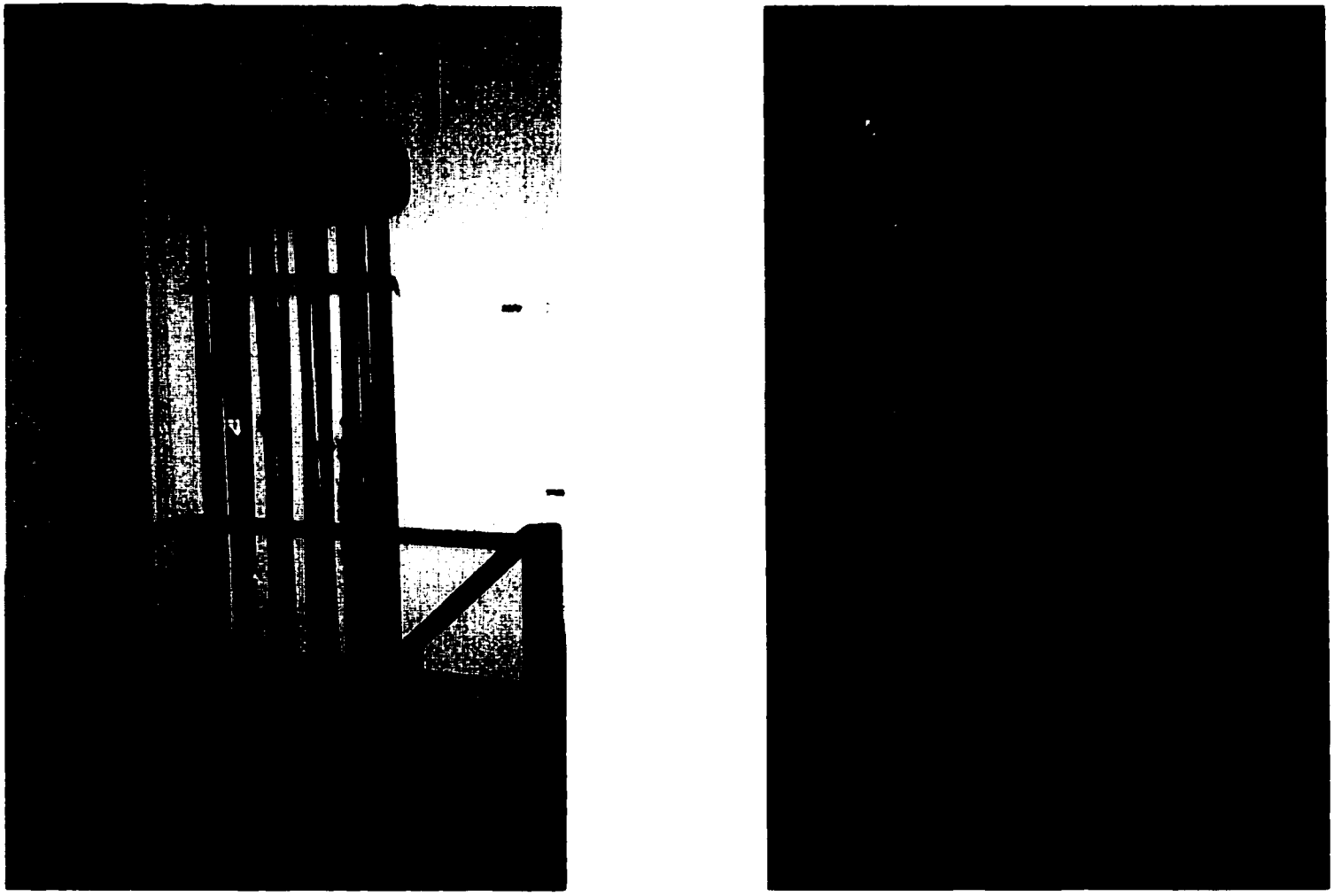

Figure 3.21 : Completed Reinforcement Cages

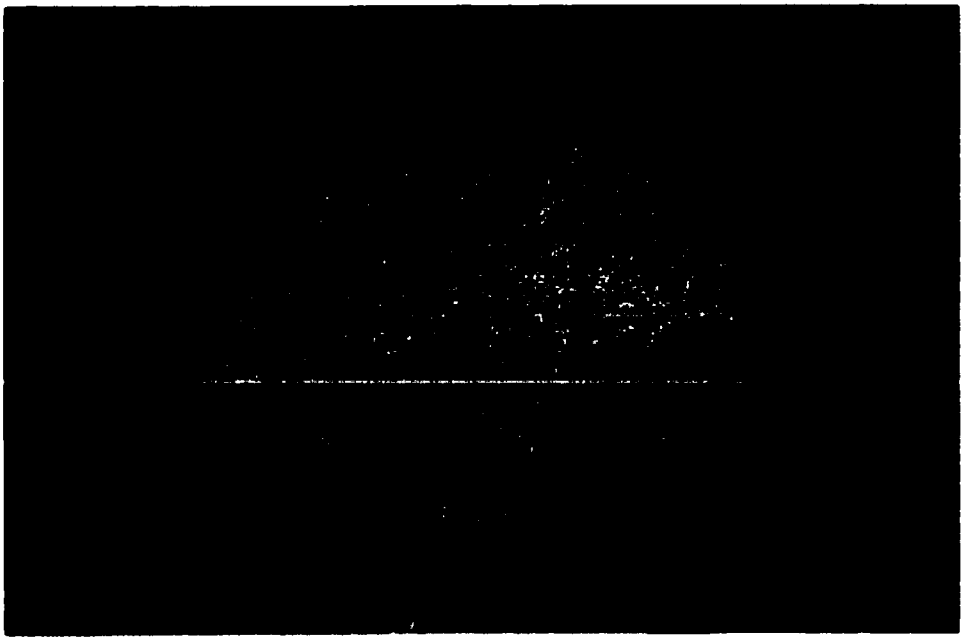

(a) Formwork Prior to Placement of Reinforcement Cage

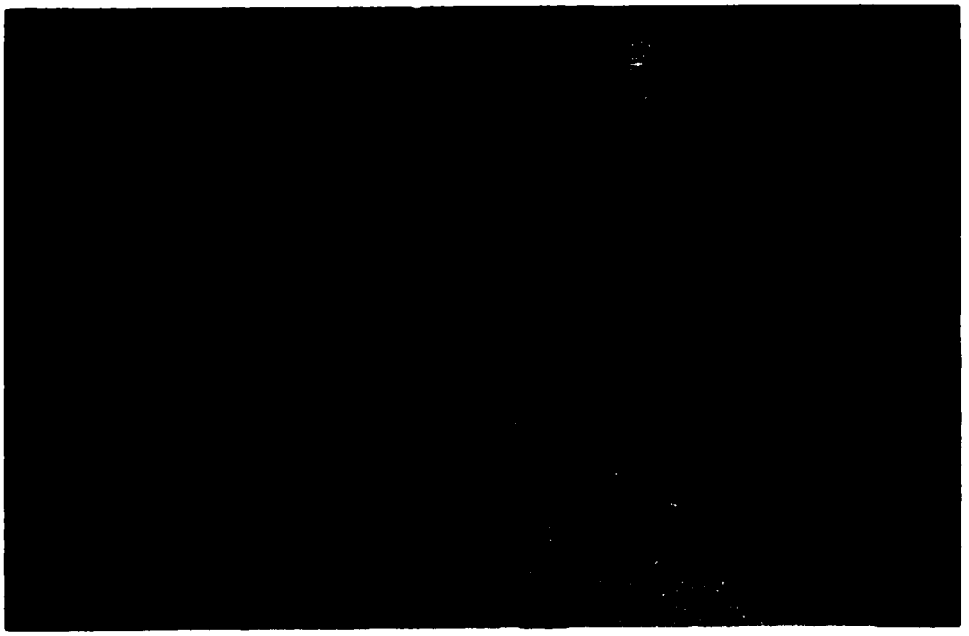

(b) Reinforcement Cages in Formwork

Figure 3.22 : Placement of Reinforcement Cages in Formwork

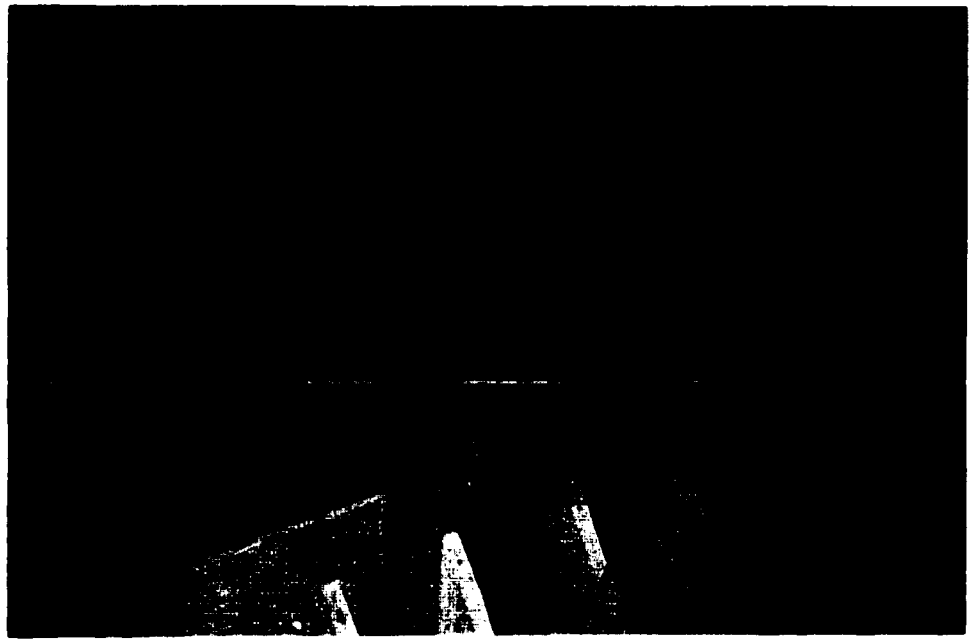

(a) Shortly Before Casting

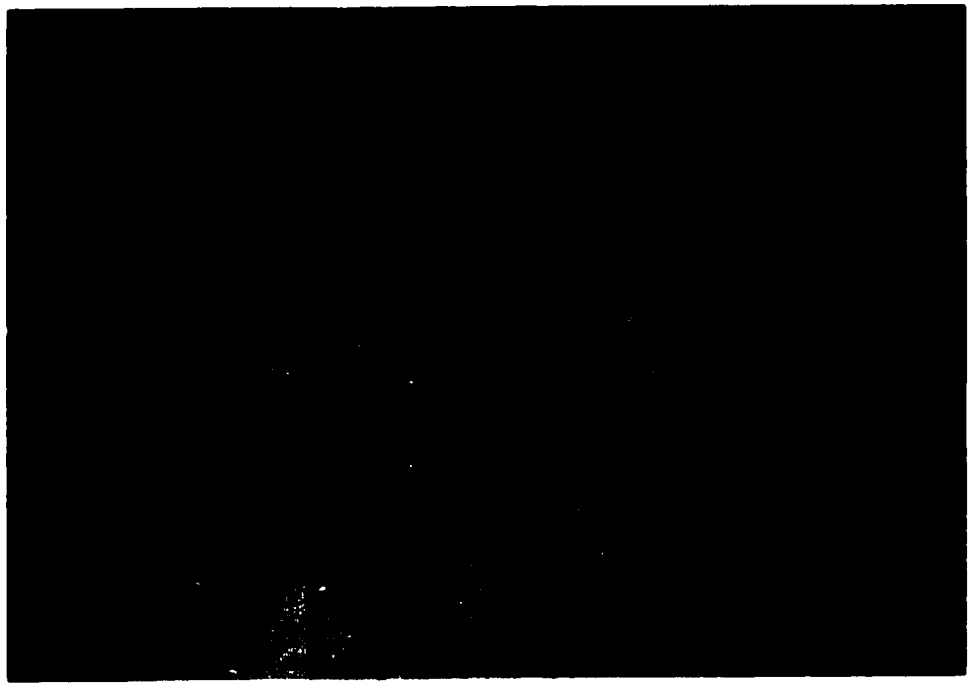

(b) At Completion

Figure 3.23 : Casting of Concrete Footings

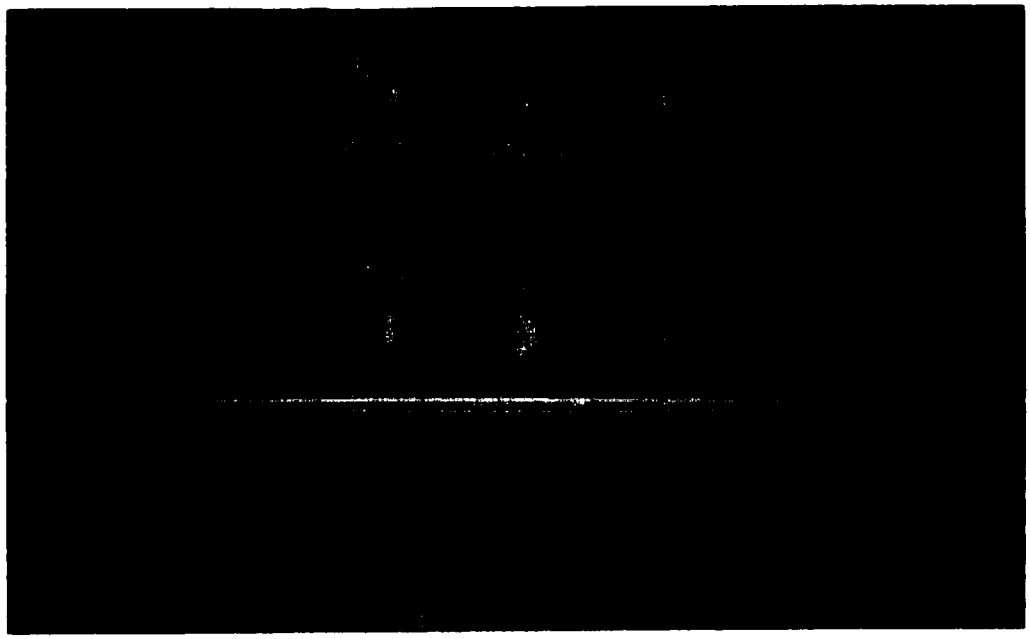

(a) Front View of Tire Template

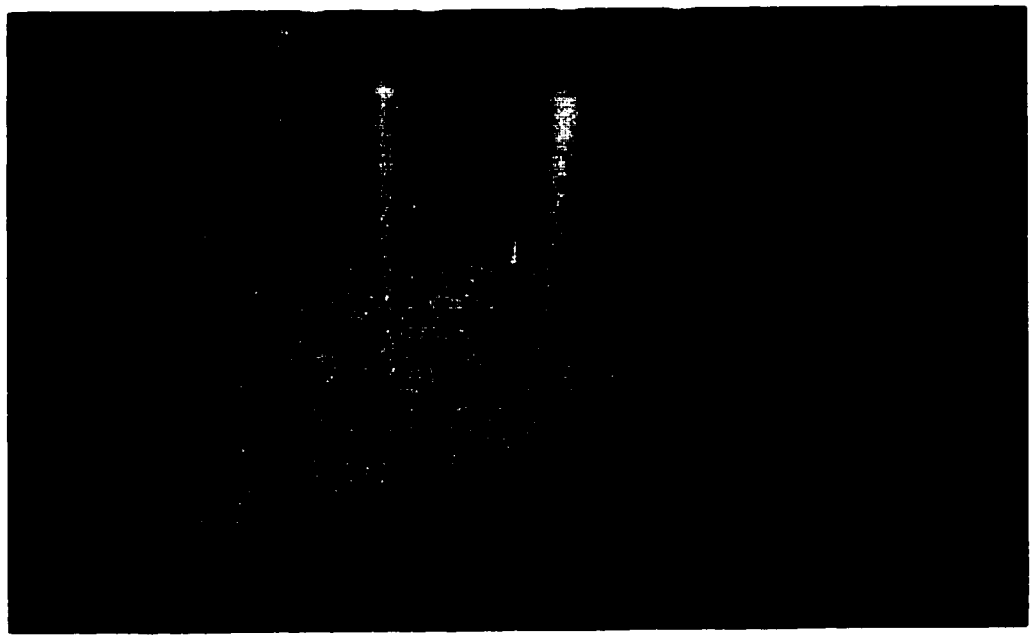

(b) Top View of Tire Template

Figure 3.24 : General Views of Tire Template

(a) Top View of the Cutter Tube

(b) Front View of Tire Inside Template

Figure 3.25 : Photographs of Tire Hole Fabrication

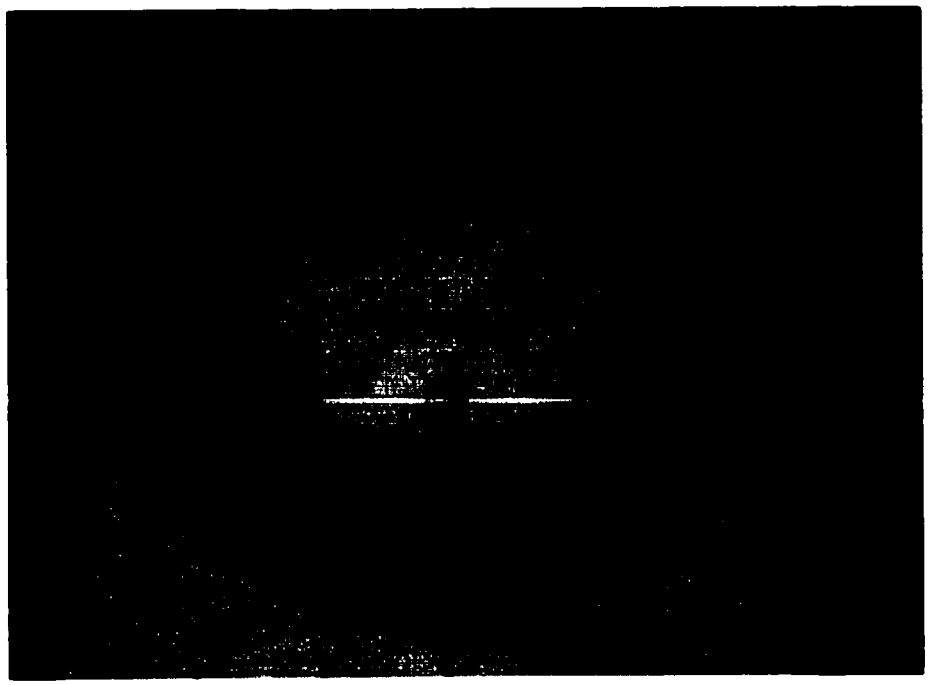

(c) Top View of the Tire in Template

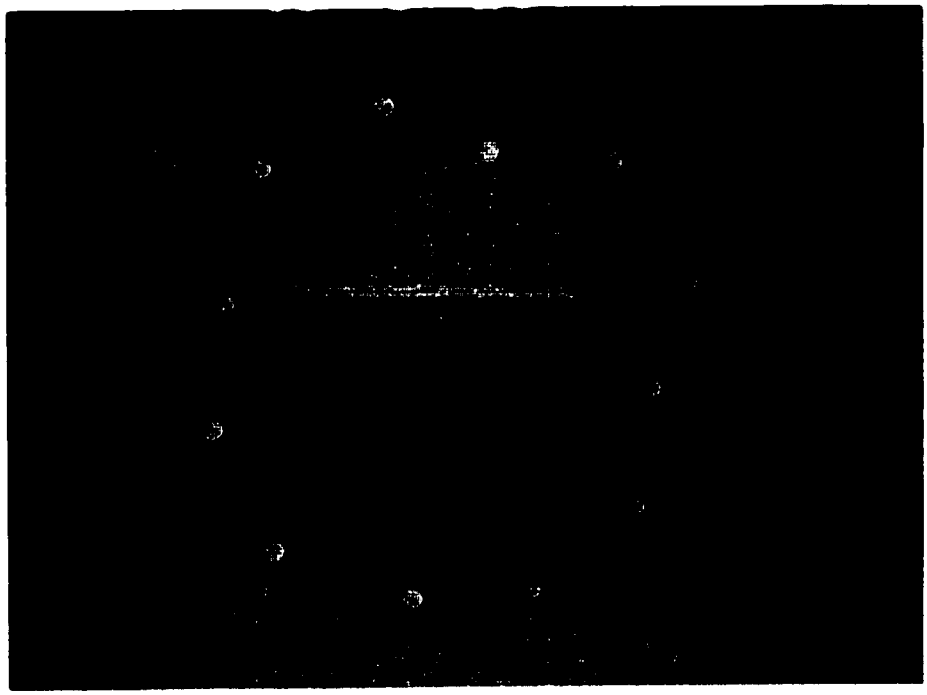

(d) Front View of the Tire After Hole Fabrication

Figure 3.25 : (Continued)

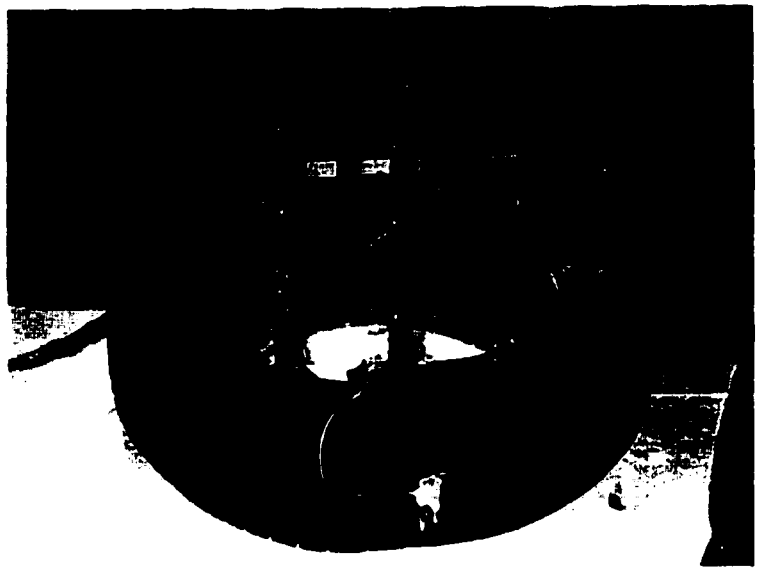

(a) First Sliding Tire in TC-1

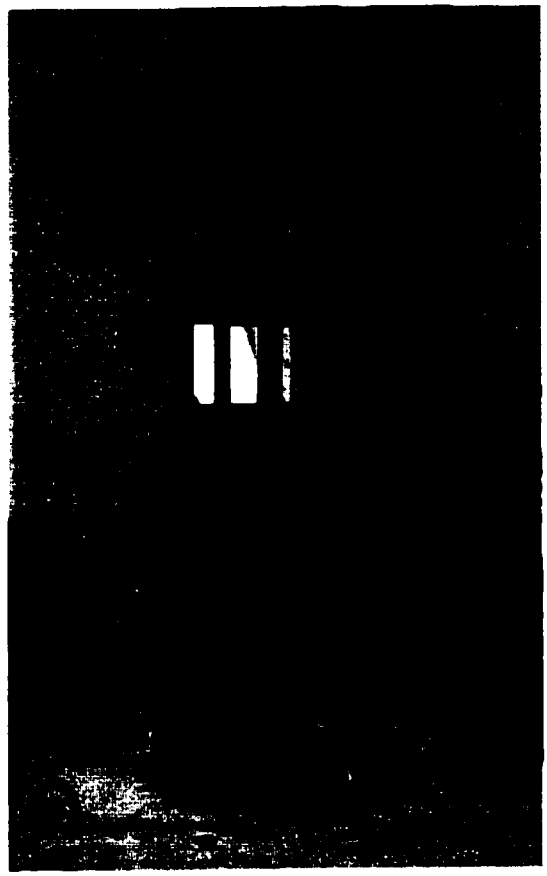

(b) Front View of Tire Sliding in TC-1

Figure 3.26 : Tire Assembly for Columns TC-1 and TC-2

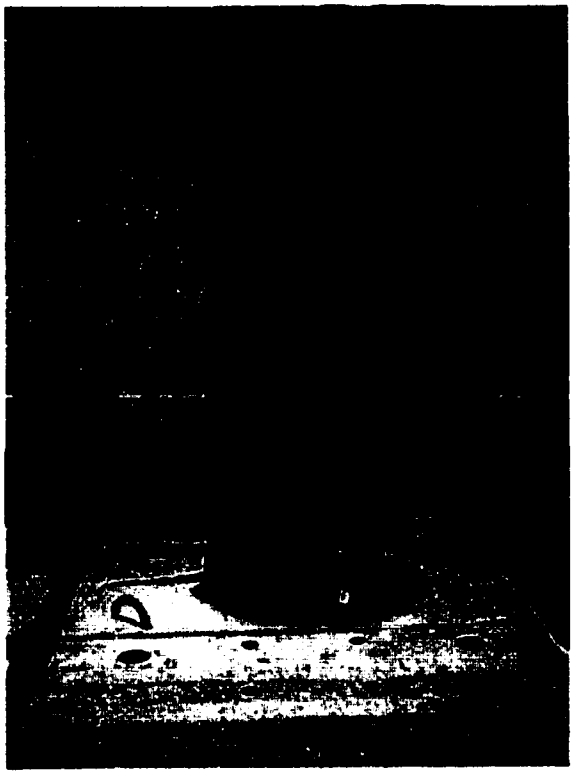

(c) Front View of TC-1 After Tire Assembly

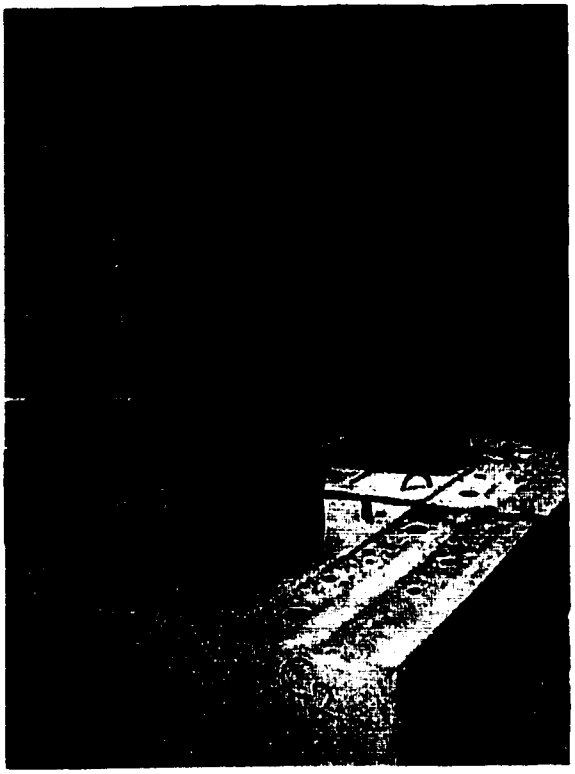

(d) Side View of TC-1 and TC-2 After Assembly

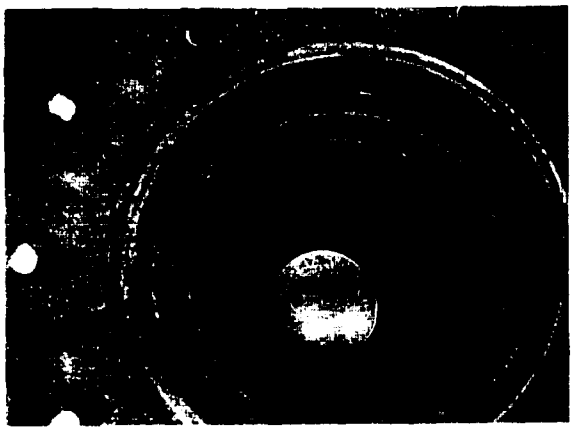

(e) Top View of TC-1

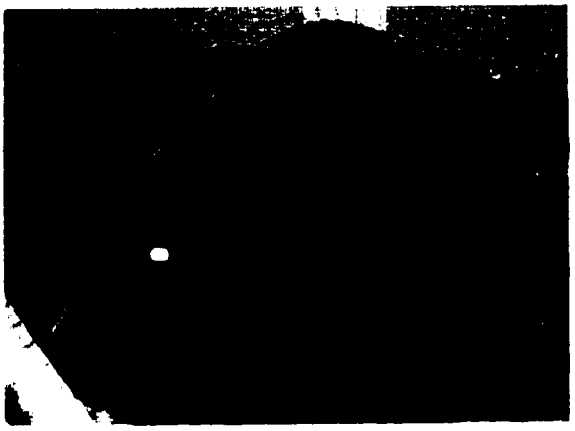

(f) Close-Up View of TC-2 at the Top

Figure 3.26 : (Continued)

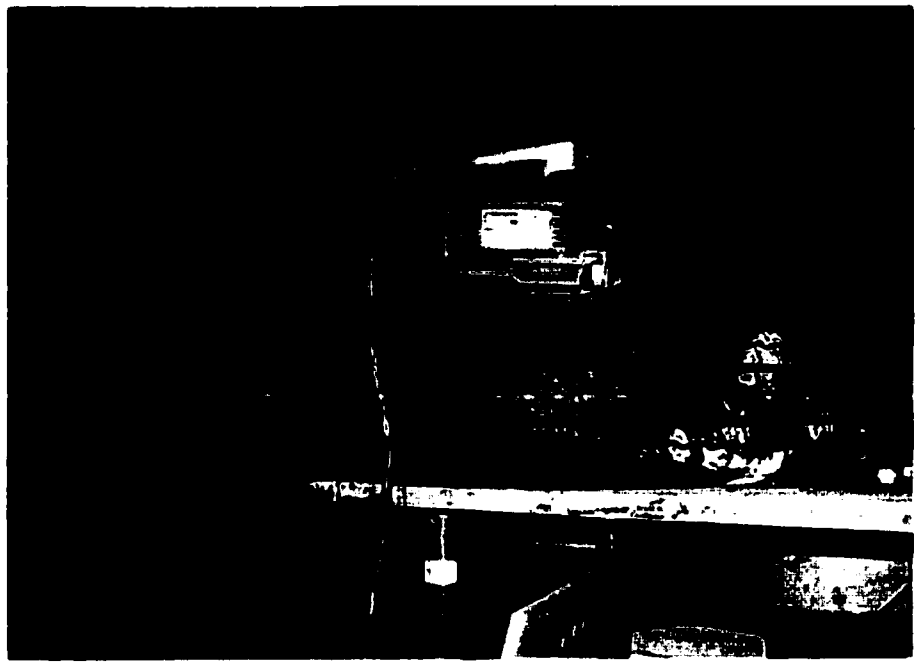

(a) Cutting the Tire with Jigsaw

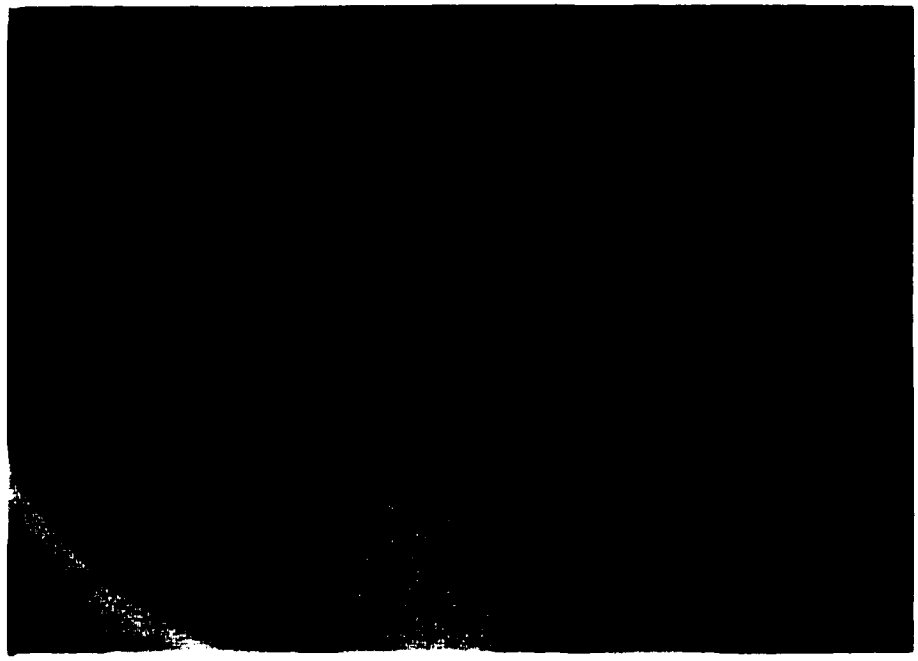

(b) Close-Up View of Tires After Removal of Sidewalls

Figure 3.27 : Procedure of Cutting the Sidewall of Tires for Columns TC-3 and TC-4

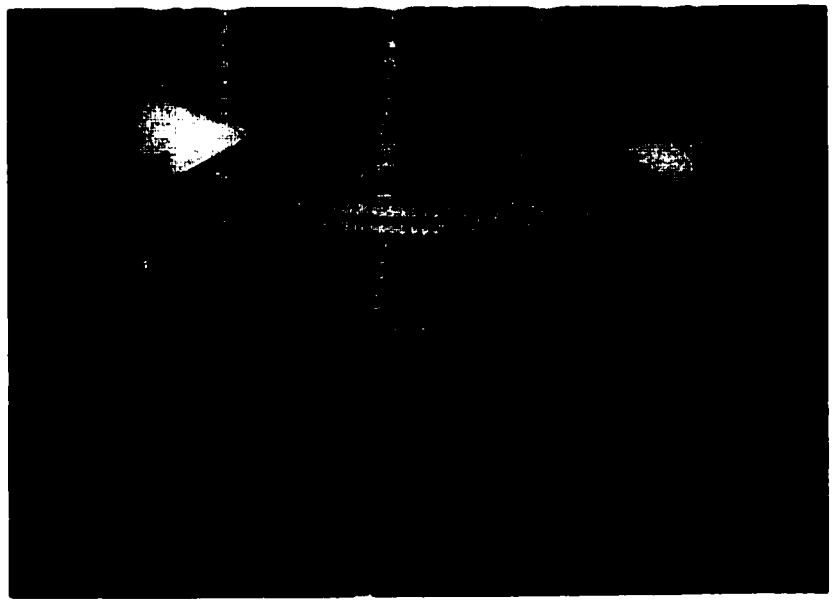

(a) Front View of First Three Tires in TC-3

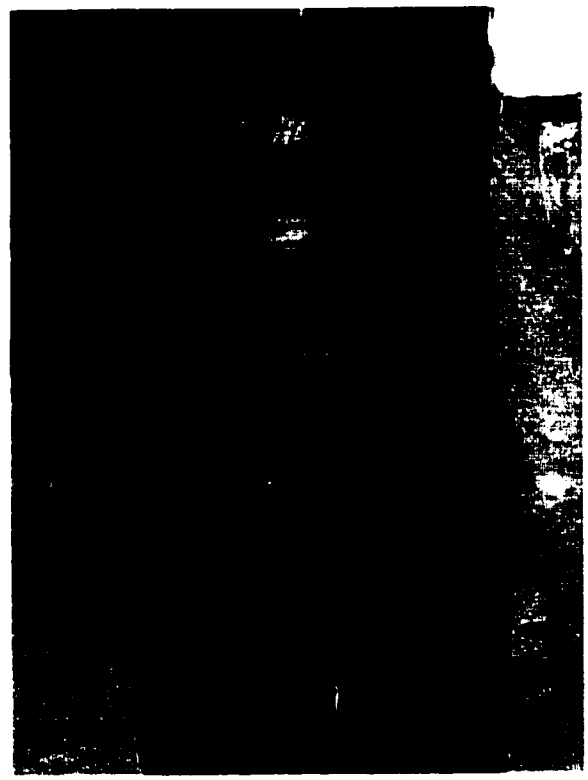

(b) Front View of TC-3

Figure 3.28 : Procedure of Placing the Tires Around Longitudinal Reinforcement in TC-3 and TC-4

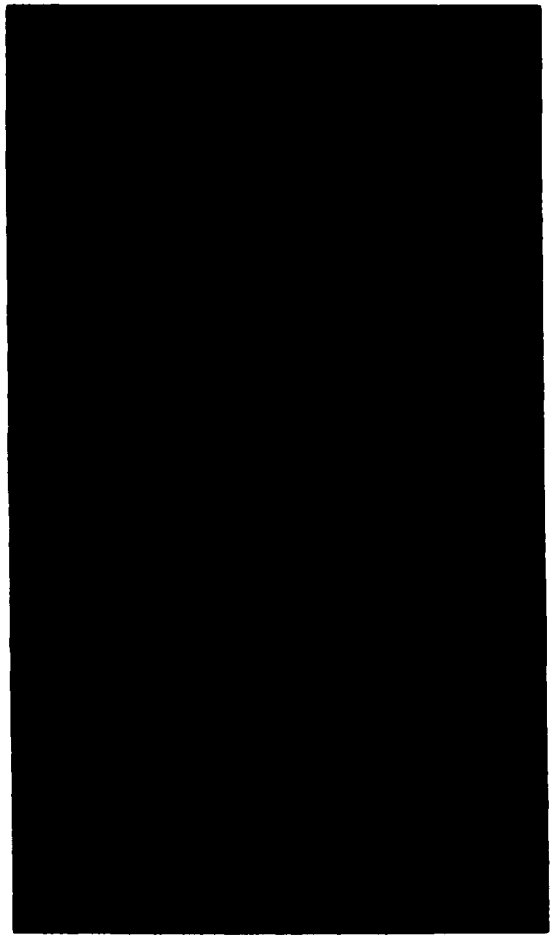

(c) Front View of Completed Column TC-3

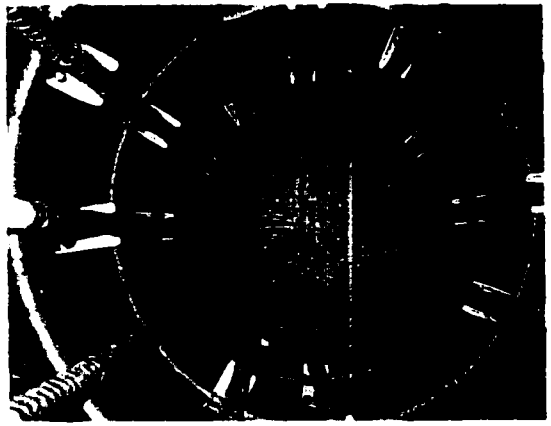

(d) Top View of TC-3

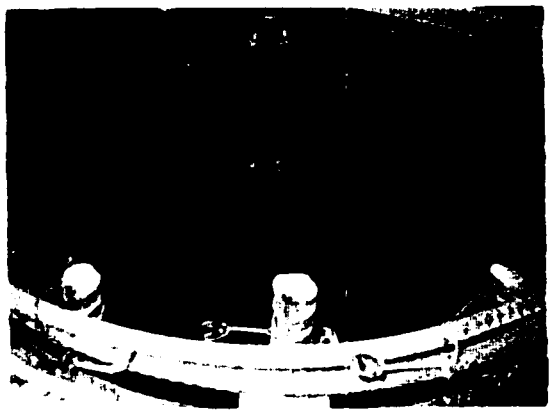

(e) Close-Up View of TC-3 at the Top

Figure 3.28 : (Continued)

(a) Sliding the First Tire in TC-5

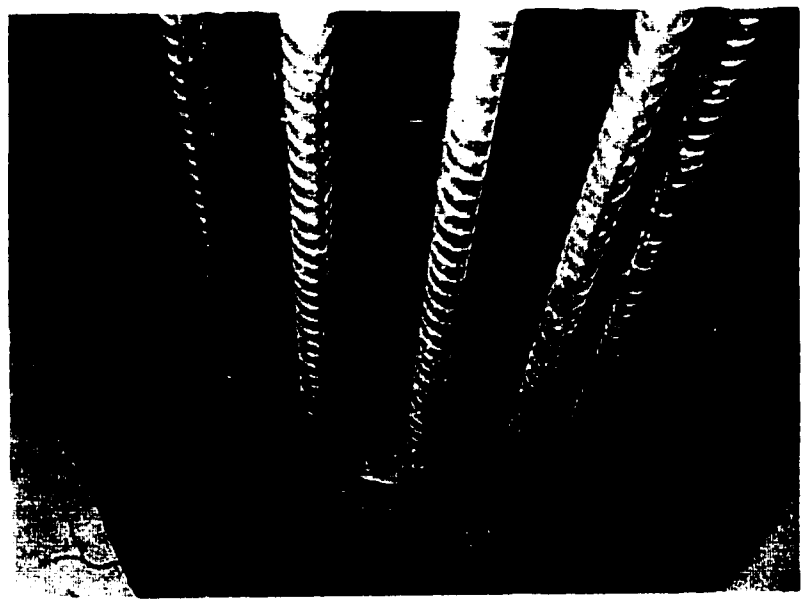

(b) Assembly in Process for TC-6

Figure 3.29 : Tire Assembly for Columns TC-5 and TC-6

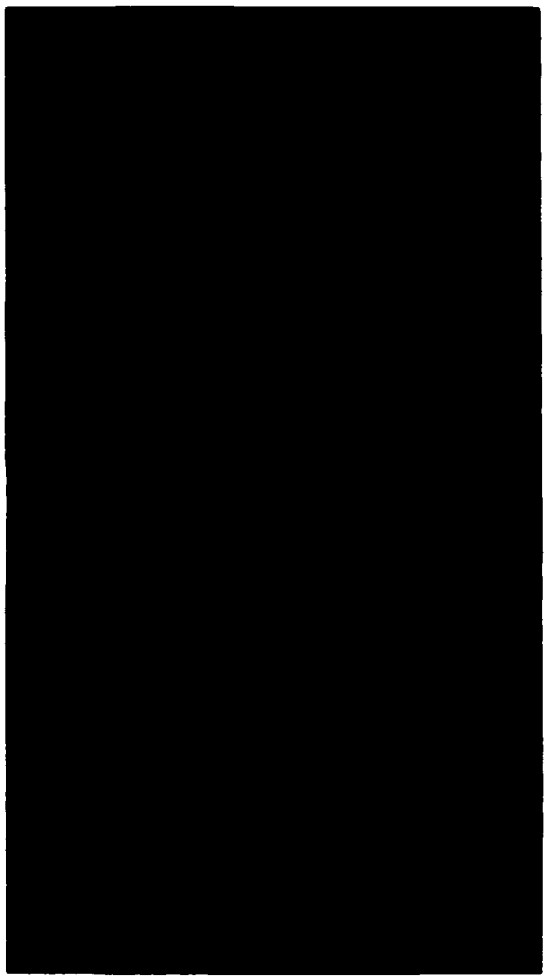

(c) Front View of TC-6 After Tire Assembly

(d) Top View of TC-5

(e) Close-Up View of TC-5 at the Top

Figure 3.29 : (Continued)

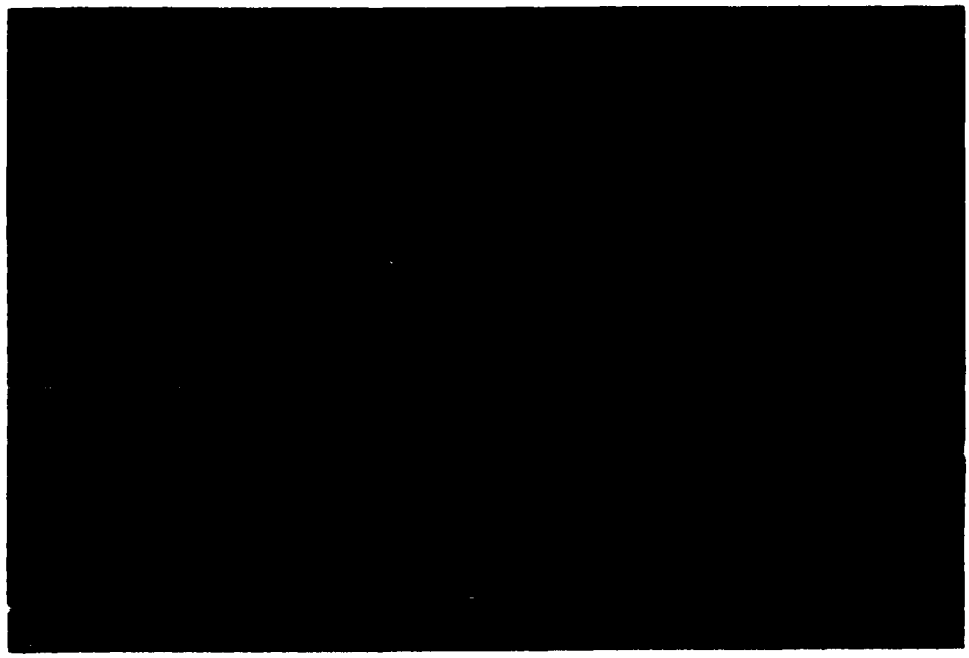

(a) Shortly Before Casting

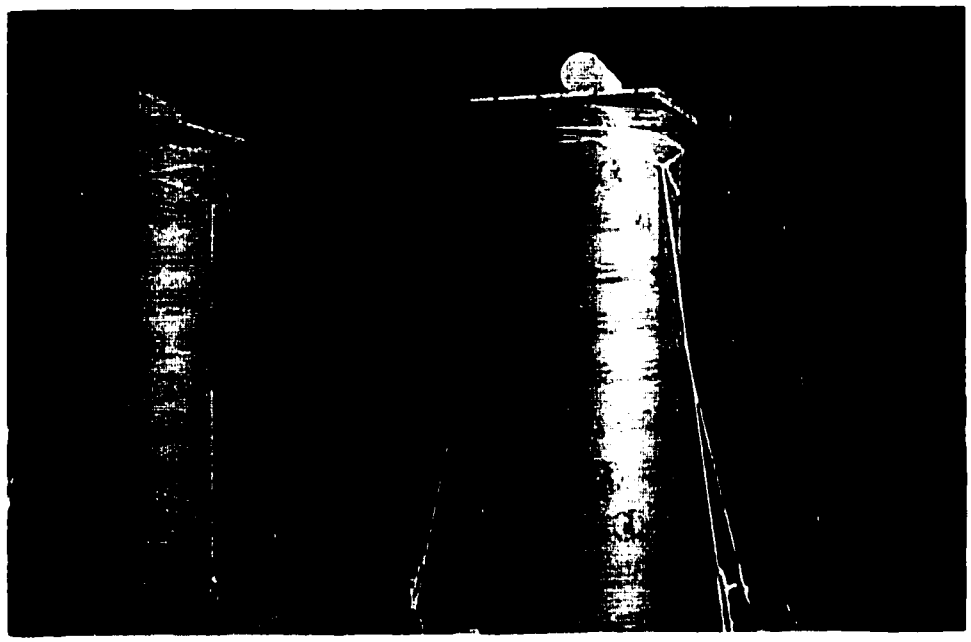

(b) At Completion

Figure 3.30 : Casting Column Specimens

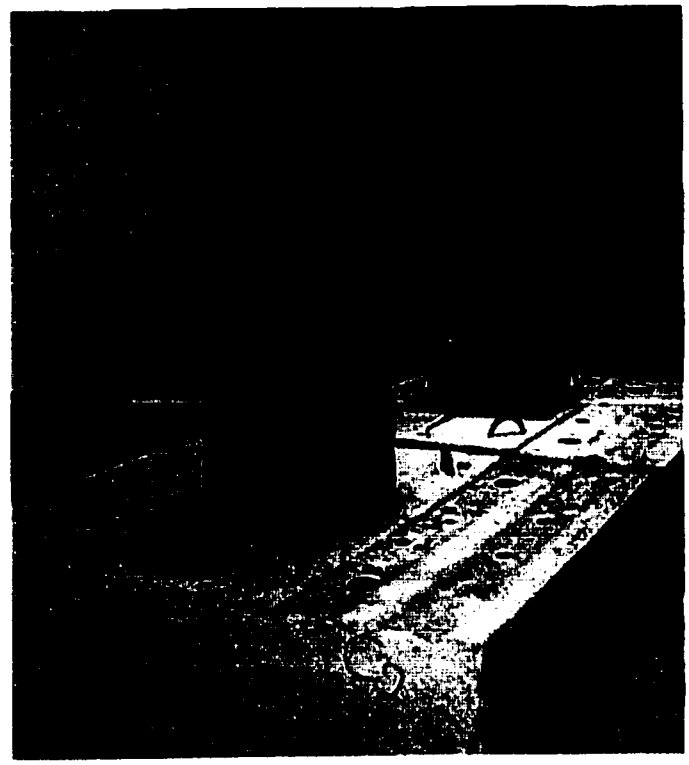

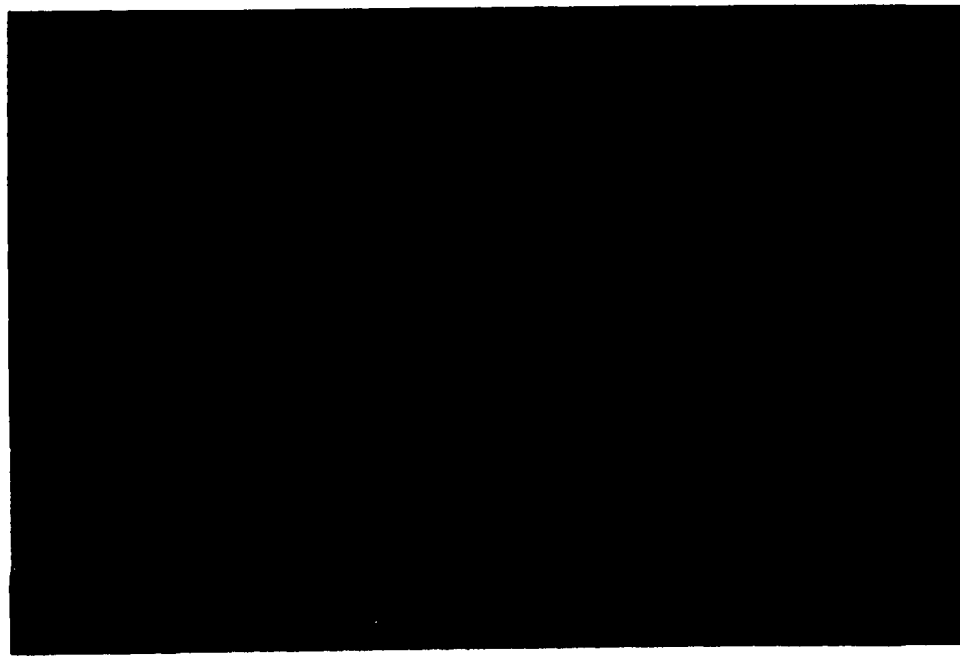

Figure 3.31 : Curing of Specimens in the Laboratory

(a) Data Acquisition System and MTS Controller

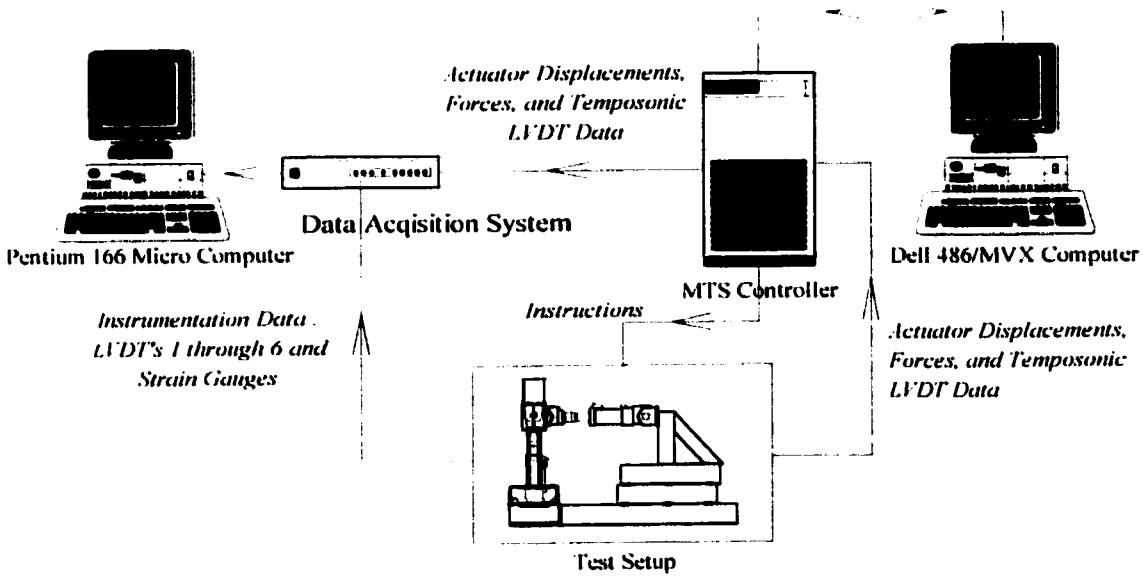

(b) Schematic Network Diagram

Figure 3.32 : Data Acquisition System, MTS Controller, and Network Diagram

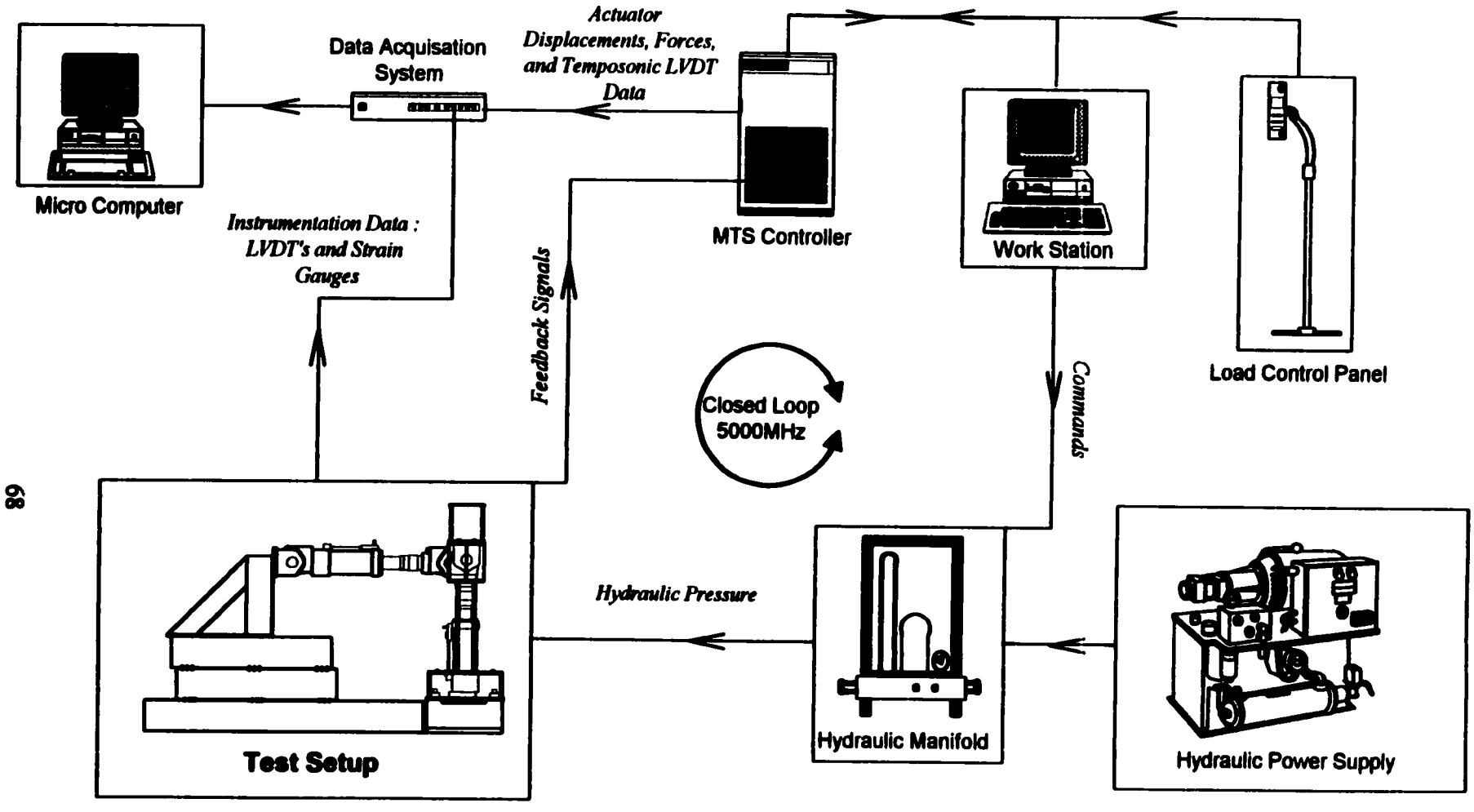

Figure 3.32 : (Continued)

Plan View

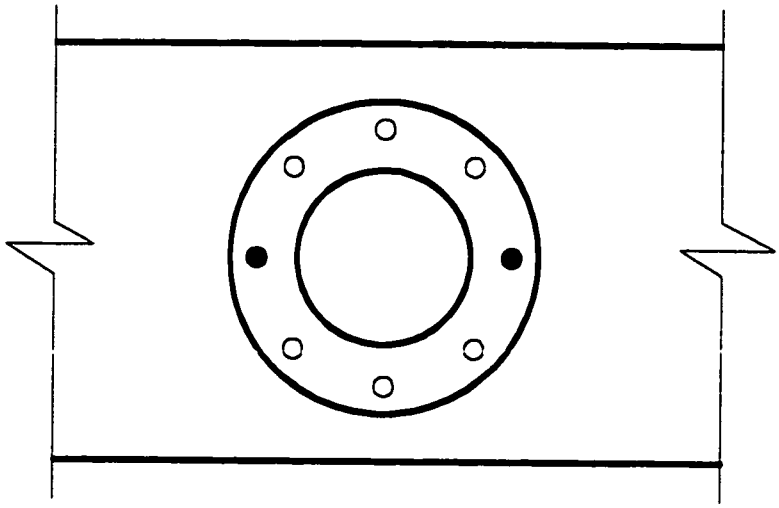

Elevation View

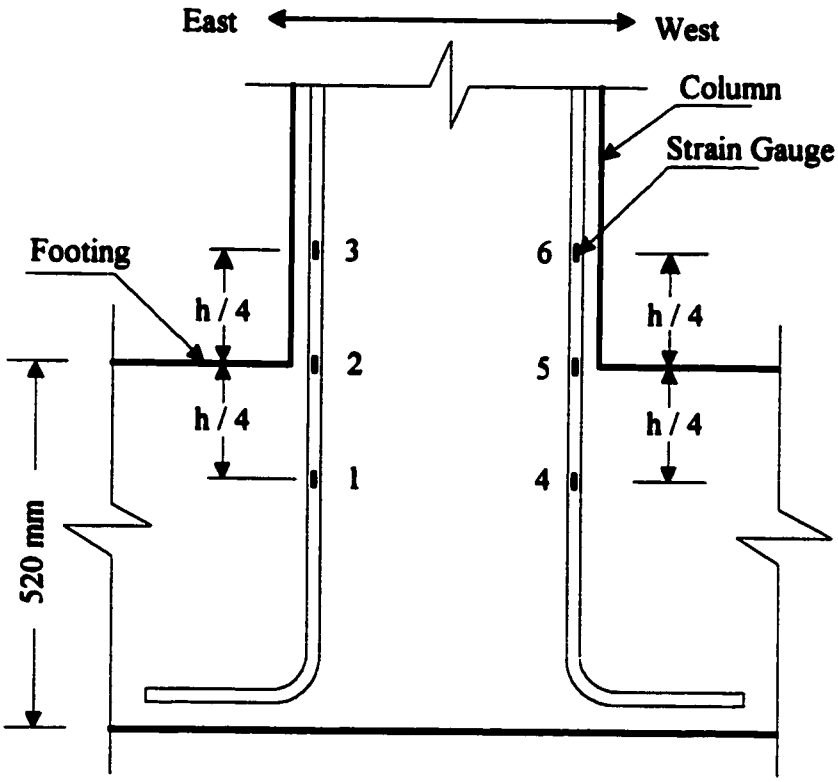

h = depth of column cross-section (545 mm)

Figure 3.33 : Location of Strain Gauges on Longitudinal Reinforcement in all Specimens

Gauges	Location
1,7	Longitudinal bar, 135 mm into footing
2,8	Longitudinal bar, at column-footing interface
3,9	Longitudinal bar, 135 mm above footing
4,10	First stirrup, 135 mm above footing
5,11	Second stirrup , 410 mm above footing
6,12	Third stirrup, 685 mm above footing

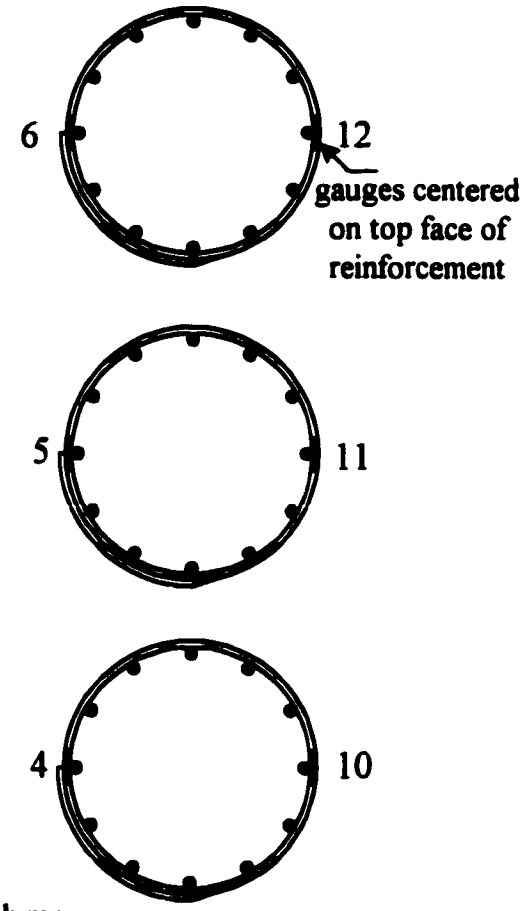

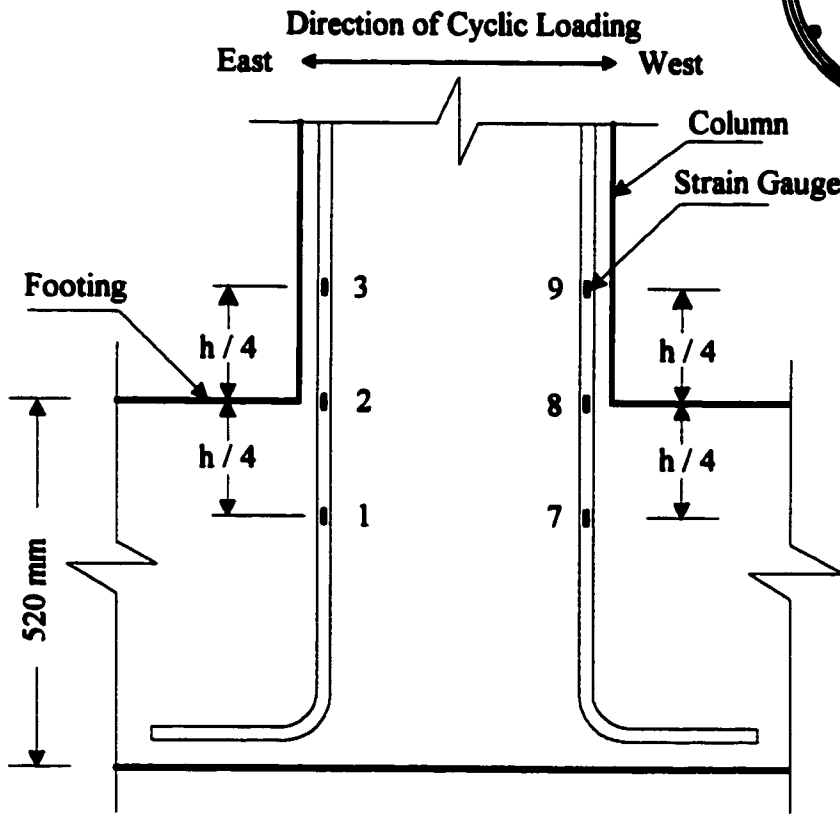

h = depth of column cross-section (545 mm)

Figure 3.34 : Location of Strain Gauges on Transverse Reinforcement for Columns TC-3 and TC-4

Gauges	Locations
7,8,9	First tire from the bottom on the east and west
10,11	First tire from the bottom on the south and north
12,13,14	Second tire from the bottom on the east and west
15,16	Second tire from the bottom on the south and north
17,18,19	Third tire from the bottom on the east and west
20,21	Third tire from the bottom on the south and north

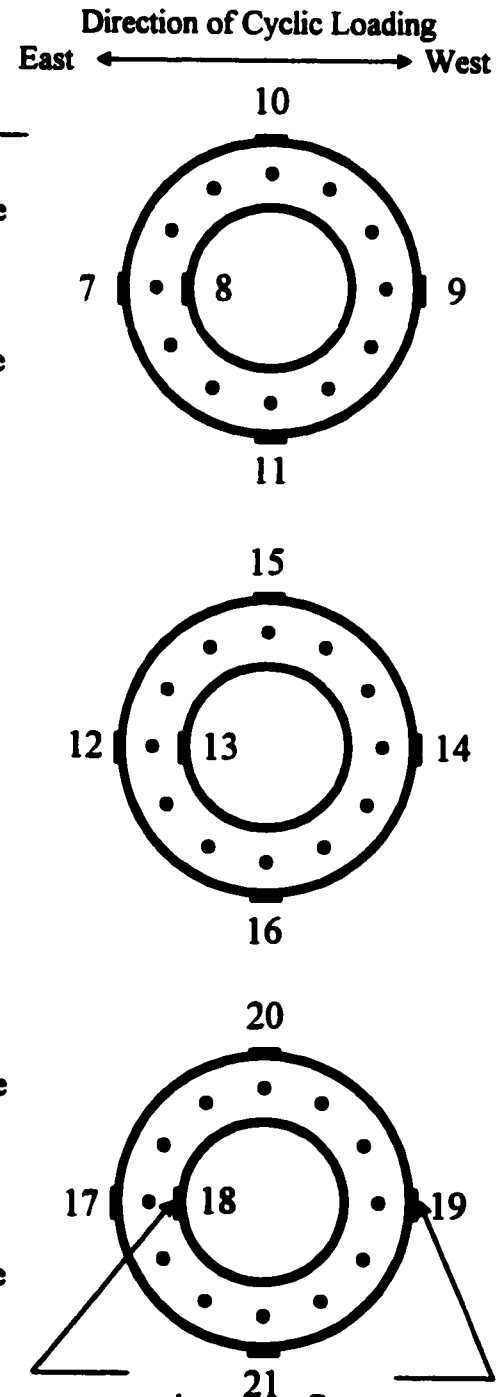

Note that gauge 1 to 6 are for longitudinal reinforcement

Gauges centered on top face of the rim

Gauges centered on front face of the tread part

a) Column TC-1

Figure 3.35 : Location of Strain Gauges on Tires

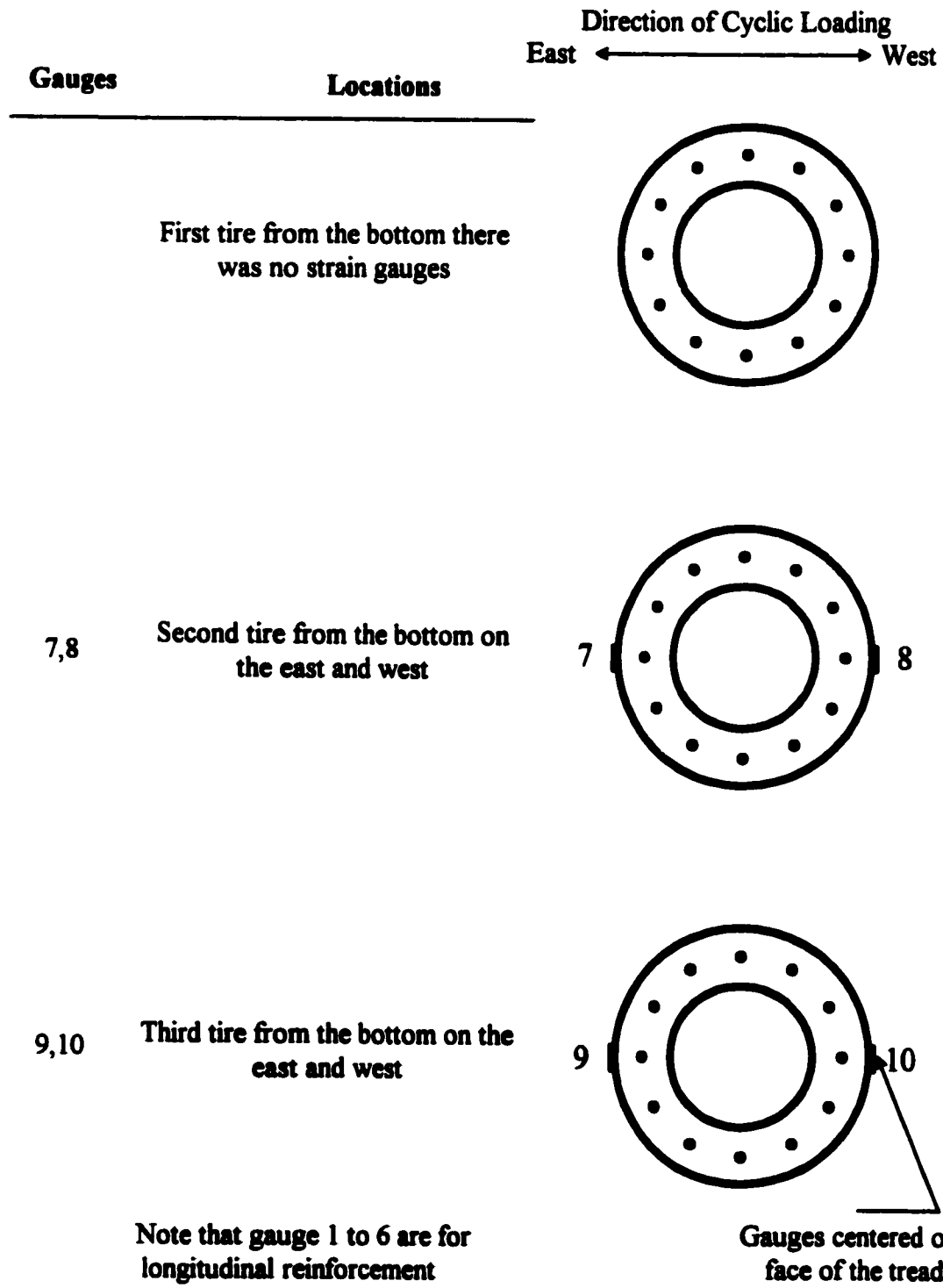

b) Column TC-2

Figure 3.35 : (Continued)

Gauges	Locations
13,14	First tire from the bottom on the east and west
15,16	First tire from the bottom on the south and north
17,18	Second tire from the bottom on the east and west
19,20	Second tire from the bottom on the south and north
21,22	Third tire from the bottom on the east and west
23,24	Third tire from the bottom on the south and north

Note that gauge 1 to 12 are for longitudinal and transverse reinforcement

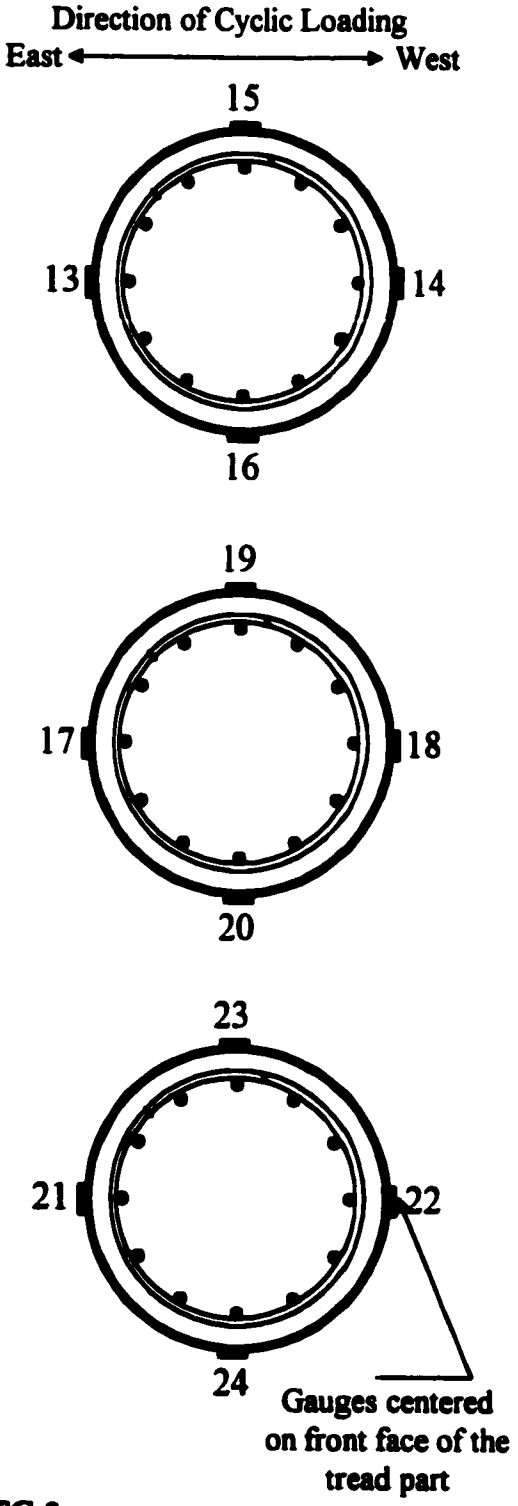

c) Column TC-3

Figure 3.35 : (Continued)

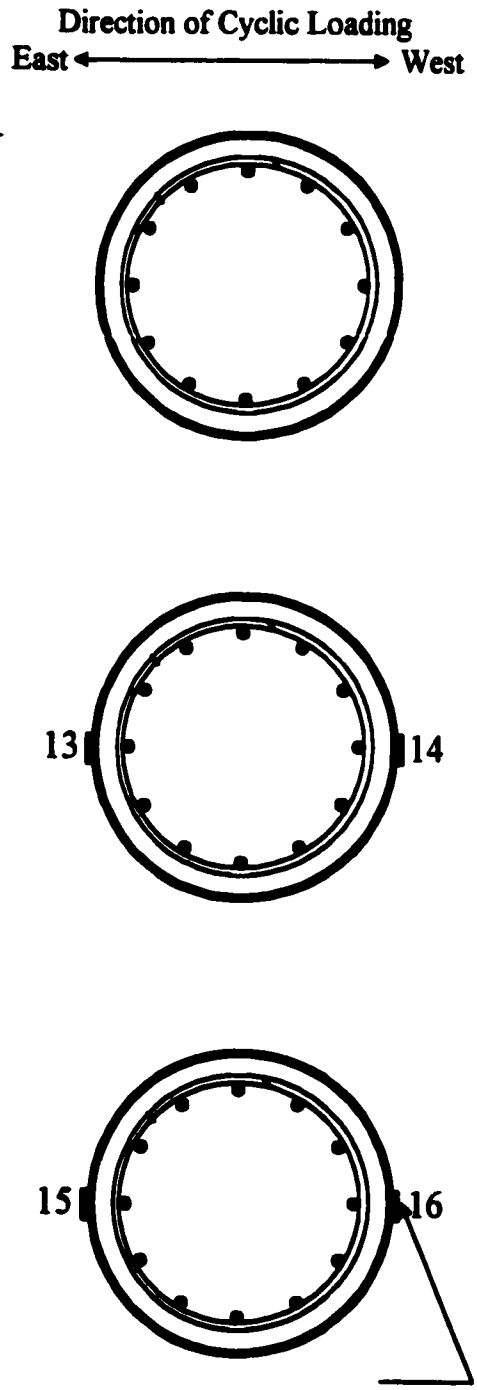

d) Column TC-4

Figure 3.35 : (Continued)

Gauges	Locations
7,8,9	First tire from the bottom on the east and west
10,11	First tire from the bottom on the south and north
12,13,14	Second tire from the bottom on the east and west
15,16	Second tire from the bottom on the south and north
17,18,19	Third tire from the bottom on the east and west
20,21	Third tire from the bottom on the south and north
	Note that gauge 1 to 6 are for longitudinal Reinforcement

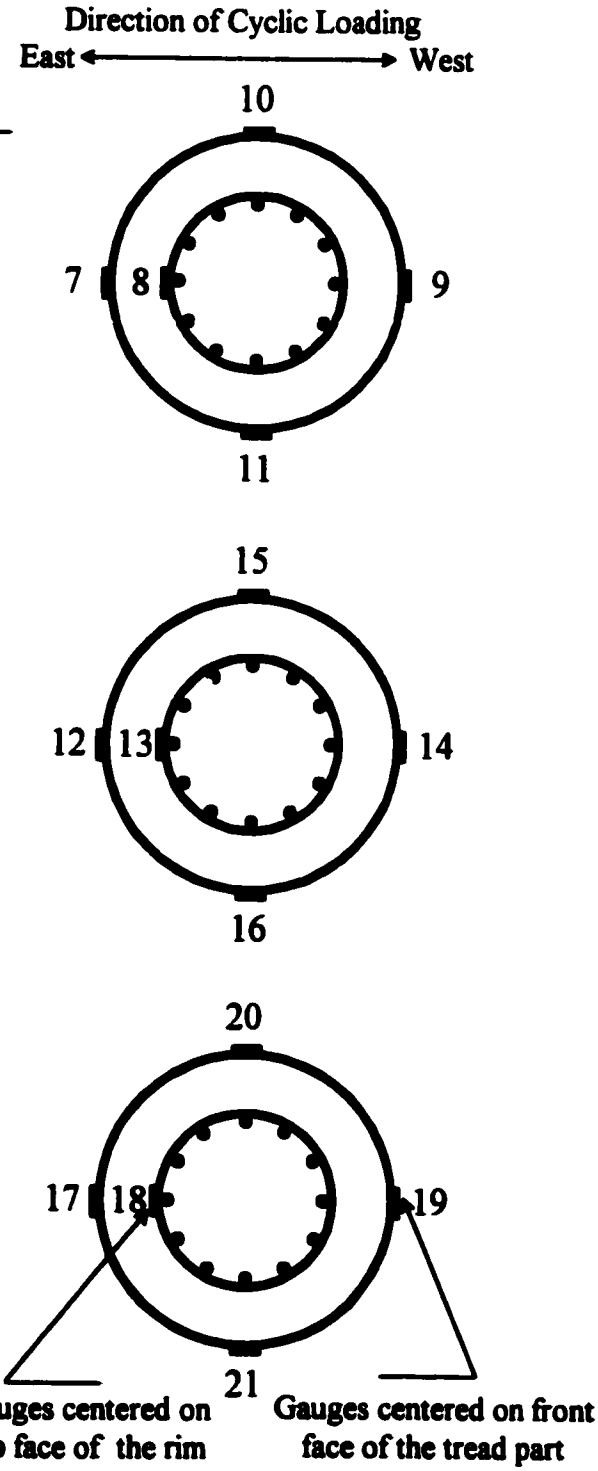

e) Column TC-5

Figure 3.35 : (Continued)

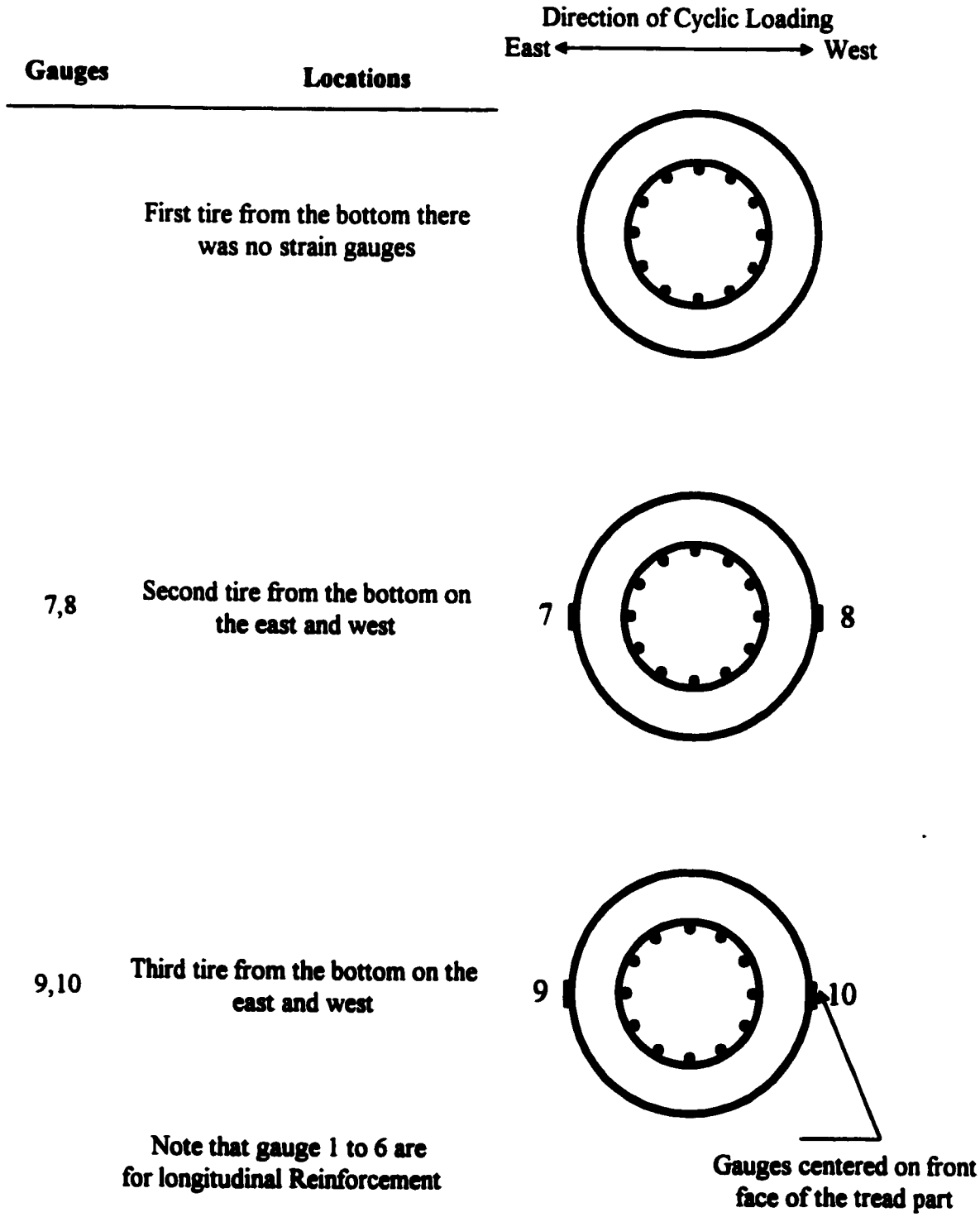

f) Column TC-6

Figure 3.35 : (Continued)

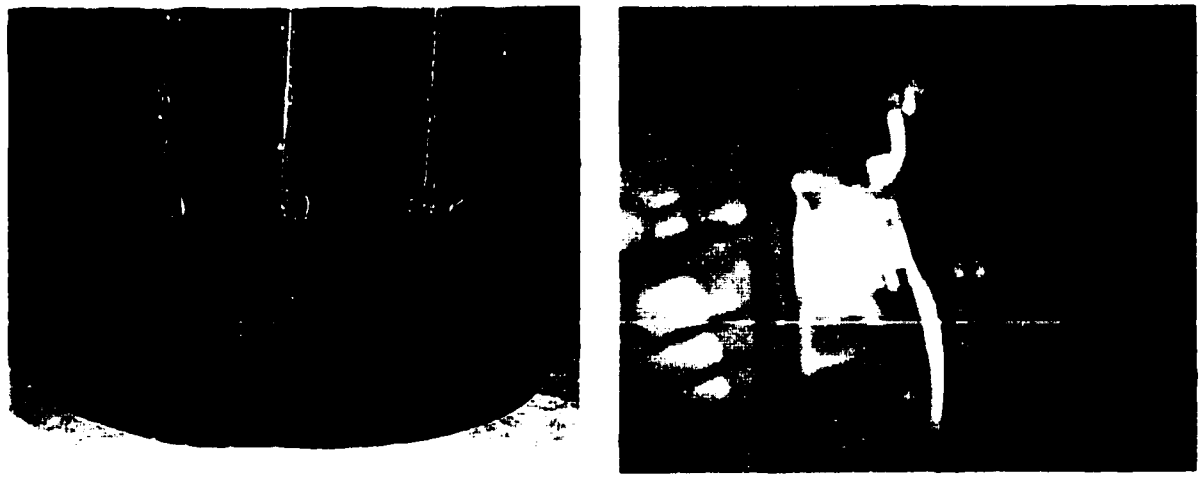

(a) Front View for Strain Gauges on Tread for Columns TC-1, TC-2, TC-5, and TC-6

(b) Top View for Strain Gauges on the Rim for Columns TC-1, TC-2, TC-5, and TC-6

Figure 3.36 : Photographs Showing the Locations of Strain Gauges on Tires for Columns TC-1, TC-2, TC-5, and TC-6

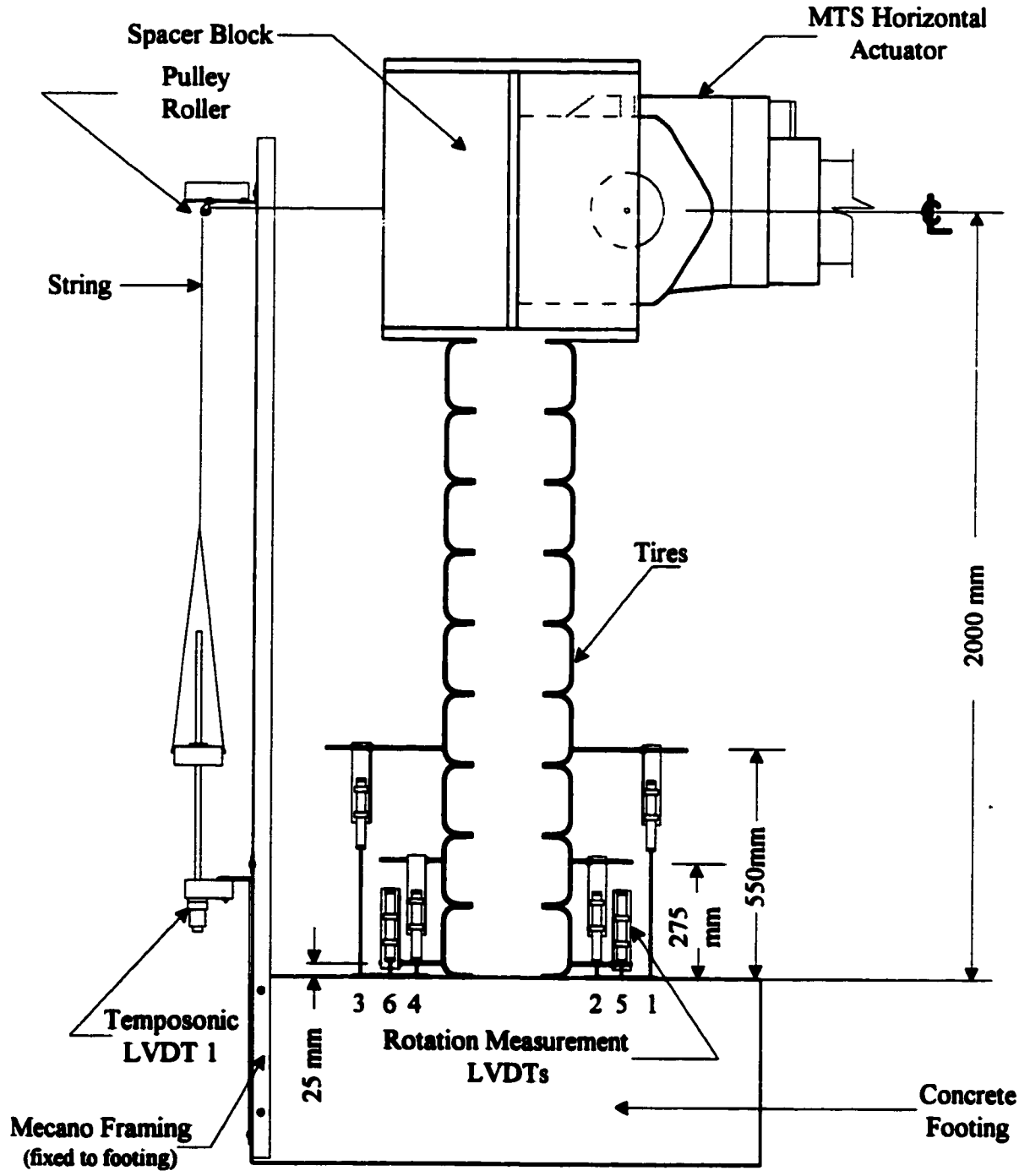

Figure 3.37 : Instrumentation for Displacement Measurements

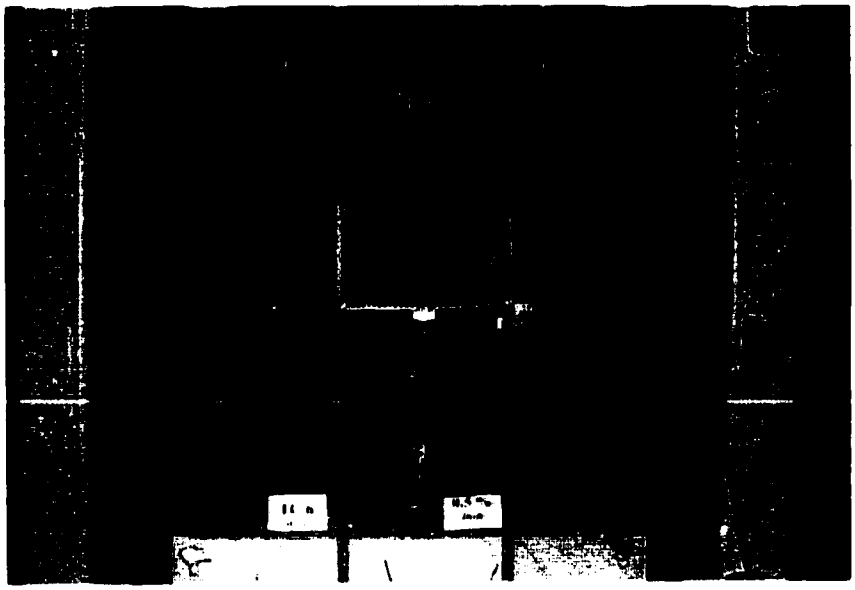

(a) West View

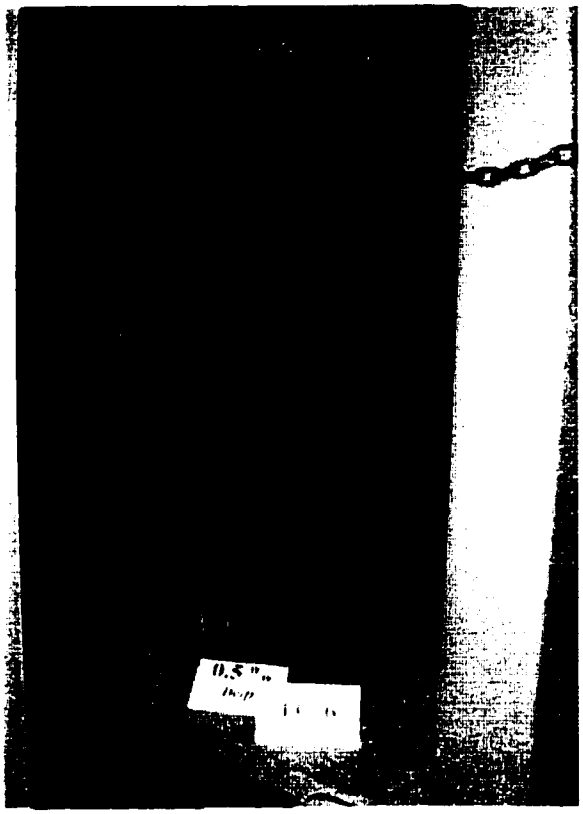

(b) East View

Figure 3.38 : Photographs of Instrumentation

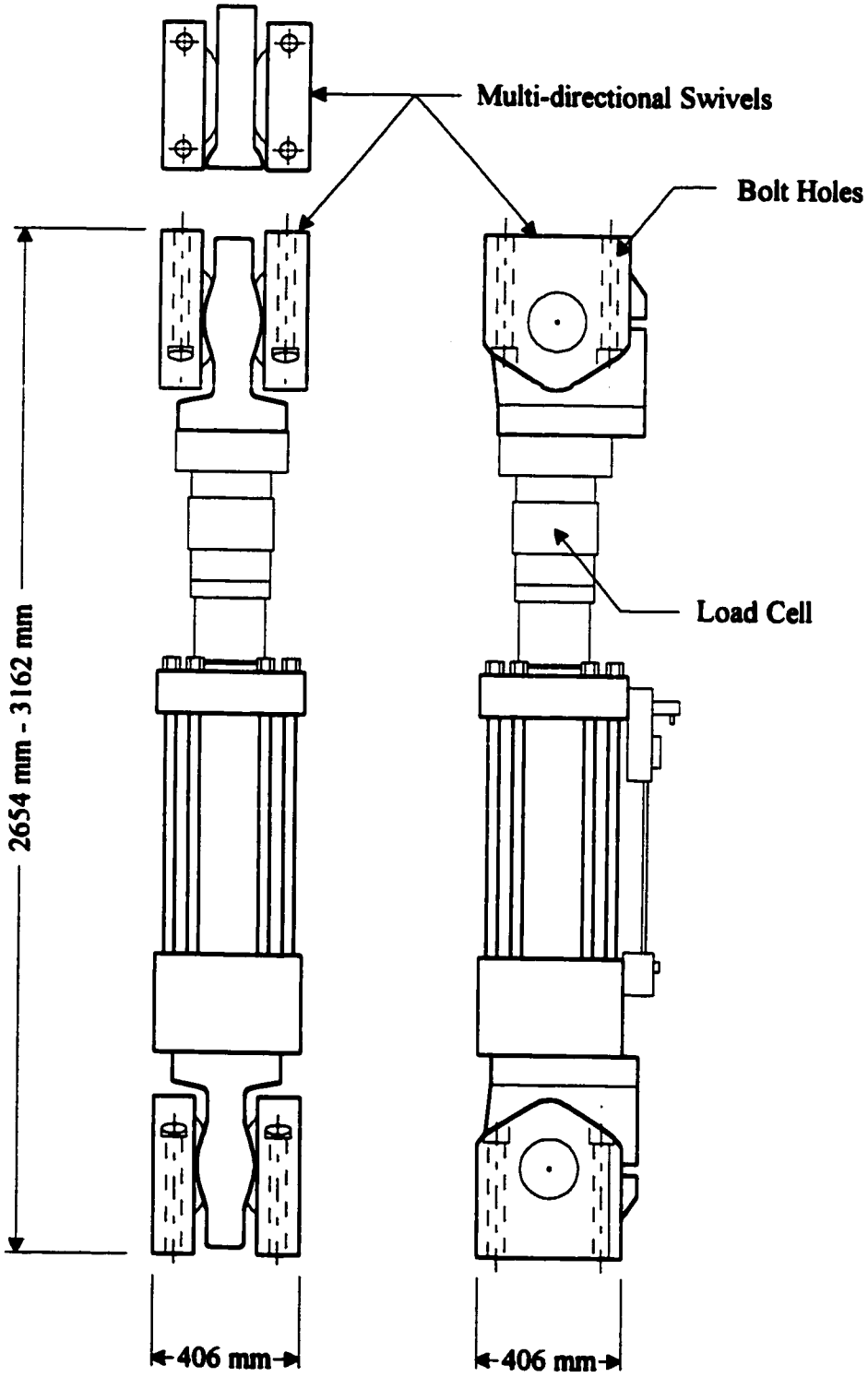

Figure 3.39 : Details of the MTS Actuators

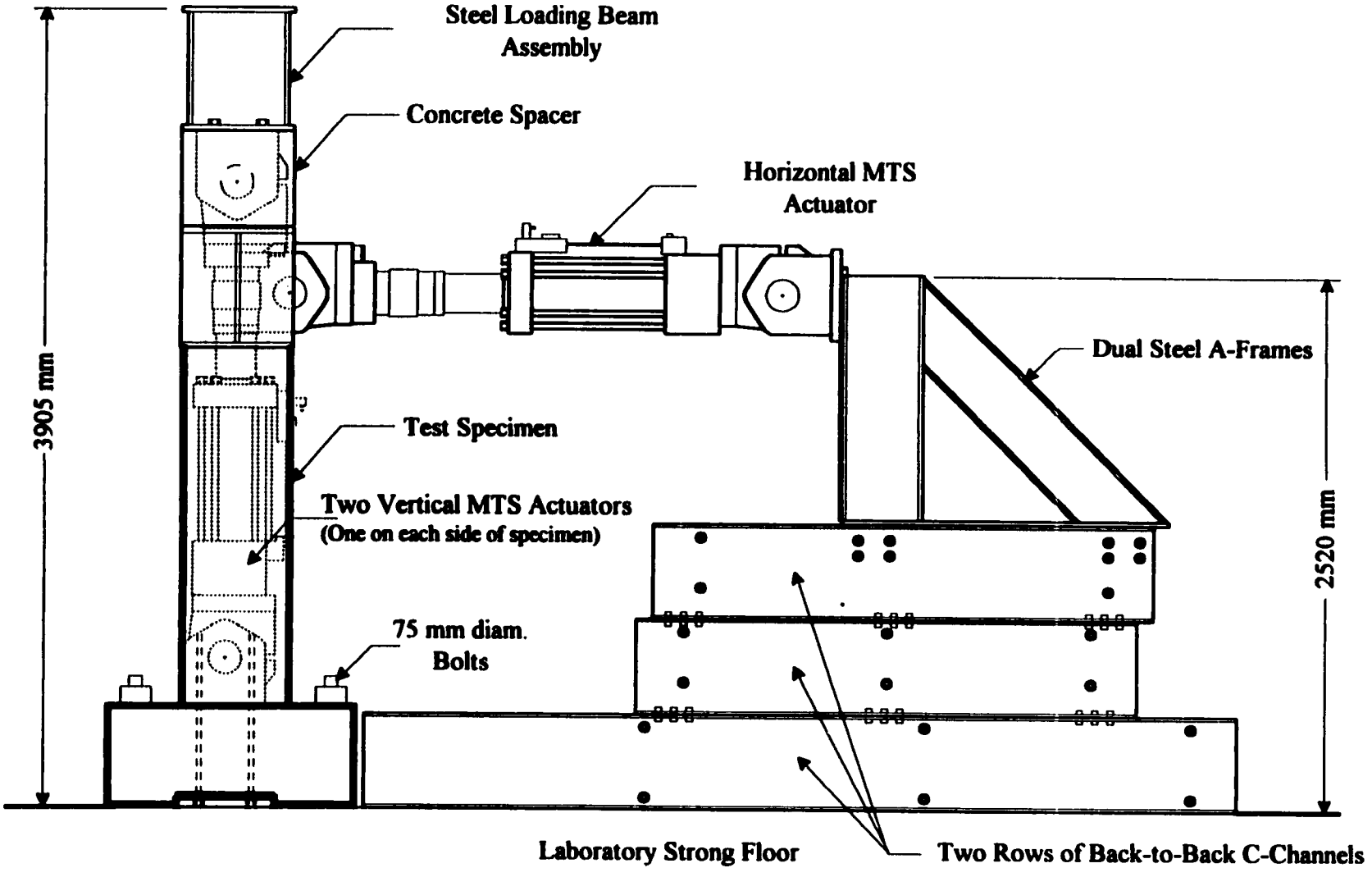

Figure 3.40 : Side Elevation of the Test Setup

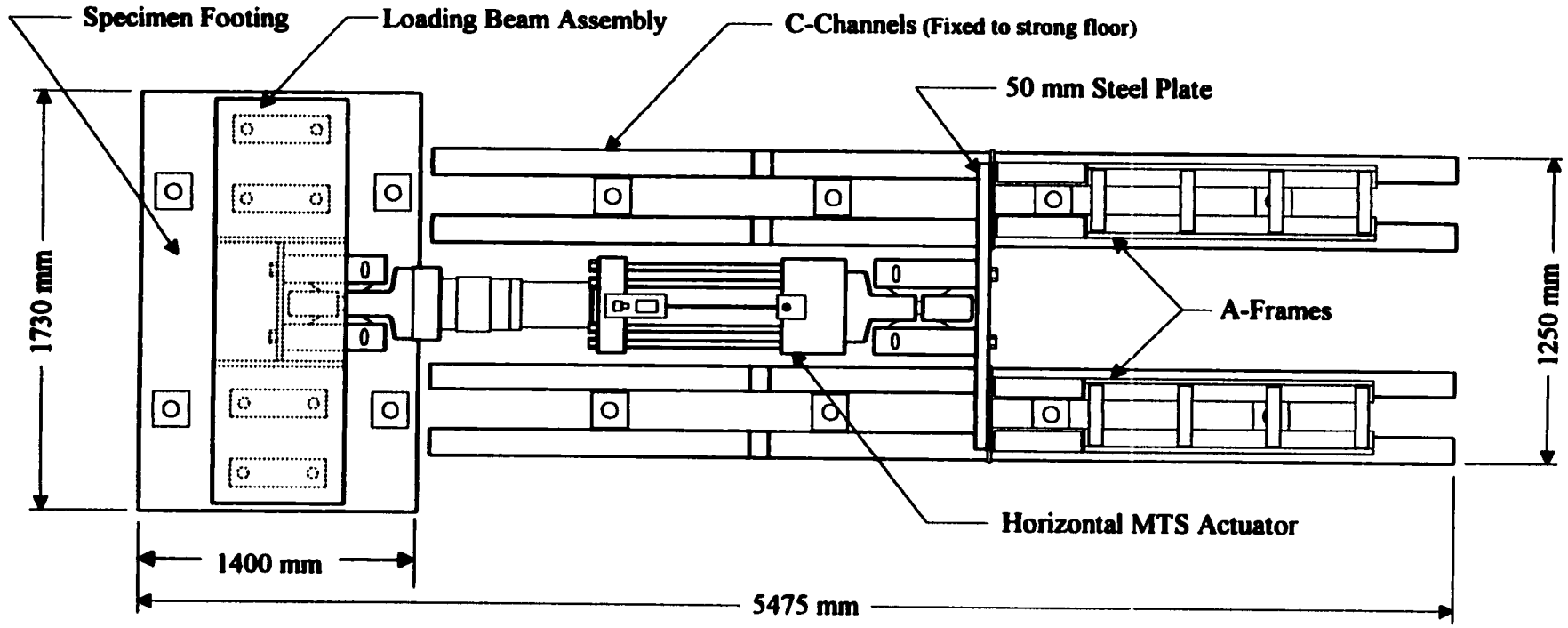

Figure 3.41 : Plan View of Test Setup

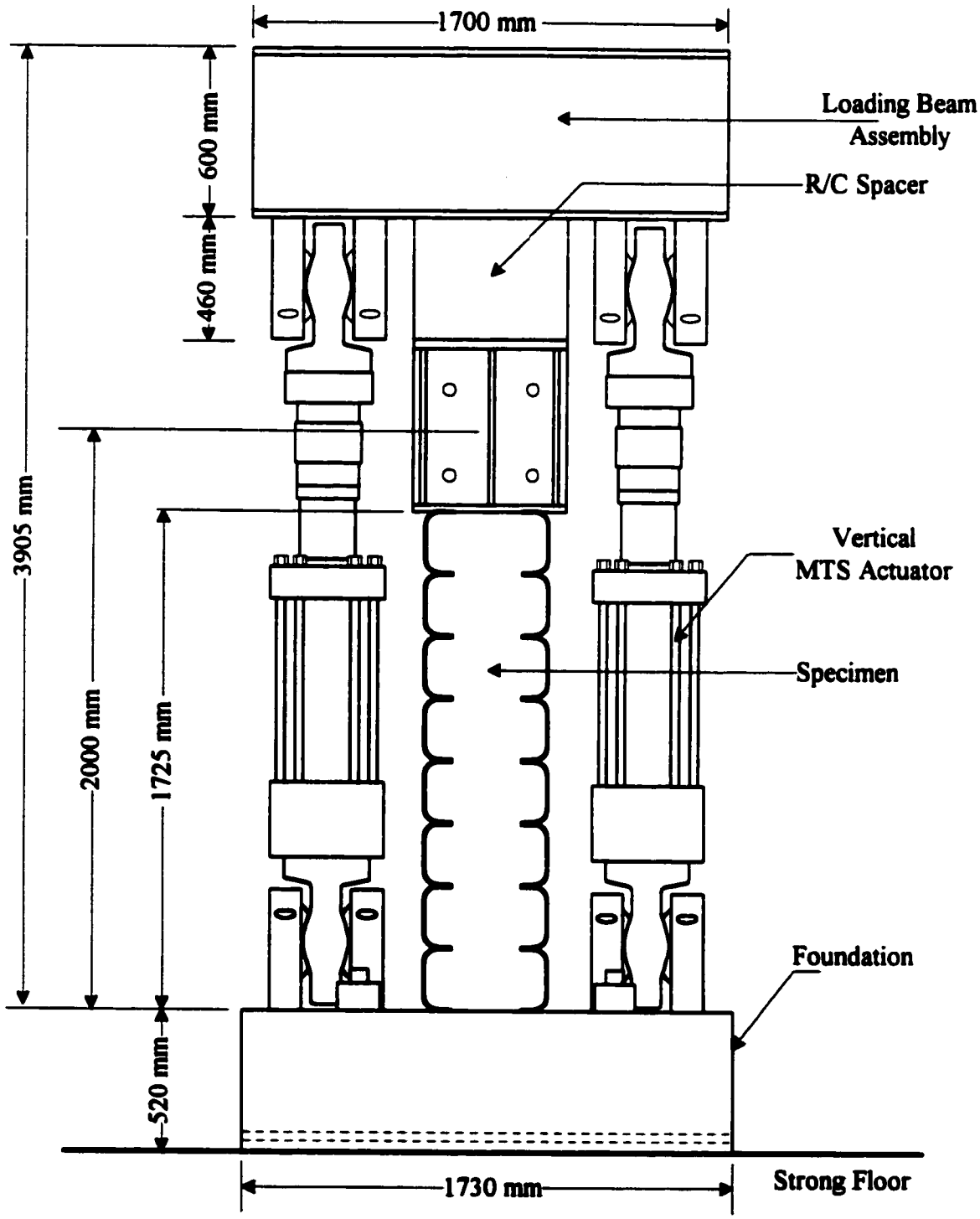

Figure 3.42 : Front Elevation of the Test Setup

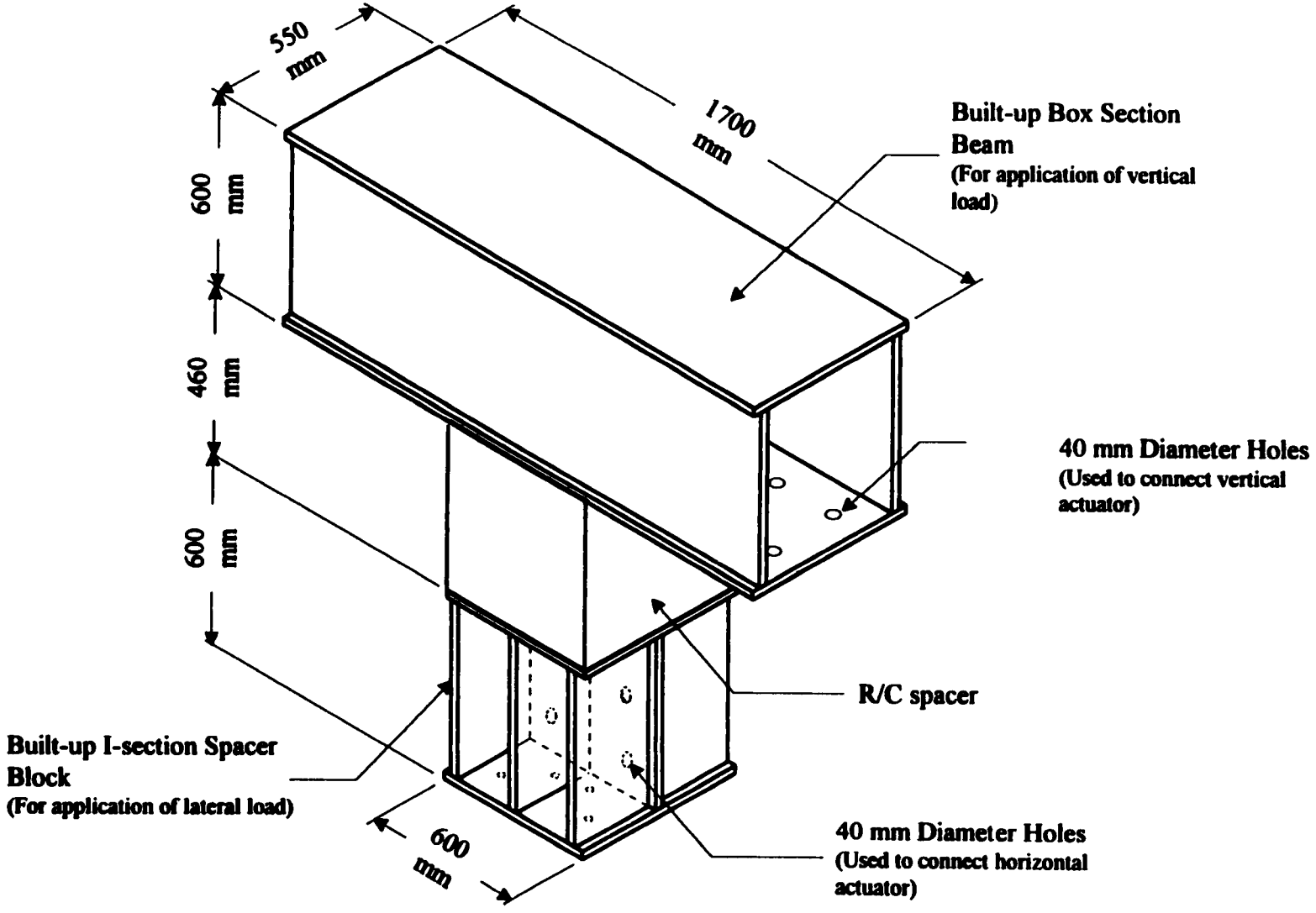

Figure 3.43 : Details of Loading Beam Assembly

(a) Front View

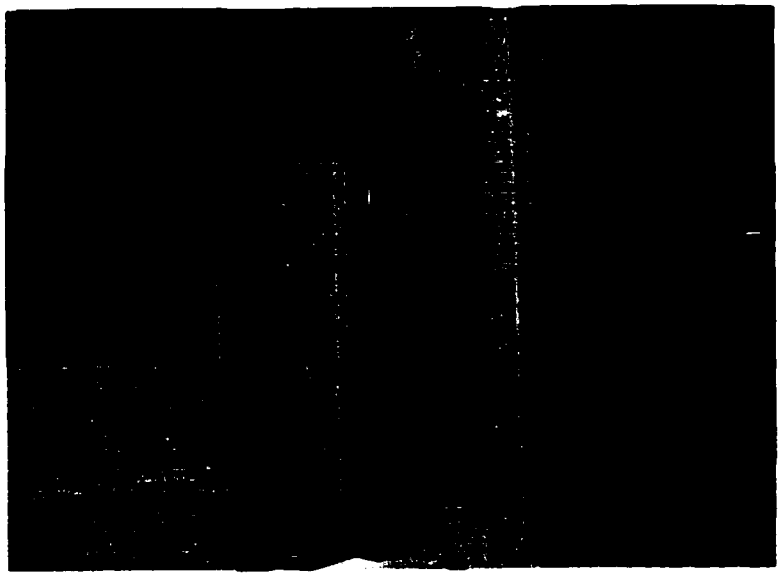

(b) Side View

Figure 3.44 : General Views of Lateral Restraint Frames

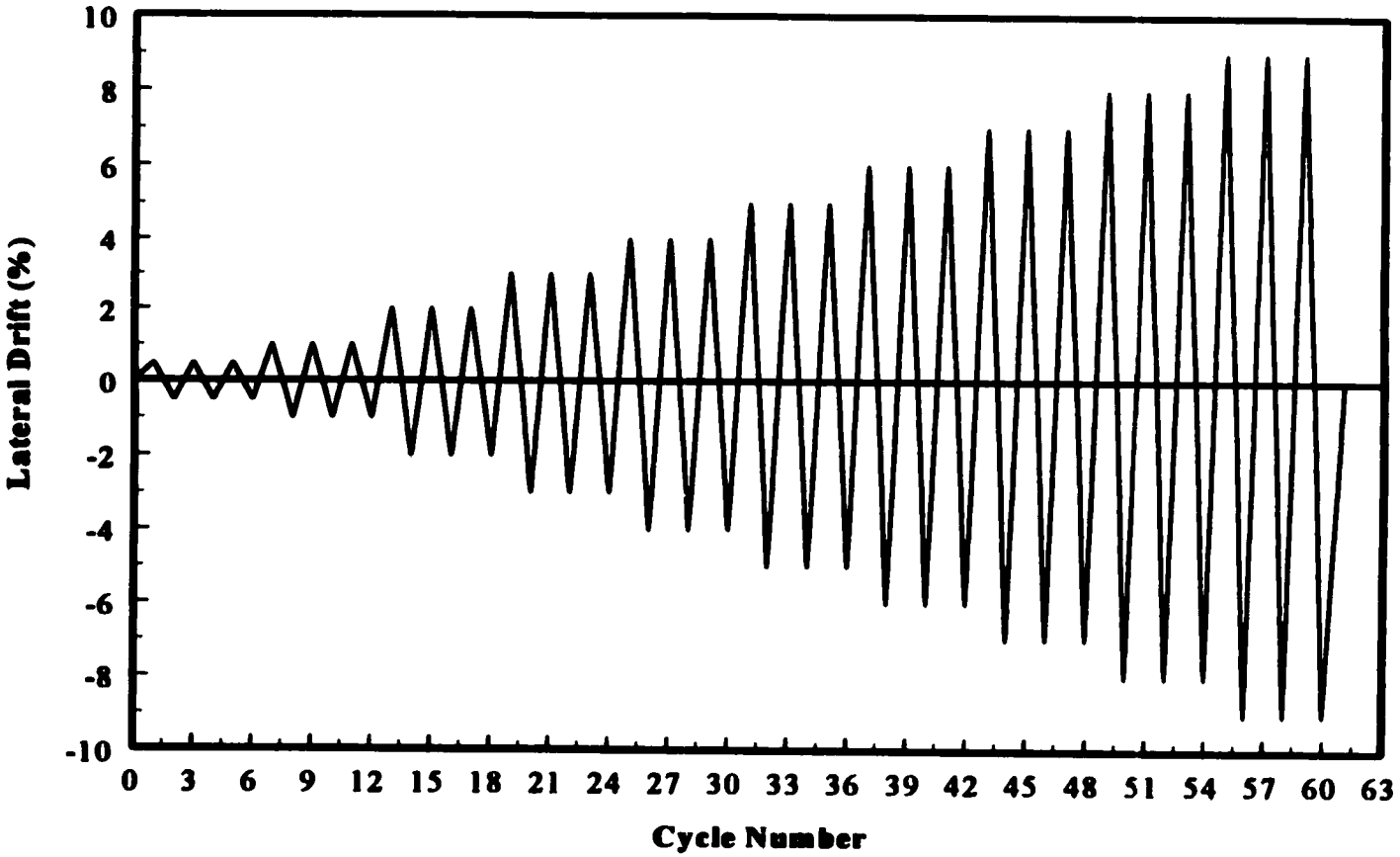

Figure 3.45 : Loading Program

CHAPTER 4

Test Results and Evaluation of Data

4.1 General

The test data and the observed behavior for each column are presented and discussed in this chapter. The column specimens were tested either under a low or high level of constant axial load, accompanied by lateral displacement reversals. The observed behavior as well as strain, displacement and force data for columns were recorded during the tests. Photographs were taken at the end of each drift level, as well as at different stages of loading when significant changes occurred in behaviour. The hysteretic behaviour is presented in terms of force-displacement and moment-displacement relationships. Strains in longitudinal and transverse reinforcement, as well as strains in the tread and rim of tires are presented and discussed. Hysteretic moment-total rotation, moment-anchorage slip rotation, and moment- flexural rotation relationships are also presented and discussed.

4.2 Observed Behaviour of Columns

Unlike conventional reinforced concrete columns, observation of damage in tire covered columns tested in the current research project was limited to rupturing of tires within the hinging region, and subsequent crushing and/or spalling of cover concrete at large inelastic deformations. Column behaviour was explained with reference to experimentally recorded hysteretic relationships. Lateral forces used to plot force-displacement hysteretic relationships, were net horizontal force components resisted by columns. These forces were obtained by subtracting the horizontal components of axial forces applied on columns. Moments used to plot hysteretic relationships were computed as the net lateral force times the shear span, plus

the vertical component of axial force times the horizontal displacement Δ, (P- Δ effect). The force-displacement relationships reflect degradation in lateral force resistance caused by P-Δ effects, as well as damage to columns, while the relationships for moments show only the strength decay caused by column damage.

Three sets of rotation readings were obtained from each column by means of six LVDTs. The first set consisted of rotations due to combined flexure and anchorage slip within distance "h" from the column-footing interface (h is the cross-sectional diameter of column, equal to 545 mm). This was referred to as total rotation of the assumed hinging region relative to the footing. The second set also gave total rotations, but this time within h/2 from the column-footing interface. The last set was intended to reflect the rigid-body rotation of the column base, caused by the extension of longitudinal column reinforcement within the footing, and was recorded at approximately 25 mm above the column-footing interface. All rotation readings were discontinued to be recorded shortly before the end of testing to safeguard the instrumentation against possible damage. Flexure rotations of the hinging region were obtained by subtracting the anchorage slip components from the total recorded.

The columns were loaded until one of the following conditions occurred: (a) rupture one of the tires in the hinging region which resulted in the spalling of concrete and a subsequent damage, or (b) the lateral load capacity of the column drop by 20%, i.e., down to 80% of the peak resistance. The amount of damage on each column varied depending on the level of axial force and the degree of confinement provided by reinforcement, including tires. A discussion of column behaviour is provided below for each specimen.

4.2.1 Column TC-1

Column TC-1 was confined by whole tires. The longitudinal steel reinforcement consisted of 12#20 (19.6 mm diameter) bars. There was no conventional transverse reinforcement in this column. Holes were made in the sidewall of the tires by a tire template, and the longitudinal

bars were inserted through the sidewalls as the tires were staked on top of each other. The column was tested under a constant compressive force of 1000 kN, which represented 11% of its concentric capacity. The actual test started with the application of full axial load, followed by lateral load reversals in displacement control mode.

During the first three cycles at 0.5% lateral drift, no damage was observed and the maximum lateral load recorded was 127 kN. The longitudinal reinforcement developed strains to indicate yielding during the third cycle at 1% drift. The strains in the extreme longitudinal bar on the east side reached 0.22% at column footing interface and 0.29% at a height of 135 mm above the footing surface. At 135 mm below the footing surface, no yielding was recorded until after 2% drift. Strains on the tread and rim of the second tire on the east side reached 0.25% and 0.2% at the first cycle of 3% drift and 0.26% and 0.3% at the end of the third cycle of the same drift level. The strain in the rim of the first tire reached 0.24% at this level of deformation. The strains in longitudinal reinforcement, at 135 mm above the footing, reached 0.7% to 0.89% during the first cycle of 4% drift, indicating higher strains and possibly higher expansion of concrete at locations above the base. At the end of 4% drift cycles, the strain in the extreme longitudinal reinforcement at 135 mm below the footing reached 0.37%. The maximum lateral load at 4% drift was 196 kN. No damage was visible until the end of 4% drift, as evidenced by Fig. 4.1.

At the beginning of 5% drift, Gauges 2, 8, and 10 were damaged. Subsequently, the second tire from the bottom started to separate from the base due to the formation of a crack at column-footing interface. The strain in the tread of the second tire reached a maximum value of 0.42% at the end of 5% drift cycles. The column survived 6% drift without any sign of severe damage, but most of the strain gauges were damaged. LVDTs 3 and 4 were out of stroke during the second cycle of 7% drift. There was a significant drop in load resistance at 7% lateral drift, which could be attributed to the rupturing of longitudinal reinforcement in tension. The first and second tires from the bottom started to separate from each other, at the first cycle at 8% drift, exposing the longitudinal reinforcement. However, there was no

buckling of longitudinal reinforcement observed.

This column developed 6.5% lateral drift prior to developing 20% decay in lateral force resistance. At the end of 8% drift the lateral load dropped down to 40% of peak resistance, and the test was stopped due to a safety concern, though there was no extensive damage observed. The duration of the test for this column was about three and a half hours. Figure 4.1 shows the behaviour of column TC-1 during selected stages of testing. All pictures were taken at the last cycle of each drift level.

The hysteretic force-displacement and moment-displacement relationships are illustrated in Figs. 4.2 and 4.3. These relationships indicate that the column developed ductile behaviour and show stable hysteresis loops up to 6% drift. There was no significant strength decay up to 6.5% drift. The decay in load resistance dropped by about 40% during the first cycle of 8% drift due to the rupture of longitudinal reinforcement. Hysteretic moment-total rotation, moment-anchorage slip rotation, and moment-flexural rotation relationships are shown in Figs. 4.4, 4.5 and 4.6, respectively, where Figs. 4.4 and 4.6 include total and flexural rotations at h and h/2 distances above the footing (h=550 mm). Figure 4.5 indicates that approximately 2/6th of the total rotation was caused by anchorage slip, and 4/6th caused by flexure.

The strain gauge data are plotted in Figs. 4.7 and 4.8. It should be noted that most of the strain gauges were damaged during 5% to 6% drift cycles, before the end of test. Therefore, the data shown do not provide strains beyond this deformation level.

4.2.2 Column TC-2

Column TC-2 was identical to TC-1. However, this column was subjected to a higher axial load of 1900 kN, which represented 21% of its concentric capacity. The actual test started with the application of full axial load, followed by lateral load reversals that were applied in the displacement control mode.

The column capacity was different than that of the companion column (TC-1). The maximum lateral load recorded at 0.5% drift was 135 kN. The load resistance increased to 200 kN at the end of 1% drift. Strain Gauges 2, 3, 5 and 6 were damaged during the preparation of column, prior to test. The treads in the third tire developed high strains relatively early in testing, reaching 4.37% on the east side, at the beginning of 2% drift cycles. The strain gauge on the east side was damaged and stopped functioning at this load stage. The longitudinal reinforcement at 135 mm below the column-footing interface yielded, developing 0.244% strain at the end of 3% drift cycles. Because Gauges 2,3,5 and 6 had been damaged, it was not possible to obtain strain gauge readings at column-footing interface and at 135 mm above the column-footing.

The second tire showed signs of excessive deformation during 4% drift cycles, developing 0.43% transverse strain on west treads. This was attributed to the tendency of longitudinal reinforcement to buckle, which was prevented by the tire. The Column survived 4% lateral drift without any drop in load resistance. At the first cycle of 5% drift, the first tire from the bottom ruptured and opened up. When the column was pushed further to start the second cycle, the sidewall of the tire at the column-footing interface ruptured on the west side, exposing cracked concrete inside. When the second cycle at 5% drift was applied, the first tire opened up widely, followed by the rupturing of steel within the treads on the north-east side of the third tire. The column could not survive the sudden rupturing of the first and third tires from the bottom. The test was discontinued at the end of 5% drift. Figure 4.9 shows the behaviour of Column TC-2 during selected stages of testing. The duration of the test for this column was two hours.

The hysteretic lateral force-lateral displacement and moment-lateral displacement relationships obtained during testing are shown in Figs. 4.10 and 4.11. These relationships indicate that the column showed ductile behaviour and stable hysteresis loops up to 4% lateral drift. There was no significant strength decay until this level of deformation, though subsequently the column capacity dropped by 21% during the second cycle of 5% drift, when the tires ruptured.

Figures 4.12, 4.13 and 4.14 show hysteretic moment-total rotation, moment-anchorage slip rotation, and moment-flexural rotation relationships for Column TC-2, respectively. Figure 4.13 indicates that, approximately 1/4th of the total rotation was caused by anchorage slip, leaving 3/4th to flexure.

Figures 4.15 and 4.16 illustrate the strain gauge data for longitudinal reinforcement and treads of tires. There was no strain gauge on the rim of tires in this column. Most of the gauges were damaged at about 4% drift. Hence, the strain readings could not be recorded beyond this deformation level.

4.2.3 Column TC-3

The tire configuration used in this column was different than that used in TC-1 and TC2. The tires in this case were used without their sidewalls, with longitudinal bars enclosed by the treaded parts of tires. The confinement to column concrete was provided by the treaded parts of tires, as well as circular hoops that were used to tie the longitudinal bars with a spacing of 275 mm. The column was subjected to axial compression of 1900 kN, which represented 21% of its concentric capacity. The actual test started with the application of full axial load, followed by lateral load reversals applied in displacement control mode. The strain gauge number 6 was damaged during construction, prior to testing.

The load resistance observed was completely different from those of the two previous columns, because of the difference in cross-sectional characteristics. This column showed the highest lateral load resistance. The maximum lateral load recorded at 0.5% drift was 265 kN. This load resistance increased to 342 kN at the end of 1% drift. Yielding of longitudinal reinforcement in extreme east and west bars were observed at this deformation level, with strains reaching to 0.23%. Yielding of transverse hoop reinforcement was also recorded, with tensile strains reaching 0.7% at 685 mm from column-footing interface (third hoop). The strain in the extreme tension bar, at column-footing interface on the west side, reached 1.12%

at the end of 1% lateral drift. Also, at 135 mm above and below the column-footing interface, the strains in longitudinal reinforcement reached 0.24%. The tensile strains in longitudinal reinforcement reached 1.03% and 0.63% at column-footing interface on the east side, and at 135 mm above the footing, respectively, at the end of the 2% drift cycles.

There was no strength degradation during the first cycle at 3% drift, though a wide crack was observed between the first and second tires. At the end of 3% drift cycles, all strain gauges on longitudinal reinforcement developed tension and compression yielding. The bar on the extreme west side developed a tensile strain of 1.23%.

At the beginning of 4% drift, the second tire showed signs of expansion, and the space between the tires became wider, exposing cracked concrete in between. Significant strength decay was observed at this stage. Column capacity dropped suddenly by 34% during the first cycle of 4% drift. Gradual spalling of concrete between the tires occurred near the top of the first tire when the second cycle was applied at 4% drift. Progression of cover spalling was observed at the top and bottom of the second and third tires during subsequent cycles. Spalling became more clear after the sudden rupture of the second tire from the bottom, on the west side. The second tire ruptured completely into two pieces, and the concrete cover spalled off completely within this region, when the cycles at 4% drift were completed. The longitudinal reinforcement buckled within the same region and the load dropped sharply to 200 kN. The test was then terminated. Figure 4.17 shows the behaviour of Column TC-3 at selected stages of testing. The duration of the test for this column was one hour and fifteen minutes.

The hysteretic curves for lateral force-lateral displacement and moment-lateral displacement relationships obtained from test data are shown in Figs. 4.18 and 4.19. These relationships indicate that the column showed stable hysteresis loops up to 3% lateral drift. There was no significant strength decay up to 3% drift but the column capacity dropped by 34% during the first cycles of 4% drift where the rupture of the second tire was observed. Figures 4.20, 4.21

and 4.22 show hysteretic moment-total rotation, moment-anchorage slip rotation, and moment-flexural rotation relationships, respectively, for Column TC-3. Figure 4.21 indicates that approximately 1/3th of the total rotation was caused by anchorage slip, and 2/3th caused by flexure. Figures 4.23 and 4.24 illustrate the strain gauge data for longitudinal and transverse reinforcement, respectively. The strain gauge data for tire treads are shown in Fig. 4.25. These data are limited to the deformation range beyond which the gauges stopped functioning.

4.2.4 Column TC-4

Column TC-4 was companion to TC-3, with the exception of the level of axial load applied. This column was tested under a lower axial load of 1000 kN which corresponded to 11% of its concentric capacity. The actual test started with the application of full axial load followed by lateral load reversals applied in the displacement control mode. Strain Gauges number 6 was damaged during construction, prior to the beginning of the test.

The lateral load capacity of the column was lower than that recorded for the companion column TC-3, tested under a higher axial load. The maximum lateral load recorded at 0.5% drift was 199 kN. The load resistance increased up to 263 kN at the begging of 1% drift. Tensile strains in longitudinal reinforcement reached 0.7% and 1.2% at the column-footing interface, when the lateral drift cycles were completed at 1% and 2%, respectively. Yielding of reinforcement at 135 mm below and above the footing was observed at the end of 1% and 2% drift, respectively, with strains reaching 0.2%. Gauges 2 and 8 maintained high strain readings, and reached 1.33% strain at the begging of 3% drift.

Up to the end of 3% lateral drift, no visual cracks were noticed between the tires. There was no spalling observed either. At the begging of 4% drift, there were hairline cracks between the first and second tires from the base. The transverse tie reinforcement developed yielding at this load stage, showing 0.2% strain. At the second cycle of 4% drift, Gauge 4 was

damaged before reached yielding. At the end of 4% lateral drift, most of the strain gauges were damaged. The first and second tires started to separate on the east side.

Gradual spalling of concrete started to take place between the first and second tires from the base on the east side, as the column was forced to experience 5% lateral drift. A 15% reduction in lateral load resistance was recorded when the column was pulled to 5% drift towards west. On the west side there was no significant reduction in lateral force, because the crack between the tires was too small compared to the one on the east side. Spalling of concrete extended to the west side when the column was loaded to the first cycle at 6% drift. At the end of 6% drift, 20% strength decay was observed as laterally expanding concrete pressured the second tire to stretch excessively so the space between the tires became wider and more visible. This eventually led to the spalling of large pieces of concrete up to the third tire level.

The first tire started to rupture at the beginning of 7% drift. Extensive damage was observed at this deformation level, especially on the east side of the column. Rupturing of the longitudinal bars were noticed on the east and west sides during the second cycle of 7% drift. Testing was discontinued at this drift level due to a safety concern. Figure 4.26 shows some views of Column TC-4 during selected stages of testing.

The hysteretic curves for the lateral force-lateral displacement and moment-lateral displacement relationships obtained from test data are shown in Figs. 4.27 and 4.28. These relationships indicate that the column was able to sustain its lateral load capacity up to 5% drift and showed stable hysteresis loops up to 6% drift. There was no significant strength decay up to 5% drift but the column capacity dropped by 20% during the second cycle of 6% drift, when the concrete crushing was observed at the first and second tire locations. Figures 4.29, 4.30 and 4.31 show hysteretic moment-total rotation, moment-anchorage slip rotation, and moment-flexural rotation relationships, respectively, for Column TC-4. One of the LVDTs within h/2 did not give reliable results, and hence the plots for that case are not

shown in Figs. 4.29 and 4.31. Figure 4.30 indicates increased penetration of yielding into the footing, relative to Column TC-4, because of the lower axial load applied on this column. It was found that, at the end of testing, approximately 2/5th of the total rotation was due to anchorage slip, and the remaining 3/5th was caused by flexure.

Figures 4.32 and 4.33 illustrate the strain gauge data for longitudinal and transverse reinforcement, respectively. Strain measurements taken from the treads are shown in Fig. 4.34. These readings of strain gauges do not contain the data till the end of test, because most of the gauges were damaged at early stages of loading.

4.2.5 Column TC-5

The configuration of column TC-5 was different from the previous columns. This column had its longitudinal reinforcement placed inside the rim of tires, while whole tires were stacked on top of each other to form transverse confinement reinforcement. There was no conventional transverse reinforcement in this column, in the form of ties. The column was tested under a constant compressive force of 1900 kN, which represented 21% of its concentric capacity.

The test started with the application of full axial load, followed by lateral load reversals, which were applied in displacement control mode. No damage was observed during the three cycles at 0.5% drift. The maximum lateral load recorded was 113 kN. At the end of 1% drift, the third tire developed 0.23% strain in the rim, on the east side. The column survived 2% drift without any visible damage. Strain measurements on longitudinal reinforcement indicated increased values, developing 0.77% and 0.99% on the east and west sides of column-footing interface (Gauge 2 and 5), at the end of 2% drift. The strains reached 0.2% at a height of 135 mm above the footing surface (Gauge 3 and 6) at the same load stage. Strain data for the east longitudinal reinforcement, 135 mm below the footing surface, was not available because the gauge had been damaged prior to testing. Strains indicated by gauge 5 were higher than those

measured by gauge 2, and reached 1.4% strain at the end of 3% drift. Strains in the rim of the second and third tires reached 0.42% and 0.32% at the same load stage.

During 4% lateral drift, most strain gauges showed strains beyond yielding, up to 0.8%. At the end of this deformation level, noise of stretching steel was heard, possibly de-bonding from the treaded rubber in the tires. The strain readings on the rim and treads of the second and third tires showed increased strains, though no visible rupture was observed. The column developed 5.5% drift without any sign of strength decay in lateral force resistance. During the second and third cycles at 5% drift, the rupturing noise of the steel in treads was noticeable once again, indicating increased expansion of concrete at second and third tire locations. The gauges on the rims of the first, second, and third tire broke loose due to high pressure exerted by longitudinal bars. Also, some of the LVDTs went out of stroke range, and removed.

During the first cycle at 6% drift, there was no decay in lateral force resistance, but the noise of rupturing steel in the tires continued as the strain gauges broke loose one by one. The failure was initiated by rupturing of the steel in the second and third tires on the west side, which led to the complete rupturing of these tires, exposing concrete. The column failed during the third cycle at 6% lateral drift due to the buckling of longitudinal reinforcement. Upon reaching the third cycle at 6% drift, the second and third tires were fractured into two pieces, with crushed concrete exposed within the column, followed by the buckling of longitudinal reinforcement. Testing was terminated right at this stage, as the column was found to be unsafe to continue loading. Figure 4.35 shows selected views of Column TC-5 during testing. The duration of the test for this column was one hour and forty-five minutes.

The hysteretic curves of the lateral force-lateral displacement and moment-lateral displacement relationships obtained from test data are shown in Figs. 4.36 and 4.37. These relationships indicated that the column was able to sustain the lateral load up to the second cycle of 6% drift without significant strength decay. The column showed stable hysteresis loops up to the beginning of 6% lateral drift before the capacity dropped by 55% during the

third cycle of 6% drift. The enhanced behaviour relative to Column TC-2 was attributed to improved stability of longitudinal reinforcement provided by the rims.

Figures 4.38, 4.39 and 4.40 show the hysteretic moment-total rotation, moment-anchorage slip rotation, and moment-flexural rotation relationships, respectively. Figure 4.39 indicates that approximately 1/8th of the total rotation was caused by anchorage slip, leaving the remaining 7/8th to flexure.

Figures 4.41 and 4.42 illustrate the strain gauge data. These readings are mostly limited to deformation cycles within the first 5% drift, after which the gauges were damaged due to excessive deformations and/or crushing of concrete.

4.2.6 Column TC-6

Column TC-6 was identical to Column TC-5. However, TC-6 was tested under a lower axial load of 1000 kN, which corresponded to 11% of column concentric capacity. The actual test started with the application of full axial load, followed by incrementally increasing deformation reversals.

The observed behaviour at early stages of loading was very similar to that of TC-5. However, the load resistance was different because of the lower axial compression imposed. During the three cycles at 0.5% drift, no damage was observed and the maximum lateral load recorded was 97 kN. This value was the lowest ever recorded in the test program. At the end of 1% drift cycle, the strain in extreme longitudinal bar reached 0.85% on the west side, at the column-footing interface (Gauge 5). The strain gauge at this location seized to function shortly thereafter. Strains in the extreme longitudinal bars reached 0.2% and 0.65% at the column-footing interface on the east side, and at 135 mm below and above the footing (Gauge 4 and 6), respectively, at the end of 2% drift. The strains on the tread of the third tire reached 0.92%, at the same deformation level. The strains continued to increase with imposed drift.

The strain in Gauge 6 (135 above the footing surface) reached 1.3% at the end of 4% drift, while the strain in the tread of the second tire reached 0.21%. During 5% drift cycles, some of the strain gauges in the longitudinal reinforcement recorded inelastic strains, reaching up to 1.0%. There was no visible damage in the column until the end of 5% drift cycles. A crack was noticeable at the column-footing interface when the column was loaded to 6% drift. Most of the strain gauges broke loose during the 7% drift cycles, while LVDT 1 went out of stroke range. Similar damage was observed to the gauges during the subsequent cycles at 8% drift. There was no significant strength decay until the third cycle of 9% drift. As the third cycle at this deformation level was applied, the noise of rupturing longitudinal reinforcement could be heard one after the other. The steel in the treads also ruptured, resulting in a droop of about 11% in load resistance. The progression of damage continued until the second cycle of 10% drift, at which stage the column resistance dropped suddenly to 50%. The subsequent cycle led to the rupturing of the second tire on the west, which resulted in the crushing of core concrete. Testing was discontinued at this stage due to the significant loss in strength. The duration of the test for this column was two hours and forty-five minutes. Figure 4.43 shows performance of Column TC-6 during selected stages of testing.

The hysteretic curves of the lateral force-lateral displacement and moment-lateral displacement relationships obtained experimentally are shown in Figs. 4.44 and 4.45. These relationships indicate that the column was able to sustain the imposed load up to the end of 8% drift, and continued showing stable hysteresis loops up to beginning of 9% drift. There was no significant strength decay up to the second cycle of 9% drift, but the column showed a significant loss in strength at the end of 9% drift. The capacity of the column dropped by about 50% during the first cycle of 10% drift due to the sudden rupture of the second tire and the crushing of concrete. The improvement in behaviour relative to Column TC-1 was attributed to improved support provided for the longitudinal reinforcement inside the rim.

Figures 4.46, 4.47 and 4.48 show the hysteretic moment-total rotation, moment-anchorage slip rotation, and moment-flexural rotation relationships, respectively, for Column TC-6.

Figure 4.47 indicates that, approximately 3/6th of the total rotations was caused by anchorage slip, and the remaining 3/6th was caused by flexure. Anchorage slip rotations of TC-6 were roughly twice the values recorded for TC-5. This difference was due to the difference in the level of axial load, depicting higher slip rotations under lower axial compression.

Figures 4.49 and 4.50 illustrate the strain gauge data recorded. These readings reflect the strains obtained until the gauges were damaged at approximately 8% drift, though some were damaged prior to testing, during construction.

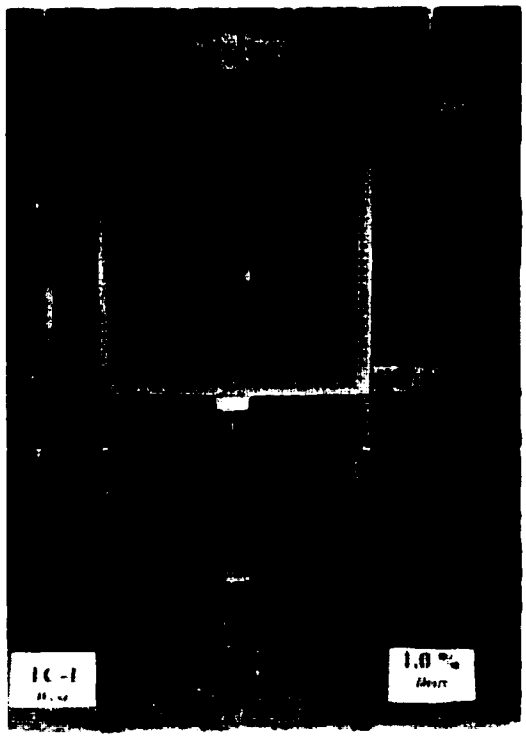

(a) At 1% Drift

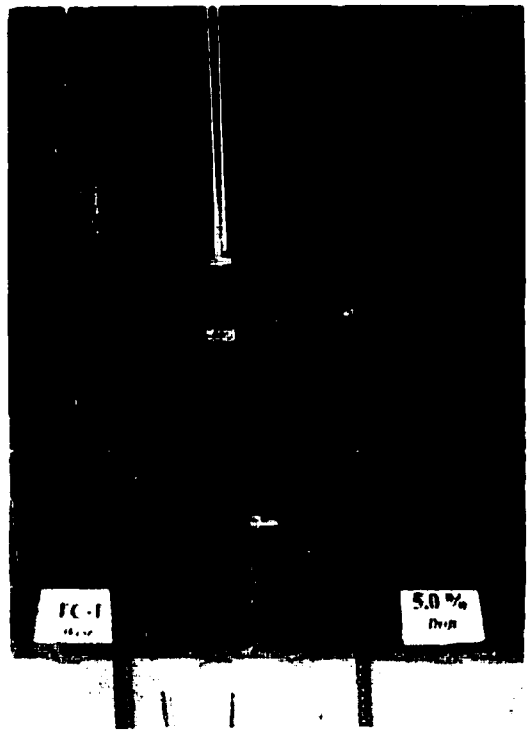

(b) At 5% Drift

(c) At 6% Drift, Close-up View

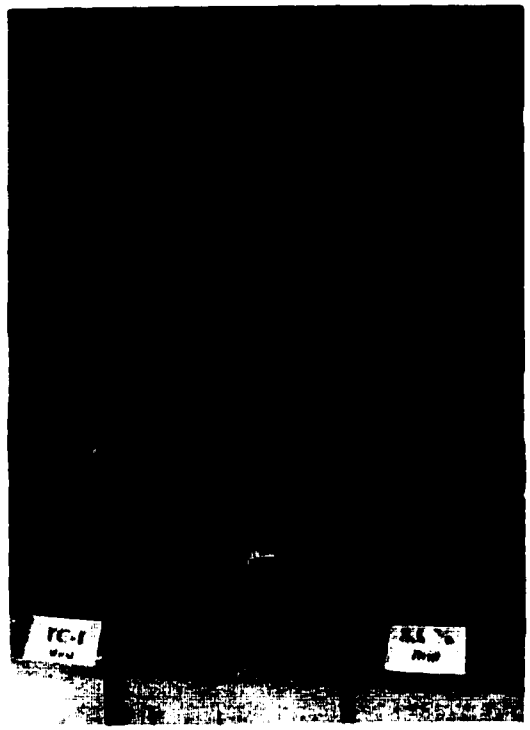

(d) At 8% Drift

Figure 4.1 : Behavior of Column TC-1 During Selected Stages of Testing

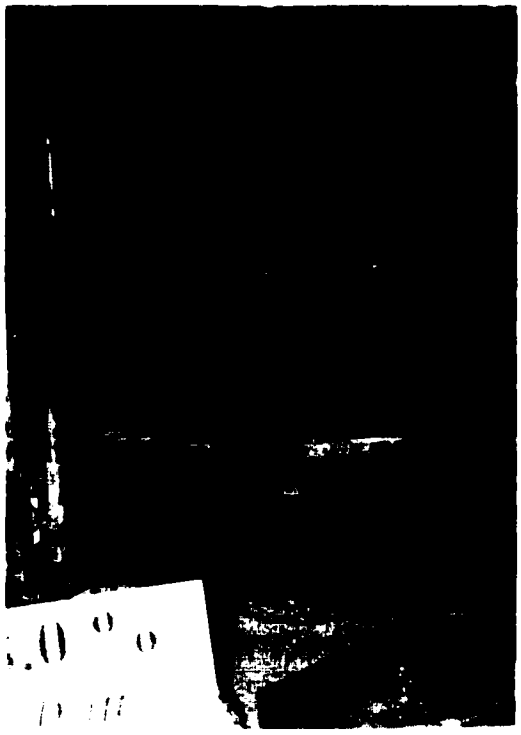

(e) Last Cycle of 8% Drift

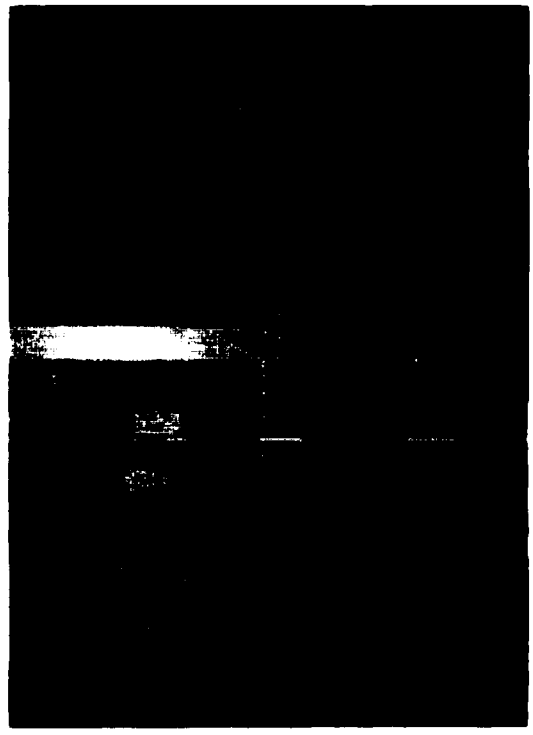

(f) Vertical Actuator At 8% Drift

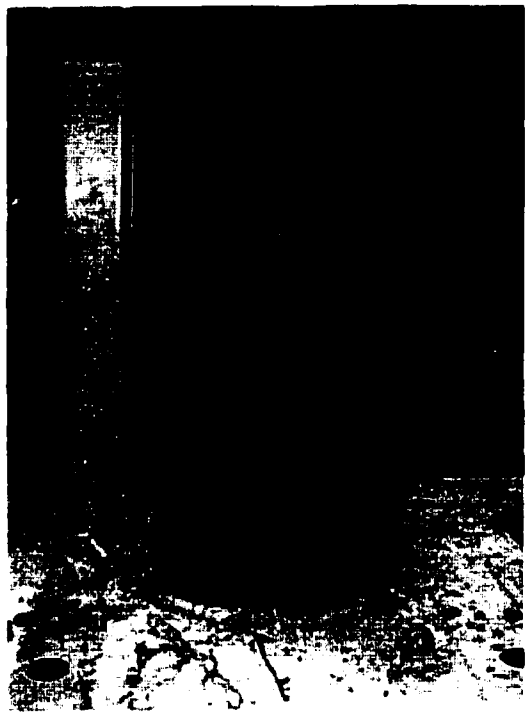

(g) Front View at the End of Test

Figure 4.1 : (Continued)

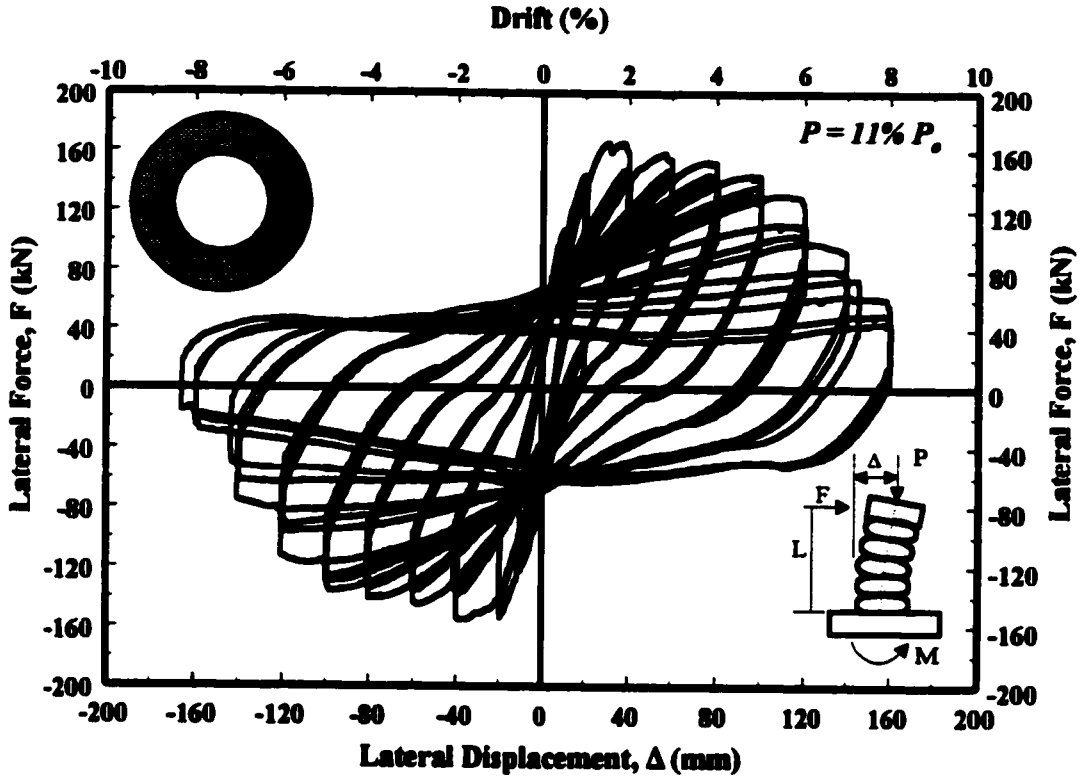

Figure 4.2 : Hysteretic Force-Displacement Relationship for Column TC-1

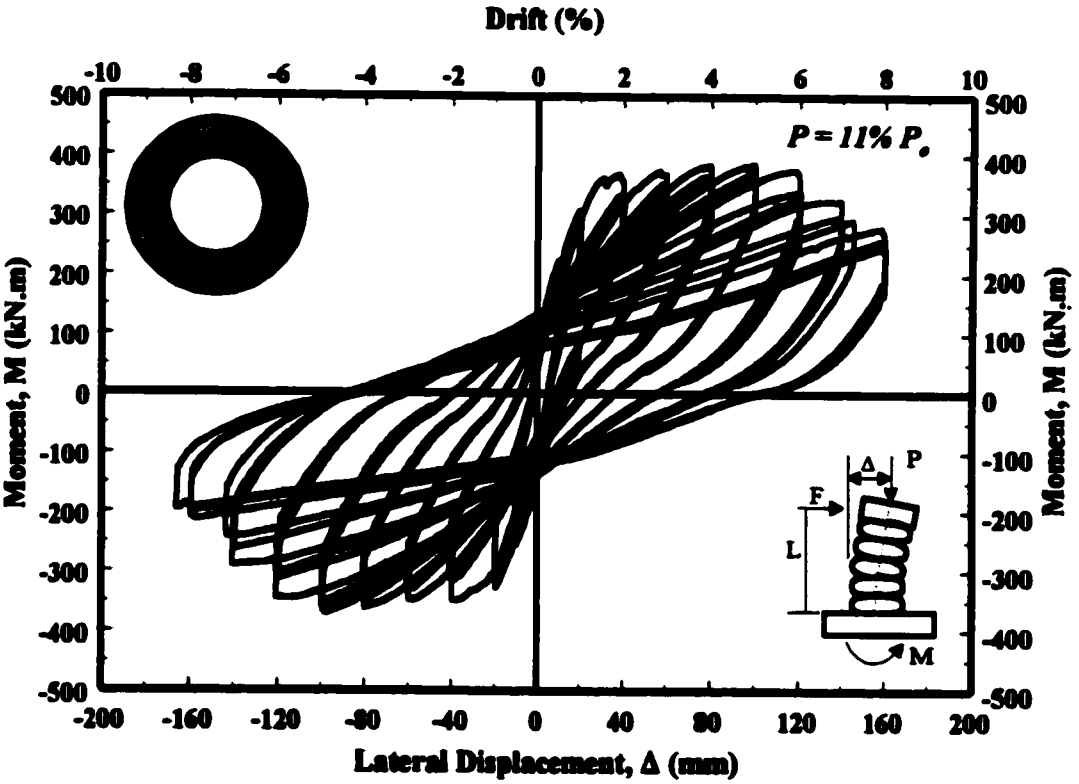

Figure 4.3 : Hysteretic Moment-Displacement Relationship for Column TC-1

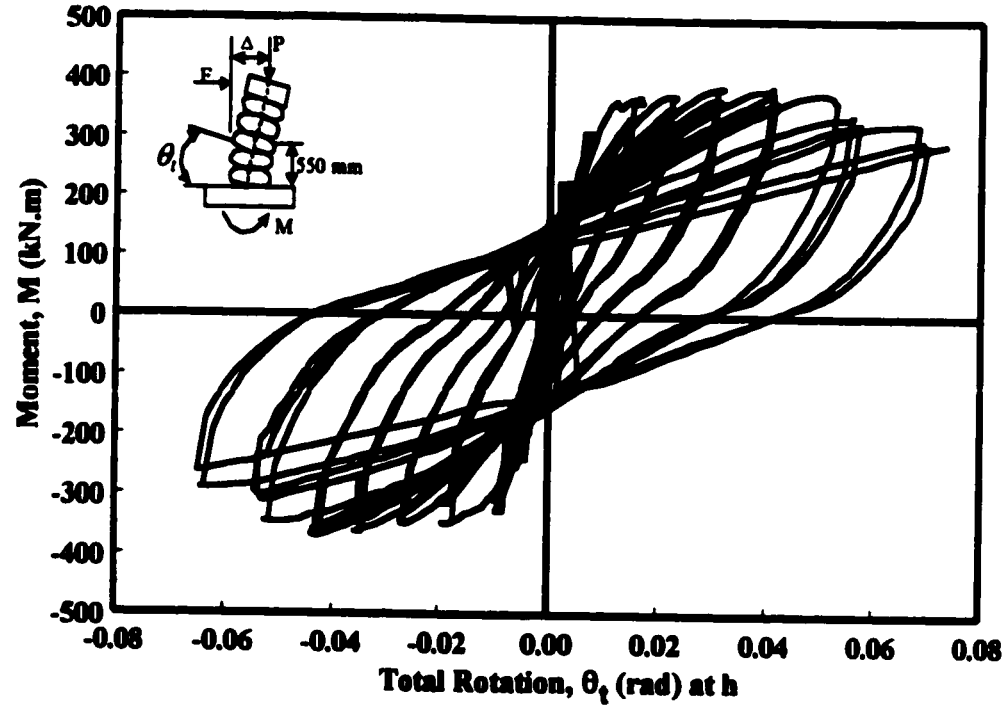

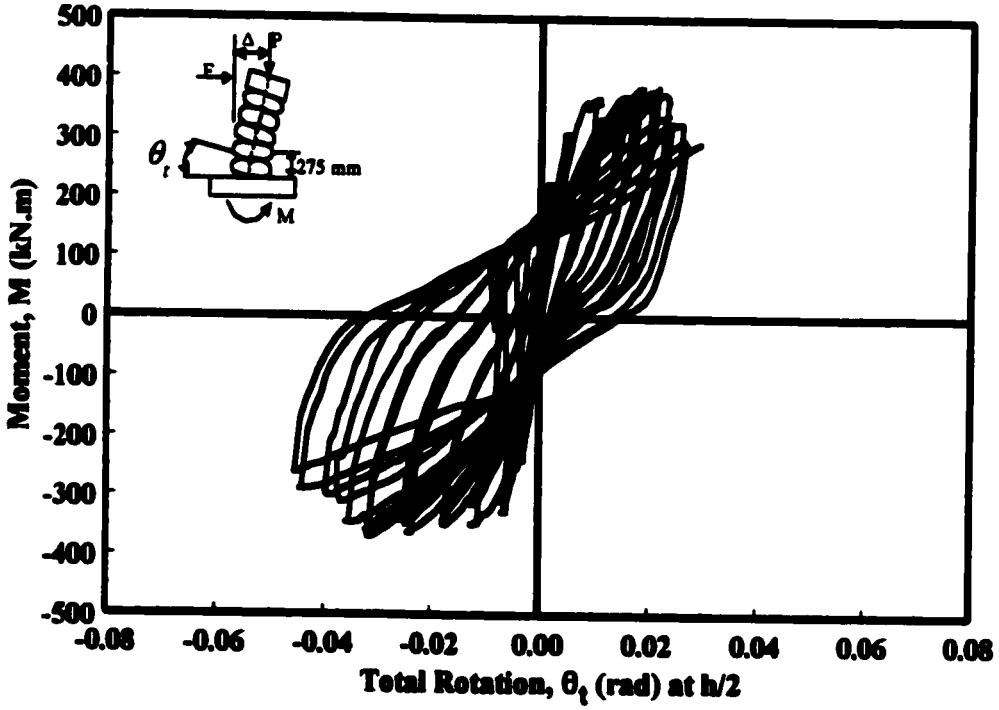

Figure 4.4 : Moment-Total Rotation Relationship for Column TC-1

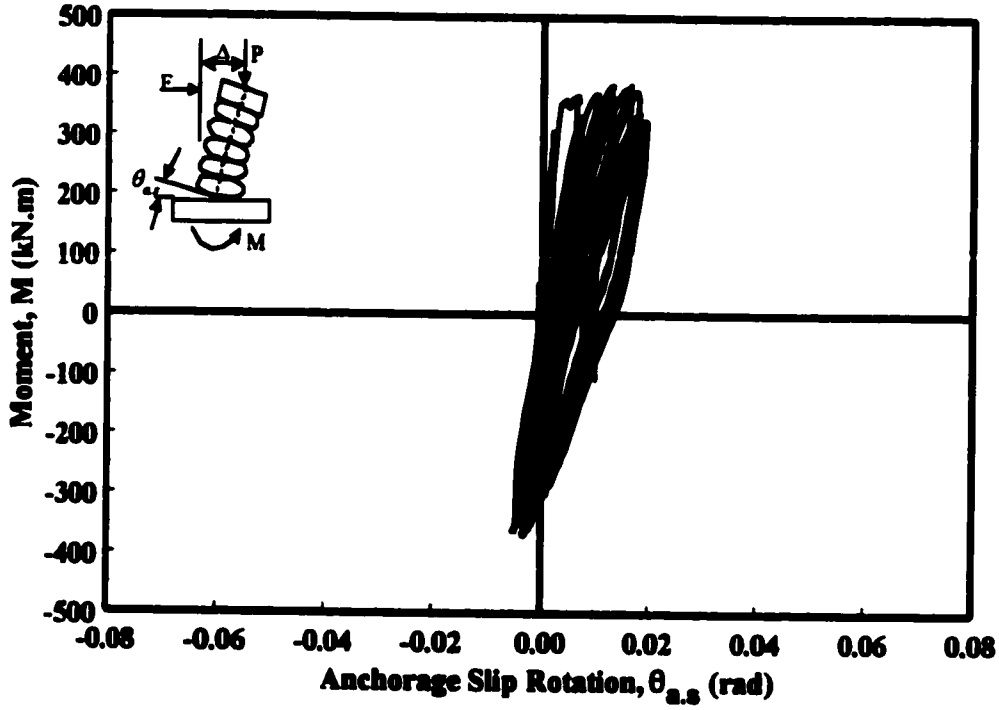

Figure 4.5 : Moment-Anchorage Slip Rotation Relationship for Column TC-1

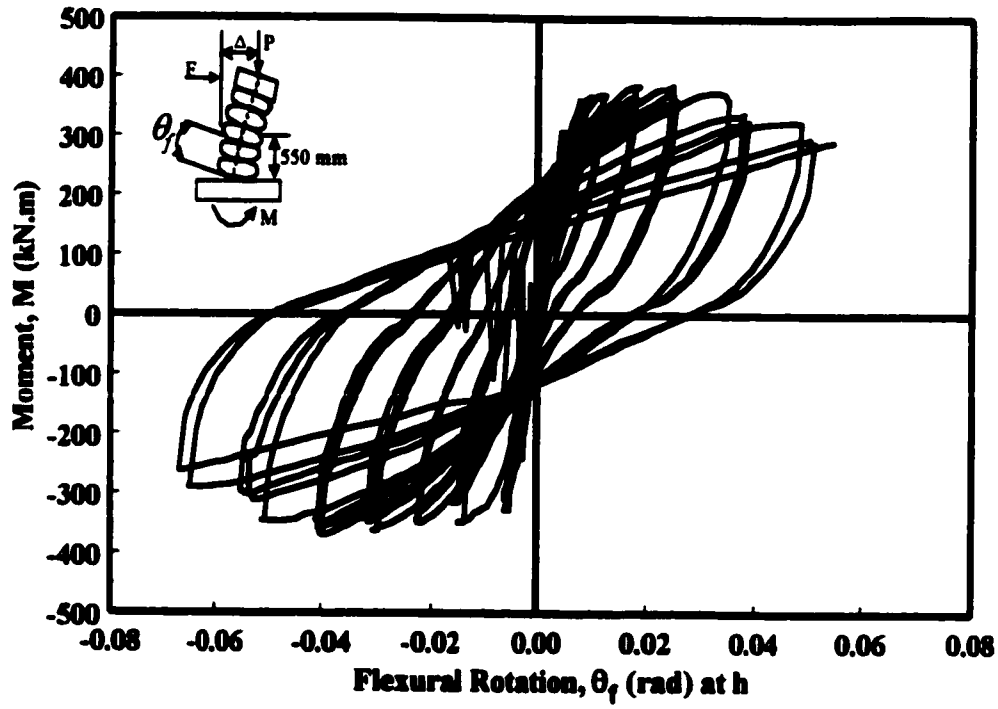

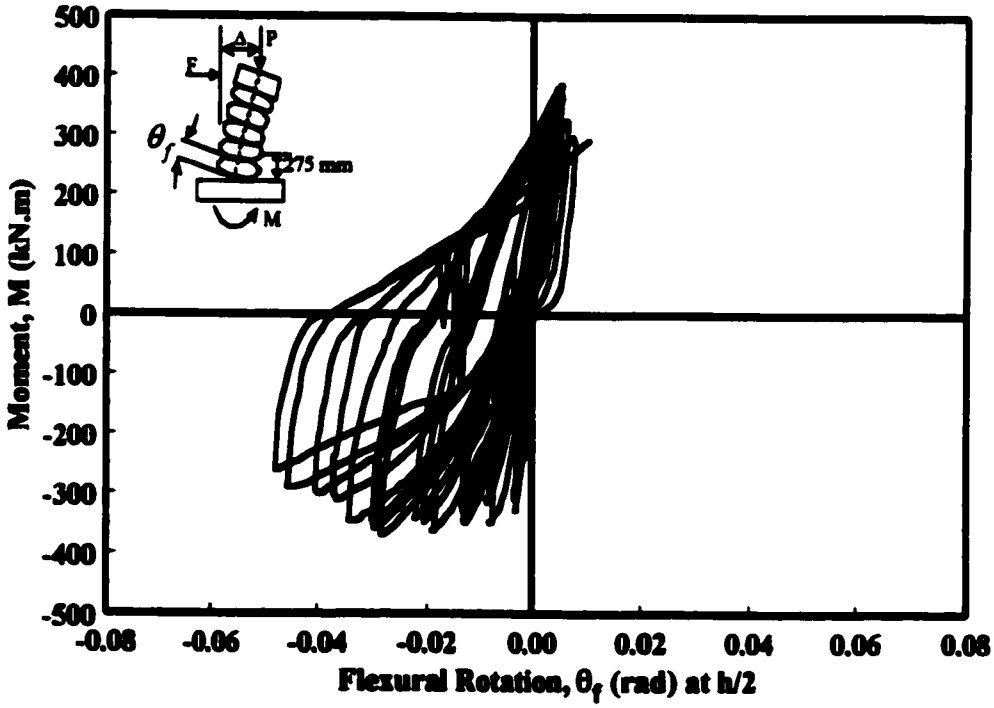

Figure 4.6 : Moment-Flexural Rotation Relationship for Column TC-1

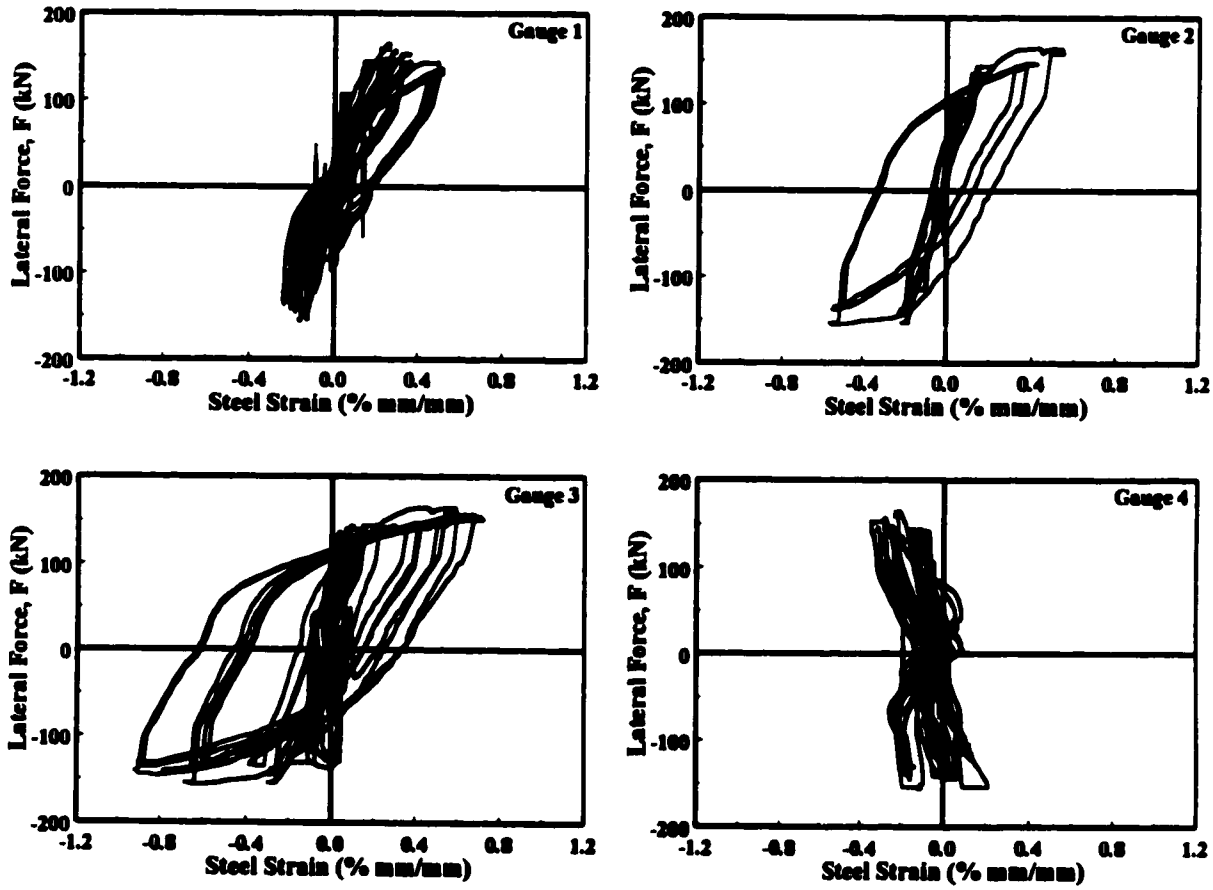

Figure 4.7 : Strain Gauge Data for Longitudinal Reinforcement in Column TC-1

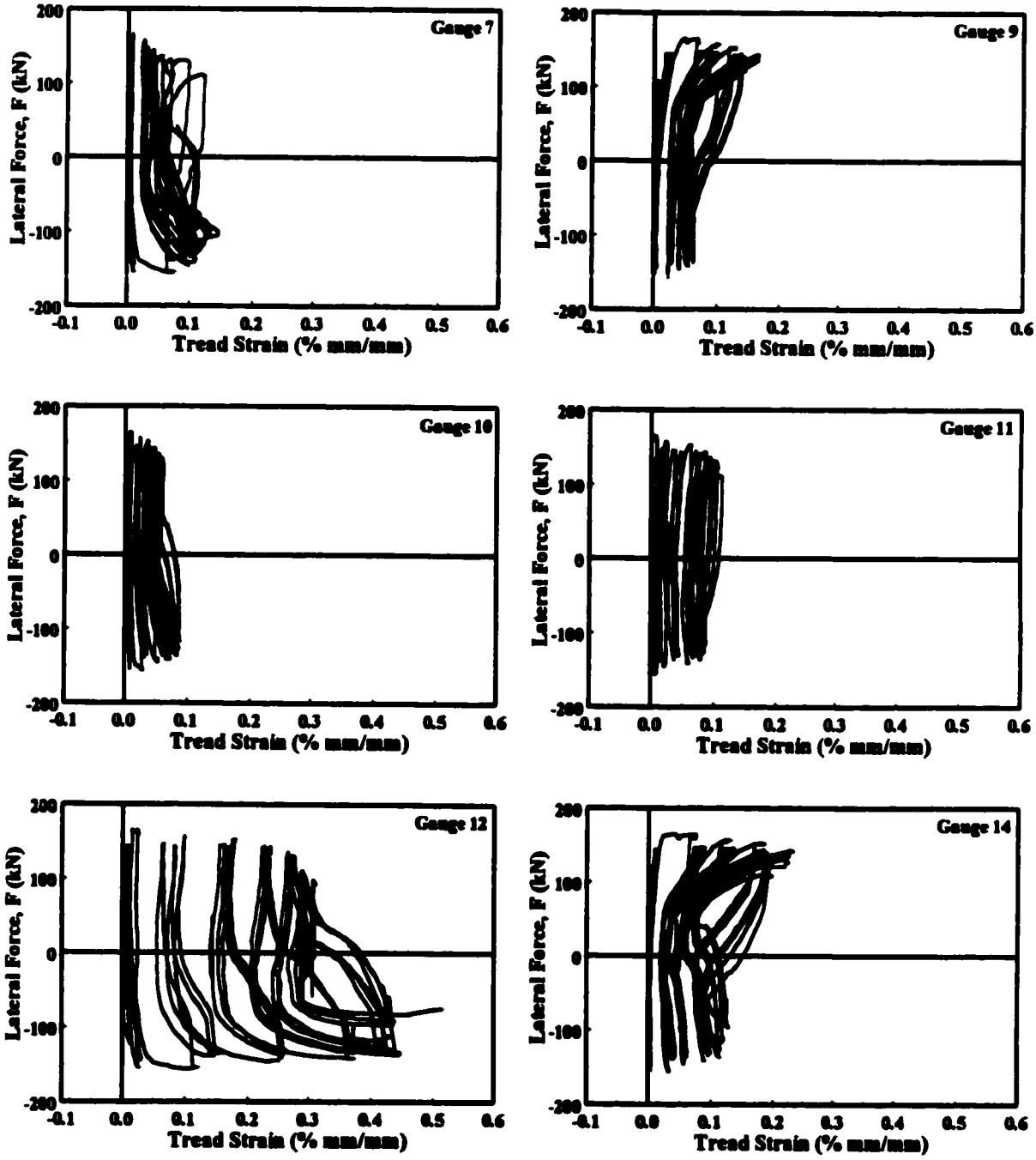

Figure 4.8 : Tire Strains in Column TC-1, Measured on Treads

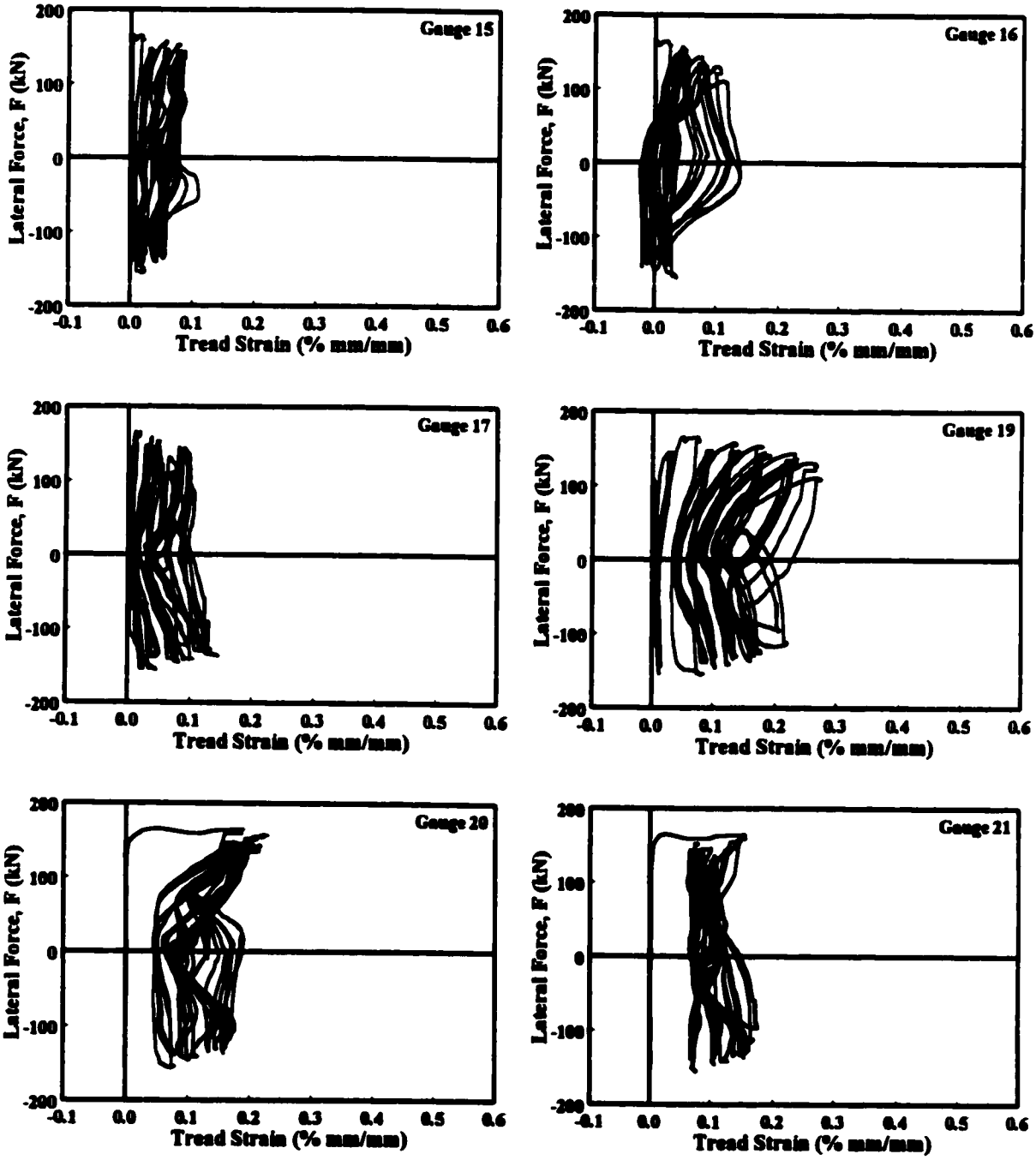

Figure 4.8 (Continued) : Tire Strains in Column TC-1, Measured on Treads

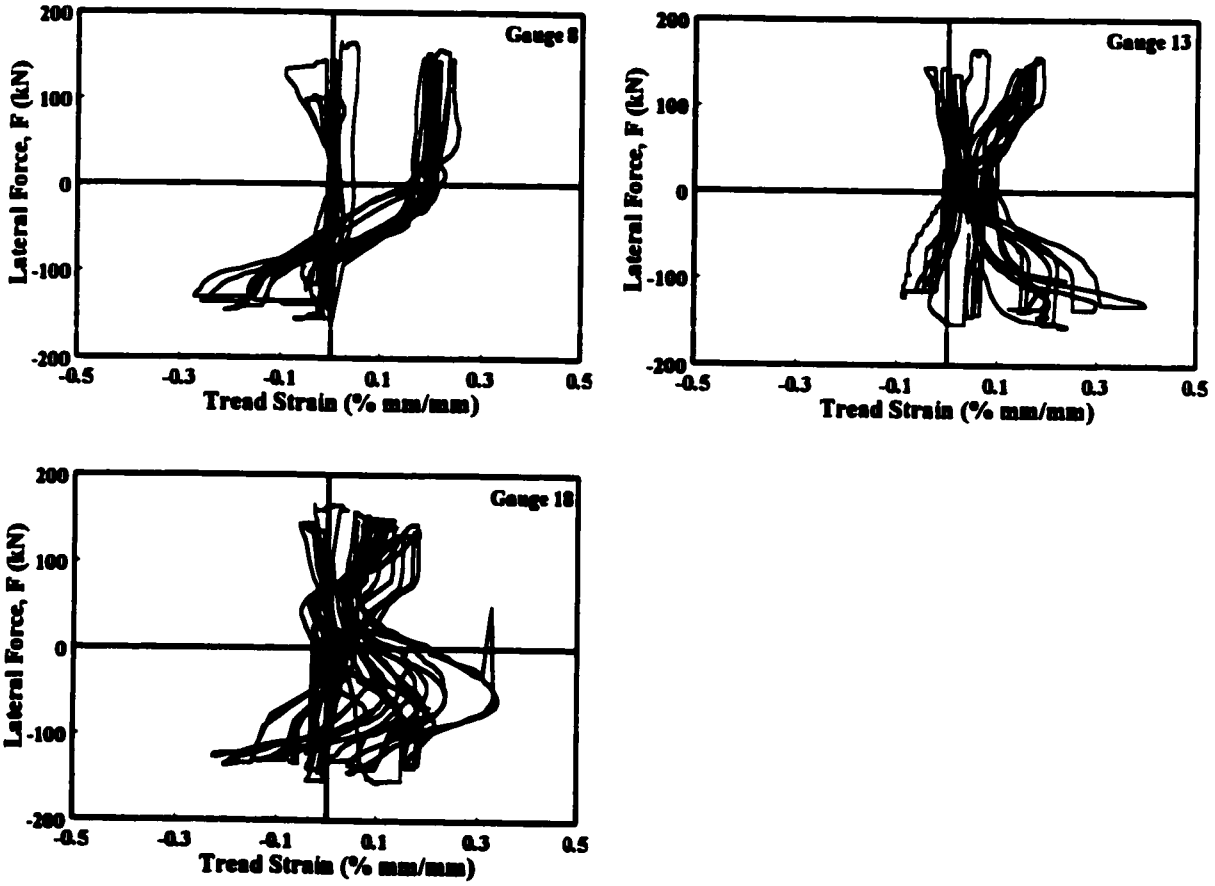

Figure 4.8 (Continued) : Tire Strains in Column TC-1, Measured on Rims

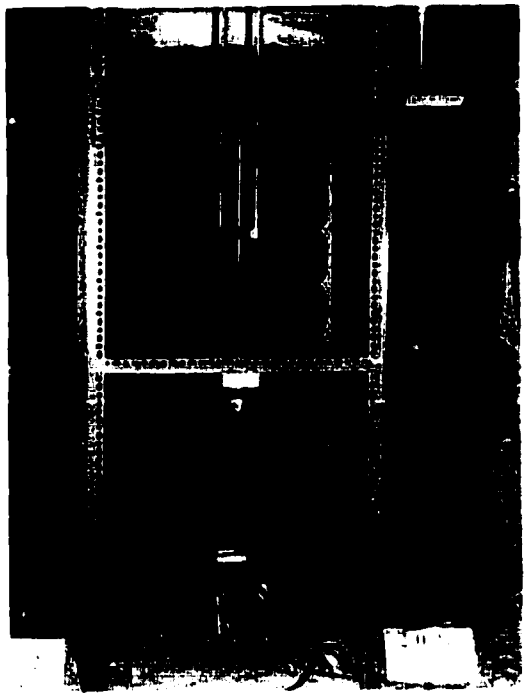

(a) At 2% Drift

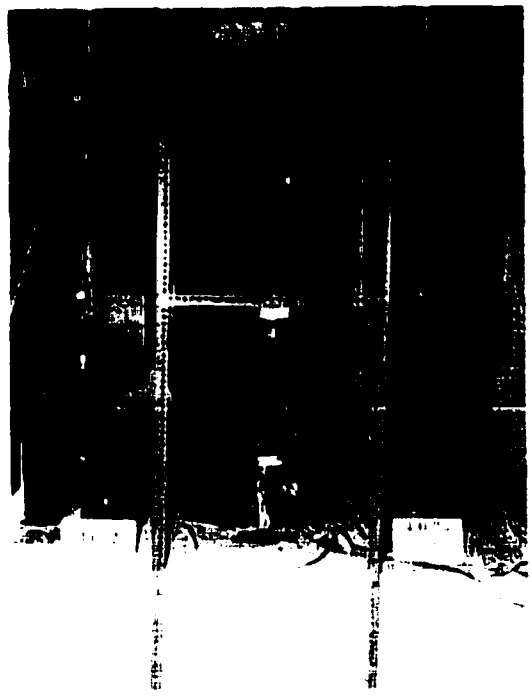

(b) At 4% Drift

(c) At Second Cycle of 5% Drift

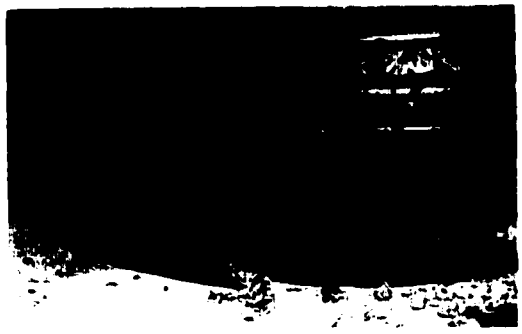

(d) Close-up View at End of Test

(e) North-East View of Third Tire

Figure 4.9 : Behavior of Column TC-2 During Selected Stages of Testing

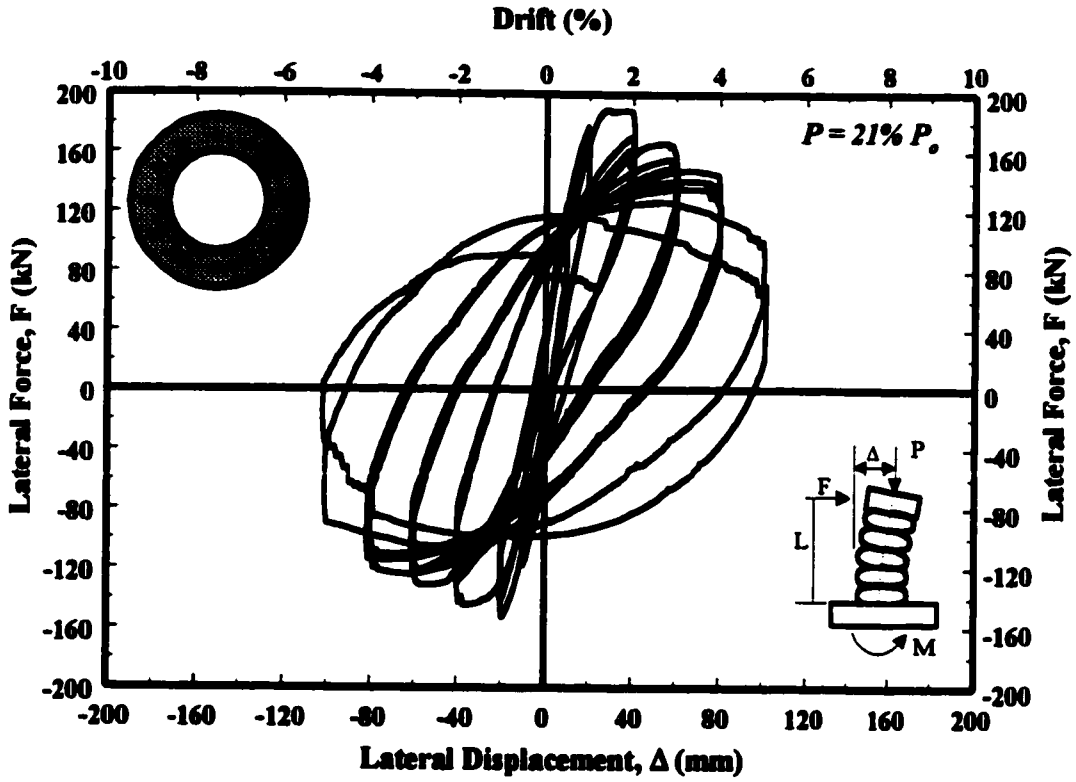

Figure 4.10 : Hysteretic Force-Displacement Relationship for Column TC-2

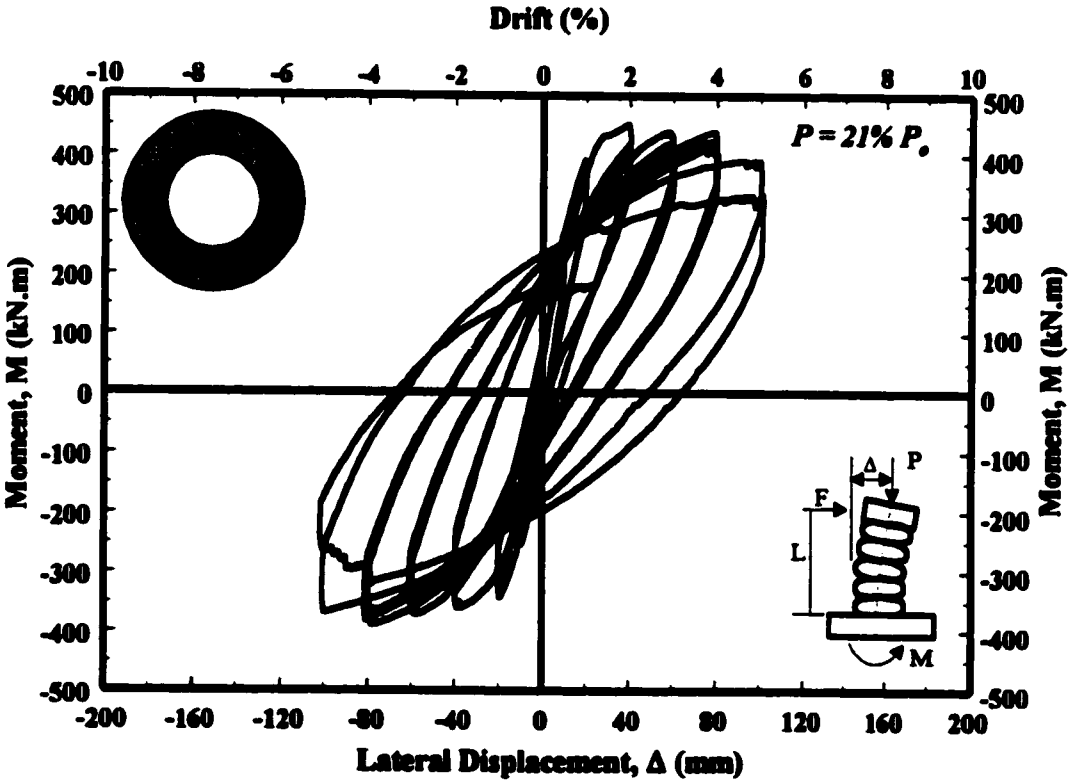

Figure 4.11 : Hysteretic Moment-Displacement Relationship for Column TC-2

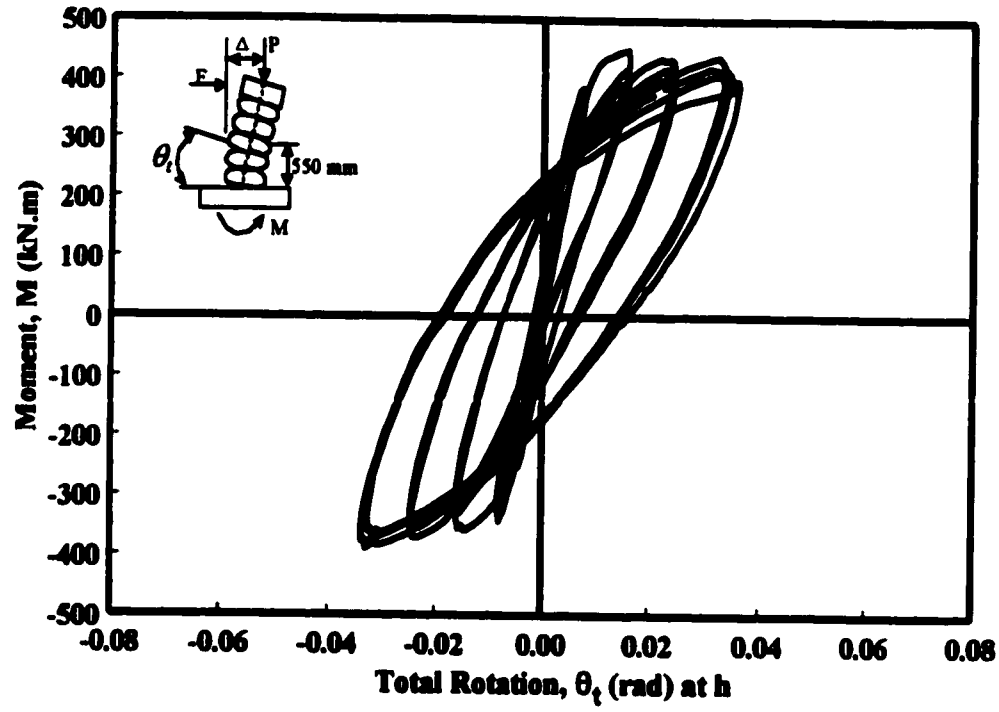

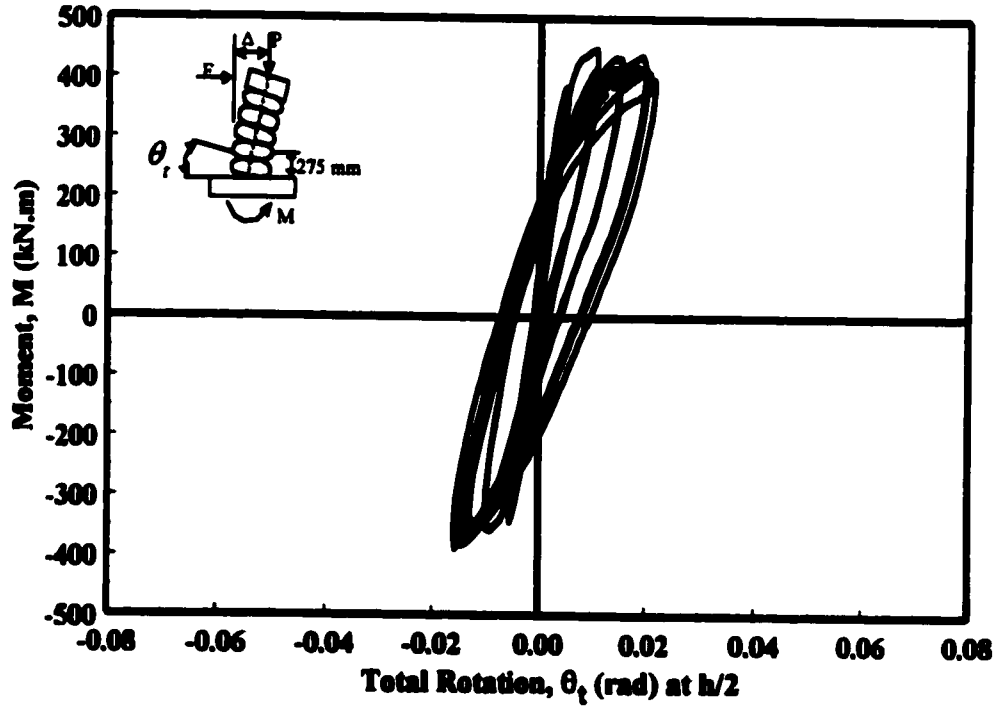

Figure 4.12 : Moment-Total Rotation Relationship for Column TC-2

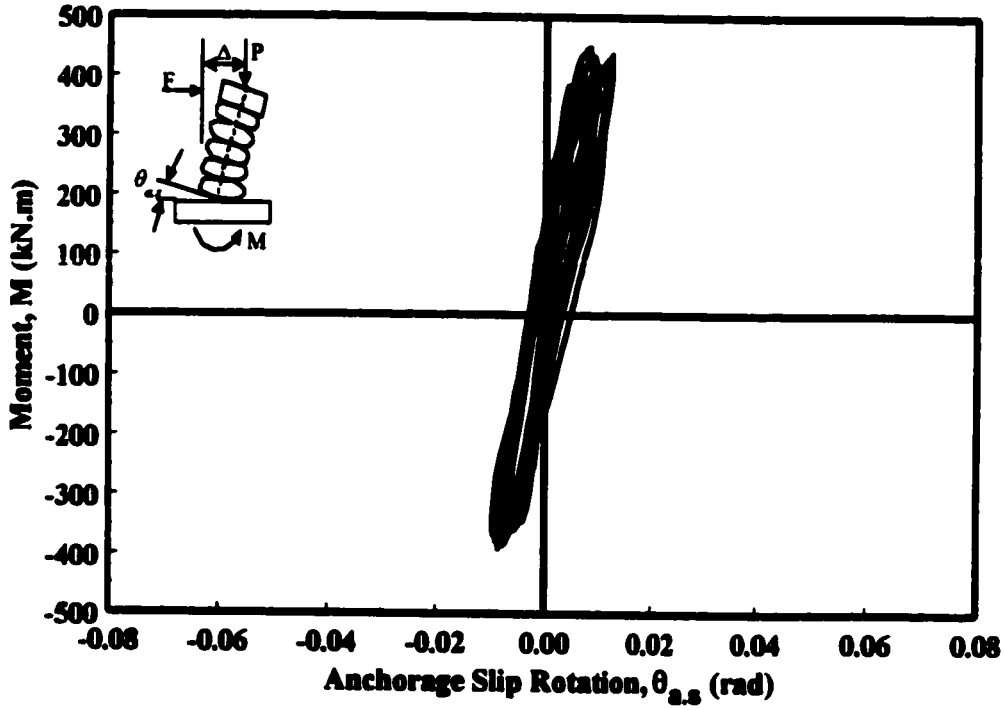

Figure 4.13 : Moment-Anchorage Slip Rotation Relationship for Column TC-2

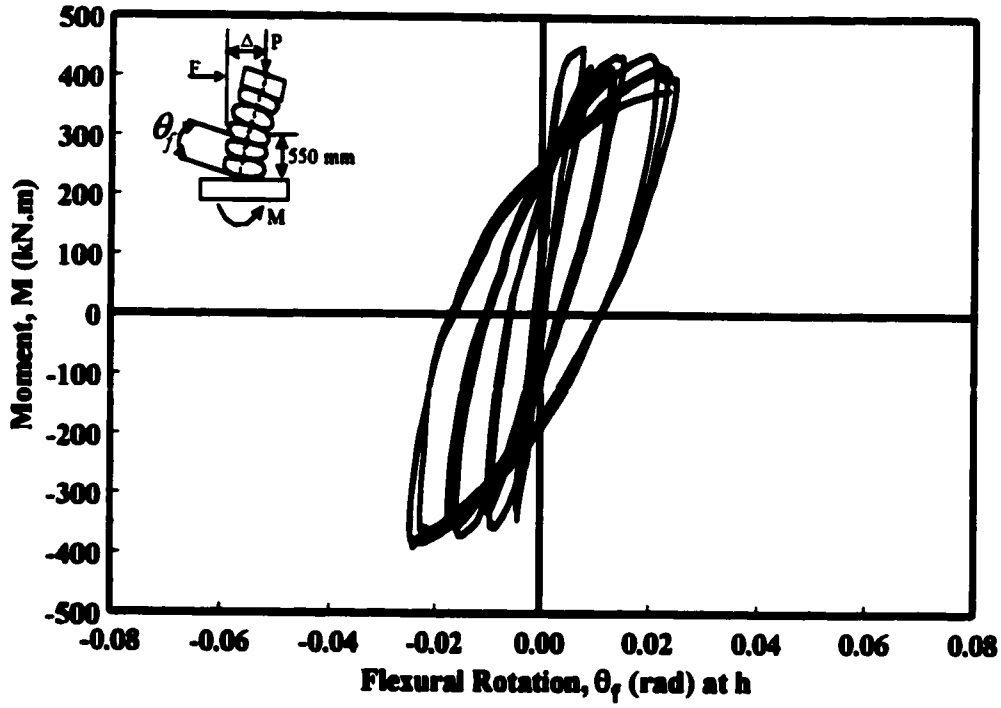

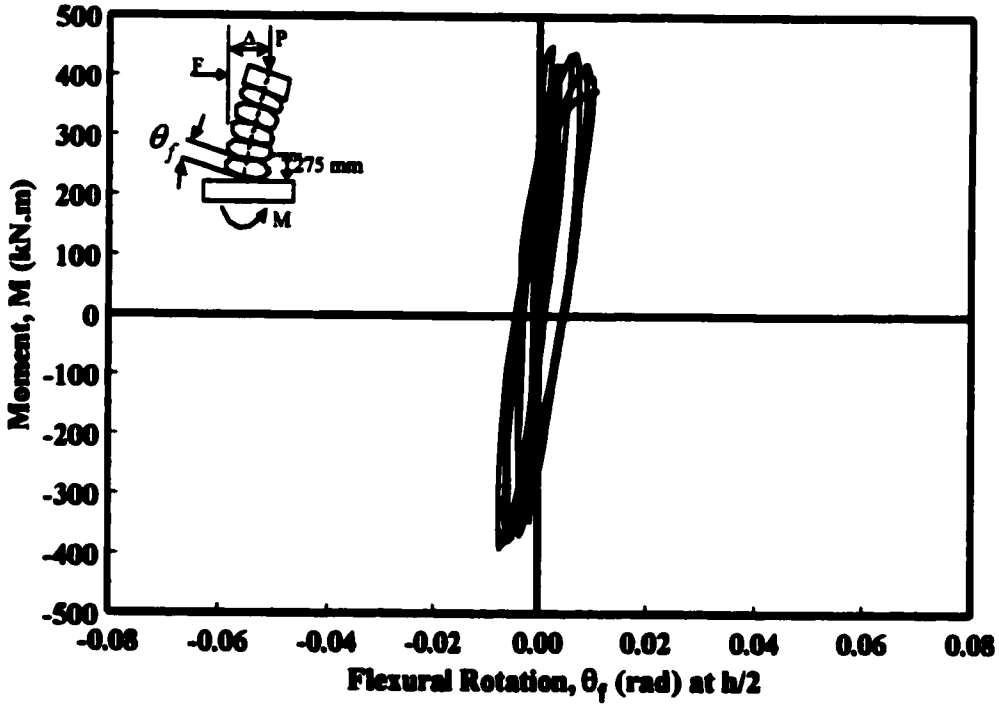

Figure 4.14 : Moment-Flexural Rotation Relationship for Column TC-2

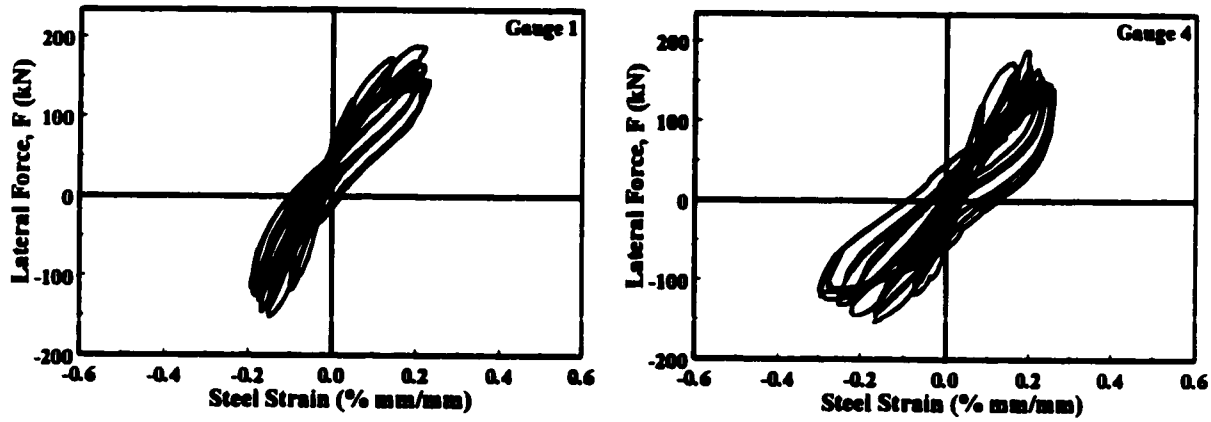

Figure 4.15 : Strain Gauge Data for Longitudinal Reinforcement in Column TC-2

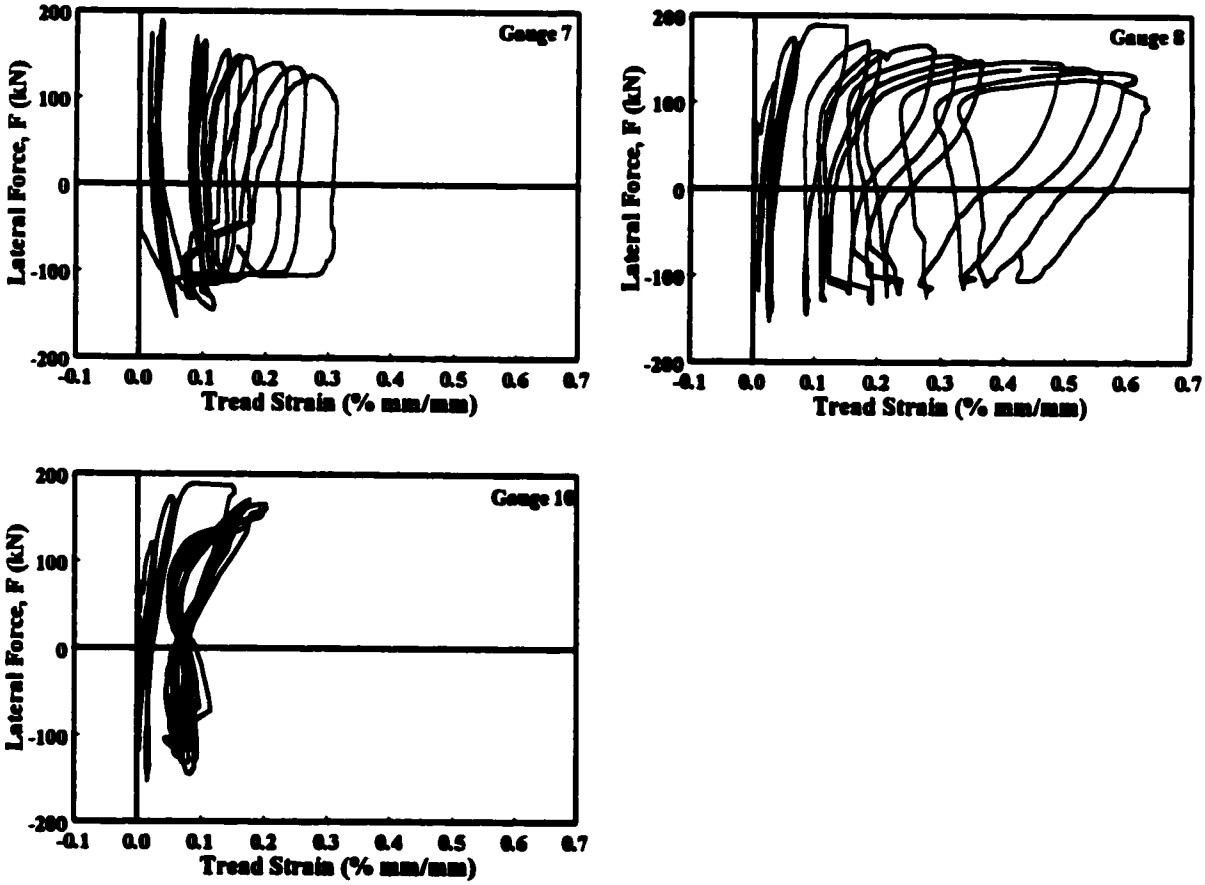

Figure 4.16 : Tire Strains in Column TC-2, Measured on Treads

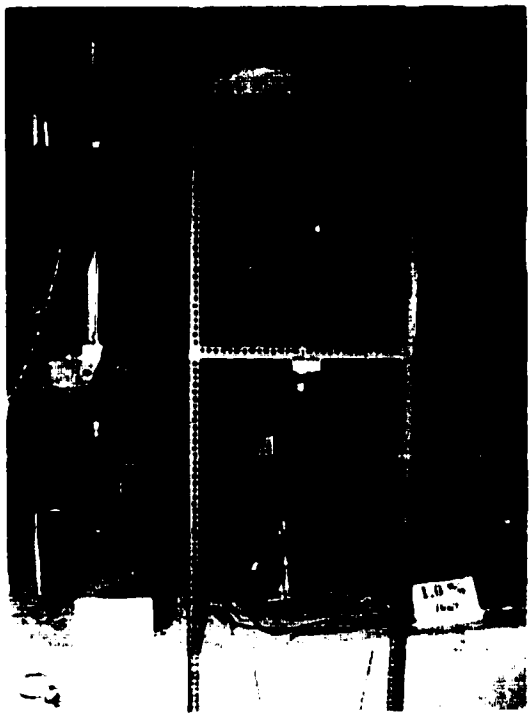

(a) At 1% Drift

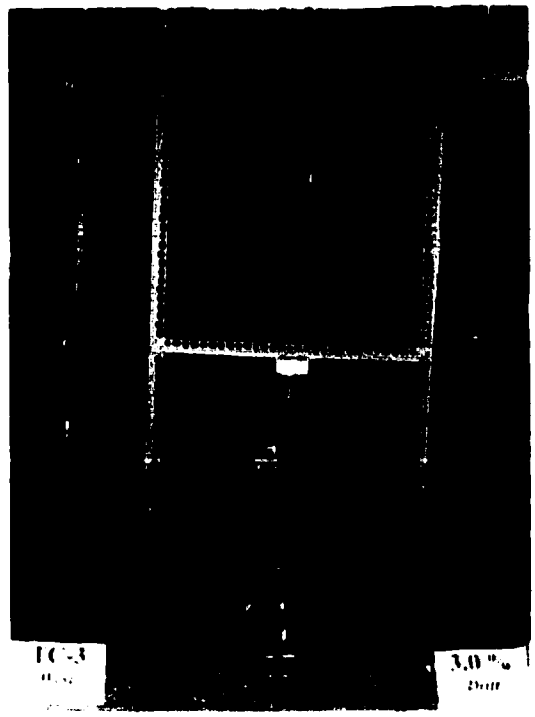

(b) At 3% Drift

(c) Close-up View At 4% Drift

(d) Rupturing of Second Tire

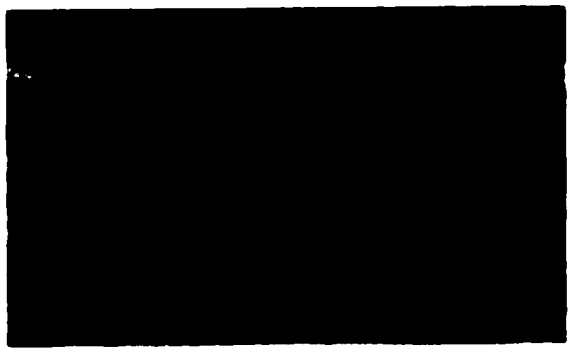

(e) Buckling of Longitudinal Bars

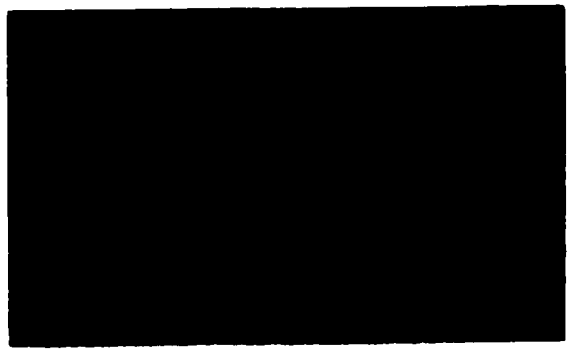

(f) At End of Test

Figure 4.17 : Behavior of Column TC-3 During Selected Stages of Testing

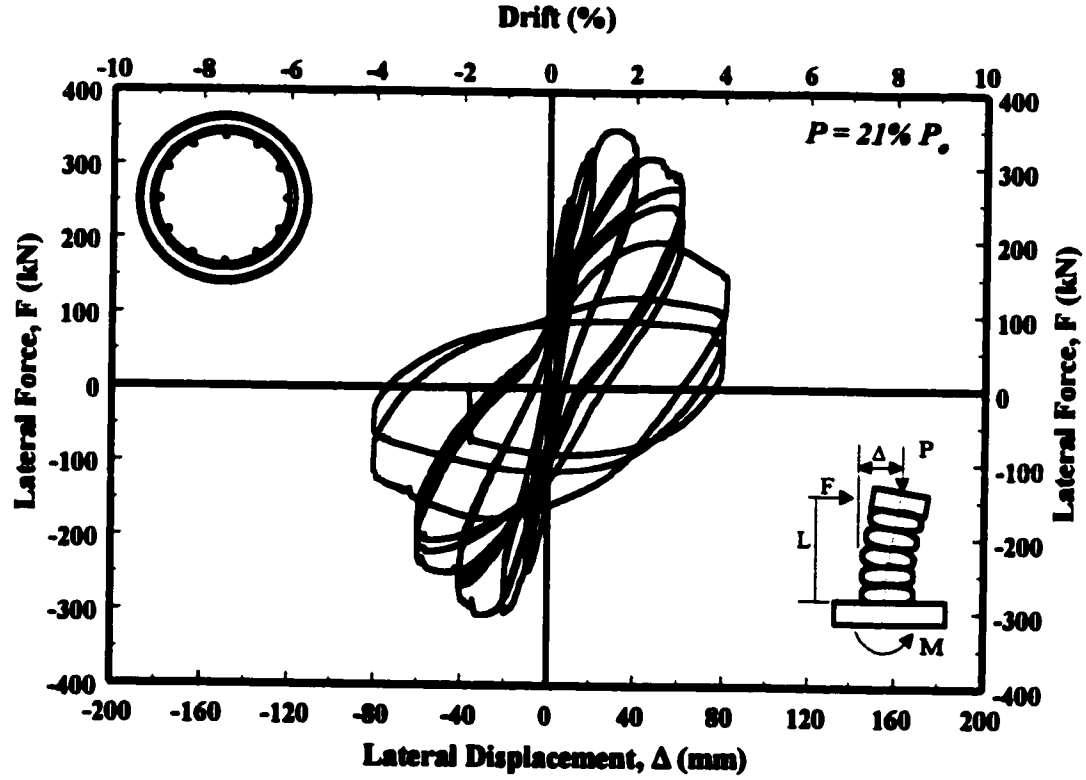

Figure 4.18 : Hysteretic Force-Displacement Relationship for Column TC-3

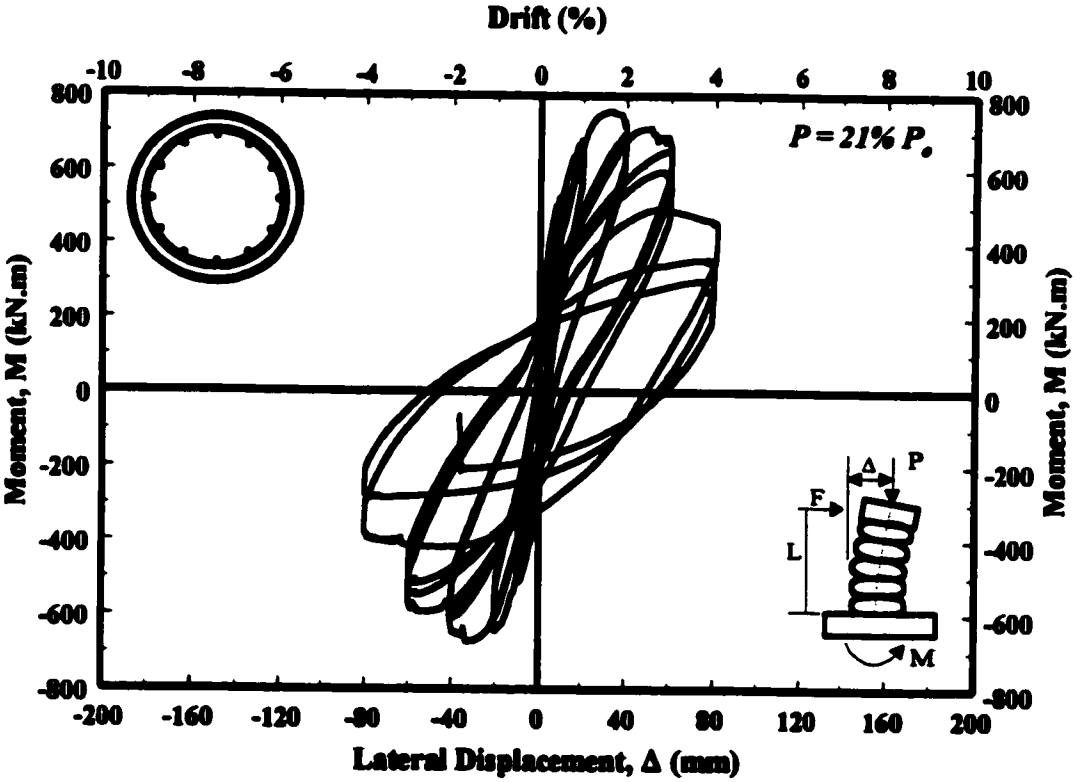

Figure 4.19 : Hysteretic Moment-Displacement Relationship for Column TC-3

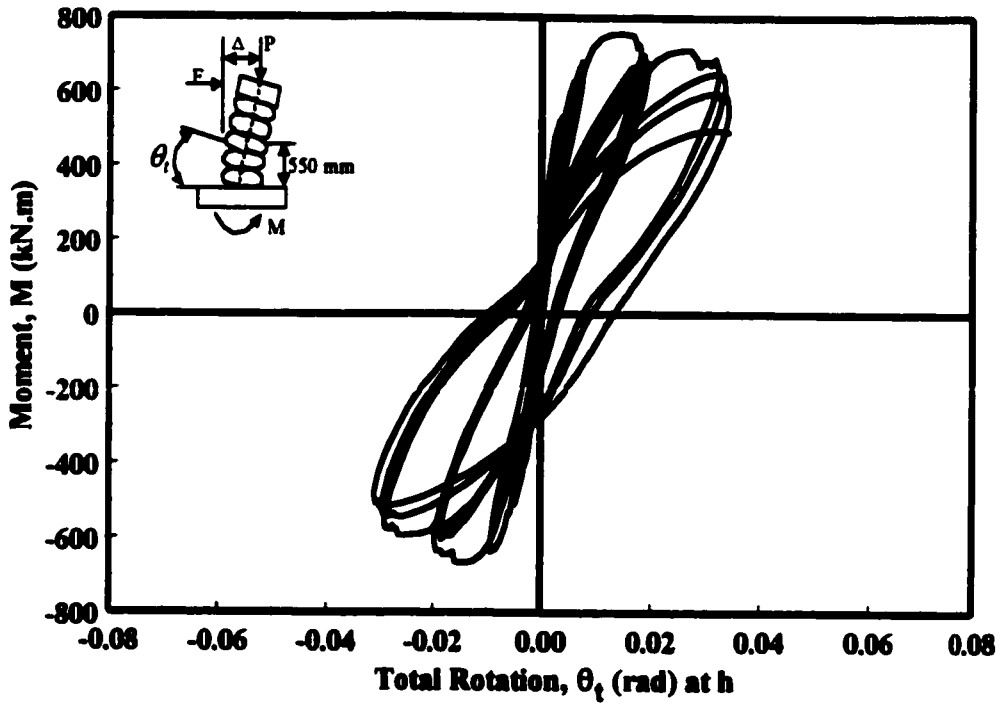

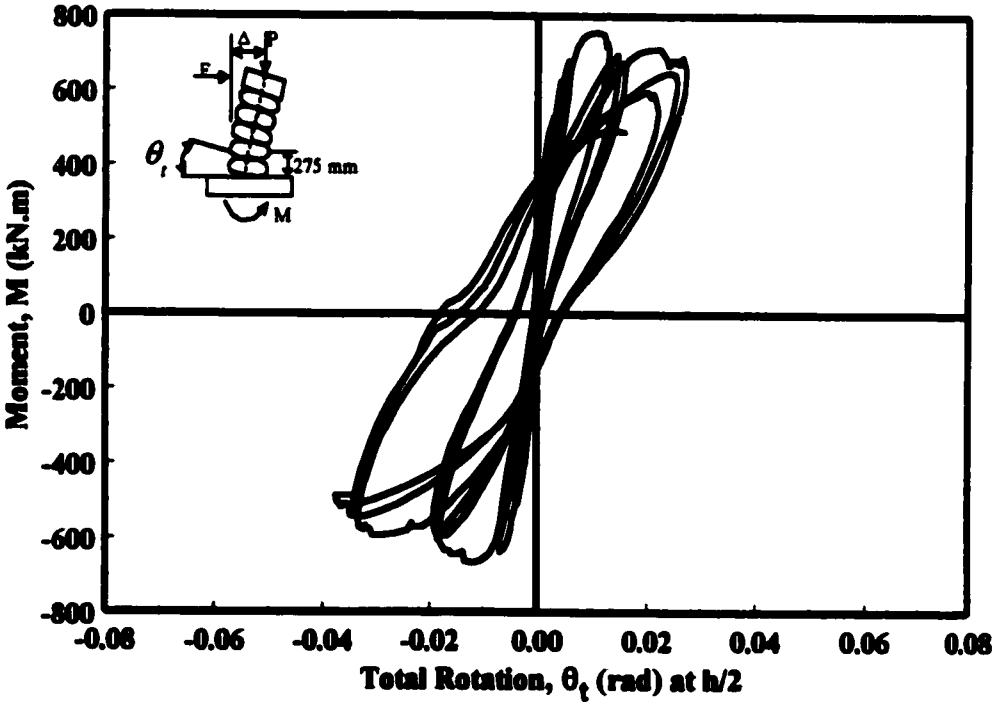

Figure 4.20 : Moment-Total Rotation Relationship for Column TC-3

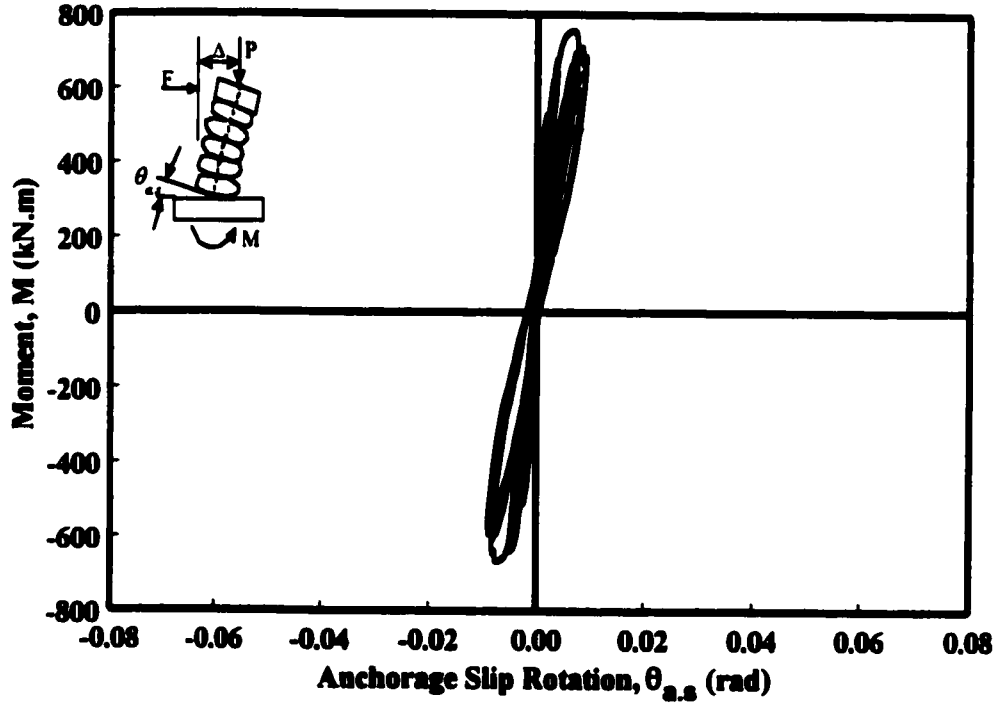

Figure 4.21 : Moment-Anchorage Slip Rotation Relationship for Column TC-3

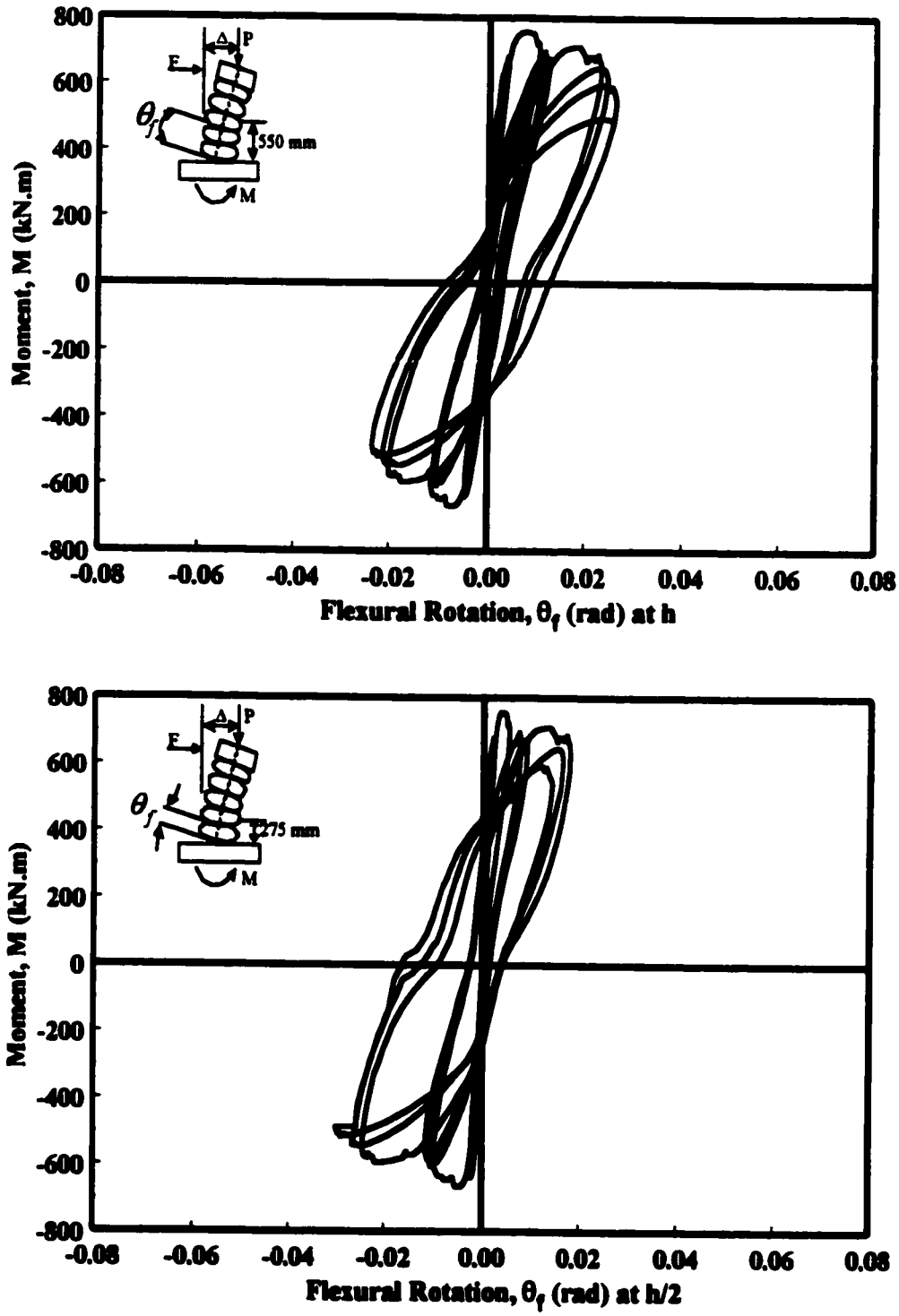

Figure 4.22 : Moment-Flexural Rotation Relationship for Column TC-3

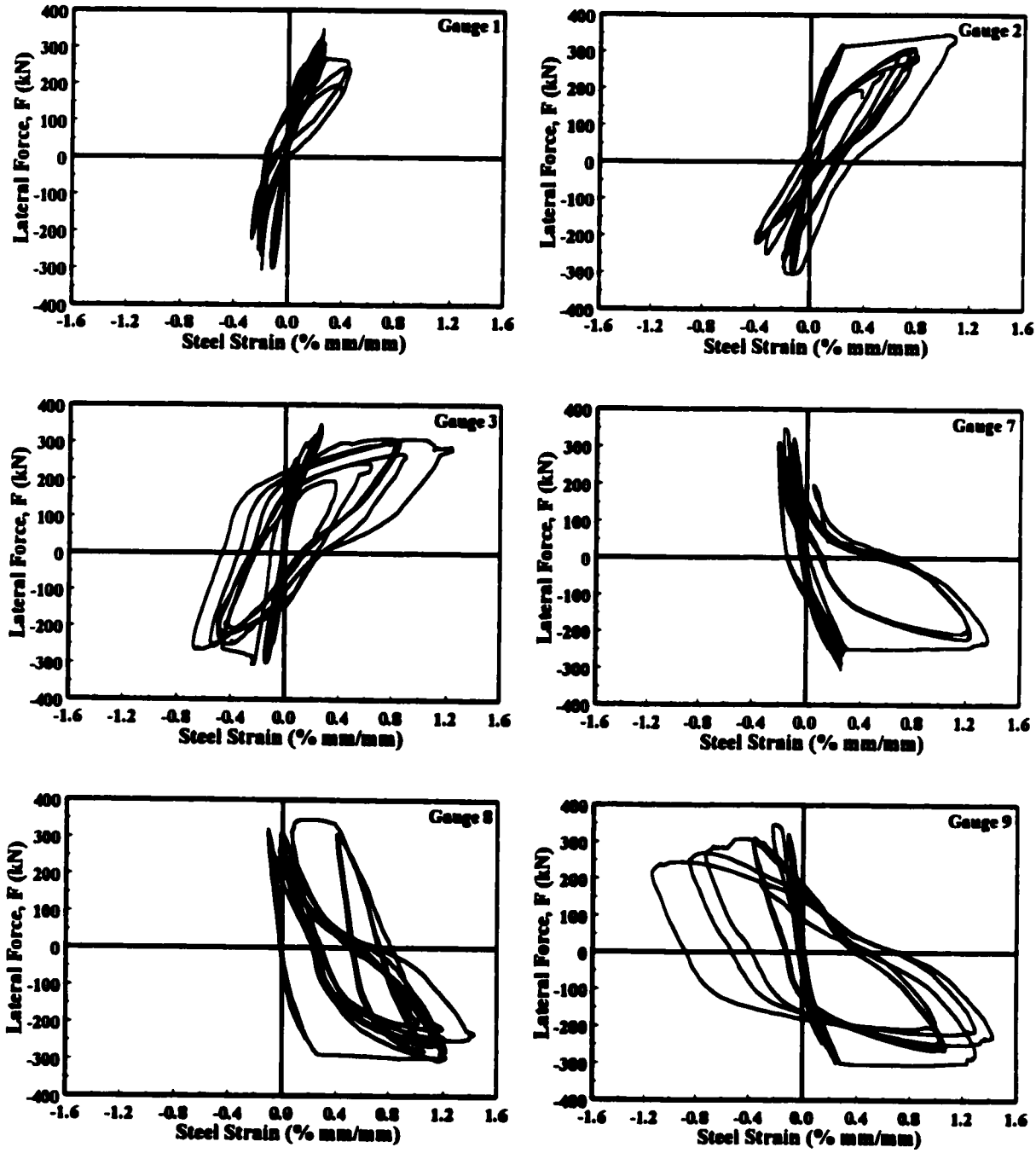

Figure 4.23 : Strain Gauge Data for Longitudinal Reinforcement in Column TC-3

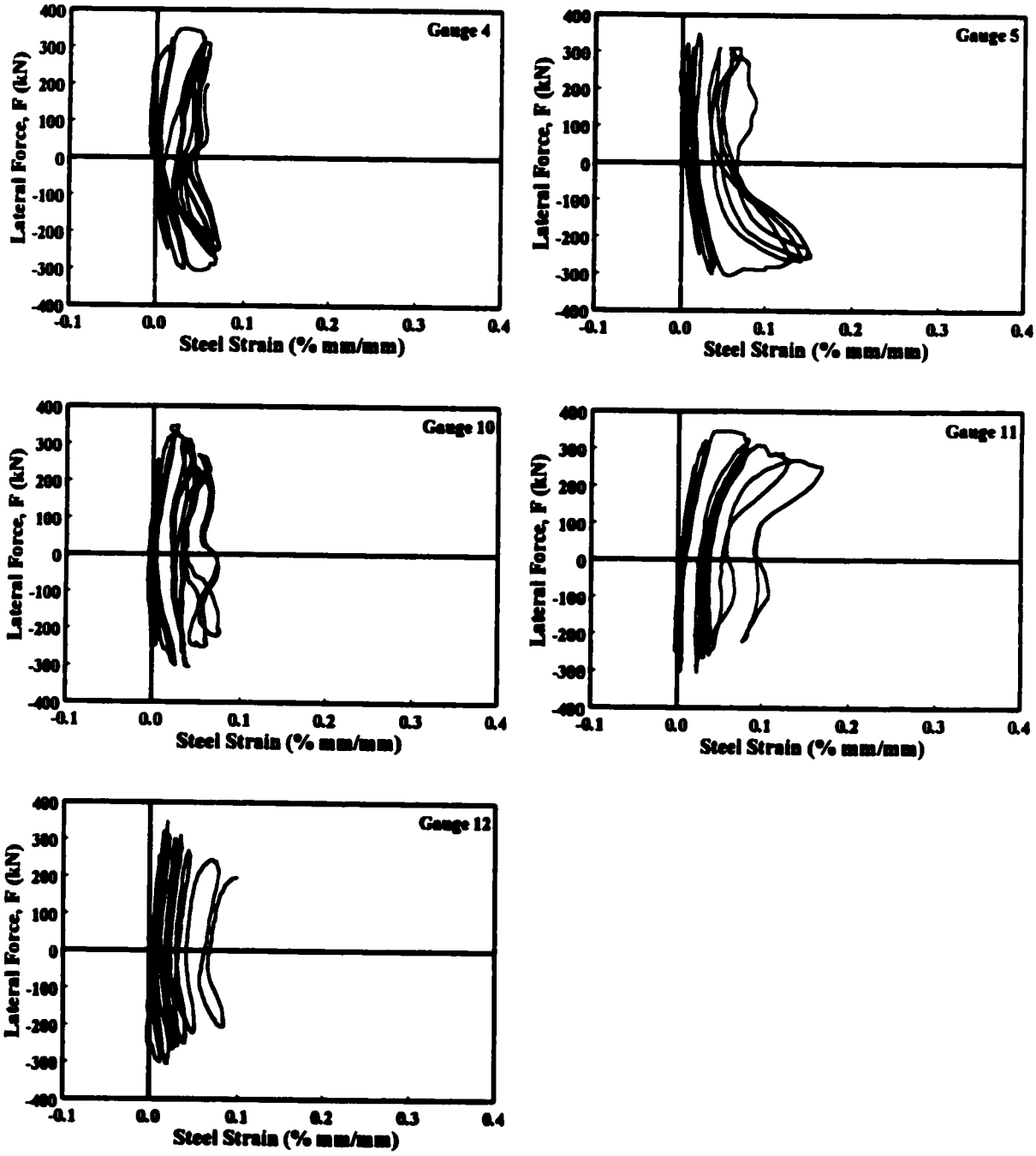

Figure 4.24 : Strain Gauge Data for Transverse Reinforcement in Column TC-3

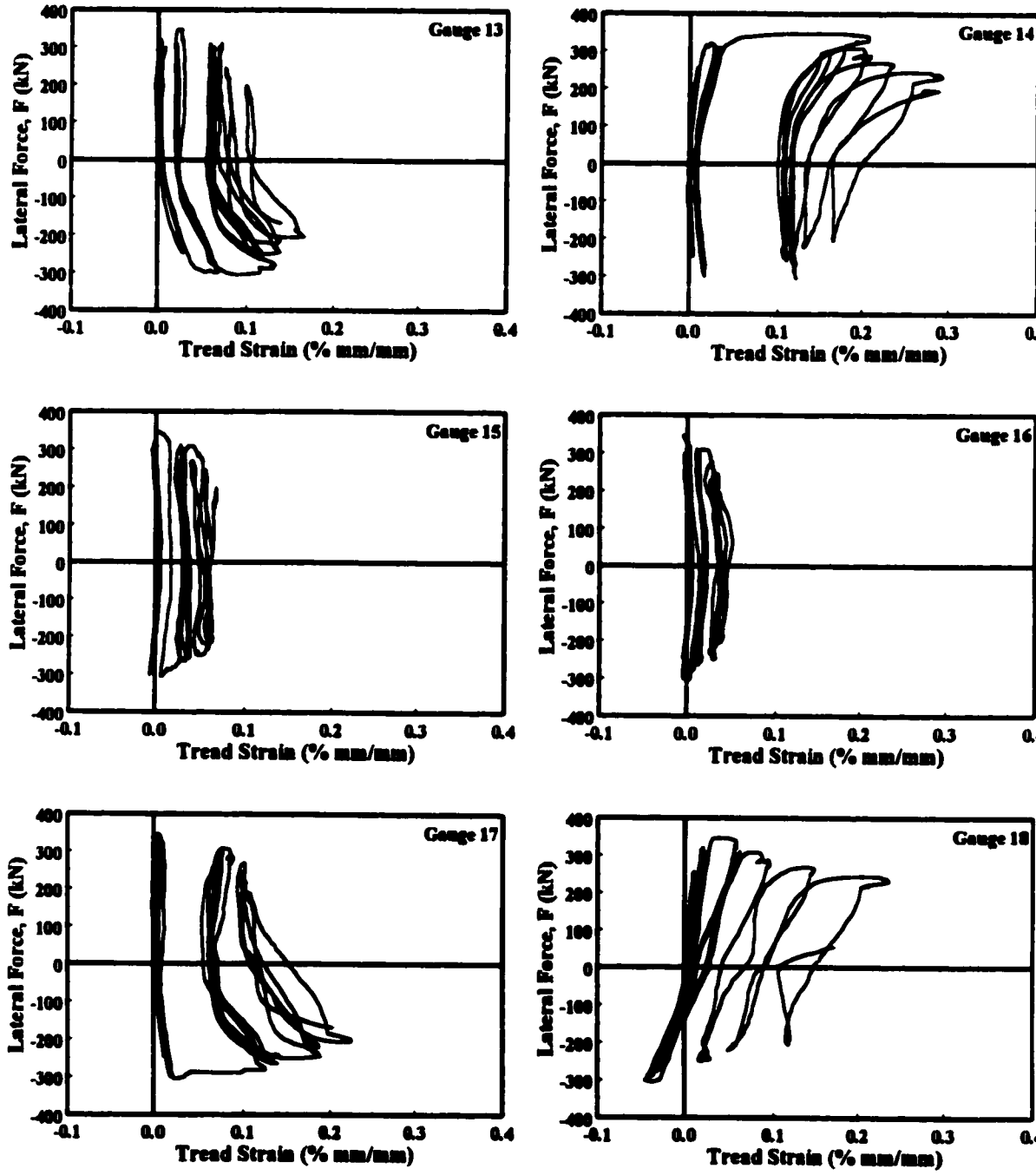

Figure 4.25 : Tire Strains in Column TC-3, Measured on Treads

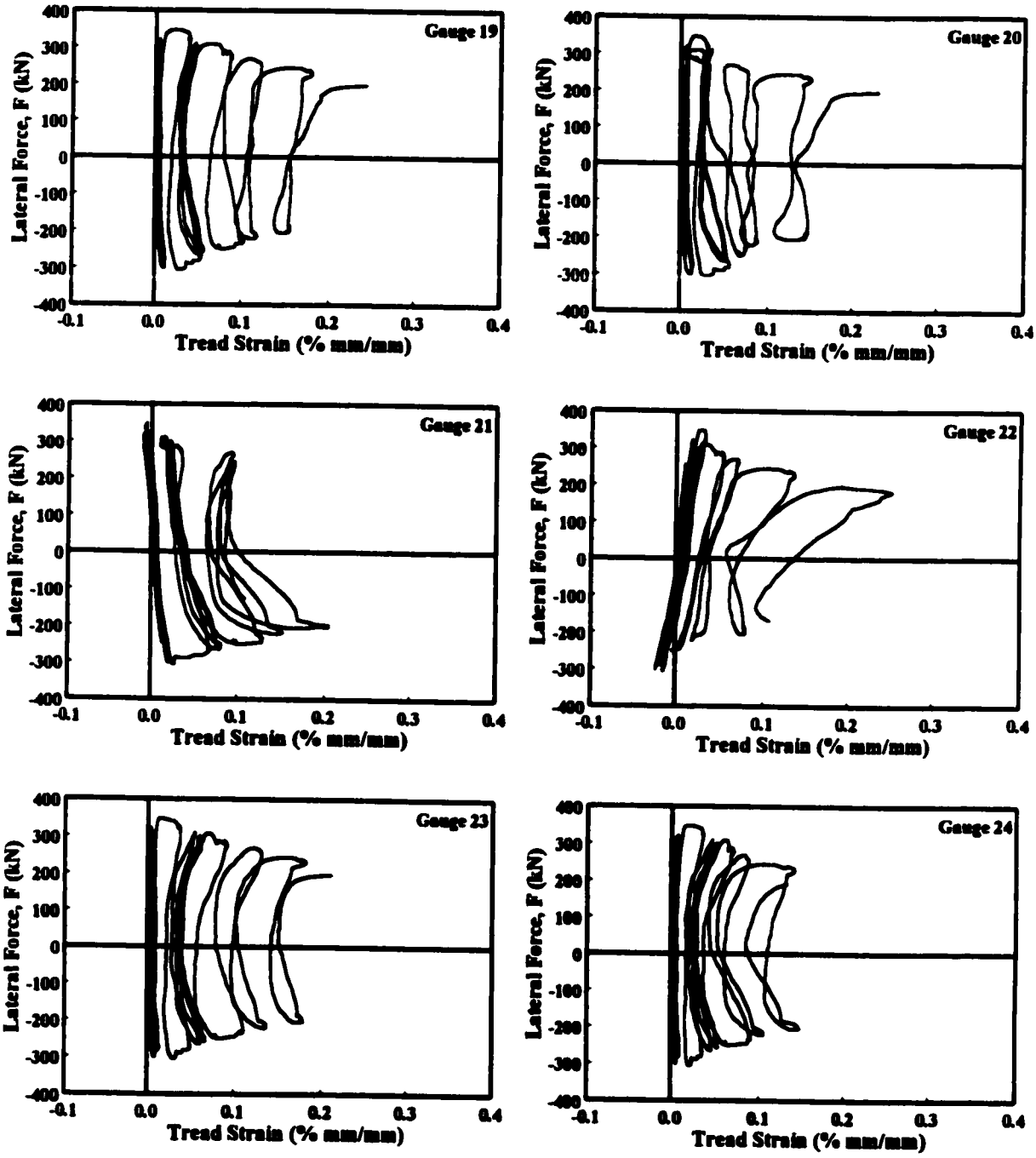

Figure 4.25 (Continued) : Tire Strains in Column TC-3, Measured on Treads

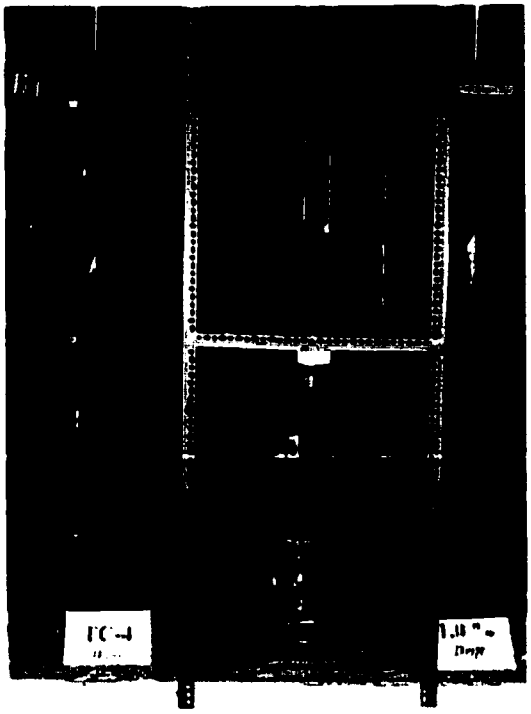

(a) At 1% Drift

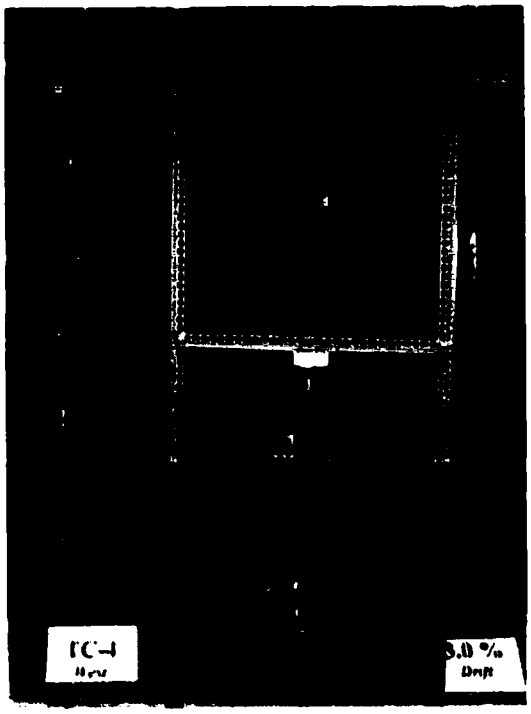

(b) At 3% Drift

(c) At 4% Drift

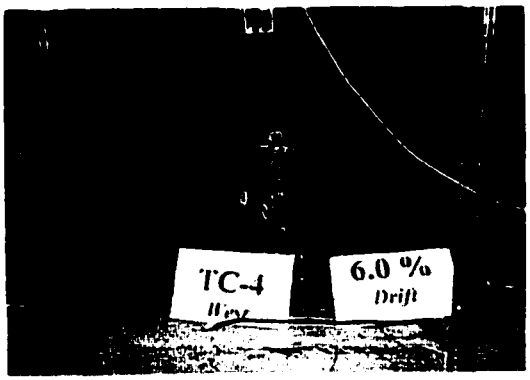

(d) At 6% Drift (West View)

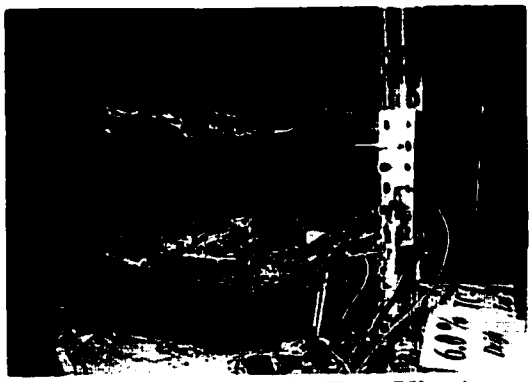

(e) At 6% Drift (East View)

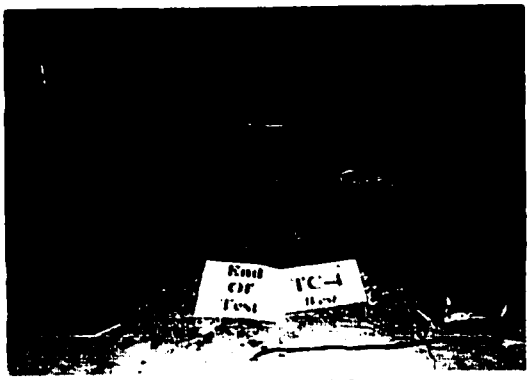

(f) At End of Test

Figure 4.26 : Behavior of Column TC-4 During Selected Stages of Testing

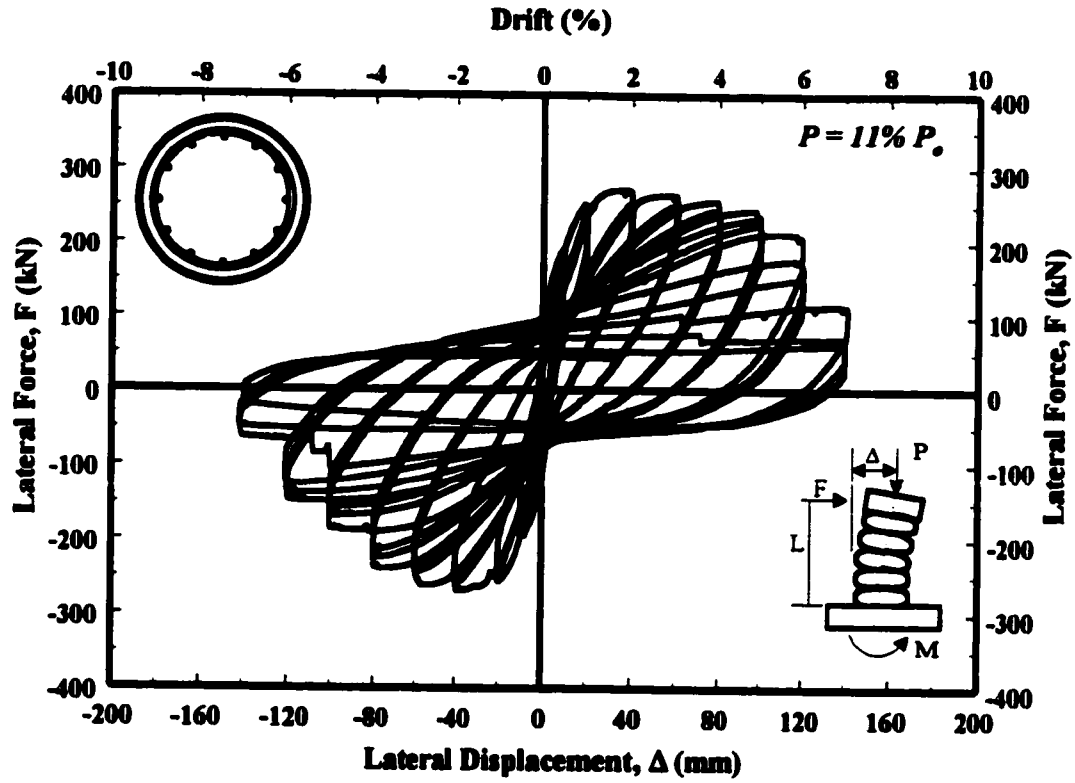

Figure 4.27 : Hysteretic Force-Displacement Relationship for Column TC-4

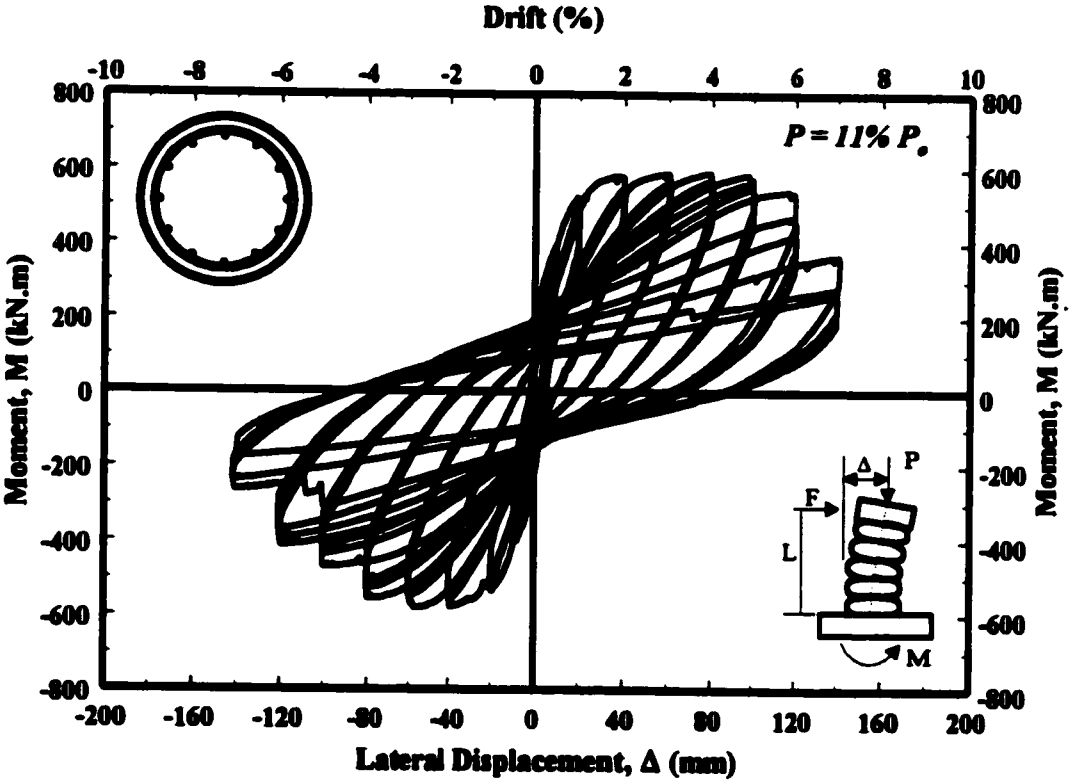

Figure 4.28 : Hysteretic Moment-Displacement Relationship for Column TC-4

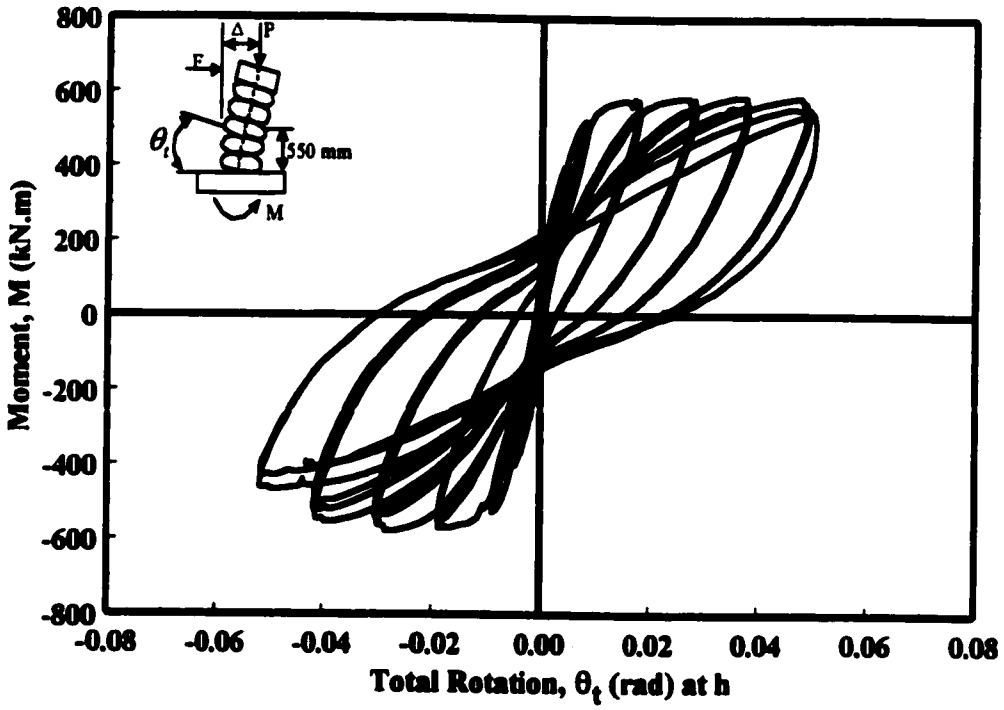

Figure 4.29 : Moment-Total Rotation Relationship for Column TC-4

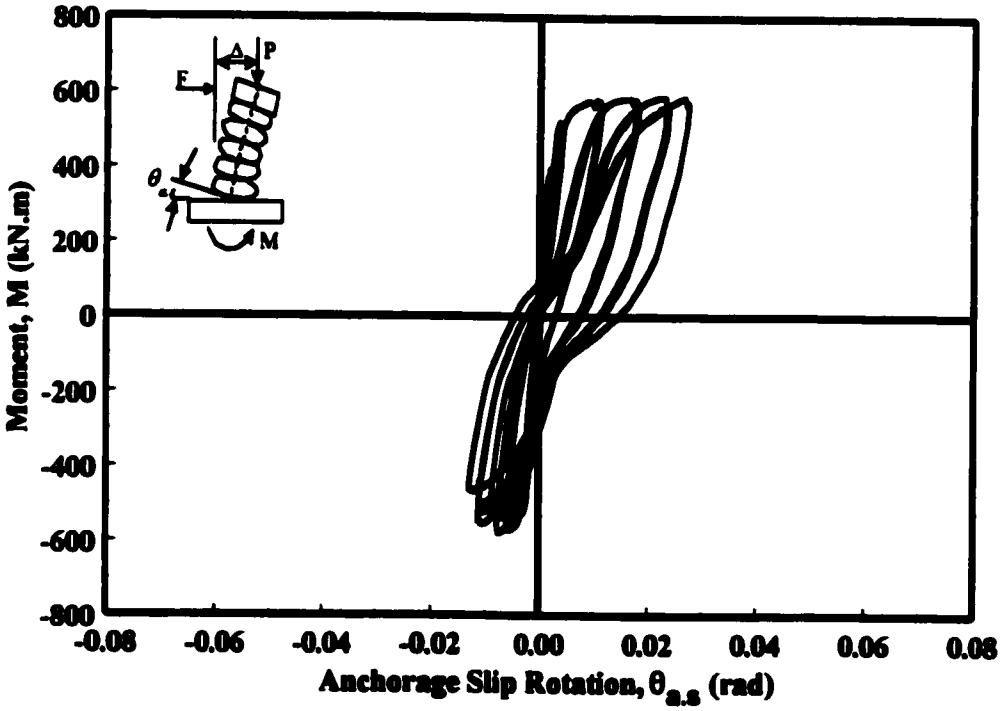

Figure 4.30 : Moment-Anchorage Slip Rotation Relationship for Column TC-4

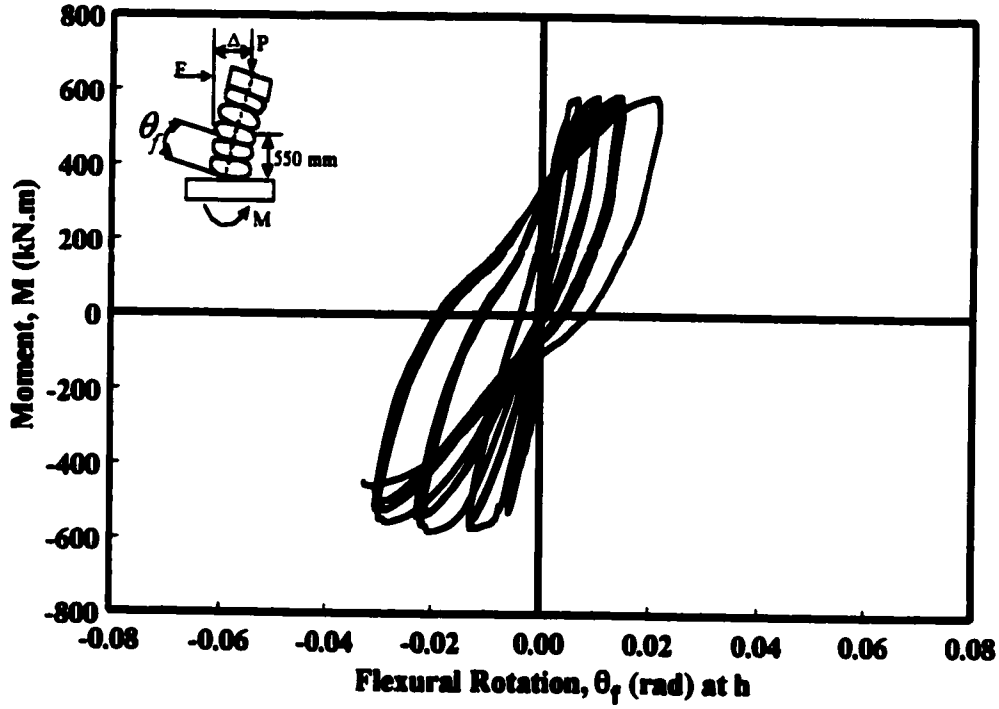

Figure 4.31 : Moment-Flexural Rotation Relationship for Column TC-4

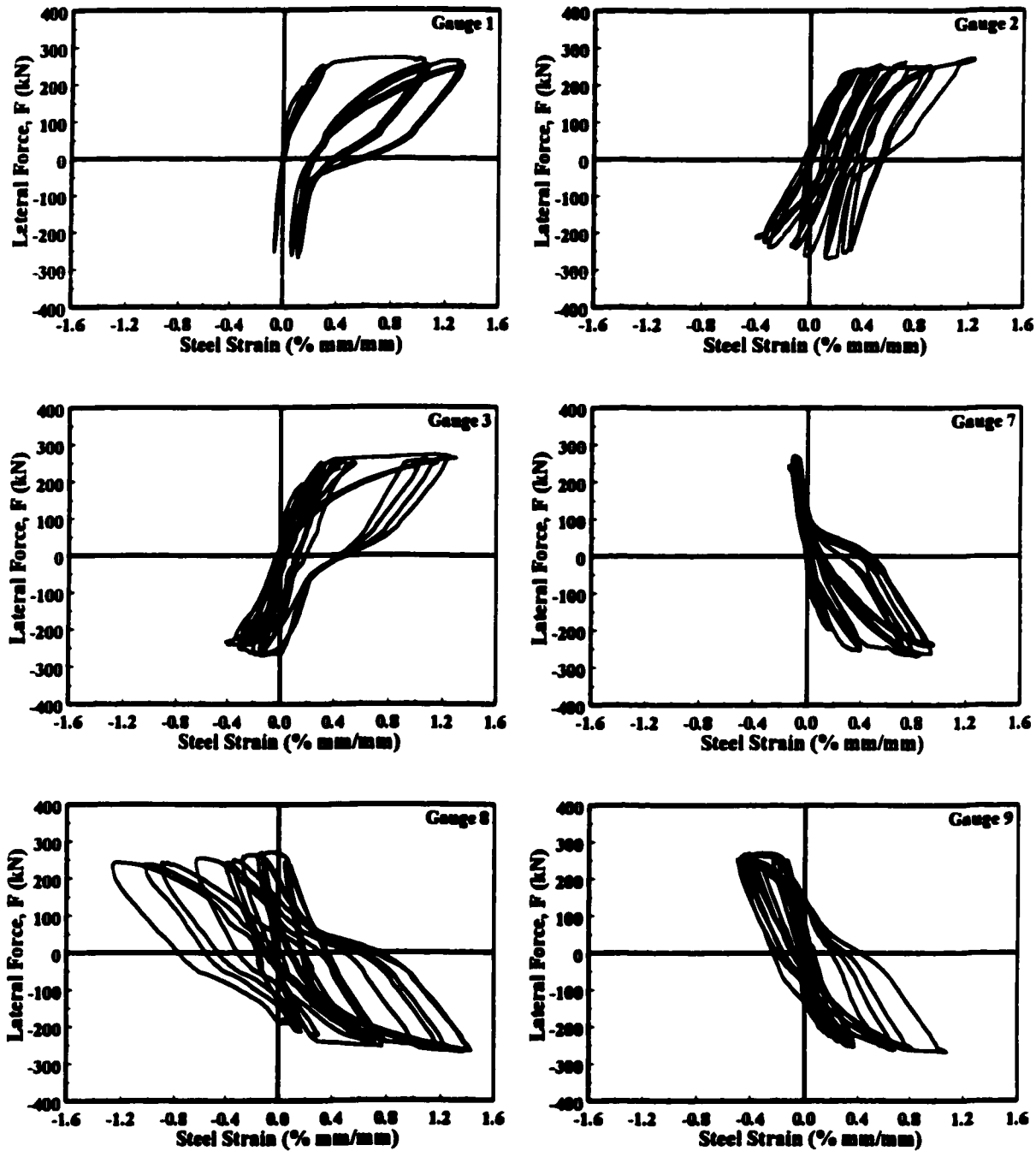

Figure 4.32 : Strain Gauge Data for Longitudinal Reinforcement in Column TC-4

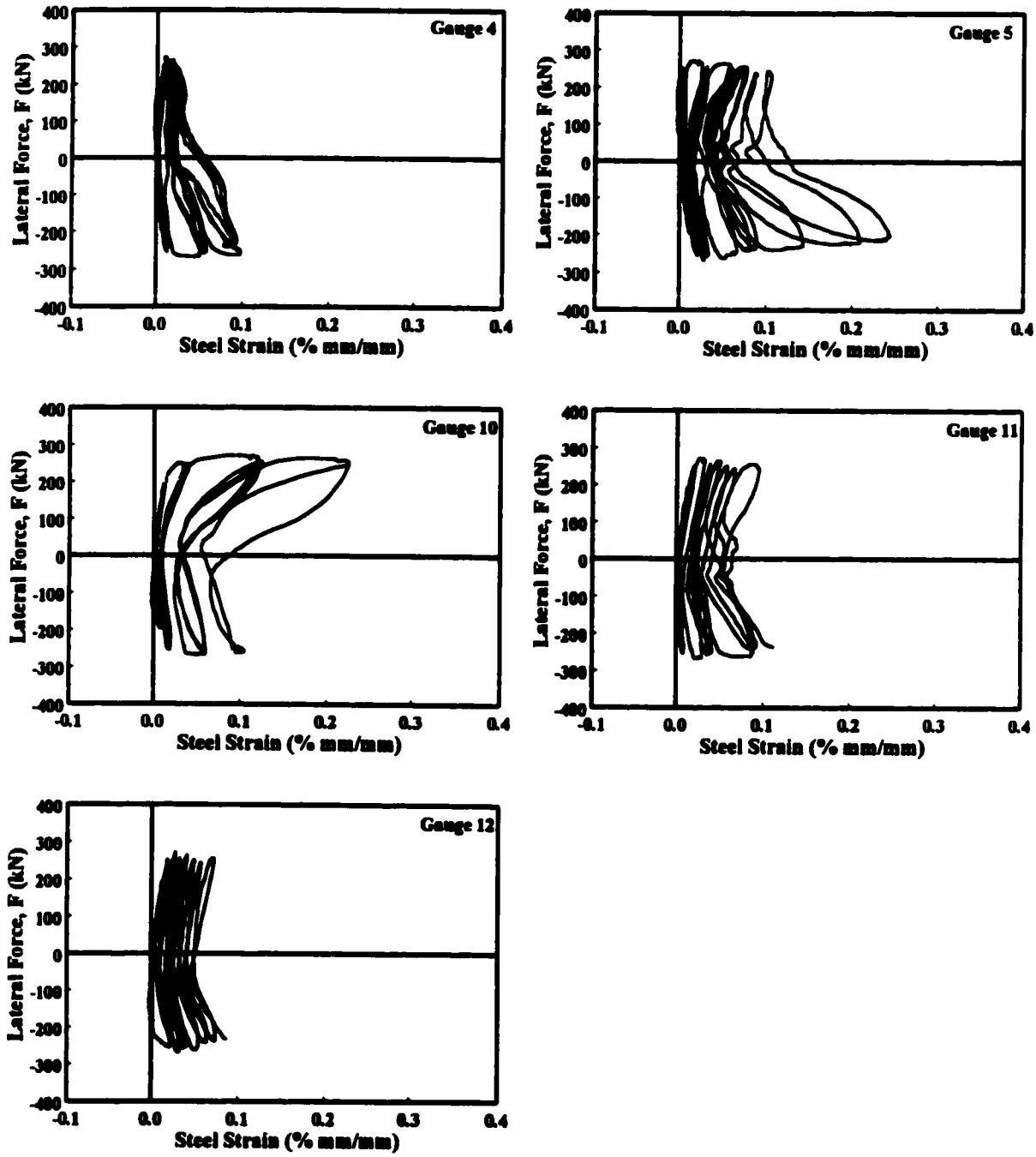

Figure 4.33 : Strain Gauge Data for Transverse Reinforcement in Column TC-4

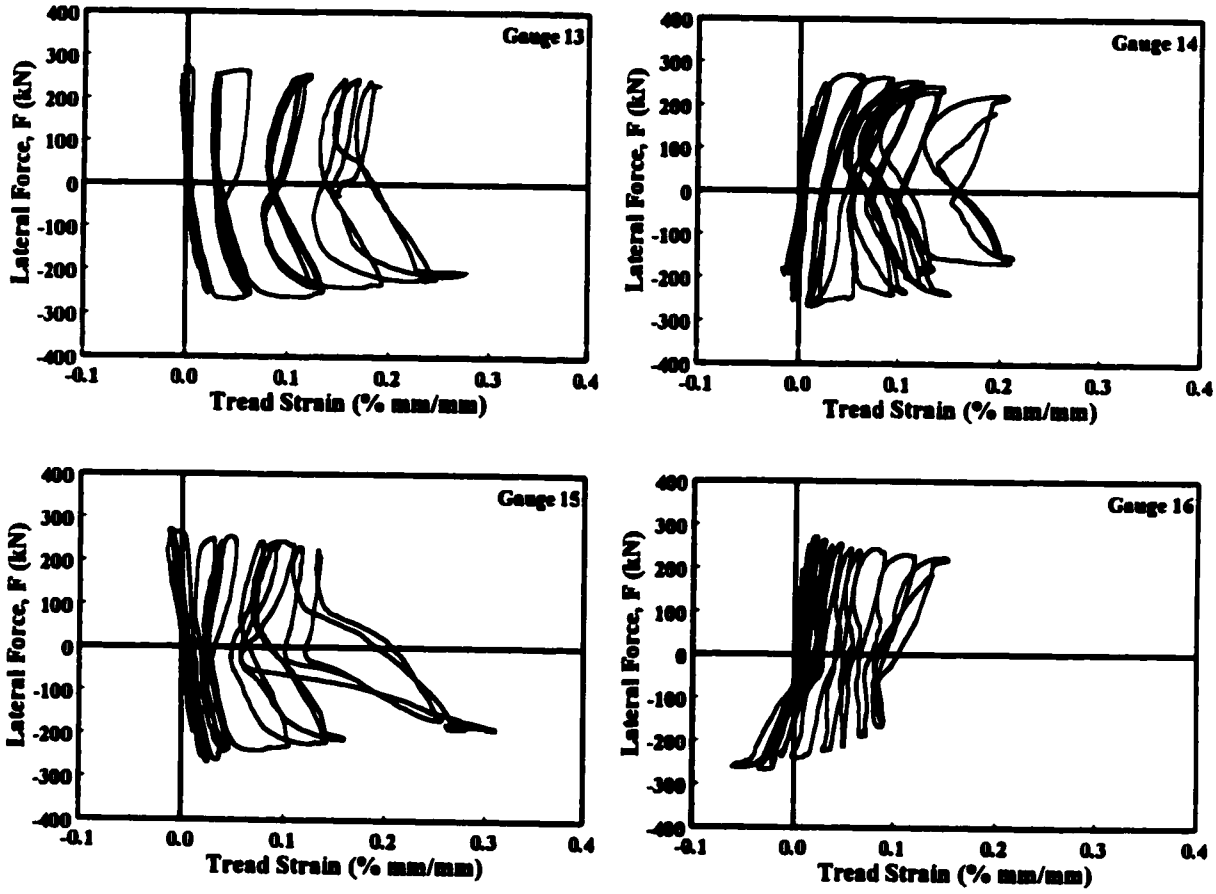

Figure 4.34 : Tire Strains in Column TC-4, Measured on Treads

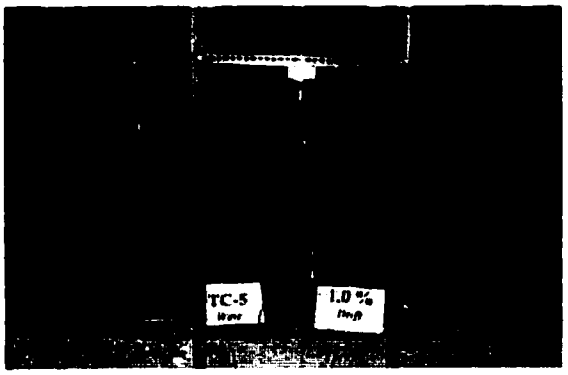

(a) At 1% Drift

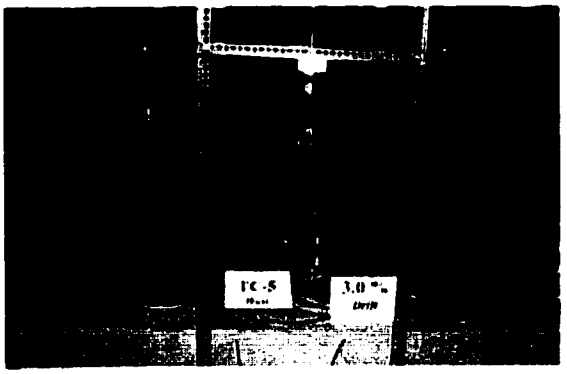

(b) At 3% Drift

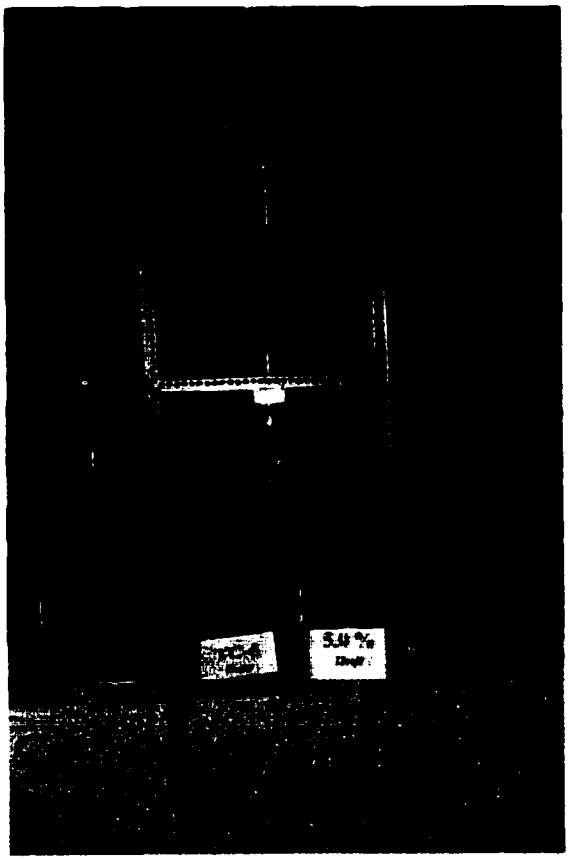

(c) At 5% Drift

(d) At 6% Drift

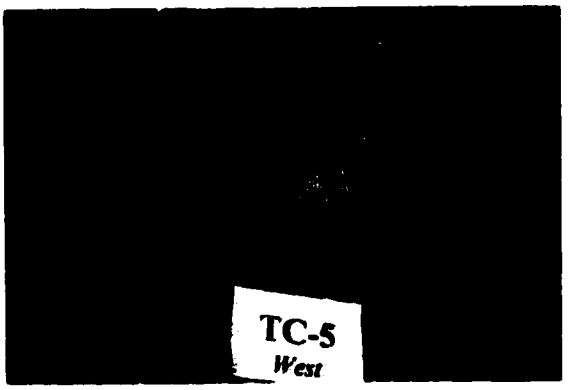

(e) At End of Test

Figure 4.35 : Behavior of Column TC-5 During Selected Stages of Testing

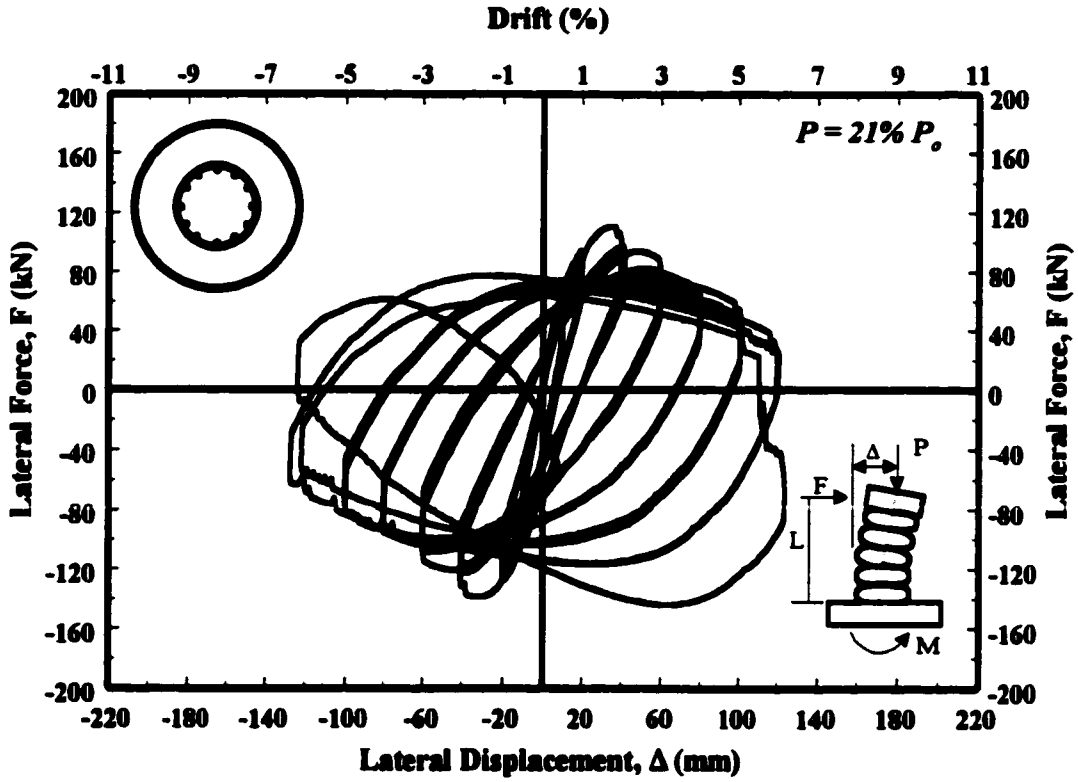

Figure 4.36 : Hysteretic Force-Displacement Relationship for Column TC-5

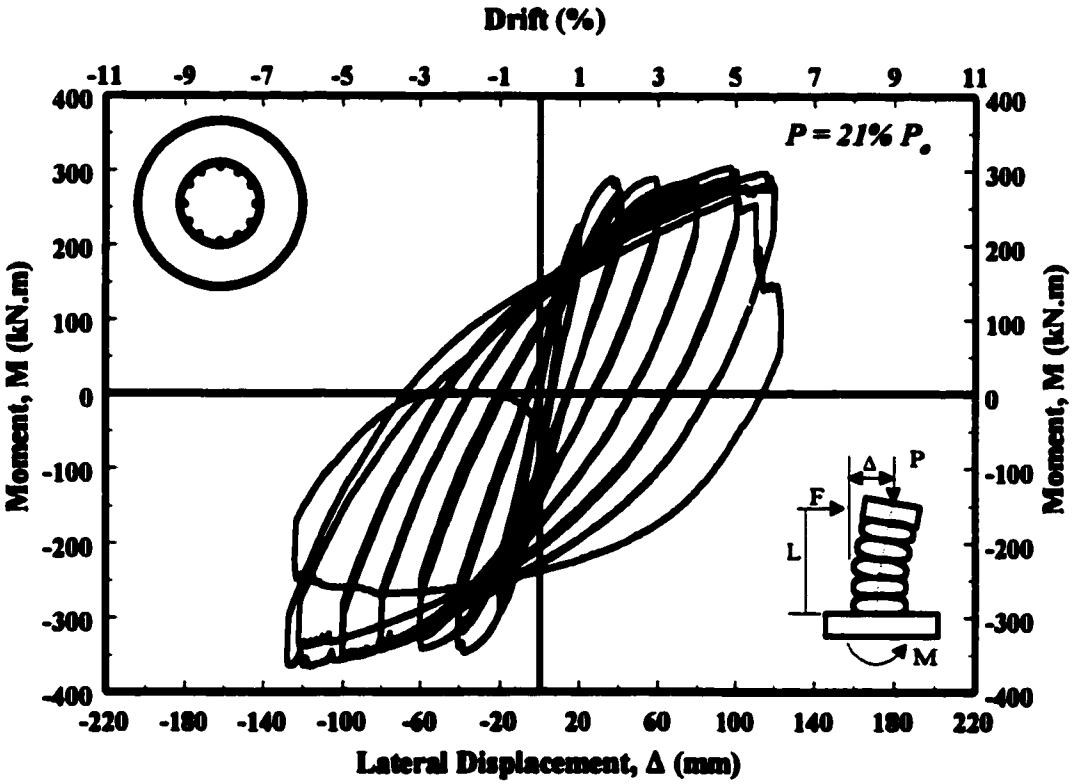

Figure 4.37 : Hysteretic Moment-Displacement Relationship for Column TC-5

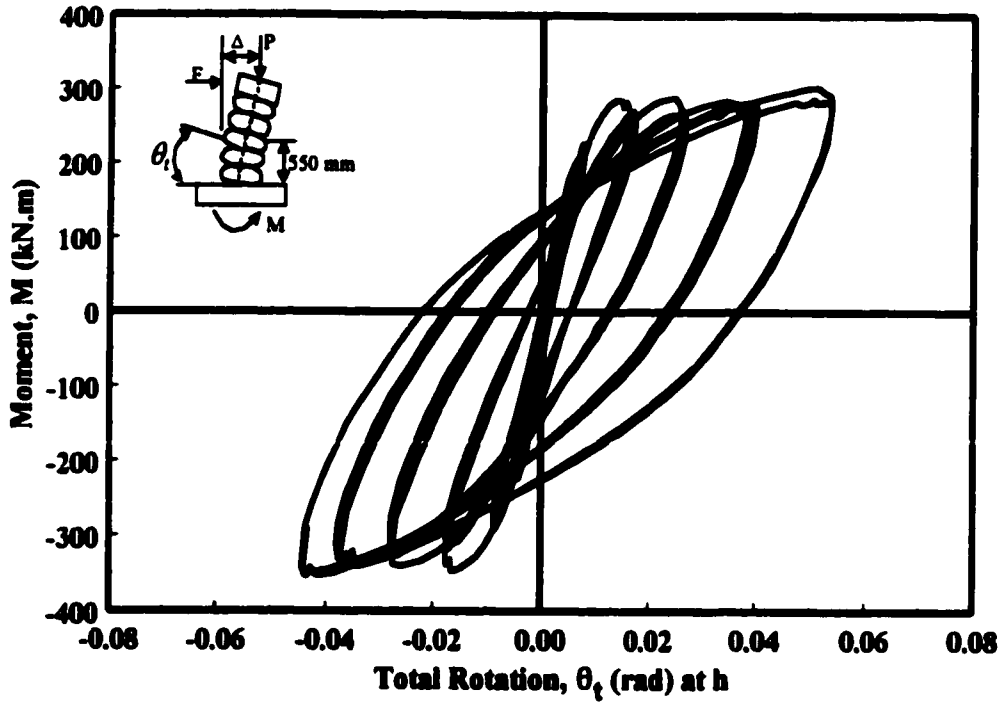

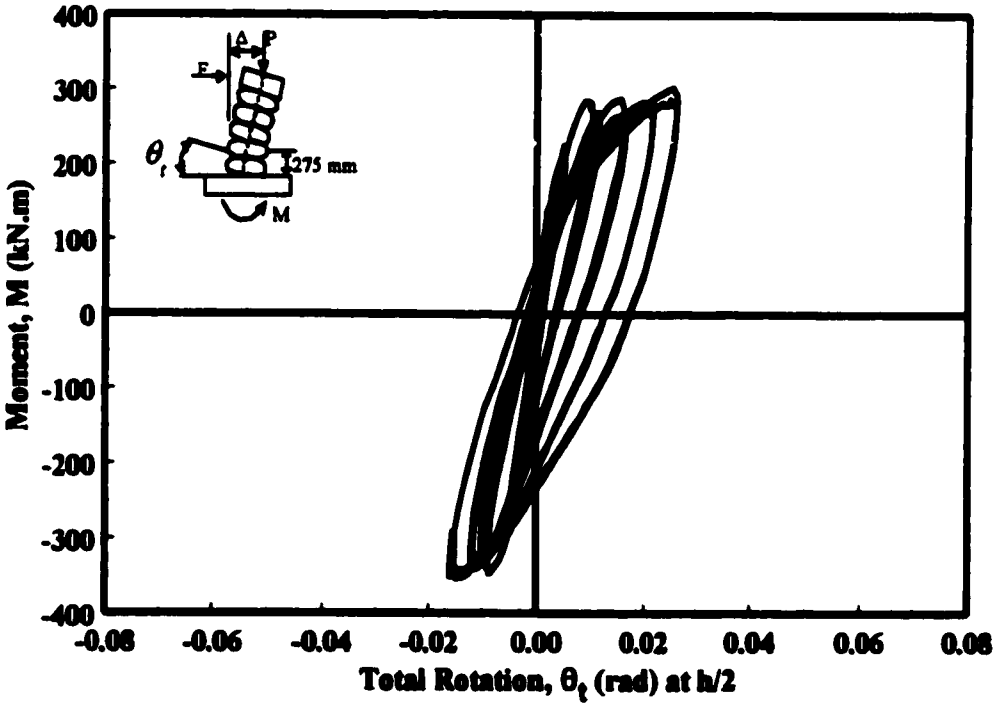

Figure 4.38 : Moment-Total Rotation Relationship for Column TC-5

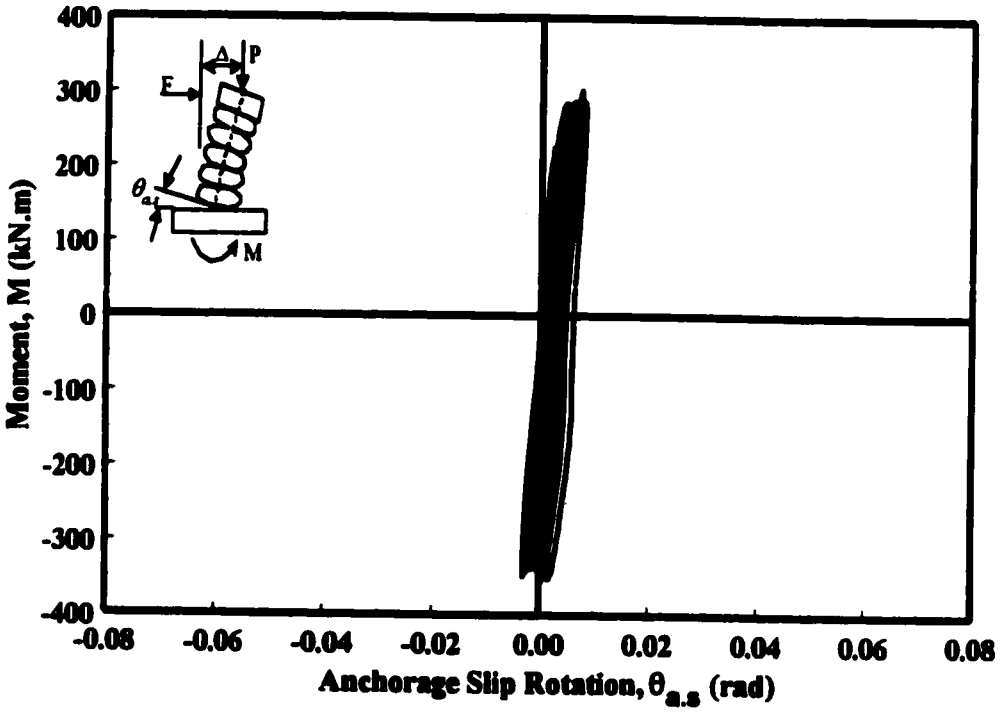

Figure 4.39 : Moment-Anchorage Slip Rotation Relationship for Column TC-5

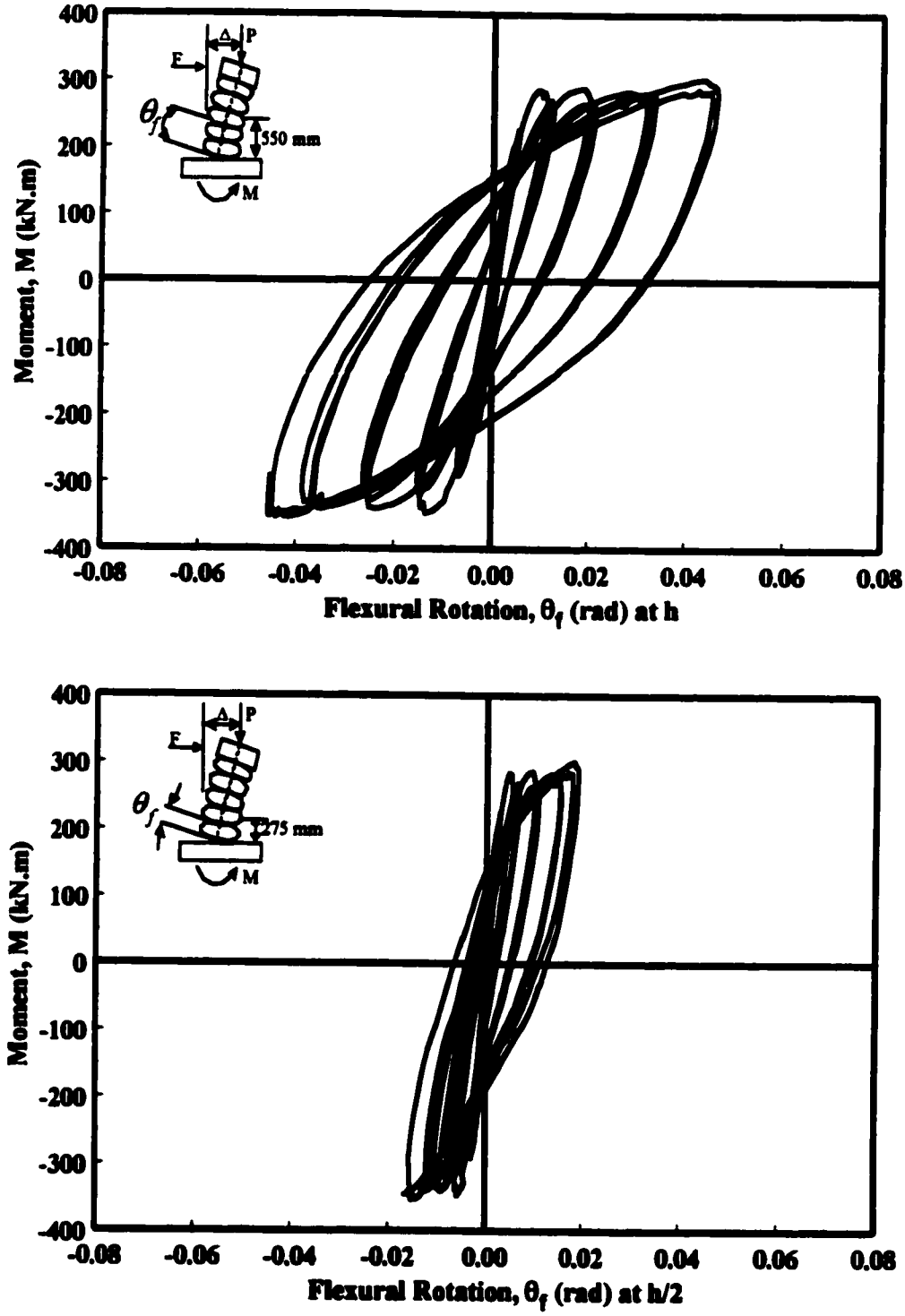

Figure 4.40 : Moment-Flexural Rotation Relationship for Column TC-5

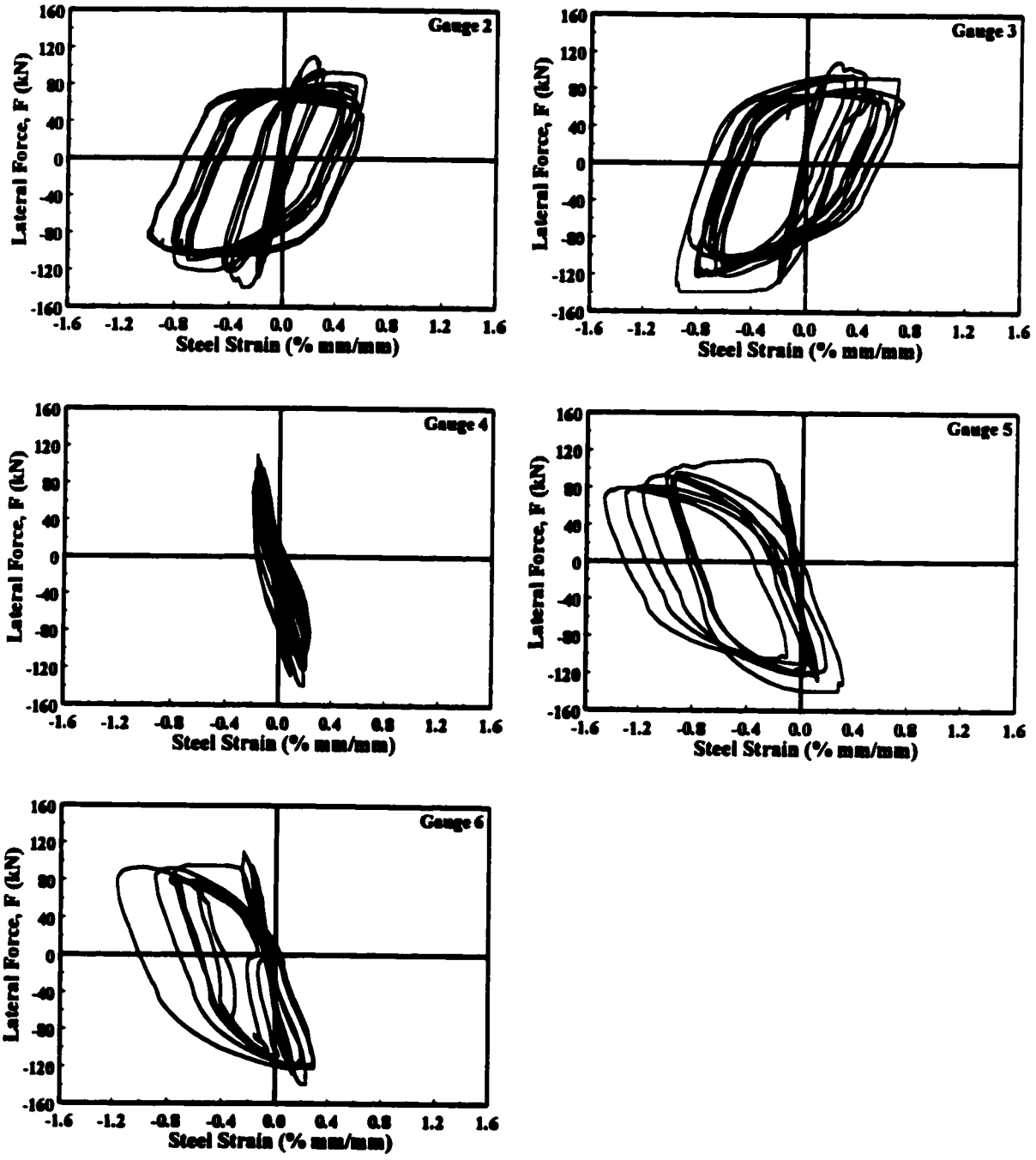

Figure 4.41 : Strain Gauge Data for Longitudinal Reinforcement in Column TC-5

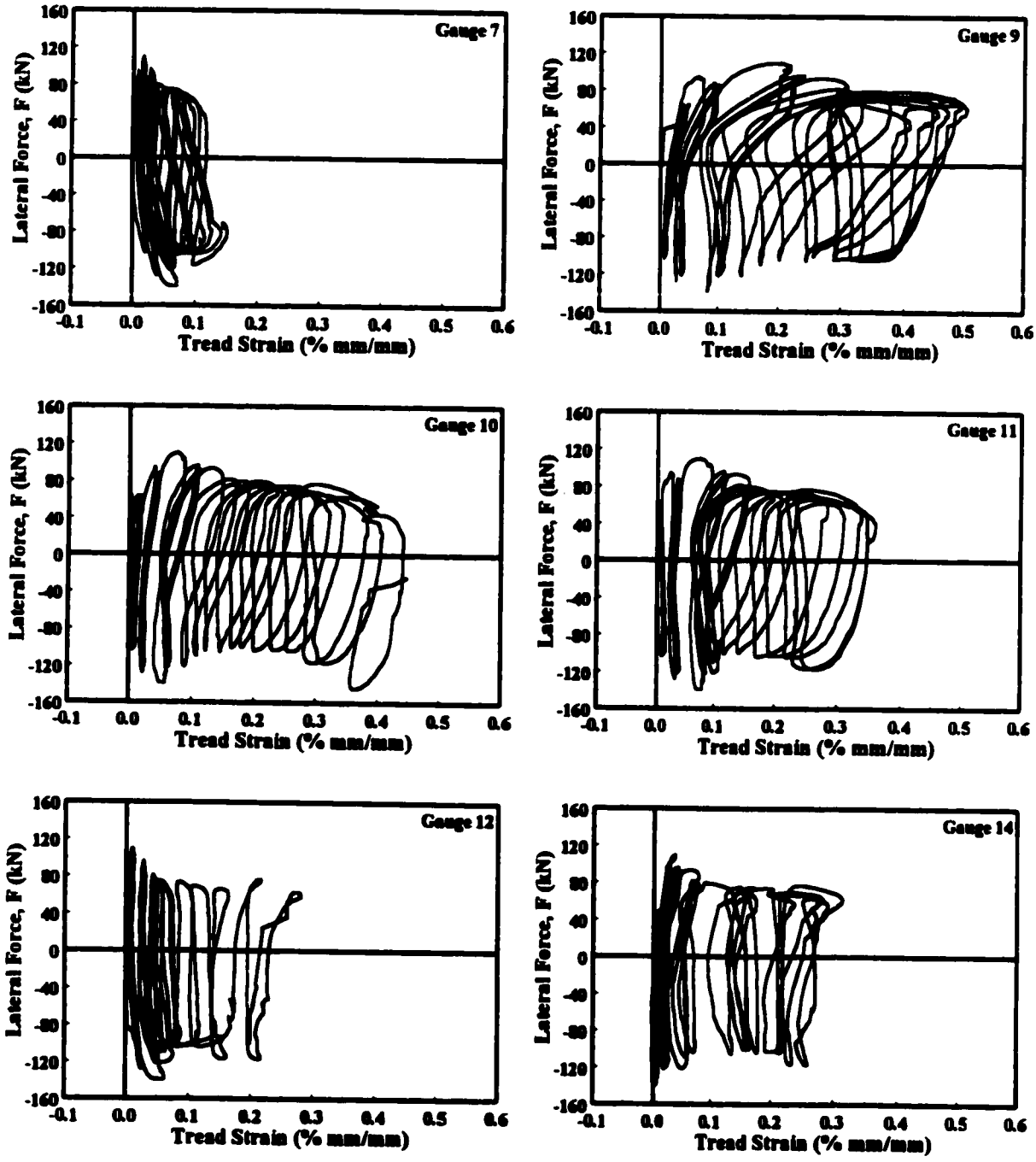

Figure 4.42 : Tire Strains in Column TC-5, Measured on Treads

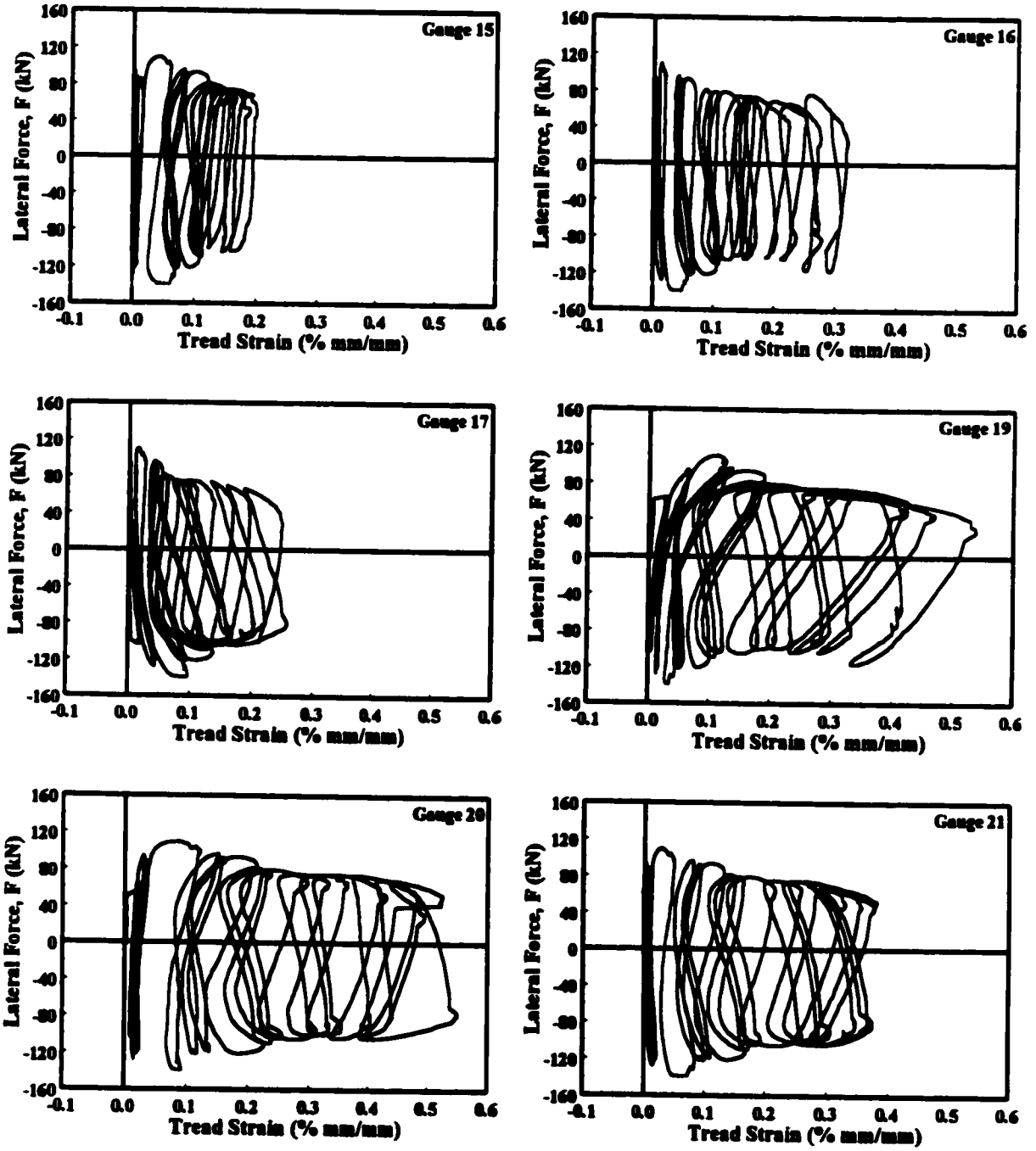

Figure 4.42 (Continued) : Tire Strains in Column TC-5, Measured on Treads

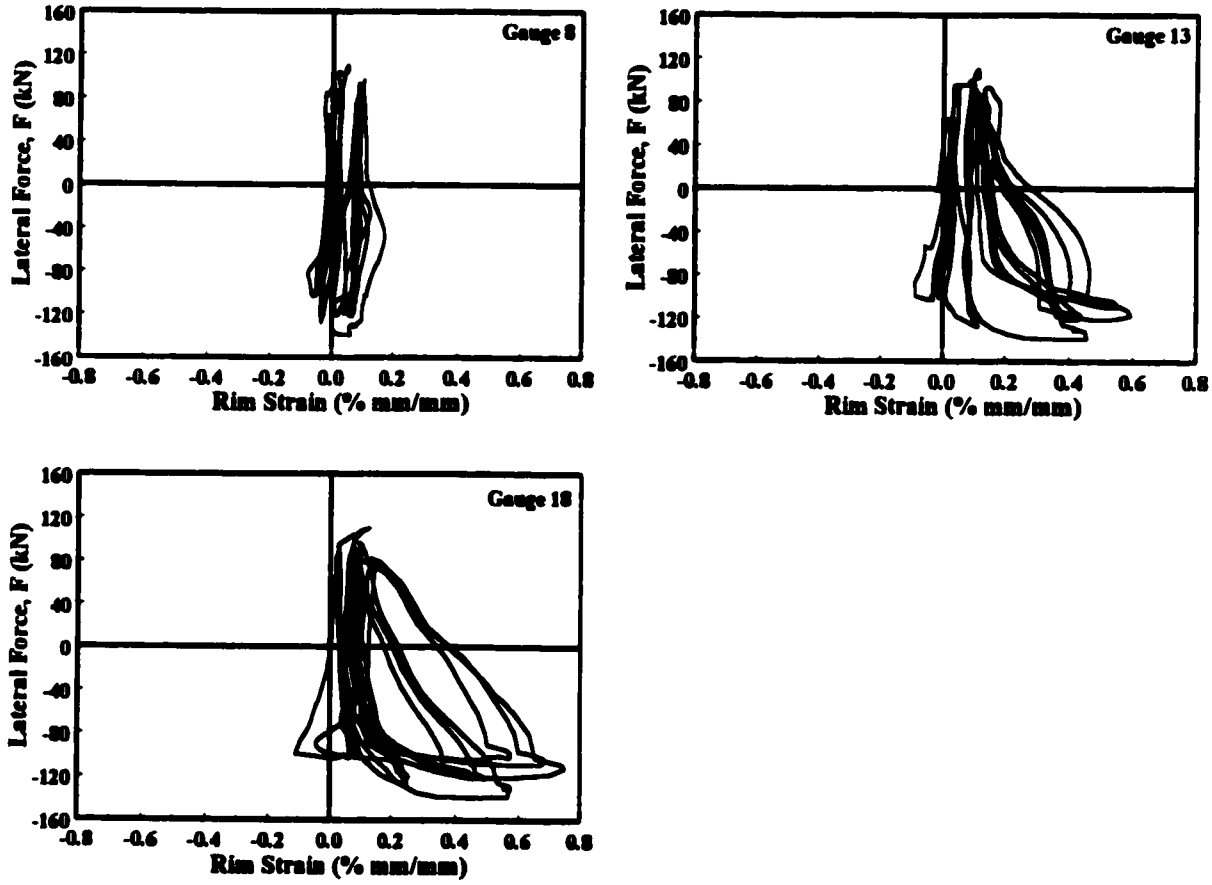

Figure 4.42 (Continued) : Tire Strains in Column TC-5, Measured on Rims

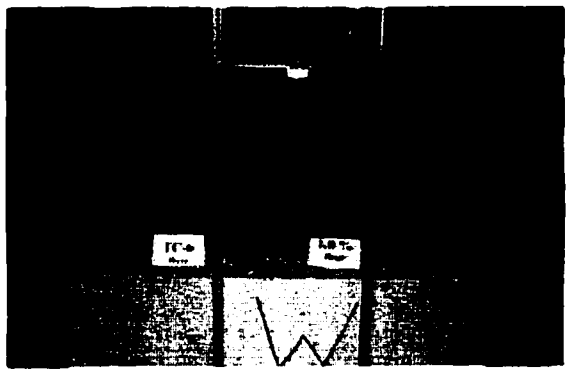

(a) At 1% Drift

(b) At 5% Drift

(c) At 6% Drift, Close-up (West View)

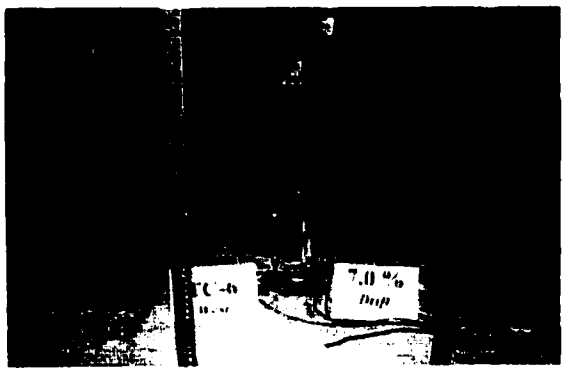

(d) At 7% Drift

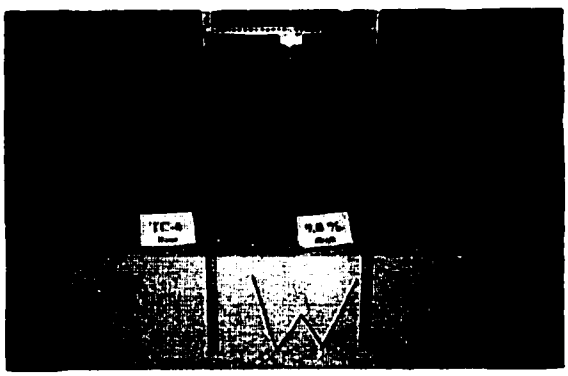

(e) At 9% Drift

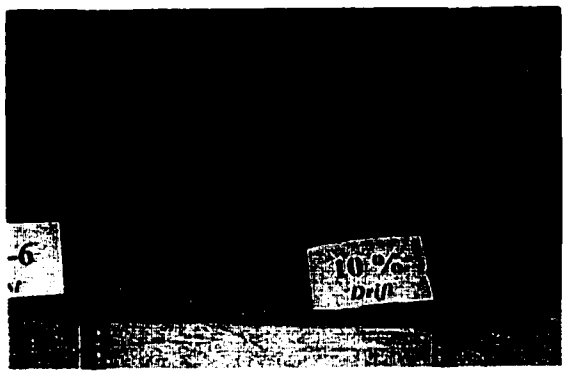

(f) At 10% Drift

Figure 4.43 : Behavior of Column TC-6 During Selected Stages of Testing

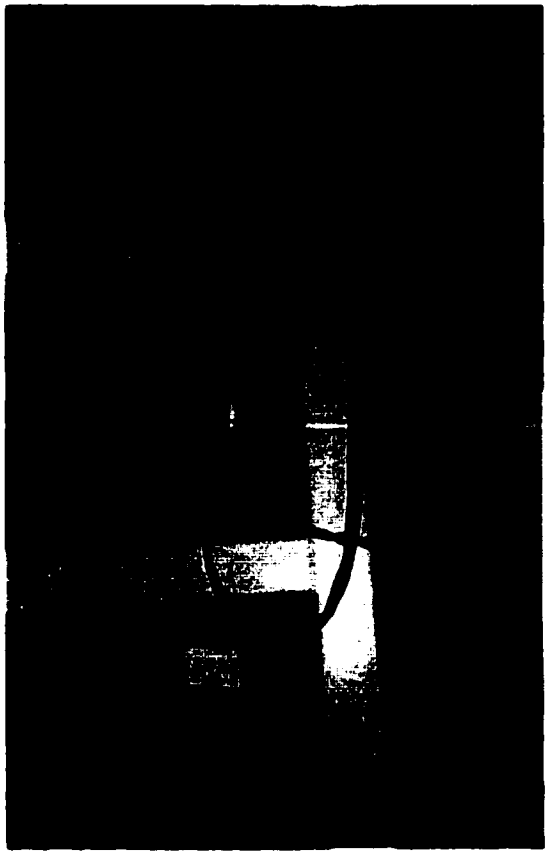

(g) South View At 8% Drift

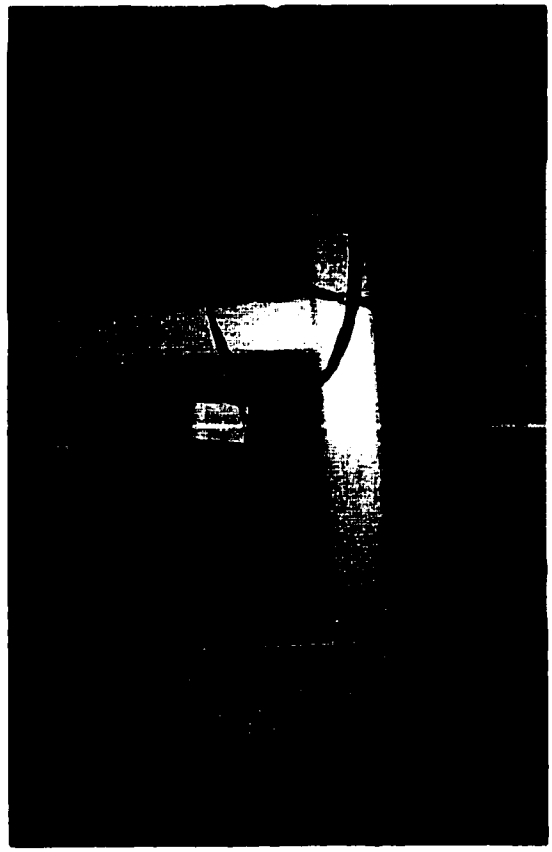

(h) South View At 10% Drift

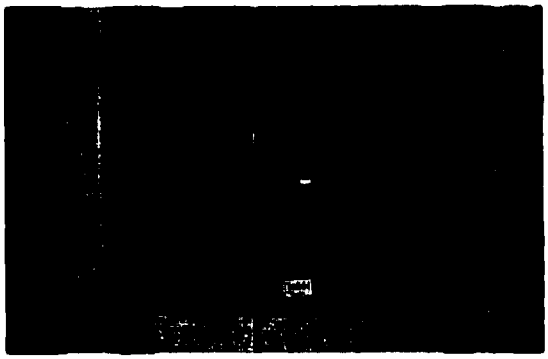

(i) At End of Test (Front View)

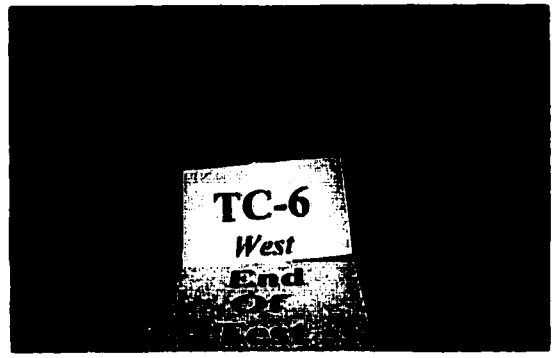

(j) At End of Test (West View)

Figure 4.43 : (Continued)

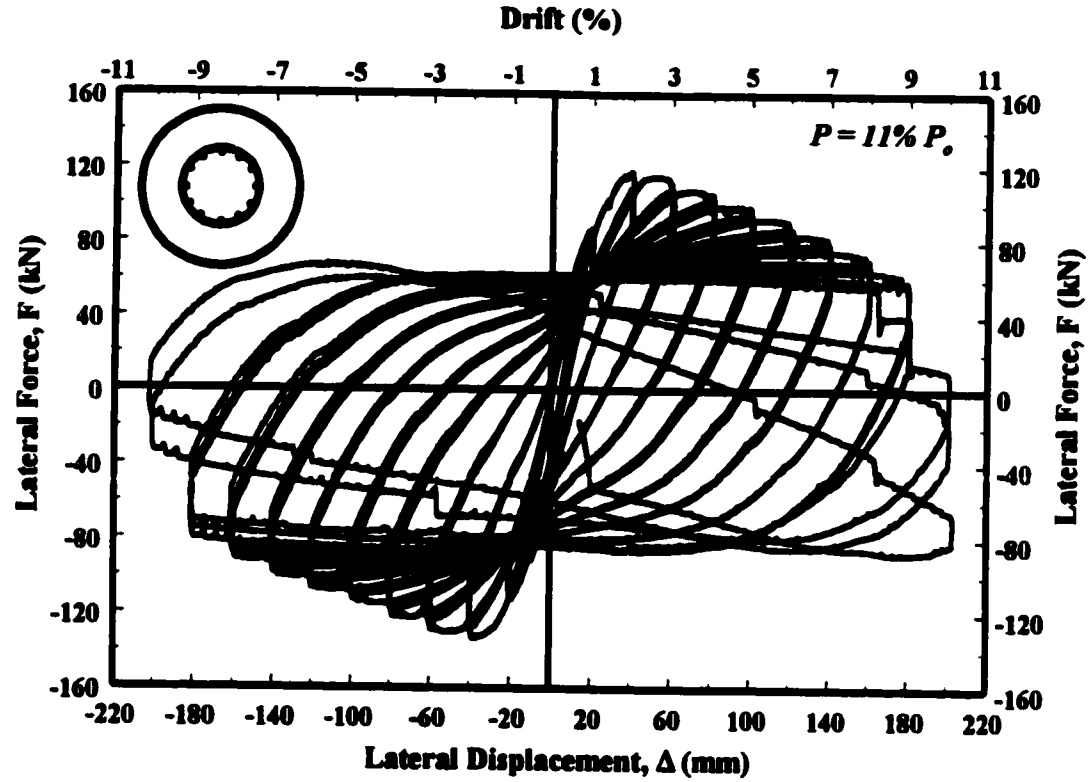

Figure 4.44 : Hysteretic Force-Displacement Relationship for Column TC-6

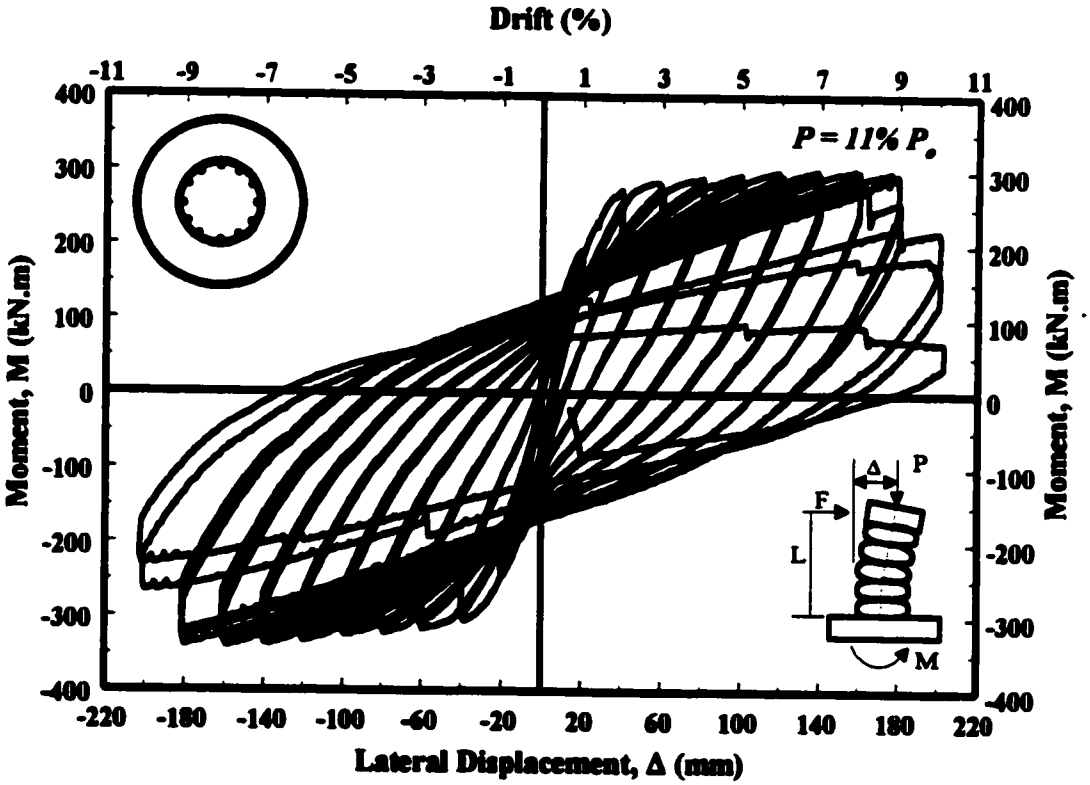

Figure 4.45 : Hysteretic Moment-Displacement Relationship for Column TC-6

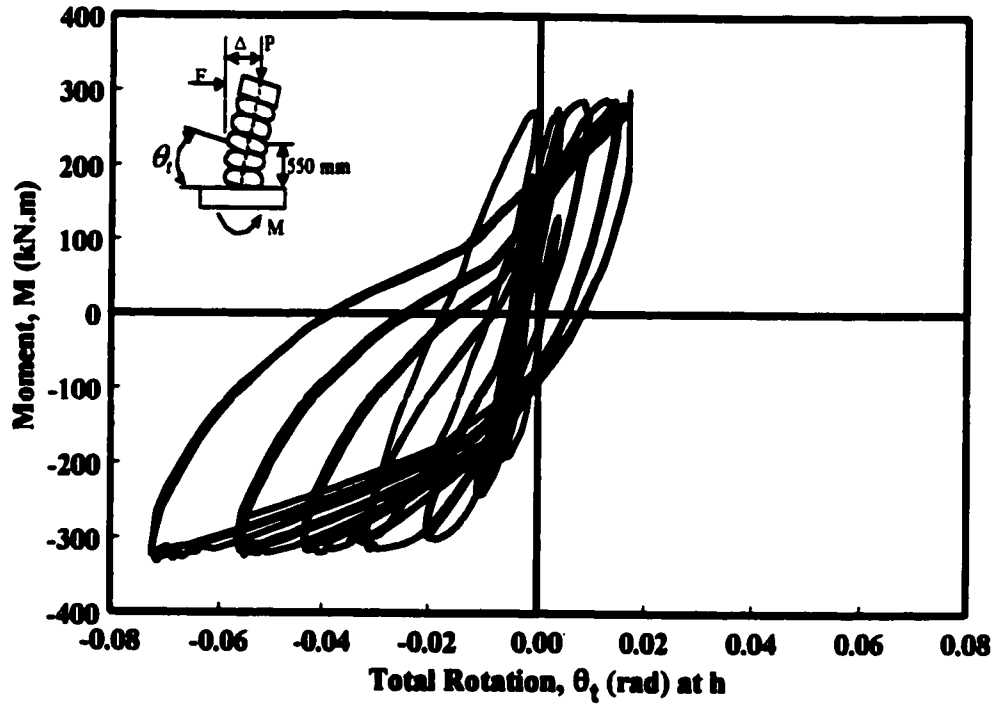

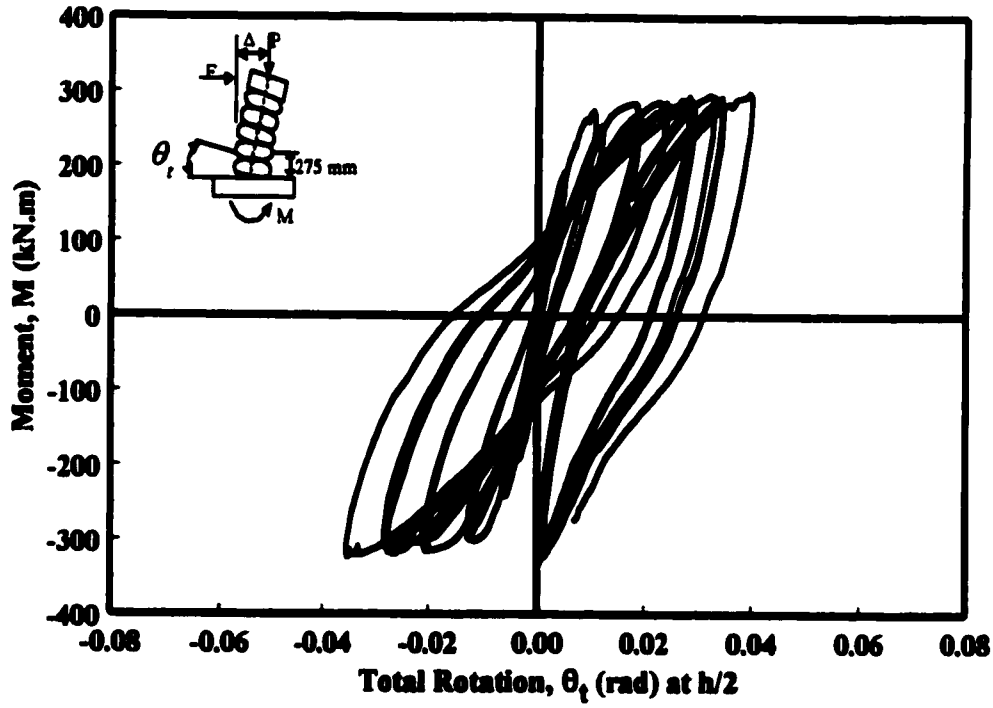

Figure 4.46 : Moment-Total Rotation Relationship for Column TC-6

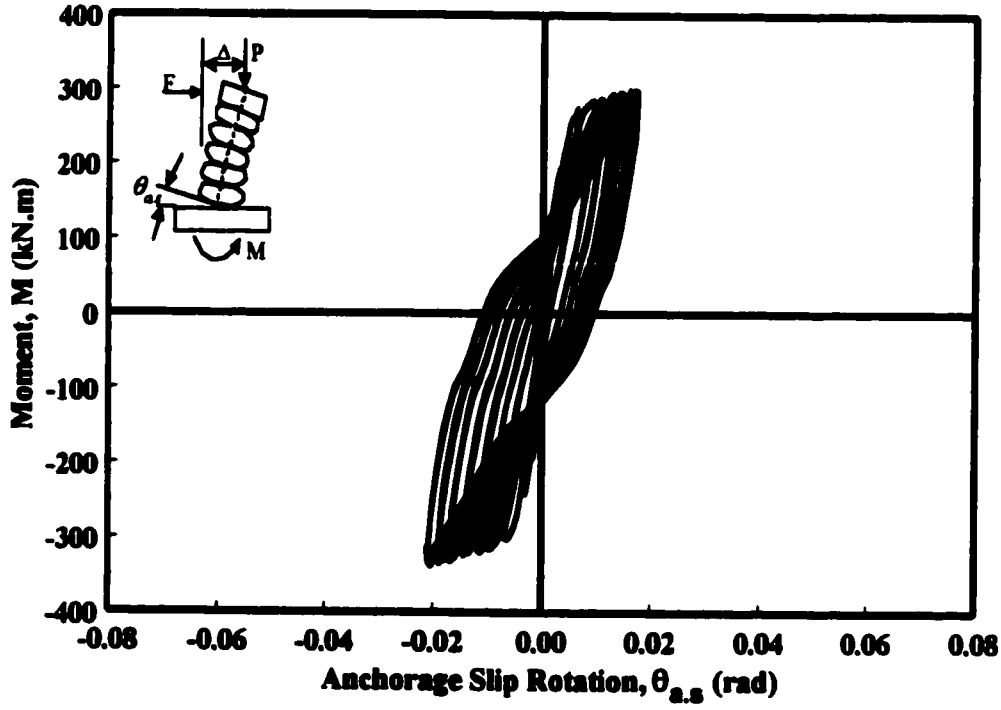

Figure 4.47 : Moment-Anchorage Slip Rotation Relationship for Column TC-6

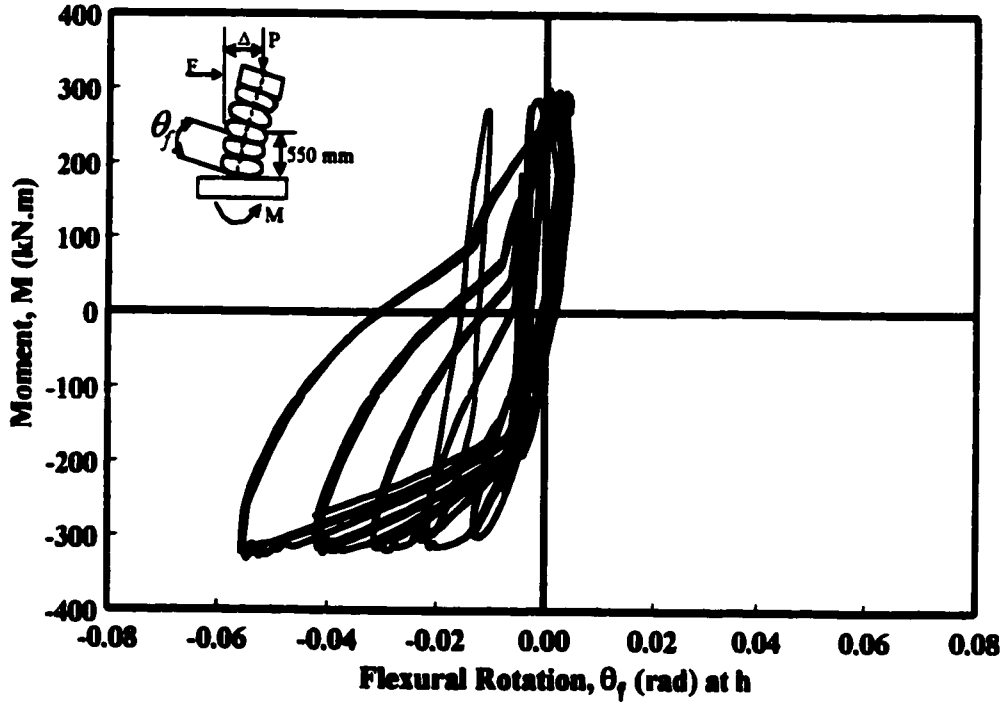

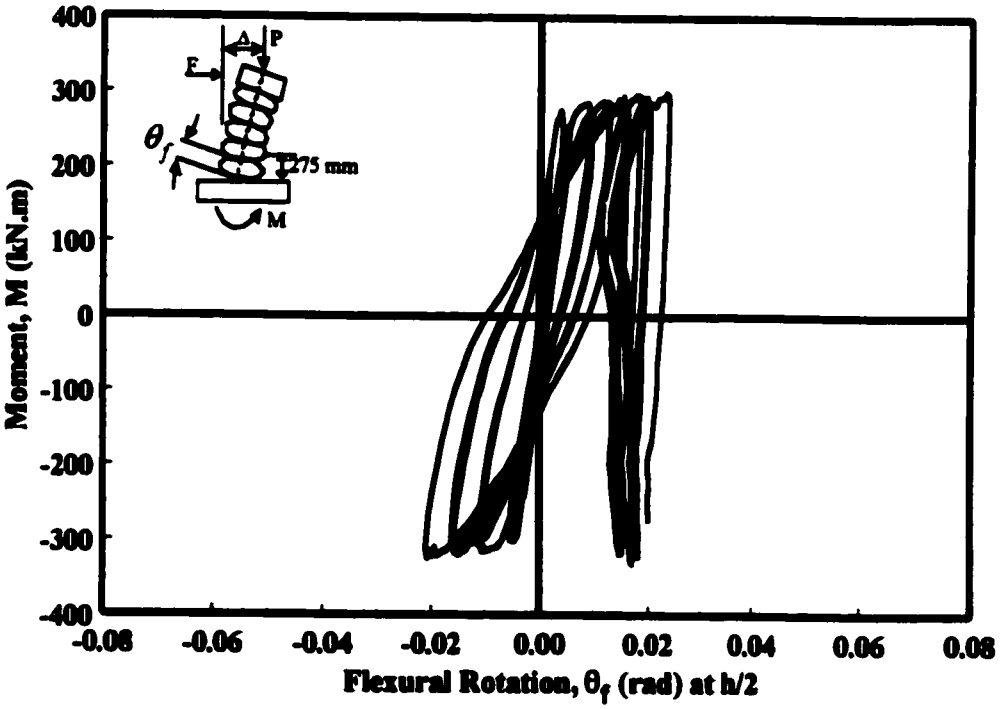

Figure 4.48 : Moment-Flexural Rotation Relationship for Column TC-6

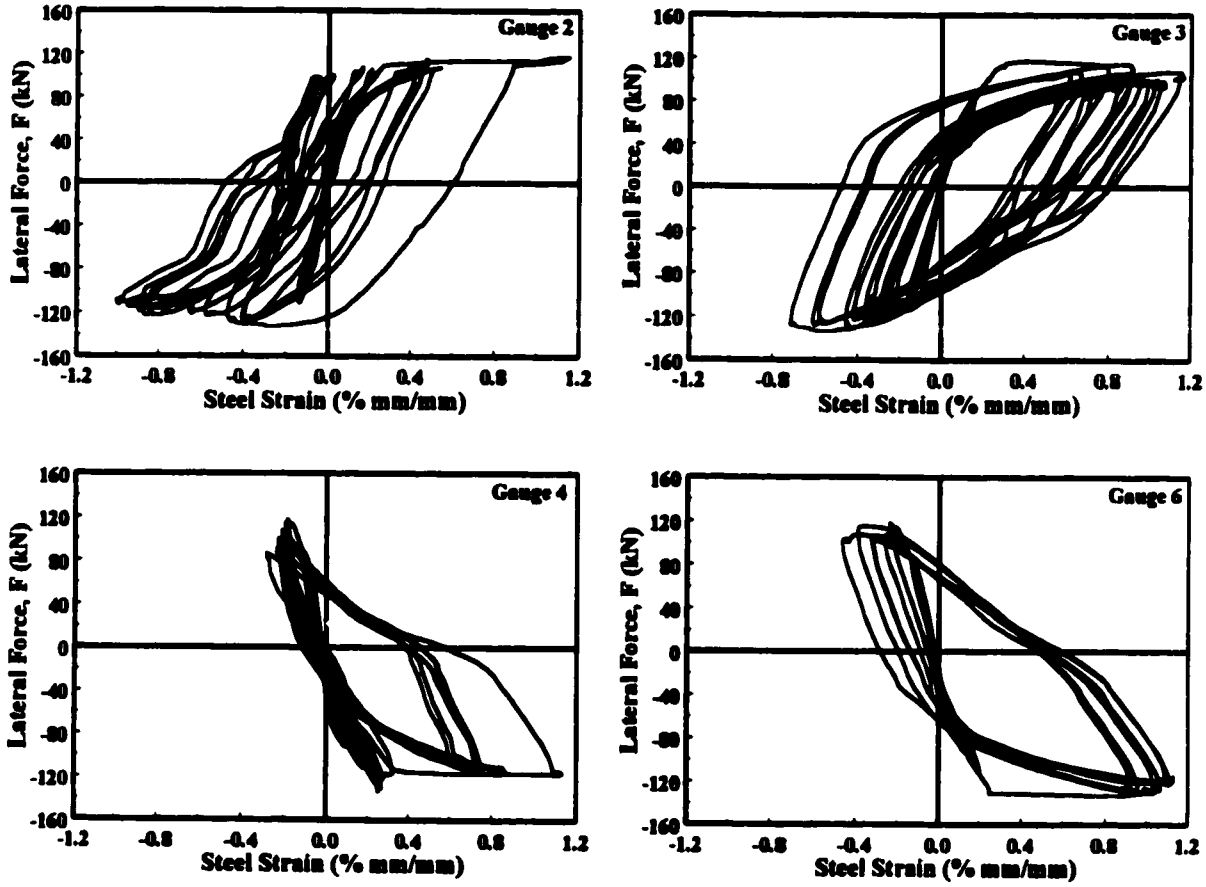

Figure 4.49 : Strain Gauge Data for Longitudinal Reinforcement in Column TC-6

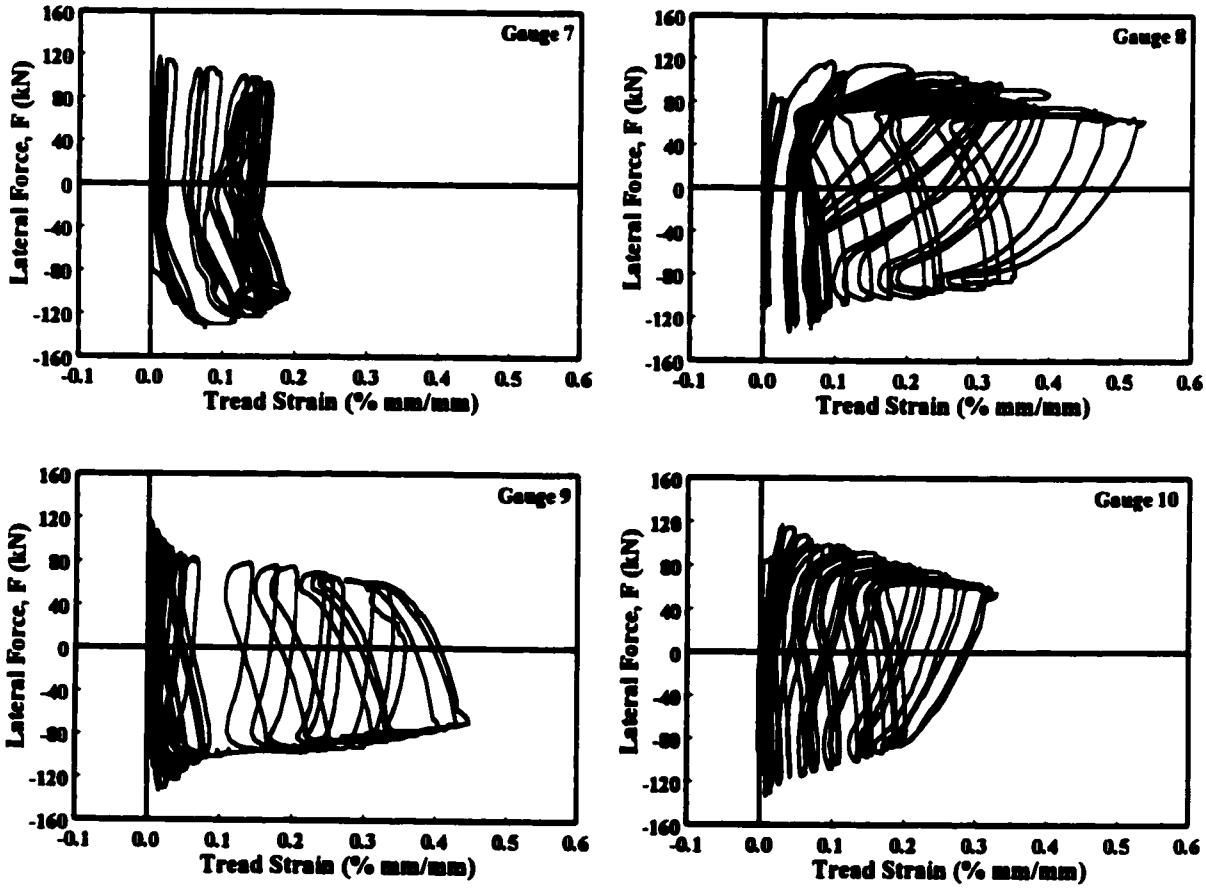

Figure 4.50 : Tire Strains in Column TC-6, Measured on Treads

CHAPTER 5

Column Analysis and Effects of Test Parameters

5.1 General

The test results obtained from the experimental phase of research are evaluated, analyzed and discussed in this chapter. The columns tested were analyzed to establish their inelastic force-displacement relationships. This was done, using the computer program COLA (COLumn Analysis). The comparisons of analytical and experimental results for the six columns tested, as well as the effects of different test parameters are presented and discussed. Test data and the observed behavior of each column, in terms of force-displacement, moment-displacement and moment-rotations relationships, are presented and discussed in Chapter 4.

5.2 Column Analysis

Strength and deformation characteristics of columns were computed analytically using a computer program (COLA) developed by Yalcin (1997). The analysis results are then compared with experimental data to assess the applicability of analytical procedures developed for columns reinforced with conventional reinforcement to the columns reinforced with scrap tires. Additional analyses were also conducted to compare flexural capacities of columns with those computed on the basis of the current Building Code (CSA A23.3). The shear capacity was not calculated, as the columns were clearly in the flexure-dominant range.

COLA is a column analysis program which conducts sectional and member analyses. The sectional analysis is consistent with the standard plane-section analysis used for flexural behaviour. The superiority of the program COLA, relative to others, is the ability to model

both concrete and reinforcing steel behaviour in the inelastic range, while considering concrete confinement, bar buckling, and anchorage slip. Once the sectional behaviour is established, in the form of moment-curvature relationship, the program then conducts member analysis. An algorithm developed by Razvi and Saatcioglu (1996) is used to simulate the formation and progression of plastic hinging in columns. Secondary deformations due to P-Δ effects are considered. The program computes inelastic deformations through integration of curvatures. Inelastic rotations and displacements are computed from the distribution of curvatures along member height. Both the ascending and descending branches of force-displacement relationship are constructed, latter being especially important to establish the inelastic capacity of columns. The column can be analyzed under combined axial compression and flexure, with cross-sectional shapes consisting of rectangle, square, and circular. Two input files are used to specify material, geometric and loading characteristics of columns. The output consists of all pertinent files for listing and/or plotting the results. Each material model, as well as sectional and member response can be generated by using the output files. Moment-axial force relationship is also plotted to assess sectional characteristics of column. The analysis results provide complete insight into the strength, as well as deformability (ductility) of columns.

5.2.1 Column Strength

Column flexural capacity was established by following two separate approaches. First, the moment capacity was computed using program COLA, with appropriate material models, including the effect of concrete confinement and stress-strain relationships obtained form standard cylinder tests and tension coupon tests. Second, the Building Code (CSA A23.3-1994) approach was employed, which ignores concrete confinement as well as steel strain hardening. Both capacities are compared in Table 5.1 with experimentally recorded strength values.

The results in Table 5.1 indicate that the analytical results, produced by using COLA slightly

overestimate flexural moment capacities of the first two (TC-1 and TC-2) and last two columns (TC-5 and TC-6), but underestimate flexural capacities of columns TC-3 and TC-4. This may be attributed to the approximation involved in calculating the area of steel in treaded regions and rims of tires, as well as the cross sectional and core areas enclosed by tires. For TC-1, TC-2, TC-5 and TC-6, the average of steel areas in treads and rims were used, along with a core area equal to the entire cross-sectional area of column. It is important to recall that COLA was prepared for conventional reinforced-concrete columns, and the use of tires as transverse reinforcement requires some approximations. However, these approximations are only limited to the aspects of transverse reinforcement, which is only used for the purpose of determining the effects of concrete confinement. Once the confined concrete stress-strain relationship is established, the main sectional and member analyses remain the same. In general, the comparisons shown in Table 5.1 show good correlations, and indicate that the same analysis tools that are used for conventional reinforced-concrete columns can also be used in analyzing tire-reinforced columns. The analytical results also indicate that the amount of confinement provided in columns does not increase column strength significantly, though column ductility is increased substantially.

5.2.2 Column Deformability

Deformability (ductility) can be defined as the ability to withstand inelastic deformation reversals without a significant loss in strength. By improving inelastic deformability, column performance during an earthquake is improved significantly. The computer program COLA was developed for inelastic column analysis under monotonically increasing load (Push-over analysis). Hence, the force-deformation or moment-displacement relationships produced by the program is in the form of a monotonic curve, rather than a hysteretic curve. However, it has been shown by previous research that a monotonic curve, in flexure dominant members, provides a good estimate of the envelope (backbone) for hysteretic relationship (Karasan and Jirsa 1970).

Analytical moment-displacement relationships, generated by COLA, are compared with hysteretic moment-displacement relationships obtained from column tests, in Figs. 5.1, 5.2 and 5.3. The correlation between the two is good, indicating that inelastic deformations and hence deformability of tire-reinforced concrete columns can be computed by using the same analysis technique used for conventional reinforced concrete columns. Generally, however, all analytical results showed slightly lower deformabilities than experimental results.

The moment-displacement relationships shown in Figs. 5.1 and 5.3 indicate that the confinement of core concrete in Columns TC-5 and TC-6 results in higher column deformability than that in TC-1 and TC-2. However, the lateral load resistance is significantly lower in TC-5 and TC-6, when compared with TC-1 and TC-2, due to the reduced internal lever arm associated with the location of longitudinal reinforcement. The reduction in peak resistance, for the same level of axial compression, was approximately 14 to 19%.

5.3 Effects of Test Parameters

The effects of test parameters are investigated by comparing hysteretic moment-displacement relationships of companion columns. The experimental program was designed to investigate the effectiveness of scrap steel belted tires as transverse confinement reinforcement. The test parameters included; the arrangement of tires and longitudinal reinforcement, as well as the level of axial compression. Six columns were tested to investigate three different reinforcement arrangements at two different levels of axial load.

5.3.1 Effect of Reinforcement Arrangement

Three different arrangements of tires and longitudinal reinforcement were considered. The first arrangement consisted of whole tires placed on top of each other, with longitudinal bars punched through the sidewalls (TC-1 and TC-2). The second arrangement consisted of tires without sidewalls and rims, enclosing longitudinal reinforcement, with side walls completely

removed (TC-3 and TC-4). In addition to the tires, this longitudinal bars were tied together by means of 11.3 mm diameter (No.10) circular ties with overlapping ends, at 275 mm (h/2) spacing. The third arrangement consisted of longitudinal bars placed inside the rims of tires (TC-5 and TC-6). Two companion columns were constructed using each arrangement, and were tested at different axial load levels. The longitudinal reinforcement of each column consisted of twelve 19.5 mm diameter (No. 20) deformed bars.

Figure 5.4 compares the experimental hysteretic moment-displacement relationship for all columns. Columns TC-1 and TC-2 behaved well with stable hysteresis loops, showing gradual strength decays beyond the peak load. TC-1 withstood up to 6% drift with no significant strength degradation and TC-2 withstood 4% drift. Similar behavior was observed in the third arrangement (TC-5 and TC-6) under the same level of axial load except that TC-6 and TC-5 developed higher deformabilities than TC-2 and TC-1, respectively. This may be explained by the increased support provided to longitudinal reinforcement in the former columns, as well as lower shear forces associated with lower flexural capacities of the same columns.

Moment capacity in the third arrangement (TC-5 and TC-6) was low due to the smaller moment arm between the longitudinal bars. Column TC-6 had extremely ductile behavior and showed stable hysteresis loops up to 9% lateral drift without any significant strength degradation. During the first cycles at 10% drift, TC-6 experienced increased strength decay exceeding 25% of the peak load. Both of these columns displayed ductile behavior and showed stable hysteresis loops.

Column TC-4, without the side walls, featured similar behavior as TC-1 and TC-6 in terms of deformability. However, in terms of strength, TC-3 and TC-4 developed higher lateral force resistance because of the larger moment arm between the longitudinal bars. Column TC-4 had ductile behavior and was able to sustain stable hysteresis loops up to 4% lateral drift without significant strength degradation. After the cycles at 4% drift there was slow and gradual strength loss in column ductility.

The damage observed in TC-3 and TC-4 after testing indicated that the joints between the tires opened widely and tires stretched out and ruptured. Because individual tires worked as independent single units, once the sidewalls and the rims were removed, the tires became extremely flexible and weak, and hence could not resist the lateral pressure exerted by concrete. This resulted in the buckling of longitudinal bars, triggering column failure at early stages of loading. This is illustrated in TC-3. The individual circular hoops used as part of column cage were not effective in stabilizing longitudinal bars, since their spacing was large and the ends were susceptible to opening under lateral pressure. Figure 5.4 indicates that columns TC-3 and TC-4 had a significant and rapid strength loss beyond the peak load, especially TC-3. However, these failure modes occurred beyond 3% to 5% lateral drift, which is usually regarded as acceptable limits for earthquake resistant columns. Test results indicated that there was no appreciable difference in strength enhancement due to tire confinement, but the improvement was essentially in column deformability. In summary, it may be concluded that the first arrangement was more effective than the second. Also, the third arrangement, had reduced strength but improved deformability, over and above those exhibited by the other two arrangements.

5.3.2 Effect of Axial Load Level

Bridge columns are usually subjected to 10% to 20% of their concentric capacities. Two levels of axial compression were used in testing the columns, corresponding to 11% and 21% of concentric capacities. This was done to investigate the effect of axial compression on strength and ductility. TC-1, TC-4, and TC-6 were tested under 1000 kN of axial load, representing 11% of their concentric capacities. TC-2, TC-3, and TC-5 columns were tested under 1900 kN of constant axial compression, representing about 21% of their concentric capacities. All other parameters remained the same within the columns in each pair.

The hysteretic moment-displacement relationships for all columns are illustrated in Fig. 5.4. These relationships illustrate the effect of axial compression on column deformability. TC-1

and TC-2 had identical characteristics except for the level of axial load. TC-2 showed lower ductility than TC-1 due to higher axial compression. TC-1 showed up to 6% drift prior to 20% strength decay and TC-2 showed 4% lateral drift at the same decay level. Similarly, the comparison of TC-6 and TC-5 indicates that, TC-5 with higher axial compression showed stable hysteresis loops up to the beginning of 6% drift, in comparison with TC-6 with lower axial compression, that showed 9% drift without any loss in strength.

The hysteretic relationships of the second arrangement indicated that, the lateral drift of TC-4 at 20% decay in moment resistance was about 6%. TC-3 had a higher axial load and could only maintain its moment resistance up to 3% drift at about the same strength decay level.

Anchorage slip and resulting rigid-body rotations at column-footing interface were monitored during testing. It was found that anchorage slip (bar extension in the footing) was small in columns tested under high axial compression, and significant in columns tested under low axial load. Therefore, the effect of anchorage slip was more noticeable in columns with lower axial load. This was to be expected as axial compression has an influence on yield penetration into the footing.

5.4 Comparisons with Regular R/C Columns

This section explains the comparisons between tire-reinforced columns, i.e., the new technology and conventional steel-reinforced concrete columns. Moment-displacement relationships for TC-1 and TC-2, are compared in Fig. 5.5 with steel reinforced columns of equivalent characteristics (BR-C6 and BR-S3), also tested at the Structures Laboratory of the University of Ottawa by Mes (1999). Column TC-1 and TC-2 were confined with tires only. The first conventionally reinforced column, BR-C6, was a circular column with a diameter of 508 mm, reinforced with 11.3 mm diameter (No.10) individual circular hoops with overlapping ends at 300 mm spacing. The second one, BR-S3, was a square column with 500 mm cross-section, again reinforced with 11.3 mm diameter (No.10) perimeter ties with 135°

bends at 300 mm spacing. The longitudinal steel used in all columns consisted of 12#20 bars and the total effective height of the columns was 2.0 m. Columns BR-C6 and BR-S3 represent typical R/C columns designed for non-seismic zones. Both were tested under 15% of P_o, where P_o represents concentric column capacity. The axial force level applied to TC-1 and TC-2 were 11% and 21% of P_o, respectively.

Figure 5.5 indicates that both BR-C6 and BR-S3 resisted lateral deformation reversals of up to 2% drift, before failing in a brittle manner by developing a 60% loss in capacity at the end of 3% drift cycles. This behavior was due to poor confinement, and shows typical unconfined column behavior. Columns TC-1 and TC-2, with the tires, showed significantly more ductile behaviour, developing 4% to 6% lateral drift with little or no strength decay. This comparison clearly indicates the superiority of concrete columns transversely reinforced with tires, over bridge columns with non-seismic transverse reinforcement. Similarly improved behaviour can only be obtained from conventionally reinforced concrete columns if closely spaced high volumetric ratio transverse steel is used in the form of spirals, closed hooks, overlapping hoops and crossties, congesting the column case while increase the cost of construction.

The tires can be used as formwork, left as transverse reinforcement, and work as protection against corrosion while providing impact resistance in the event of a traffic accident.

Table 5.1 : Column Analysis

Columns	Analytical		Experimental
	Flexural Moment Capacity		Flexural Moment Capacity
	M_{COLA}	M_{CSA}	M_{Test}
TC-1	420	412	383
TC-2	485	471	430
TC-3	707	687	720
TC-4	581	566	593
TC-5	415	374	343
TC-6	357	331	329

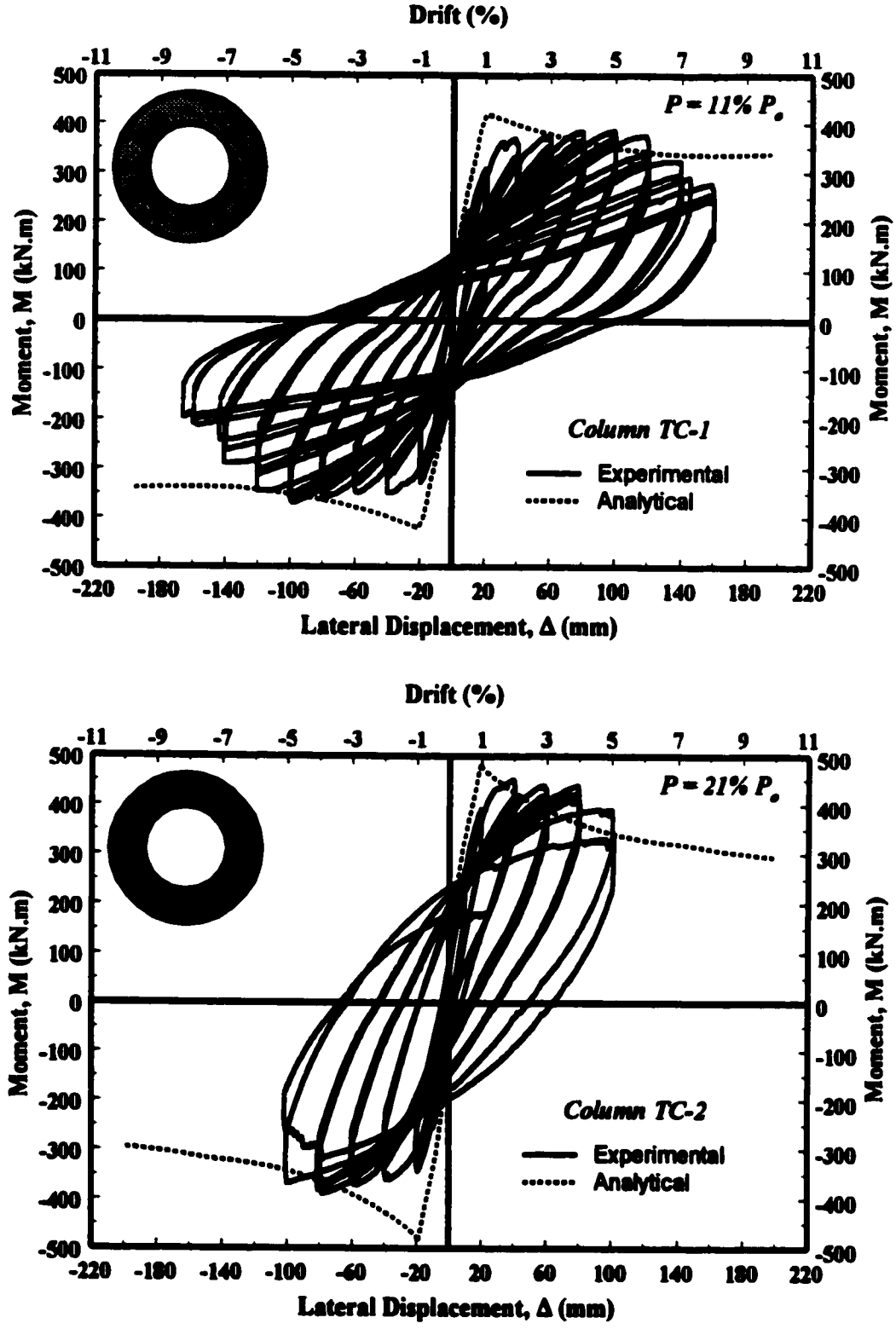

Figure 5.1 : Comparisons of Analytical and Experimental Moment-Displacement Relationships for Columns TC-1 and TC-2

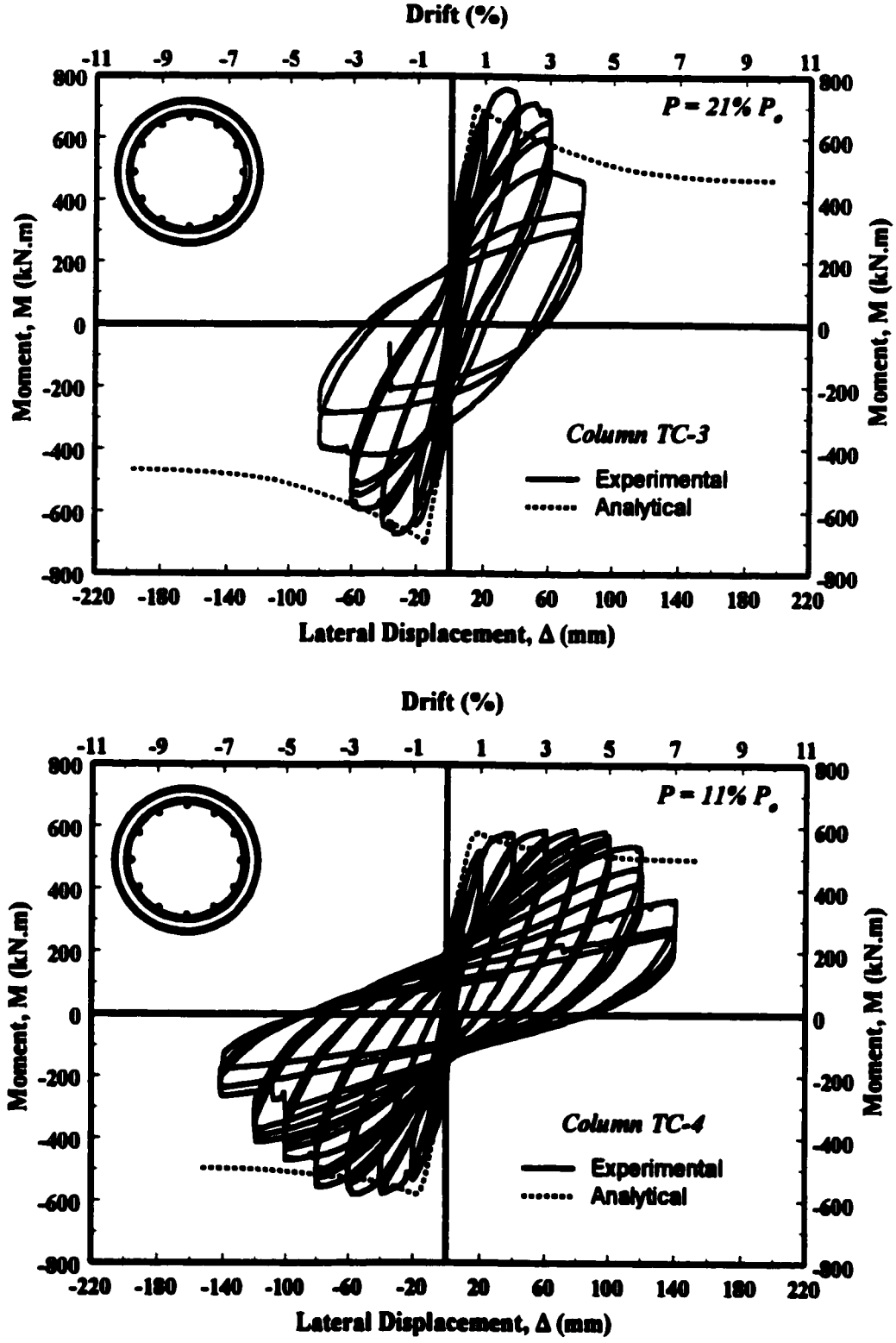

Figure 5.2 : Comparisons of Analytical and Experimental Moment-Displacement Relationships for Columns TC-3 and TC-4

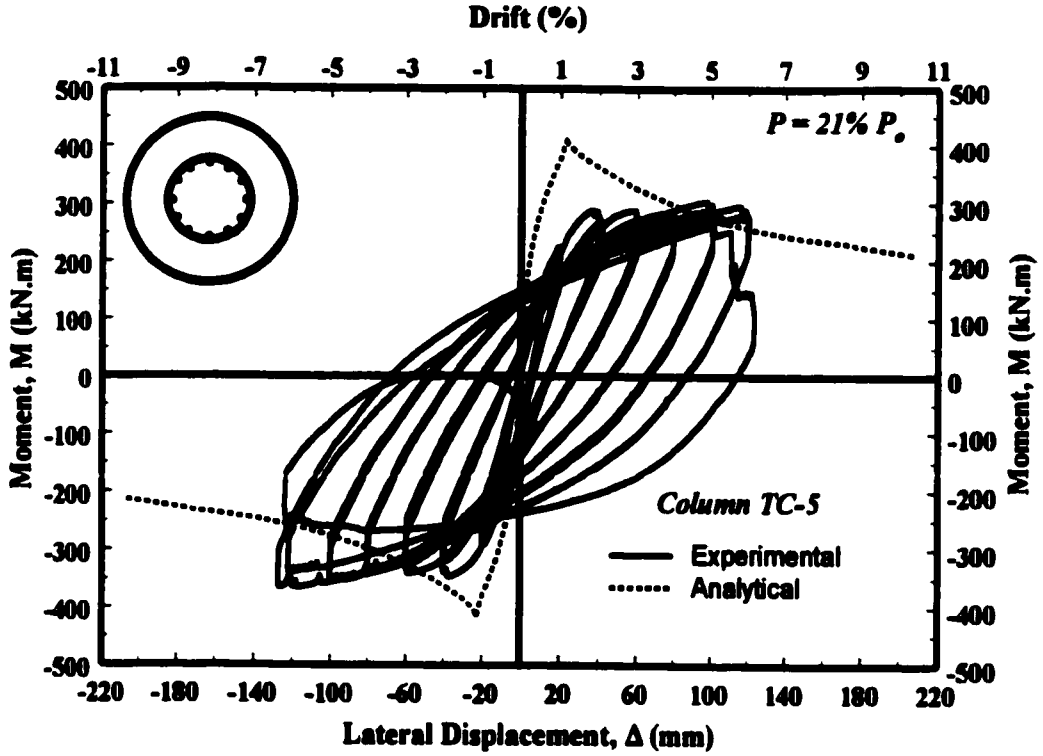

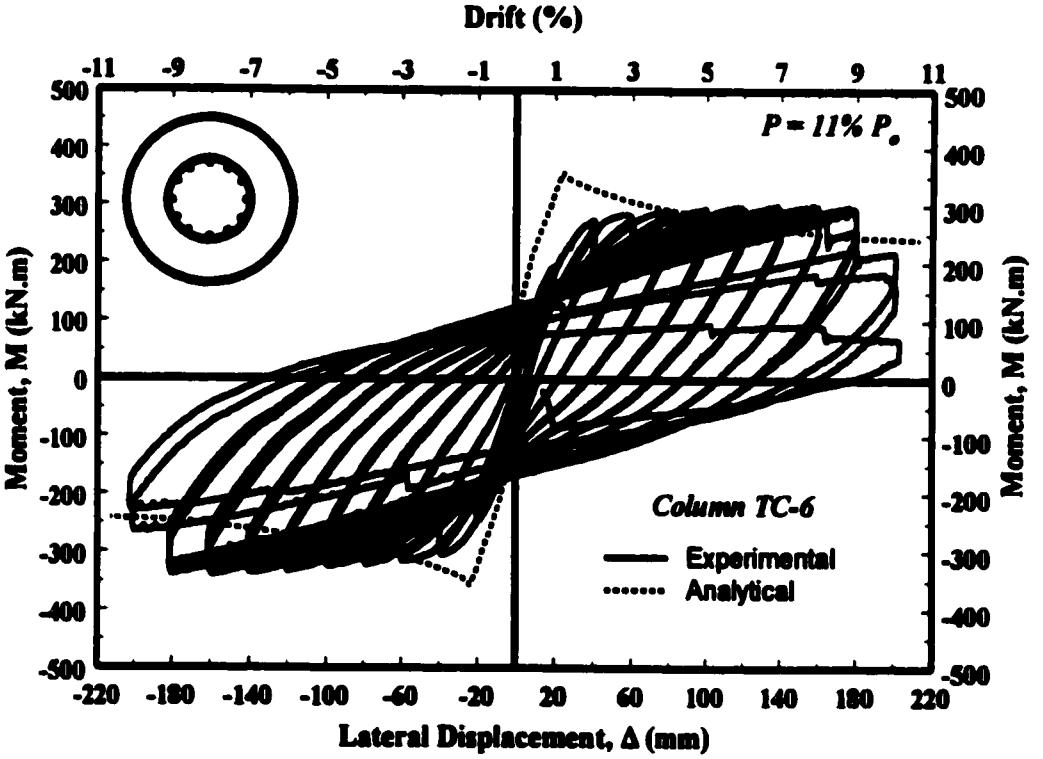

Figure 5.3 : Comparisons of Analytical and Experimental Moment-Displacement Relationships for Columns TC-5 and TC-6

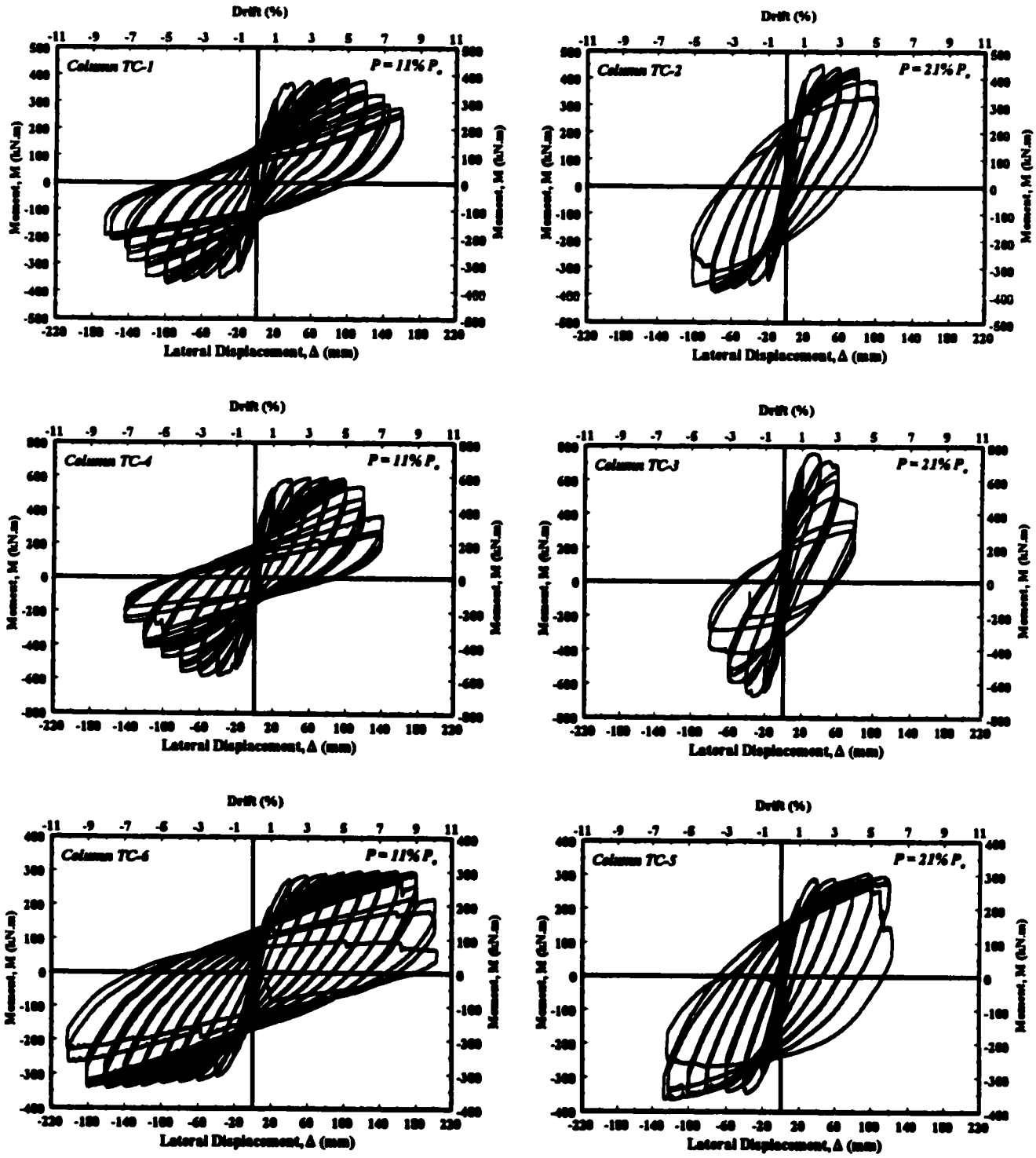

(a) P = 11% P_o

(b) P = 21% P_o

Figure 5.4 : Effects of Reinforcement Arrangement and Level of Axial Load

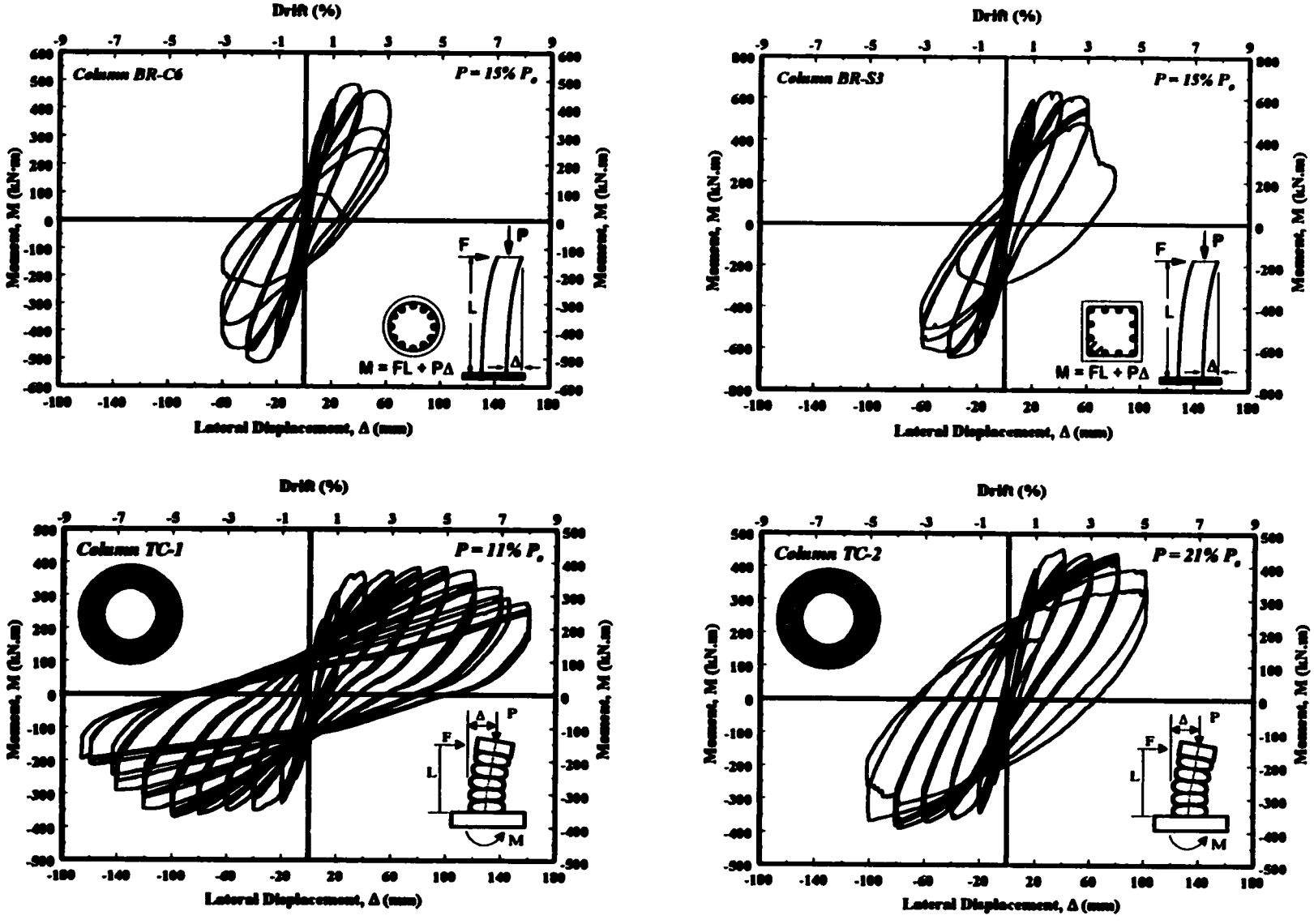

Figure 5.5 : Comparisons Between Tire-Reinforced and Conventionally-Reinforced Concrete Columns

CHAPTER 6

Summary and Conclusions

6.1 Summary

One of the concerns of Structural Engineers is to design concrete columns so that they maintain their strengths during a strong earthquake. For most framed structures to survive a major earthquake, they must undergo a large number of inelastic deformation reversals without a significant loss of strength, while dissipating energy. Many structural failures during past earthquakes have been attributed to poor column behavior in the inelastic range. In order to prevent this poor behavior, columns are designed to have adequate ductility, by suitably confining the plastic hinge regions. This is usually done by providing transverse reinforcement of sufficient amount and proper arrangement, with close spacing. Because the current requirements for concrete confinement result in congestion of column cage, and related difficulties in construction, researchers have directed their attention to new and innovative approaches to column confinement. One possible alternative for column confinement is to use steel-belted scrap tires. However, this application of tires has not been researched in the past. Hence, there is no experimental data available on columns confined with scrap tires, though confining bridge columns with steel-belted tires may be a feasible alternative.

A comprehensive investigation of the characteristics of tires used in the automobile industry has first been conducted. This involved verification of the type, diameter, and number of wires or cords in tires of different brand names. A total of six full size circular columns were designed, constructed and tested under constant axial compression and incrementally increasing lateral deformation reversals. These columns were design to investigate the effects of using various configurations of tire confinement on strength and ductility of columns. The

parameters included in the experimental program were; the arrangement of reinforcement, including the tires, and the level of axial load.

Test results were presented in the form of hysteretic force-displacement and moment-displacement relationships. The effects of test parameters were analyzed by comparing column performance. Analyses of columns were conducted using the computer program COLA, which provided analytical moment-displacement relationships (backbone curves) under monotonically increasing lateral loads. These results were then compared with those obtained experimentally. Column flexural capacities were also computed using the approach outlined in current Building Codes (ACI318-1995, CSA A23.3-1994). Conclusions drawn from the results are summarized in the following section.

6.2 Conclusions

The following conclusions can be drawn based on the experimental and analytical research presented in this thesis:

1. Columns confined with scrap tires behaved in a ductile manner, developing lateral drifts ranging between 4% and 9%. These drift levels were found to be comparable to those expected in columns confined with conventional transverse reinforcement of significantly higher volumetric ratio.

2. Among the three arrangements of tires and longitudinal reinforcement considered, those that contained whole tires performed better than that included the treaded parts only, without the sidewalls. Columns TC-1 and TC-2, with whole tires and longitudinal bars punched through the side-walls, showed ductile response and developed 4% to 6.5% drift, depending on the level of axial compression. Similarly, columns with whole tires, enclosing longitudinal reinforcement in the rims, performed in a ductile manner. In fact these columns (TC-5 and TC-6) showed even higher drift

capacities, developing 6% to 9% drift prior to experiencing significant strength decay, depending on the level of axial compression. However, this arrangement resulted in reduced internal lever arm, which led to a proportional reduction in flexural capacity.

3. The columns without the tire side-walls showed 3% or 6% lateral drift capacity, depending on the level of axial compression. The improvement observed in column deformability was limited because of the reduced rigidity of tires as well as the reduced volumetric ratio of steel in tires, resulting from the removal of the side-walls, including the rims. Therefore, this arrangement is the least favorable among the three considered.

4. The effect of axial compression is to increase flexural capacity but reduce column deformability. The increase in axial load from 11% P_o to 21% P_o resulted in approximately 2% reduction in drift capacity.

5. The hysteretic moment-displacement relationships obtained experimentally showed good correlations with the moment-displacement envelope (backbone curves) computed analytically. This implies that the analysis techniques intended for concrete columns reinforced with conventional steel reinforcement can be applied to tire-reinforced columns.

6. Both experimental and analytical research indicated that tire-reinforced concrete columns show approximately the same inelastic deformability as those expected from steel reinforced concrete columns, with much less volumetric ratio of transverse reinforcement than that required by CSA Standard A23.3. This may be attributed to the efficiency of tires with closely spaced steel wires contained, and the higher grade of steel used in tires.

7. Tire coupon tests conducted in the lab showed that the steel in tires showed almost

linear behaviour, with ultimate tensile strain of approximately 6% to 7%. The tensile strength was approximately equal to 2000 MPa to 2500 MPa.

8. The use of tires in columns as transverse reinforcement results in ductile response of column, while preventing congestion of columns cage and associated concrete placement problems. The tires further have the advantage of protecting longitudinal steel against corrosion, while providing impact resistance and energy dissipation in the event of a vehicular collusion.

9. Deformations due to anchorage slip can be significant if the axial load is low. Therefore, the effect of anchorage slip was more noticeable in columns with lower level of axial load. The columns subjected to higher axial compression developed lower yield penetration into the footing.

6.3 Recommendations for Future Research

The following recommendations are made for future research:

1. The number of steel cords inside the tire treads varied from one brand name to the other. Furthermore, different sizes of tires are available in the industry. More experimental and analytical research is needed on columns with different size and steel content of tires.

2. Tires are a combustible material. Although they are difficult to ignite, they can be a fire hazard. To eliminate the possibility of potential fire damage, further research is required to explore the use of incombustible materials such as, shotcrete as fire retarders.

3. Construction difficulties exist in placing the re-bars inside the sidewall of tires (first

arrangement). Further research is needed to design techniques for mass production for columns confined with scrap tires.

4. The current research project was limited to 6 column tests. Further testing is recommended to provide more experimental evidence on performance of tire-reinforced concrete columns.

References

[1] AB-Malek, K., and Stevenson, A., "*The effects of 42 Years Immersion in Sea Water on Natural Rubber,*" Journal of Material Sciences, No. 21, 1968, PP. 147-154.

[2] Baingo, D., "*Performance of Circular High-Strength Concrete Columns Under Lateral Load Reversals,*" M.A.Sc. Thesis, Department of Civil Engineering, University of Ottawa, Ottawa, Ontario, Canada, May 1996, PP. 211

[3] Chan, W. L., *"The Ultimate Strength and Deformations of Plastic Hinges in Reinforced Concrete Frameworks,"* Magazine of Concrete Research, Vol. 7, No. 21, November 1955, PP. 121-132.

[4] CSA, "*Design of Concrete Structures for Buildings (CAN3-A23.3-M94),*" Canadian Standards Association, Ontario, 1994, 281 PP.

[5] Drescher, A., and Newcomb, D., "*Development of Design Guidelines for Use of Shredded Tires as A lightweight Fill in Road Subgrade and Retaining Walls,*" Report Submitted to the Minnesota Department of Transportation, Report No. MN/RC-94/04, 1994, National Technical Information Service, Springfield, Virginia 22161.

[6] Eldin, N. N., and Senouci, A. B., "*Use of Scrap Tires in Road Construction,*" Journal of Construction Engineering and Management, Vol. 118, No. 3, 1992, PP. 561-576.

[7] Eldin, N. N., and Senouci, A. B., "*Rubber-Tire Particles as Concrete Aggregate,*" Journal of Materials in Civil Engineering, ASCE, Vol. 5, No. 4, November 1993, PP. 478-496.

[8] Fafitis, A. and Shah, S. P., *"Prediction of Ultimate Behavior of Confined Columns Subjected*

to Large Deformation," ACI Structural Journal, Vol. 82, July-August 1985 (a), PP.423-433.

[9] Forsyth, R. A., and Egan, J. P., "*Use of Waste Materials in Embankment Construction,*" Transportation Research Record, No. 593, 1976, PP. 3-8.

[10] Geisler, E., Cody, W. K., and Niemi, M., " *Tires for Subgrade Support,*" ASCE Paper No. 897550, Presentation. American Society of Agriculture Engineers, 1989, ASAE, St. Joseph, MI.

[11] Grira, M., "*Innovative Approaches to Column Confinement,*" Ph.D. Thesis, Department of Civil Engineering, University of Ottawa, Ottawa, Ontario, Canada, September 1998, PP. 481.

[12] Humpstone, C. C., Ayres, E., Keahy, S. G., and Schell, T., "*Tire Recycling and Reuse Incentives,*" Report No. EPA/530/SW-32c(R), 1972, Environmental Protection Agency.

[13] Karasan, I. D., and Jirsa, J. O., "*Behavior of Concrete Under Varying Strain Gradient,*" Proceedings, ASCE, Vol. 96, No. St8, August 1970, PP. 1675-1696.

[14] Kent, D. C., and Park, R., *"Flexural Members with Confined Concrete,"* Journal of Structural Division, ASCE, Vol. 97, 1971, PP. 1969-1990.

[15] Lipien, W., "*Behavior of Square High Strength Concrete Columns Under Load Reversals,*" M.A.Sc. Thesis, Department of Civil Engineering, University of Ottawa, Ottawa, Ontario, Canada, November 1995, PP. 184.

[16] Long, N. T., "*The Pneusol. Laboratoire Central des Ponts et Chaussées, Paris,*" Études et Recherches des Laboratoire des Ponts et Chaussées, Série Géotechnique, 1990 GT44.

[17] Long, N. T., "Le Pneusol: Recherche-Réalisations-Perspectives," Tése de Doctorat, Institut

National des Science Appliquées de Lyon, 1993.

[18] Mander, J. B., Priestley, M. J. N., and Park R., *"Observed Stress-Strain Behavior of Confined Concrete,"* ASCE Structural Journal, Vol. 114, No. 8, Aug. 1988(a), PP. 1827-1849.

[19] Mes, D., *"Seismic Retrofitting of Concrete Bridge Columns by External Prestressing,"* M.A.Sc. Thesis, Department of Civil Engineering, University of Ottawa, Ottawa, Ontario, Canada, January 1999, PP. 125.

[20] Mitchell, J. K., and Christopher, B. R., North American Practice in Reinforced Soil Systems. *"Design and Performance of Earth Retaining Structures,"* Geotechnical Special Publication No. 25, ASCE. Philip C. Lambe and Lawrence A. Hansen editors, 1990, PP. 322-346.

[21] O'Shaughnessy, V., *"Reinforcement of Earth Structures Using Scrap Tires,"* Ph.D. Thesis, Department of Civil Engineering, University of Ottawa, Ottawa, Ontario, Canada, November 1997, PP. 372.

[22] Ozcebe, G., and Saatcioglu, M., *"Confinement of Concrete Columns for Seismic Loading,"* ACI Structural Journal, Vol. 84, No. 4, 1987, PP. 308-315.

[23] Park, R., and Paulay, T., *"Reinforced Concrete Structures,"* John Wiley and Sons, 1975, PP. 769.

[24] Park, R., Priestley, M.J.N., and Gill, W.D., *"Ductility of Square Confined Concrete Columns,"* Journal of Structural Division, ASCE, Vol. 108, No. ST4, April 1982, PP. 929-951.

[25] Razvi, S., *"Behavior of Reinforced Concrete Columns Confined With Welded Wire Fabric,"*

M.A.Sc. Thesis, Department of Civil Engineering, University of Ottawa, Ottawa, Ontario, Canada, January 1988, PP. 152.

[26] Razvi, S., *"Confinement of Normal and High-Strength Concrete Columns,"* Ph.D. Thesis, Department of Civil Engineering, University of Ottawa, Ottawa, Ontario, Canada, June 1995, PP. 416.

[27] Razvi, S., and Saatcioglu, M., *"Behavior of Reinforced Concrete Columns Confined with Welded Wire Fabric and/or Rectilinear Ties,"* Research Report, Department of Civil Engineering, University of Ottawa, Canada, 1989(a), PP. 65.

[28] Razvi, S., and Saatcioglu, M., *"Confinement of Reinforced Concrete Columns with Welded Wire Fabric,"* ACI Structural Journal, Vol. 86, No. 5, September-October 1989(b), PP. 615-623.

[29] Saatcioglu, M., and Ozcebe, G., *"Response of Reinforced Concrete Columns to Simulated Seismic Loading,"* ACI Structural Journal, Vol. 86, No. 1, January-February 1989, PP. 3-12.

[30] Saatcioglu, M., *"Deformability of Reinforced Concrete Columns,"* Earthquake-Resistance Concrete Structures Inelastic Response and Design, ACI SP-127-10, 1991, PP. 421-452.

[31] Saatcioglu, M., *"Design of Seismic Resistant Concrete Columns for Confinement,"* Worldwide Advances in Structural Concrete and Masonry Structures Congress - Proceedings 1996. ASCE, New York, NY, USA. PP. 233-244.

[32] Saatcioglu, M., and Razvi, S., *"Strength and Ductility of Confined Concrete,"* Journal of Structural Engineering, ASCE, Vol. 118, No. 6, June 1992, PP. 1590-1607.

[33] Saatcioglu, M., Salamat, A. H., and Razvi, S. R., *"Confined Columns Under Eccentric*

Loading," Journal of Structural Engineering, ASCE, Vol. 121, No. 11, November, 1995, PP. 1547-1556.

[34] Scott, B. D., Park, R., and Priestley, M. J. N., *"Stress-Strain Behavior of Concrete Confined by Overlapping Hoops at High and Low Strain Rates,"* ACI Journal, January-February 1982, PP. 13-27.

[35] Sheikh, S. A., and Khoury, S. S., *"Confined Concrete Columns With Stubs,"* ACI Structural Journal, Vol. 90, No. 4, July-August 1993, PP. 414-431.

[36] Sheikh, S. A., and Khoury, S. S., *"A Performance-Based Approach for the Design of Confining Steel in Tied Columns,"* ACI Structural Journal, Vol. 94, No. 4, July-August 1997, PP. 421-431.

[37] Sheikh, S. A., and Uzumeri, S. M., *"Analytical Model for Concrete Confinement in Tied Columns,"* Journal of Structural Engineering, ASCE, Vol. 108, No. 5, December 1982, PP. 2703-2723.

[38] Sheikh, S. A., and Uzumeri, S. M., *"Strength and Ductility of Tied Concrete Columns,"* Journal of Structural Engineering, ASCE, Vol. 106, No. 5, May 1980, PP. 1079-1102.

[39] Sheikh, S. A., and Yeh, C. C., *"Flexural Behavior of Confined Concrete Columns,"* ACI Structural Journal, May-June 1986, PP. 389-404.

[40] Williams, J., *"Guidelines for Using Recycled Tire Carcasses in Highway Maintenance,"* Report No. FHWA/CA/TL-87/07, California Department of Transportation, Sacramento, May 1987.

[41] Williams, P. T., Besler, S., and Taylor, D. T., *"The Pyrolysis of Scrap Automotive Tires: The*

Influence of Temperature and Heating Rate on Product Composition," Fuel, Vol. 69, December 1990, PP. 1474-1482.

[42] WYMCC 1977, "*Reuse of Worn Tyres in Civil Engineering Construction,*" Report Prepared for the West Yorkshire Metropolitan County Council, April 1977.

[43] Yalcin, C., "*Seismic Evaluation and Retrofit of Existing Reinforced Concrete Bridge Columns,*" Ph.D. Thesis, Department of Civil Engineering, University of Ottawa, Ottawa, Ontario, Canada, September 1997, PP. 306.